Programa de Doctorat en Bioquímica, Biologia molecular i Biomedicina

Universitat Autònoma de Barcelona

Centre de Biotecnologia Animal i Teràpia Gènica

Departament de Bioquímica i Biologia Molecular

Facultat de Medicina

Universitat Autònoma de Barcelona

Development and optimization of the *attB* system to produce Helper-dependent Adenovirus vectors of different species

Memòria per optar al grau de Doctor en Bioquímica, Biologia molecular i Biomedicina per la Universitat Autònoma de Barcelona

Presentada per Dan Cots i Rabella

Abril de 2014

El Director: El Doctorand:

Dr. Miguel Chillón Rodríguez Dan Cots i Rabella

A les persones que estimo

Index

Abbreviations

^{o}C	Celsius degrees
Ψ	Packaging signal
A	Adenine
AAV	Adeno-associated virus
Ab	Antibody
Ad	Adenovirus
Ad5	Adenovirus serotype 5
Ad40	Adenovirus serotype 40
ADA	Adenosine deaminase
ADA^{-} SCID	Adenosine deaminase deficiency
ADP	Adenovirus death protein
APCs	Antigen-presenting cells
AdPol	Adenovirus DNA polymerase
Bp	Base pairs
C	Cytosine
CAR	Coxsackievirus and adenovirus receptor
CAV-2	Canine adenovirus serotype 2
CCR5	C-C chemokine receptor type 5
cDNA	Complementary deoxyribonucleic acid
CF	Cystic fibrosis
CFTR	Cystic fibrosis transmembrane conductance regulator
CKD	Chronic kidney disease
cm	Centimeter
CMV	Cytomegalovirus
CNS	Central nervous system
CsCl	Cesium chloride
CTL	Cytotoxic T lymphocyte
DBP	Deoxyribonucleic acid binding protein
DMD	Duchenne Muscular Dystrophy
DNA	Deoxyribonucleic acid

dsDNA Double-stranded deoxyribonucleic acid

DTT Dithiothreitol

EDTA Ethylenediamine tetra-acetic acid

EGTA Ethylene glycol tetra-acetic acid

EMSA Electrophoretic mobility shift assay

F40L Adenovirus 40 long fiber protein

F40S Adenovirus 40 short fiber protein

FACS Fluorescence-activated cell sorting

FBS Fetal bovine serum

FGAd First-generation adenoviruses

Flt3L/TK FMS-like tyrosine kinase ligand 3

G Guanine

G6Pase Glucose-6-phosphatase

GFP Green Fluorescent Protein

GSD-Ia Glycogen storage disease type Ia

hAAt Human α-1 anti-trypsin

HBsAg Hepatitis B surface antigen

HDAd Helper-dependent adenovirus

HDCAV-2 Helper-dependent canine adenovirus serotype 2

HEK Human embryonic kidney

hGAA Human lysosomal α-glycosidase

HIV Human immunodeficiency virus

HPLC High-performance liquid chromatography

HSV-1 Herpes simplex virus

ITR Inverted terminal repeat

iRNA Interference ribonucleic acid

IU Infection units

Kb Kilo-base pair

KDa Kilodalton

LTR Long terminal repeat

MCS Multiple cloning site

MHC Major histocompatibility complex

min	Minute
ml	Milliliters
MLP	Major late promoter
mM	Millimolar
MMLV	Moloney murine leukemia viruses
MOI	Multiplicity of infection
MPS	Mucopolysaccharidosis
mRNA	Messenger ribonucleic acid
MTA	Material Transfer Agreement
MW	Molecular weight
NaCl	Sodium chloride
ng	Nanogram
nt	Nucleotide
nm	Nanometer
OTC	Ornithine transcarbamylase
PCR	Polymerase chain reaction
PEG	Polyethylene glycol
PEI	Polyethylenimine
pm	Picomol
polyA	Polyadenylation sequence
pp	Physical particle
RCA	Replication-competent adenovirus
RFP	Red fluorescent protein
RNA	Ribonucleic acid
RSV	Human respiratory syncytial virus
X-SCID	X-linked severe combined immunodeficiency
SDS	Sodium dodecyl sulfate
SDS-PAGE	Sodium dodecyl sulfate polyacrylamide gel electrophoresis
SGSH	N-sulfoglucosamine sulfohydrolase
shRNA	Short hairpin ribonucleic acid
SV40	Simian vacuolating virus 40
T	Thymine

TCR	T-cell receptor
TK	Thymidine kinase
TLR	Toll-like receptor
TNF-α	Tumor necrosis factor α
TP	Adenovirus terminal protein
TU	Transducing unit
U	Units
UV	Ultraviolet
VCAM-I	Vascular cell adhesion molecule I
VIP	Vasoactive intestinal peptide
vp	Viral particles
WHV	Woodchuck hepatitis virus
X-ALD	X-linked adrenoleukodystrophy
µl	Microliters
µg	Micrograms

Summary

Helper-dependent adenovirus (HDAd) are very attractive vectors for gene therapy because they have a large cloning capacity and can infect a wide variety of cell types, regardless of their proliferation state, and result in long-term transgene expression without chronic toxicity. The production of these vectors has been widely optimized up to a level where clinical-grade productions can be achieved with very low helper-Ad contamination levels. However, this methods still need to be improved, as most of them are not scalable and therefore require an important amount of time and effort to achieve large-scale preparations.

Despite the ongoing optimization of HDAd production, there is still concern for the clinical application of HDAd vectors because the humoral immune response against the viral capsid limits their efficiency, while the innate immune response limits their biosafety. In this regard, the use of non-human-derived HDAd vectors to avoid the immune response seems to be a very promising option for their application in clinical trials. However, the production of these vectors has not been sufficiently optimized yet, generally producing low infectious titers with levels of helper contamination that do not permit their use in clinical trials.

Also, to improve the biosafety and efficacy of HDAd vectors, different strategies based on modulating the interaction between viral fiber proteins and the cellular receptors by capsid modification are currently being tested. The higher transduction efficiencies of these chimeric vectors would allow therapeutic levels of the vector using lower doses, making them safer in the clinic. Also, capsid modification could be performed to generate vectors capable of only transducing a specific target cell, allowing the control of vector tropism, and therefore avoiding a widespread distribution of the vector, which would be an important step forward in terms of biosafety. In this regard, the generation of systems to produce chimeric HDAd is very interesting, as these vectors combine the mentioned advantages of chimeric vectors and the biosafety of HDAds.

In this thesis we developed and optimized HDAd production strategies for these vectors based on the use of helper-Ad with the *attB* sequence of ΦC31 recombinase, which causes a delay on the viral life cycle of these vectors, allowing a preferential amplification of HDAd without requiring the use of cell lines with Cre recombinase expression.

Preface

In the era of new technologies and scientific breakthroughs, chronic diseases are still treated with drugs that often only target the symptomatology of these diseases, and do not intend the cure of them. In this regard the rising of gene therapy, the field of biomedicine based on the insertion of genes or the modulation of their expression has generated much expectation for its great potential to treat these diseases. However, this new technology has encountered several barriers that have slowed its widespread application in many clinical applications. Among them, the development of safer and highly effective vectors that elicit no host immune response and allow a long-term expression of the transgene is crucial for the success of gene therapy and its final implementation in clinical trials. To date, helper-dependent adenoviral vectors are one of the most promising vectors for gene therapy. However, despite their attractive characteristics (large insert capacity and low cell immune response compared with first-generation adenoviral vectors) they have several drawbacks, like the complex production process, the presence of helper contamination and the humoral host immune response they still elicit. To overcome production complexity and lower contamination the optimization of the *attB* production system seems an interesting strategy. On the other hand, the use of adenovirus of non-human origin to avoid the humoral immune response against the human adenovirus is promising. However, the production of these vectors is very inefficient and its availability is currently limited. For this reason, the development of strategies to optimize their production and titration is very interesting.

In addition, the development of chimeric adenoviruses will be helpful to increase the transduction efficiency of serotype 5 adenovirus (Ad5) vectors as well as to control their tropism. In this regard, the generation of the adenovirus 5/40S helper-dependent vector may improve the biosafety and efficiency of these vectors and will allow their application in tissues where the use of Ad5 vectors is not feasible.

Chapter 1

INTRODUCTION

1.1. GENE THERAPY

Advances towards understanding the molecular biology underlying diseases altogether with recent scientific breakthroughs in the genomics field have yielded a wealthy knowledge of the molecular basics of a wide range of human pathologies. This allowed the rising in the last few decades of biomedicine, a discipline specialized in the development of different techniques and therapies using bioactive compounds for the treatment of diseases.

1.1.1. Concept of gene therapy

Gene therapy is the field of biomedicine based on the introduction of nucleic acids in a target cell or tissue for therapeutic purposes and focused on the correction of the genetic dysfunction. While in the traditional medicine the use of drugs, radiotherapy or surgery often only treat the symptoms of genetic diseases, gene therapy focus on the correction of the genetic dysfunction. This offers unique possibilities to treat the genetic causes of diseases, such as the expression of specific genes in fatal enzyme deficiencies, or the introduction of genetic elements capable of modulating the gene expression in genetic diseases caused for gene overexpression, like Huntington disease (Franich *et al.*, 2008; Xia *et al.*, 2004). These genetic elements include iRNA (interference RNA), shRNA (short hairpin RNA), antisense sequences, and RNA aptamers or miRNA sponges. As a result of this, diseases with a known genetic malfunction are candidates to be corrected with the introduction of the appropriate nucleic acids. Nevertheless, gene therapy can also be applied to the treatment of acquired diseases like AIDS, where zinc finger nucleases are used to alter genomic sequences to create a mutation in C-C chemokine receptor type 5 (*CCR5*) to make cells resistant to HIV infection (Urnov *et al.*, 2010; Chung *et al.*, 2011) or in cancers, where the use of vectors that express toxins like thymidine kinase have a great anti-tumoral potential (Puntel *et al.*, 2010). As a result, more than 1900 gene therapy clinical trials have been recorded worldwide, mainly targeting cancers and, in a lesser extent, monogenetic diseases (http://www.abedia.com/wiley/index.html).

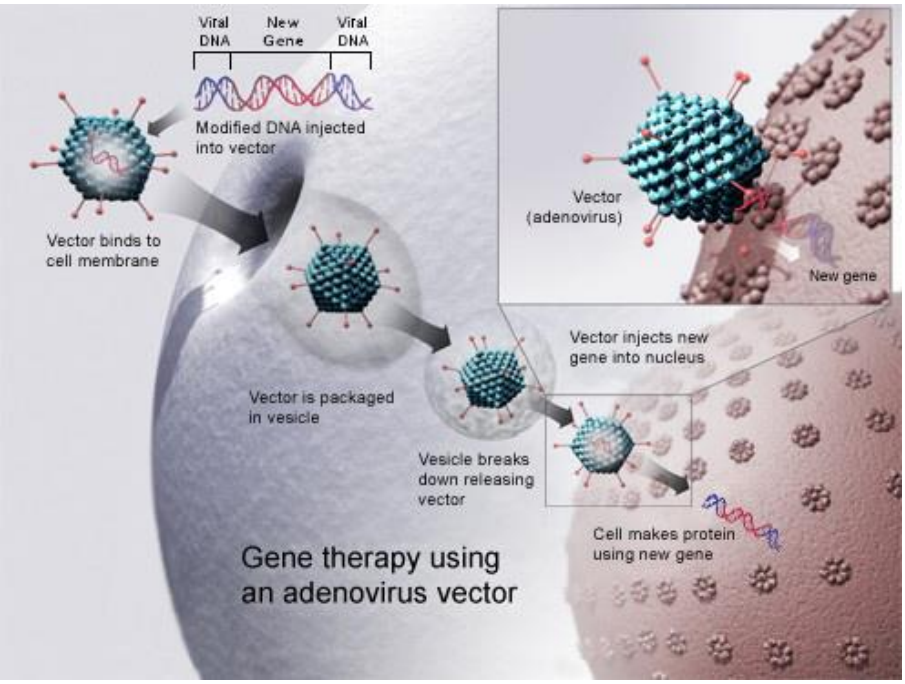

Figure 1.1. Gene therapy using an adenovirus vector. A new gene is inserted into a cell using an adenovirus. If the treatment is successful, the new gene will make functional protein to treat a disease (from Wikimedia Commons).

1.1.2. Methods of genetic administration

Gene therapy potentially represents one of the most important developments to occur in current medicine, but before it can be fully applied, certain technical problems common to all methods of gene delivery must be overcome. Usually, these treatments require a tissue-specific, efficient transgene expression throughout all the life of the patient with absence of toxic effects. For this reason, the generation of a vector capable of targeting a specific tissue with an elevate transduction efficiency and sustaining a stable, regulated gene expression without any side effects or immunogenic responses would be ideal, thus avoiding the risks of the immune response caused for successive administrations.

In this regard, the main barriers to successful gene therapy can be summarized in:

I) vector uptake, transport and uncoating, II) vector genome persistence, III) the mutagenesis by integrative vectors, IV) sustained transcriptional expression, and V) the host immune response (Figure 1.2).

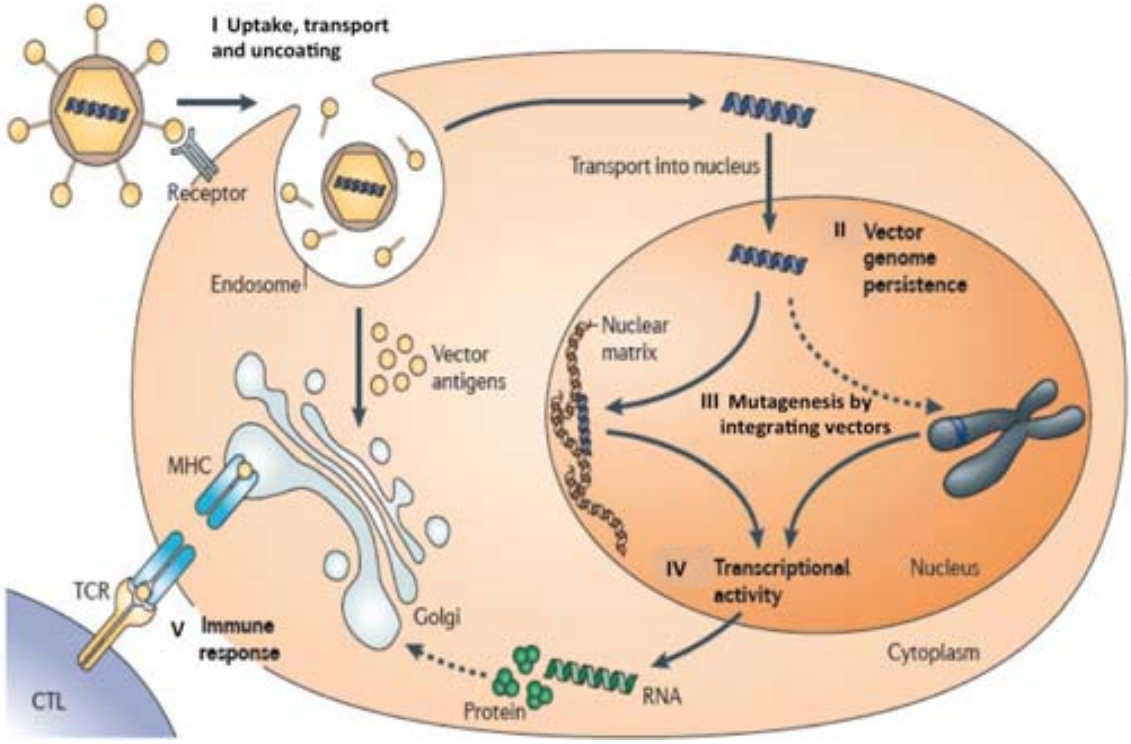

Figure 1.2. Main barriers to successful gene therapy. I) Uptake, transport and uncoating. Once internalized, most vectors enter the endosome and undergo a complex set of reactions that can result in their degradation. Viruses have evolved mechanisms for escaping the endosome as, for example, the endosome lysis. II) Vector genome persistence. Depending on the vector, the DNA can exist as an episome or it can be integrated into the chromosome. III) Mutagenesis by integrating vectors. These vectors may cause mutations by covalent attachment to the chromosome. IV) Transcriptional activity. V) Immune response, which may limit the viability of the transduced cells and therefore, the expression of the transgene product. Adapted from (Kay, 2011).

Unfortunately, even though much effort is taken in developing new vectors, a vector that perfectly address these barriers has not been described yet. Besides, different properties are needed depending on the tissue that vectors are intended to target (i.e. if they target quiescent cells or not). At present, it is considered that there is not yet an ideal vector that allows its application for all types of genetic diseases. For this reason, every vector is specifically designed for the treatment of a particular disease (Porteus *et al.*, 2006).

Gene therapy administration methods can be divided into 2 groups:

- *Ex vivo* gene therapy.
- *In vivo* gene therapy.

Ex vivo gene therapy is a technique consisting of the extraction of the patient's cells to be treated and in their further transduction and selection *in vitro* (Figure 1.3). Then, they are expanded *in vitro* and are finally introduced in the patient. The main advantages of *ex vivo* gene therapy are the high transduction level of the target cells, the minimization of immunogenic responses, and the specificity, which avoids a potential harmful effect of the vector and its therapeutic genes on the rest of the cells. However, the complexity of these protocols, altogether with the reduced number of cell types capable of being maintained *in vitro* after extraction are the main disadvantages of these strategies. The vectors used in *ex vivo* gene therapy are usually integrative, like Moloney murine leukemia viruses and lentiviruses. However, if a transient expression of the transgene is required, non-integrative vectors like adenoviruses or adeno-associated viruses can also be used. Noteworthy, *ex vivo* gene therapy shows great potential for the regeneration of different organs or tissues, like the corneal endothelium (Kampik, *et al.*, 2012), or as a good alternative to treat hematologic and immunodeficiency disorders, when combined with the use of hematopoietic stem cells (Watts *et al.*, 2011). Recently, *ex vivo* gene therapy has been applied to inactivate the HIV *CCR5* gene expression, which encodes for a receptor essential for the entry of the virus into the T lymphocytes. Thus, an adenovirus expressing a zinc finger nuclease capable to inactivate the *CCR5* gene was used in T lymphocytes or $CD34^+$ cells that were subsequently transplanted back to the patients (Cannon *et al.*, 2011).

In vivo gene therapy is based on the direct transduction of the target cells directly in the patient without any cell extraction. The advantage of *in vivo* gene therapy over *ex vivo* gene therapy is the simplicity of the method and the possibility to apply it to any tissue. However, *in vivo* gene therapy has a lower control level over the transfection process when compared to *ex vivo* gene therapy, and transduction efficiency is lower. Furthermore, it is difficult to achieve high levels of tissue specificity and there is an elevated risk of causing toxic effects produced by the direct exposure of the vectors to the organism, thus impairing the results of the therapy.

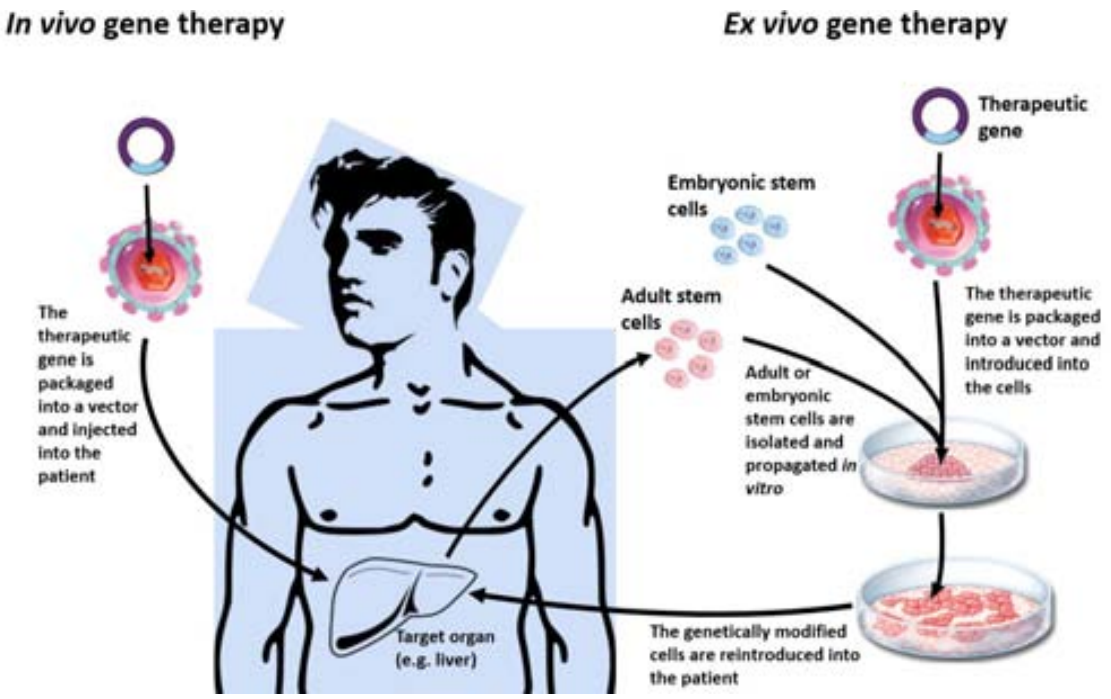

Figure 1.3. Strategies for Delivering Therapeutic Transgenes into Patients. In the *in vivo* approach to gene therapy, a therapeutic nucleic acid is packaged in to a vector (viral or non-viral) and then inserted directly into the patient. In this figure, the gene is cloned in an adenoviral genome and delivered to liver via a catheter in portal vein. The *ex vivo* approach involves harvesting adult stem cells from tissue of interest, transducing them with a gene *in vitro* , and again administering the genetically altered cells to the patient. Alternatively, embryonic stem cells can also be genetically modified and introduced to the patient.

Currently, two types of vectors are available (viral vectors and non-viral vectors). Their success will depend on their specificity for the target cells, their efficiency of transduction and their biosafety.

1.1.2.1. Non-viral vectors

Non-viral gene therapy is based on the ability to efficiently transfer genes into cells by using complexes of DNA with cationic liposomes or cationic polymers, together with the use of chemical and physical methods.

Cationic liposomes and cationic polymers complexes bound to DNA are easier to produce and have a better safety profile than viral vectors, are generally very low-immunogenic, do not have limitations regarding the length of the nucleic acid, can be targeted to specific cells and tissues and have the ability to be repeatedly administered. However, these complexes are generally too large to go across the vascular endothelial layers and, even if they enter into the cells, most end up degraded in endosomal complexes. Therefore, the greatest limitation of these vectors is the reduced

transduction levels and transgene expression compared with their viral counterparts as, in contrast of the long-last expression of proviral episomal genomes, the episomal plasmid expression does not last for long periods after entering into the nucleus (Lam *et al.*, 2010).

Non-viral gene delivery using physical transference methods is based on the use of a physical force to overcome the membrane barrier of the cells. There are many physical methods available (Table 1.1). These include electroporation, consisting of the application of an electric field that increases the permeability of the plasma membrane of the cells; the hydrodynamic system, where the high pressure originated from intravenous injection allow the injected DNA to enter the tissues; or the bioballistic method (also known as gene gun), capable of ejecting gold particles carrying plasmid DNA to introduce them into the cell nucleus (Chen *et al.*, 2002). The main advantage of these delivery systems is the simplicity in which the transgene and the regulatory elements for its expression can be directly delivered into cells without involving any substances that could be cytotoxic or immunogenic as commonly seen in viral vectors and, occasionally, on other non-viral vectors. Despite these advantages, the application of these methods is limited by their low transfection efficiency and the tissue damage that their aggressive nature may cause.

Method	Critical features for gene delivery	Advantages	Limitations
Cationic liposomes and polymers	Cationic charge	High efficiency *in vitro* Easy to produce	Low efficiency *in vivo.* May be toxic to cells or cause immune reaction.
Gene gun	Electric pulse	Good efficiency	Gene transfer limited to targeted area Needs surgical procedure for internal organs
Electroporation	Ultrasound	Site specific	Tissue damage Gene transfer limited to targeted area Needs surgical procedure for internal organs
Hydrodynamic delivery	Hydrodynamic pressure	Simplicity High efficiency Site specific	Needs catheter insertion in large animals

Table 1.1. Main characteristics of the most used non-viral vectors.

1.1.2.2. Viral vectors

Millions of years of evolution have placed viruses in favorable position of being the most effective vectors for introducing nucleic acids into the host cells, as they have developed efficient strategies to circumvent cellular barriers to ensure an effective infection. In contraposition to non-viral gene therapy, viral vectors have a specific tropism for different cell types, generally leading to a higher and longer transgene expression. However, these vectors have some drawbacks, like the high immune response they may elicit, the high costs of their production, biosafety issues and in some cases their challenging production at large scale.

There is a wide range of viral vectors available. Among the most used are found Moloney murine leukemia viruses (MMLV), lentiviruses, adeno-associated viruses (AAV), adenoviruses (Ad) and herpes simplex (HSV-1) viruses (Table 1.2). Each of these viruses have different properties that makes them appropriate for certain applications but not for others (Kay *et al.*, 2001). Viral vectors can be classified into two large groups depending on the capacity of their genome to integrate into the cellular genome (MMLV and lentiviruses) or their ability to persist in the cell nucleus primarily as an episome (AAV, Ad and HSV-1), even though the integration into the host genome cannot be completely discarded in any vector (Stephen *et al.*, 2008).

In this regard, the integration capacity of MMLV into host DNA has been used to treat genetic diseases that require permanent modification of cells, using the ability of these vectors to integrate in the host genome. Unfortunately, the integration of these vectors arises major safety concerns, as they have the risk of mutagenesis by insertion into the host genome, and the retroviral long terminal repeats (LTRs) of these vectors can activate neighboring genes, which could lead to oncogenesis. Because of these concerns, as well as the fact that they are unable to transfect non-dividing cells, gene therapy is moving towards the use of other vectors.

Another family of retroviruses, known as lentiviral vectors, and especially those derived from human immunodeficiency virus (HIV), target a wide variety of cells including quiescent and difficult-to-transduce cells such as hematopoietic precursors, neurons, lymphoid cells and macrophages, among others (Dropulić *et al.*, 2011; Kay *et al*., 2001).

Moreover, these vectors appear to have a safer profile than MMLV, as they have a), a lower risk of insertional mutagenesis and oncogenicity because of its tendency to integrate far from cellular promoters (Ciuffi, 2008) and b), the absence of a robust enhancer on their LTRs.

Among non-integrative vectors, AAV have been widely used as they efficiently transduce a wide range of quiescent and dividing cells including hepatocytes, muscle cells and cells of the peripheral and central nervous system, feature a low cellular immune response and have very low risk of insertional mutagenesis. Despite its attractive characteristics, AAV are limited by their low cloning capacity, which is unsuitable for most therapeutic genes, and for the slow expression of their transgenes, as the single-stranded AAV DNA genome has to be converted into double-stranded DNA before the transgene can be expressed (Coura *et al.*, 2010).

First-generation adenoviruses (FGAd) have a high transduction efficiency and the advantage over AAV that they have a large cloning capacity and they are easier to produce. However, these vectors elicit a cellular and humoral host immune response, leading to a transient expression of the transgene. The last generation of these vectors, known as helper-dependent adenoviruses (HDAd), while maintaining the high transduction efficiency of FGAd, improve its characteristics by the elimination of the viral genes, thus avoiding the cellular immune response against the vector. Also, the lack of viral genes allow an even higher cloning capacity in these vectors (up to 36kb), which makes them especially useful when the insertion of large genes, combinations of genes or regulatory elements is required.

Finally, HSV-1 are attractive for their extremely large cloning capacity (up to 150 kb) and the low cellular immune response they elicit, which allows a sustained transgene expression. The main limitations of these vectors are the transient expression, the generally low transduction efficiency and the latent wild-type viral activation risk.

Vector	Genetic material	Cloning capacity	Advantages	Limitations
First-generation adenovirus	Double-stranded DNA	8-10 kb	Transduces quiescent and dividing cells High efficiency of transduction Easy to produce in high titers	Transient expression Cellular and humoral host immune response
Helper-dependent adenovirus	Double-stranded DNA	~36 kb	Transduces quiescent and dividing cells High efficiency of transduction High cloning capacity No expression of viral proteins Essentially no integration	Transient expression Humoral host immune response to certain serotypes
Adeno-associated virus	Single-stranded DNA	4-5 kb	Transduces quiescent and dividing cells Sustained gene expression Low cellular host immune response Broad tropism	Insertional mutagenesis may be a problem Very low cloning capacity
Herpes simplex virus	Double-stranded DNA	~30 kb	Low cellular host immune response High cloning capacity Non-integrative	Transient expression Low transduction efficiency Latent wild-type viral activation risk
Moloney murine leukemia virus	Single-stranded RNA	8 kb	Highly effective for dividing cells High efficiency of transduction	Insertional mutagenesis Unable to transduce quiescent cells Inactivation by serum Low titter
Lentivirus	Single-stranded RNA	8 kb	Highly effective for dividing and non-dividing cells High efficiency of transduction Low cellular host immune response	Insertional mutagenesis Potential risk of recombination of pathogenic vector (HIV)

Table 1.2. Main characteristics of the most used viral vectors.

1.1.3. Gene therapy clinical assays

The first human gene transfer clinical trial was performed in 1990, when two children were treated for a form of severe combined immunodeficiency (ADA^- SCID). Transduction of their purified T cells using a retroviral vector encoding for the adenosine deaminase gene (*ADA*) allowed a temporary restoration of their immune system (Blaese *et al.*, 1995). After this successful event, expectations arose to a point where the predictions by then were that gene therapy would become a treatment for numerous diseases in just a matter of years.

However, during the following two decades, many obstacles like the ones mentioned previously (regarding vector uptake, transport and uncoating, sustained transcriptional expression, vector genome persistence, the host immune response and the mutagenesis

by integrative vectors) tempered the enthusiasm for gene therapy. Also, the translation of preclinical results into humans has been another issue to overcome, as many successful cures to treat animal models like mice or larger animals failed in the human context, suggesting notable differences in host-vector interaction among different species and leading to prudence from the scientific community when it comes to analyze preclinical results. Despite this, the gained experience from failures altogether with the development of better and safer vectors has allowed the overcome of most of these technical barriers, to the point where nowadays there are successful examples of treating specific diseases, as well as encouraging preclinical trials that will hopefully be successful in the clinic.

Since the first clinical trial, many others have been performed, involving infectious diseases, Mendelian genetic diseases, complex common diseases and cancer. Among these, the great majority are phase I clinical trials (59%), followed by phase I/II and II clinical trials (26%), with a lower number of phase II/III, III or IV clinical trials (<5%) (Figure 1.4).

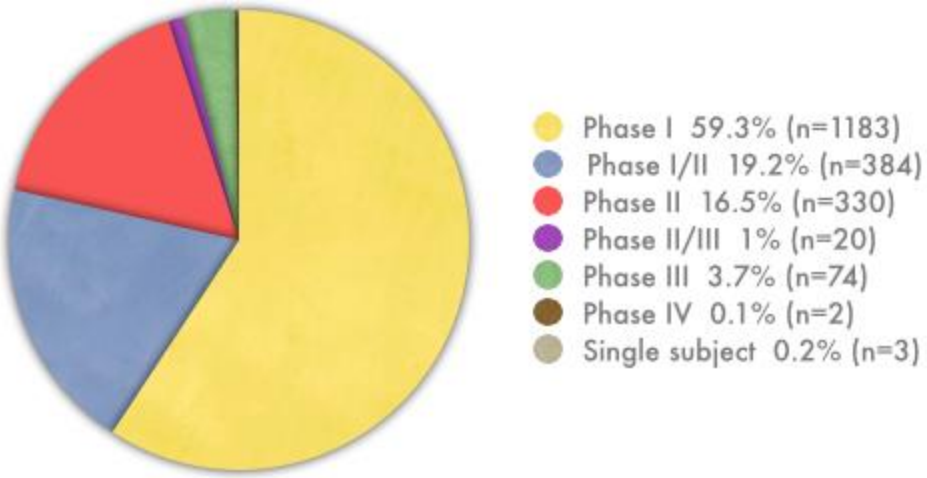

Figure 1.4. Phases of gene therapy clinical trials. From (http://www.abedia.com/wiley).

The first successful, long-last gene therapy treatment occurred in 2000 when autologous transplantation of transduced bone marrow cells using MMLV expressing the interleukin-2 receptor gamma (*IL2RG*) resulted in the restoration of the immune system in children with X-linked severe combined immune deficiency (X-SCID). Unfortunately, 5 out of the 20 patients developed leukemia due to the integration of the vector genome, which caused the overexpression of the *LMO2* proto-oncogene that is frequently

overexpressed in T-cell leukemia (Hacein-Bey-Abina *et al*., 2008). It is believed that the risk of leukemia using MMLV is transgene-specific, as when this vector encoding the *ADA* gene was used in clinical trials no cases of leukemia were described (Kohn *et al*., 2010). In contrast, when the growth-promoting *IL2RG* transgene was encoded a clonal expansion of oncogenic cells was caused, possibly due to a synergistic effect of this gene with the *LMO2* proto-oncogene. Moreover, it is considered that the LTRs of these vectors can activate neighboring genes, thus inducing oncogenesis. In this regard, the use of MMLV with self-inactivating LTRs may improve the biosafety of these vectors.

Lentiviral vectors have been used to treat different pathologies, like the X-linked adrenoleukodystrophy (X-ALD), where the progression of the neurodegeneration was halted after the administration of autologous CD34· hematopoietic cells transduced with a lentiviral vector expressing the *ABCD1* cassette (Cartier *et al*., 2009). Also, lentiviruses encoding for a β-globin cDNA have been successfully used to reverse the transfusion dependency in a patient with β-thalassemia-based anemia (Cavazzana-Calvo *et al*., 2010). Unlike MMLV, lentiviruses are able to transduce quiescent cells while maintaining the capability to integrate into the host genome. For this reason, the safety profile of these vectors is not totally predictable.

Adenoassociated vectors have been used in retina to treat patients with Leber´s congenital amaurosis, leading to an improvement in vision parameters in some patients (Simonelli *et al*., 2010). Also, because AAV efficiently transduce skeletal and cardiac muscle, they have been used with interesting results for treating heart failure (Hajjar *et al*., 2008; Zsebo *et al*., 2014), and muscular dystrophies (Bowles *et al*., 2012). These vectors have been also systemically administered for liver-based treatment of factor IX deficiency, resulting in a moderate increase of factor IX expression levels (up to 11% of normal levels) (Nathwani *et al*., 2011). Finally, this vectors have been used in the CNS to target neurodegenerative diseases like Parkinson´s disease (Muramatsu *et al*., 2010; Eberling *et al*., 2008) and, more recently, mucopolysaccharidosis type IIIA (Tardieu *et al*., 2014). Results of these assays showed different results depending on the development stage of the disease, indicating the importance of early treatment.

Among the viral vectors, adenoviruses are the most used in clinical trials in humans (23%) (Figure 1.5). This can be explained by the following factors: they can infect a large number of cell types (both in quiescent cells as division), modern production techniques allow the modification of its capsid and thus its cell tropism, and they are easy to produce at high levels of up to 10^{13} IU/ml (Palmer *et al.*, 2003). Also, adenoviruses are generally not integrative, which avoids insertional mutagenesis. However, these vectors have also some disadvantages, like the induction of a high dose-dependent immune response, both humoral, preventing possible future repeated administrations, and cellular, mediated by T lymphocytes.

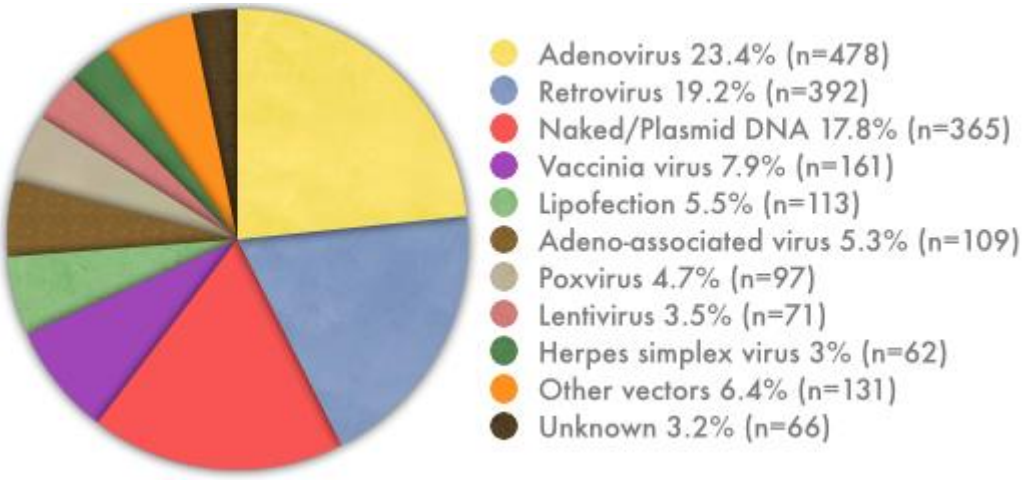

Figure 1.5. Vectors used in gene therapy clinical trials. From (http://www.abedia.com/wiley).

Adenoviral vectors reached an unwanted popularity in September 1999 when a second generation adenovirus, caused the first death related to gene therapy in a patient suffering from ornithine transcarbamylase deficiency. Eighteen hours after the administration of the vector via hepatic artery injection the patient developed a strong systemic inflammatory response, disseminated intravascular coagulation and multiple organ failure that led to his death several hours later. It is believed that this fatal outcome was due to the high dose of the vector ($6{\cdot}10^{13}$ vp), the highly immunogenic nature of adenovirus, and the poor condition of the patient (Raper *et al*., 2003).

Despite this episode that lowered the widespread application of gene therapy clinical trials and indicated the need for further research to improve biosafety, adenoviral vectors have been successful in animal models for many diseases, like type 1 (Li *et al.*, 2012) and type 2 diabetes (Samson *et al*., 2008), Pompe disease (Kiang *et al*., 2006),

Crigler-Najjar syndrome (Dimmock *et al*., 2011) and brain tumors (Puntel *et al*. 2010), among others.

1.2. ADENOVIRUSES

The first human Ad was isolated in 1953 from human glands and tonsils adenoids (Rowe *et al.*, 1953). The adenovirus group was accepted in 1956 by the International Committee of Viral Taxonomy where they were classified in the family of Adenoviridae (Enders *et al.*, 1956), consisting of two genera: Mastadenovirus and Aviadenovirus.

Adenoviruses are associated with mild, self-limiting diseases of the upper respiratory tract and gastroenteritis but can also cause severe conjunctivitis and pharyngitis. However, most infections are asymptomatic in immunocompetent individuals (Jozkowicz *et al.*, 2005; Hong *et al.*, 1997; Tomko *et al.*, 1997). It is important to mention that in opposition of other viruses, adenovirus has not been associated with any neoplastic disease in humans (Benihoud *et al.*, 1999). More than 100 different species of adenoviruses have been identified from mammals, birds and reptiles, all maintaining a similar architectural structure and chemical composition. More than 50 serotypes of human adenovirus serotypes have been described and classified into 7 subgroups (A-G) depending on their ability to hemoagglutinate red blood cells (Aoki *et al.*, 2011; Seto *et al.*, 2011). Among them, Ad5 and Ad2 are the most studied, both belonging to the subgroup C, and are commonly used for gene therapy (Russell *et al.*, 2000).

Species	Serotype	Infection	Primary receptor
A	12, 18, 31	Intestine	CAR
	16, 21, 50	Respiratory tract, eye	CD46
	11, 34, 35	Respiratory and/or urinary tract, eye	CD46
	3, 7, 11, 14	Respiratory and/or urinary tract, eye	DSG-2
C	1, 2, 5, 6	Respiratory tract	CAR
D	8-10, 13, 15, 17, 19, 20, 22-30, 32, 33, 36, 38, 39, 42-49, 51	Eye, intestine	CAR
	8, 19, 37	Eye	Sialic acid, GD1a
E	4	Respiratory tract, eye	CAR
F	40, 41	Intestine	CAR
G	52	Intestine	-

Table 1.3. Classification of the 52 Adenovirus serotypes based on receptor usage and tissue tropism. From (Cupelli *et al.*, 2011).

The Ad has been studied for several decades as a biomedical application. In the mid-twentieth century it was widely used in the armed forces of the United States as a vaccine against respiratory diseases. Within this field, conducted studies allowed further knowledge of the immune response against Ad and its adverse effects.

1.2.1. Adenovirus biology

Adenoviruses are non-enveloped viruses, sized between 70 and 100nm (Fabry *et al.*, 2005) with a very condensed double-stranded linear DNA (Akusjarvi *et al.*, 1984) covered by a proteic icosahedral capsid without envelope (Figure 1.6). The capsid consists of 3 major proteins: the hexon proteins, the penton proteins and the fiber proteins (Ginsberg *et al.*, 1966). The hexon proteins, distributed in trimmers, are the majority of the capsid (720 copies). Each penton protein (240 copies), which is located at the vertex of the capsid, has a *fiber* protein bound. These fiber proteins consists of 3 main elements: the N-terminal tail, which is bound to the penton base, the shaft, with repetitive motifs of 15 residues approximately (Rux *et al.*, 2004) and the C-terminal knob, which binds to the cellular receptor and promotes the internalization of the viral protein.

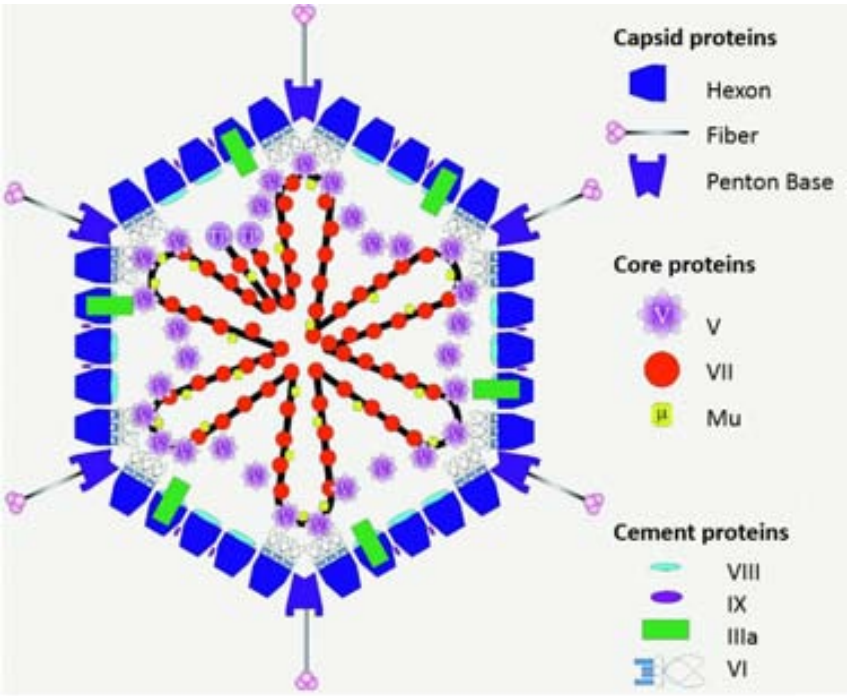

Figure 1.6. Structure of adenovirus. The locations of the capsid and cement components are reasonably well defined. In contrast, the disposition of the core components and the virus DNA is largely conjectural. Adapted from (Russell *et al.,* 2000).

Adenoviruses also are also composed of minor proteins that have the function of accommodating and stabilizing the genome in the capsid (Vellinga *et al.*, 2005). The structural proteins of the virion are designated from the protein II to the XII depending on the molecular weight that they present on a SDS-PAGE polyacrylamide gel (Van Oostrum *et al.*, 1985). IIIa, VI, VIII and IX proteins are associated with the hexon proteins, while V, VII, mu (X), XI and XII proteins bind the viral genome to the capsid (Rux *et al.*, 2004).

Besides structural proteins, adenoviruses also have non-structural proteins for the development of the different phases of their viral cycle. These phases include the endosomal escape of the virus by the adenoviral protease (Leopold *et al.*, 2007), the liberation of the adenoviral genome from the capsid, the replication of the viral DNA by the TP, DBP and AdPol proteins, and the packaging of the viral genome by IVa2 and L155K proteins, among others (Zhang *et al.*, 2000; Ostapchuk *et al.*, 2005).

1.2.2. The adenoviral genome

The adenoviral genome contains approximately 36 Kb of double stranded DNA, flanked by two ITR (inverted terminal repeats) ranging 103 and 165 bp (Shinagawa *et al.*, 1987). The packaging signal (Ψ) is about 200 nucleotides of the 5 'end, and it is essential for the encapsidation of the viral genome into the capsid through its interaction with several cellular and viral proteins. The genome is divided into two set of genes: the early genes (*E1A*, *E1B*, *E2*, *E3* and *E4*), which are transcribed early in cell cycle before viral DNA replication, and late genes (*L1*, *L2*, *L3*, *L4* and *L5*), which are transcribed after the initiation of DNA replication (Figure 1.7).

The *E1A* transcription unit encodes two major E1A proteins with an important role in activating the transcription of the virus and the induction of the host cell to enter an S phase-like state. The two major E1B proteins are involved in the stimulation of the viral mRNA transport, blocking both E1A-induced apoptosis and host mRNA transport. The *E2* region is divided in two sub-regions: the *E2A* encoding the DNA-binding protein, and the *E2B* that encodes the viral DNA-polymerase. The *E3* region encodes at least seven immunomodulatory proteins specifically involved in host immune evasion. The *E4* region encodes at least six proteins involved in the nuclear exportation of mRNA, the transcriptional and transductional regulation, enhancement of the late gene expression, and decrease host protein synthesis.

Alternative splicing of a single transcript, referred to as late region genes, gives rise to all the mRNA encoding virion structural proteins. The expression of late region genes is regulated by the common major late promoter (MLP).

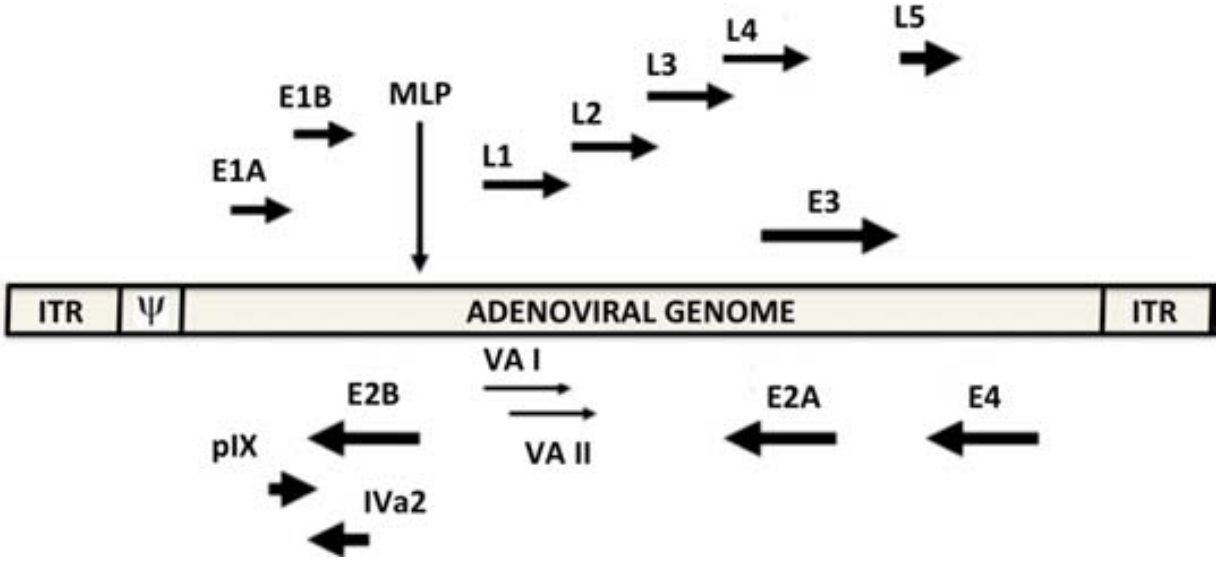

Figure 1.7. Transcription map of human adenovirus serotype 5. The Ad5 genome (~36 kb) is divided into four early region transcription units (*E1–E4*), five families of late mRNA (*L1–L5*), which are alternative splice products of a common late transcript expressed from the major late promoter (MLP) and four smaller transcripts (*pIX*, *IVa*, and *VA* RNA's *I* and *II*). The inverted terminal repeats (ITRs) are located at the termini of the genome and are involved in viral DNA replication, and the packaging signal (Ψ) at 5' is involved in packaging of the genome into virion capsids. Adapted from (Vetrini *et al.,* 2010).

1.2.3. Adenovirus cell entry

Adenovirus has a strictly regulated infection cycle where multiple viral and cellular proteins interact to complete the viral replication program to generate infectious virus particles. Initiation of infection by serotype 5 adenovirus is dependent on the binding of the adenovirus fiber knob protein with the Coxsackievirus and Adenovirus receptor (CAR) expressed on the target cells. Even though these viruses use CAR as their primary attachment receptor, they can also use heparan sulfate proteoglycans for the internalization of the virus to the cell, MHC-I and VCAM-I (Bergelson *et al.*, 1997; Hong *et al.*, 1997; Dechecchi *et al.*, 2001). Also, recent studies indicate that the cell attachment during systemic infection may rely on the association of soluble serum cofactors with the capsid (Shayakhmetov *et al.*, 2005; Parker *et al.*, 2006; Alba *et al.*, 2009). Nevertheless, other authors indicate in more recent studies that the ability of FX to enhance Ad5 liver transduction is caused by the ability of FX to protect Ad5 from neutralization by the classical complement pathway (Xu *et al.*, 2013).

After the attachment of the serotype 5 adenovirus to the cell receptors, a subsequent interaction between the arginine-glycine-aspartic acid (RGD) motif present on the virion penton base and $\alpha_v\beta_3$ or $\alpha_v\beta_5$ integrins of the host cells leads to clathrin-mediated endocytosis (Meier *et al.*, 2004; Smith *et al.*, 2010). Then, Ad5 traffics to early endosomal compartments prior to endosomal escape (Gastaldelli *et al.*, 2008). Within the endosome, the adenovirus capsid partially disassembles upon acidification (Figure 1.8). This process leads to the release of protein VI (pVI), an internal capsid protein with the hability to rupture endosomal membranes, allowing the partially disassembled virion to enter the cytoplasm (Wiethoff *et al.*, 2005; Maier *et al.*, 2010; Moyer *et al.*, 2011). After the endosomal escape, Ad5 traffics through the cell along the microtubule network (Suomalainen *et al.*, 1999) and reach the nucleus, docking at the nuclear pore and delivering the Ad5 genome to the nucleus (Chardonnet *et al.*, 1970).

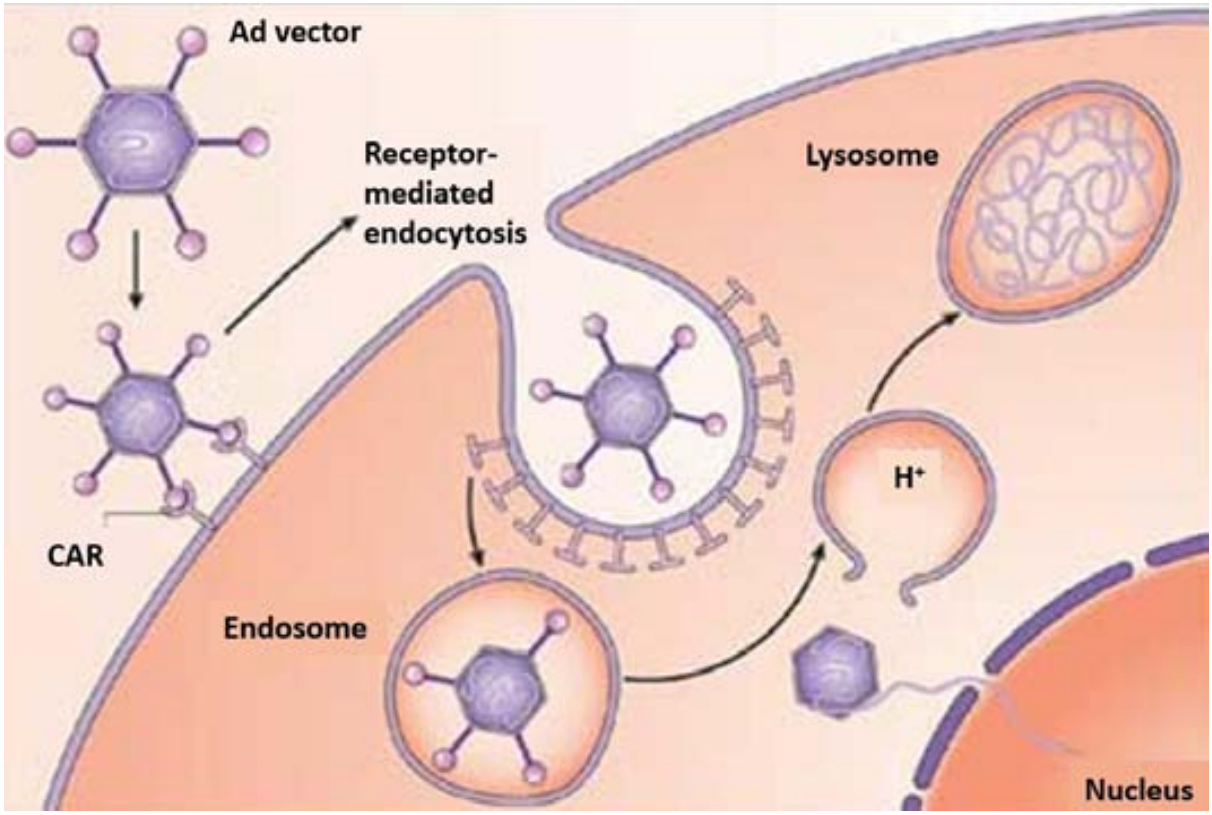

Figure 1.8. Adenovirus cell entry, escape from the endosome and nuclear internalization. Adenovirus virions bind to the coxsackie adenovirus receptor (CAR) and integrins on the plasma membrane, and enter the cell by receptor-mediated endocytosis. As the endosome acidifies (H^+), the capsid is broken down and released from the endosome. Then, double-stranded viral DNA is released from the degraded capsid, traffics through the cell by the microtubule network and finally enters the nucleus through the nuclear pore. Adapted from (Davidson and Breakefield, 2003).

It has been suggested that the major capsid protein, hexon (Smith *et al.*, 2008; Bremner *et al.*, 2009), and pVI (Wodrich *et al.*, 2010) influences microtubule-dependent trafficking of adenovirus virions in the cytoplasm. Other proteins, like nuclear filament protein Nup214, hsc70 and histone H1 are implicated in nuclear import of the viral DNA (Saphire *et al.*, 2000; Trotman *et al.*, 2001; Strunze *et al.*, 2011). It is important to mention that serotype 5 adenovirus entry to the cell and its posterior trafficking is a complex subject that constantly generates new data. In this regard, recent investigations suggest that ubiquitination of viral and host proteins has an important role by influencing a variety of processes such as cell entry (Wodrich *et al.*, 2010), trafficking, and posterior viral replication (Harada *et al.*, 2002; Blackford *et al.*, 2010).

1.2.4. Adenovirus packaging

Packaging of the adenoviral genome is a complex process where different viral proteins interact with the packaging signal of the virus (Ψ) to encapsidate the viral genome in a polar process to form a mature viral particle (Ostapchuk *et al.*, 2005). The packaging process begins with the formation of the procapsid and recognition of the procapsid by viral DNA. It has been widely demonstrated that the packaging domain, located between 200 and 400 nucleotides after the 5' end of the viral genome, is essential for the encapsidation of viral DNA (Hearing *et al.*, 1987). More specifically, this domain is located between 198 and 358 nucleotides of the Ad5 genome (Hearing *et al.*, 1987), and consists of a series of repeated sequences, 7 in Ad5, termed A- repeats. These regions have a characteristic motif: 5'-TTTGN_8CG-3', which is conserved among the different serotypes of Ad (Weiss *et al.*, 1997; Grable *et al.*, 1990). Among the A-repeats, the most important for Ad5 are A1, A2, A5 and A6 (Grable *et al.*, 1990). It has been demonstrated that each A-repeat is independent of the others. Because of this, Ad genomes with different artificial packaging signals have been generated including existing A-repeats, with comparable packaging efficiency as the wild type packaging signal (Schmid *et al.*, 1998). Interestingly, the packaging domain can be located at either end of the viral genome, as genomes with packaging domains at both ends are viable (Hearing *et al.*, 1983). The distance of Ψ from the 5' or 3' ends of the genome is crucial for optimal packaging activity, although some flexibility in its location is tolerated. Concerning this, when the distance between the ITR and Ψ is 655 nucleotides or more, virus viability is severely compromised,

but when the distance between the ITR and Ψ is increased only up to 271 nucleotides, fully viable viruses are produced (Hearing *et al.*, 1987).

As far as 12 viral proteins that intervene with the packaging process have been described, including IVa2, L1 52/55K, L4 100K, L4 33K and L4 22K. Also, in this process, nuclear factors like Oct-1 and COUPTF1 bind to the packaging signal (Shmidt *et al.*, 1998). It has been described that IVa2 protein interacts with the CG sequence of the A-repeat, thus generating a protein complex with the protein L1 52/55K (Gustin *et al*., 1996) in an essential step for the packaging process (Zhang *et al.*, 2001). Once this complex is formed, L4-22K protein interacts with the TTTG motif (Ostapchuk *et al.*, 2006). Of note, it has been demonstrated that the L1 52/55K protein interacts *in* vivo with the packaging signal in absence of the IVa2 protein, suggesting that L4-22K protein could recruit L1 52/55K protein in the packaging process (Perez-Romero *et al.*, 2005; Christensen *et al.*, 2012). The binding of all these proteins to the packaging signal forms a protein complex that guides the adenoviral genome to one of the vertices of the viral capsid, where the packaging initiates (Figure 1.9).

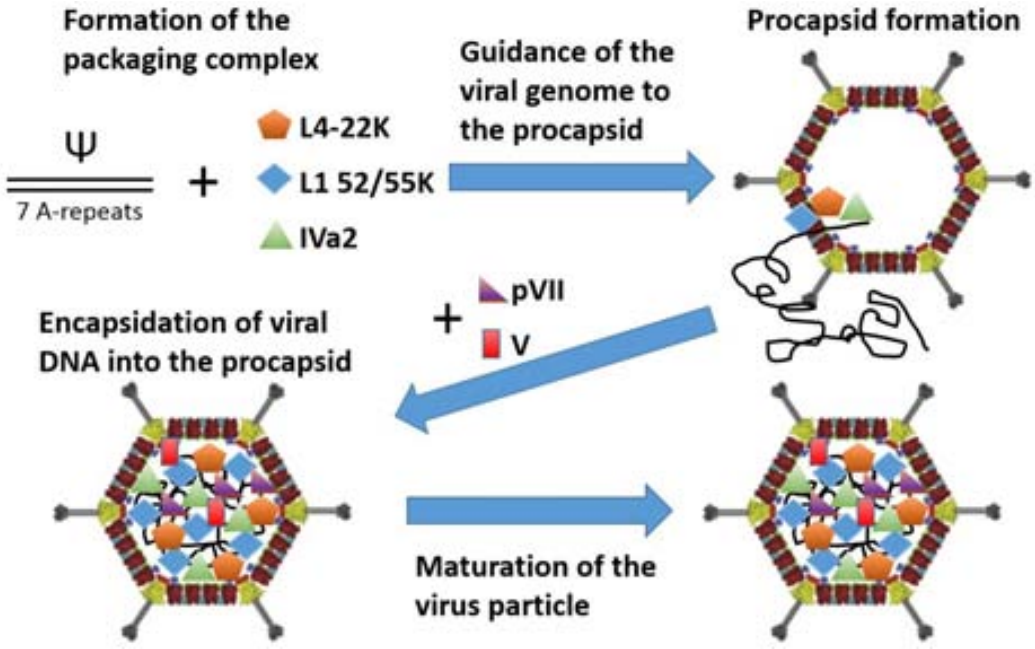

Figure 1.9. Classical model for packaging/assembly of adenovirus. The packaging process is initiated by the formation of the packaging complex with the binding of L4-22K, L1 52/55K and Iva2 to Ψ. Then, the packaging complex is guided to the procapsid, allowing its formation. Consecutively, viral DNA is encapsidated into the procapsid. Protein V and protein pVII are found in these particles containing full-length DNA. This process is completed by the maturation of the virus particle, with a density of 1.35 g/cm^3.

Even though most authors support this classical packaging theory, it is important to mention that other studies suggest another mechanism by which the packaging complex is formed (Alba *et al*., 2011). In this modified theory the packaging complex on the viral DNA would act as an initiator of the formation of a procapsid/DNA assemblage, a process that would be followed by the incorporation of the DNA into the procapsid.

During the Ad assembly process, the density of the viral particle varies from 1.29 to 1.35 g/cm^3. This appears to reflect the insertion of viral DNA into an empty capsid, as well as virion maturation during the packaging process (Ostapchuk *et al.*, 2005).

1.2.5. Adenovirus maturation

Once the adenoviral genome is inserted into the viral capsid, the DNA has to be efficiently accommodated and condensed, binding to different proteins that attach it. To become an infectious particle, the immature adenoviral particle uses an Ad-synthesized protease, called adenain, which is transported into the capsid and mediates the final steps of mature particle formation via the cleavage of a number of virion proteins including pIIIa, pVI, pVII, pVIII, pTP, X and L1-52/55K (Weber *et al.*, 2003). This adenoviral protease, which is encoded by the *L3* gene and has a weight of 23 KDa, is synthesized as an immature form to be later activated by cofactors. It has also been described that this protein not only acts at the latter phases of the viral cycle but can also be important in other stages of the viral cycle. In this regard, it has been published that adenain digests cytokeratin 18, leading to a reorganization of the cellular cytoskeleton, debilitating the cell and leading to the liberation of the virion by cell lysis. Another protein involved in the latter phases of the viral cycle is the adenovirus death protein (ADP), also known as E3-11.6K protein. This protein is required for the cellular lysis and the subsequent liberation of the viral particles to the exterior of the cell. It has been described that *ADP* mutant adenovirus (Ad*ADP*$^-$) remains in the cell nucleus and cannot efficiently exit the cell.

When an adenovirus is amplified and centrifuged in a CsCl or saccharose gradient, different bands can be found in an established order, which correlate with different maturation and packaging stages. The less dense or lighter bands correspond to the empty capsids and is located in the superior fragment of the CsCl gradient. These particles contain all the major

capsid proteins, as well as the proteins that bind to the viral genome. This pre-viral band has a density in CsCl gradient of 1.285g/cm^3, and includes hexons, pentons and IX proteins assembled with 100K, pVIII and pVII proteins, which are hypothesized to be the first steps of the formation of the icosahedrical structure of the capsid. This band is known as light particle, but some authors may also include IIIa, 50K, 39K, 28K and pVI proteins as well as part of the viral genome, which would place these particles in a CsCl gradient density ranging between 1.295 g/cm^3 and 1.315g/cm^3.

In the following maturation step, heavy intermediates are produced, and the 100K, 39K and 28K proteins are not present. In addition, the viral genome enters into the capsid together with the V and VII proteins, reaching a CsCl gradient density of 1.37g/cm^3. Next, the viral protease digests VI, VII and VIII proteins, converting them to pVI, pVII and pVIII polypeptides and thus transforming the heavy intermediate to a young viral particle, with a CsCl gradient density ranging between 1.34 g/cm^3 and 1.35g/cm^3. When all the VI, VII, VIII and X precursors and pTP (DNA-Terminal Protein) are completely digested and the 50K protein is exchanged for the V protein the mature particle is generated, with a CsCl gradient density of 1.345 g/cm^3.

1.3. ADENOVIRAL VECTORS

1.3.1. First-generation adenoviruses

Adenoviruses are only associated with mild, self-limiting diseases (Horwitz *et al.*, 1990). However, to avoid propagation and possible adverse effects when used in gene therapy, adenoviral vectors must be replication deficient. To this end, first-generation adenoviruses (FGAd) were generated. The first FGAd contained the whole viral genome with the exception of the *E1* region, which encodes proteins necessary for the expression of the other early and late genes, leading to the replication of the viral genome. Of note, the deletion of the *E1* region allowed the cloning of up to 5.1Kb transgene in the viral genome without impairing the vector productivity and stability (Bett *et al.*, 1993). Later, other first-generation adenovirus were generated, lacking the *E1* region and also the *E3* region to increase biosafety and provide more space for transgene expression cassettes. The *E3* region is not essential for viral replication *in vitro* as it encodes products that counteract host defense mechanisms, so its presence in the producer cells was not necessary (Wold, 1993). *E1-E3* deleted FGAds allow the entry of a therapeutic gene of up to 8.2Kb.

In order to produce first-generation adenoviruses, these vectors should be amplified in cells that constitutively express the *E1* region *in trans*. The first generated cell line for the production of FGAd vectors was HEK-293 (Graham *et al.*, 1977). This cell line was generated after transformation with a fragment of the adenovirus containing the *E1* region. Even though these cells were very productive, they allowed the recombination between homologous regions of the viral genome and the *E1* region that was inserted to the cellular genome, hence producing viruses with the functional *E1* region and with the capability to replicate (RCA, *replication-competent adenovirus*) (Lochmuller *et al.*, 1994). To avoid the formation of RCA, several cell lines containing a minimum *E1* region with no homology with the viral genome were generated: 911 (Fallaux *et al.*, 1996) N52.E6 (Schiedner *et al.*, 2000) and PER.C6 (Fallaux *et al.*, 1998). However, despite these improvements, *in vivo* residual expression from remaining adenoviral genes triggers a cytotoxic T lymphocyte (CTL) immune response towards infected cells, which finally leads to the elimination of the transduced cells and, therefore, to the loss of transgene expression (Yang *et al.*, 1994).

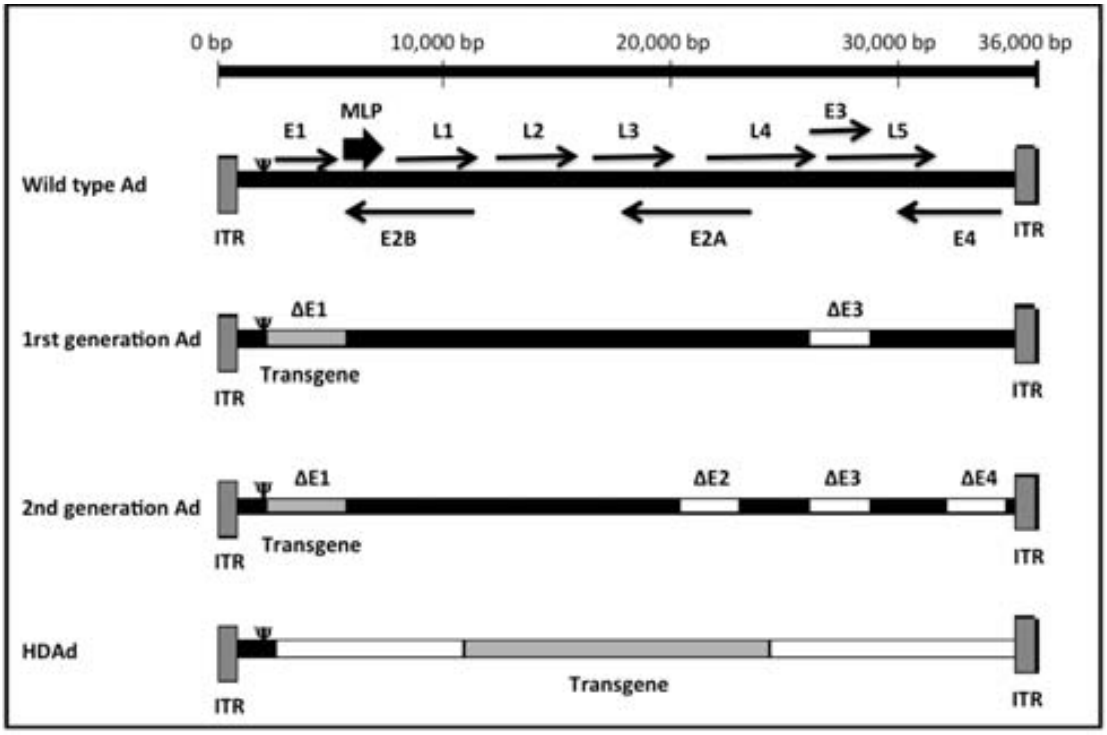

Figure 1.10. Representation of adenovirus serotype 5 genome and the different vector generations. *E1-E4*: early regions. *L1-L5*: late regions. MLP: major late promoter. Ψ: packaging signal. Adapted from (Alba *et al.,* 2005).

1.3.2. Second-generation adenoviruses

In order to reduce the immune response caused by the administration of first-generation adenoviruses and to increase cloning capacity, second-generation adenoviruses were generated. These vectors combine different deletions in early regions (*E2* and/or *E4* plus *E1* or *E1* and *E3*), that reduce residual expression of viral proteins and permit to accommodate up to 14 kb and hence increase the vector cloning capacity (Amalfitano *et al.*, 1998; Armentano *et al.*, 1997) (Figure 1.10). The generation of these vectors led to the creation of new cell lines capable of providing *in trans* the proteins necessary for the replication of the Ad (Zhou *et al.*, 1996; Amalfitano *et al.*, 1996; Wang *et al.*, 1995; Brough *et al.*, 1996). However, these vectors did not improve FGAds, since due to residual gene expression from remaining viral genes they had the same problems in terms of immunogenicity and toxicity (Danthinne *et al.*, 2000).

1.3.3. Third-generation adenoviruses (also known as gutless or helper-dependent adenoviruses)

To finally solve the problems caused by cellular immunogenicity elicited from the viral vector, third-generation adenoviruses, alternatively referred as helper-dependent vectors (HDAd), gutless or high capacity adenovirus were generated. In these vectors only the ITR ends (5' and 3') and the packaging signal of the adenoviral genome (Ψ) are present in the vector, altogether with the therapeutic gene and DNA stuffer necessary to complete the 36kb for the correct packaging of the genome (Parks *et al.*, 1997) (Figure 1.10). These characteristics make HDAds one of the most promising vectors for gene therapy because of their lack of viral genes and their large cloning capacity (up to 36 kb), which makes them more useful than other vectors such as the first-generation adenoviruses (up to 8 kb) (Kochanek *et al*., 1999) or adeno-associated viruses (5 kb cloning capacity) (Grieger *et al*., 2012), especially when the insertion of large genes, combinations of genes or regulatory elements are required. Moreover, in contrast to first-generation adenoviruses (FGAds), the lack of any viral coding region minimizes the cellular immune response, promoting safer and more prolonged transgene expression. Finally, because of its non-integrating nature (Stephen *et al*., 2010), HDAd vectors have a negligible risk of insertional mutagenesis while they still mediate efficient transduction to a wide variety of cell types and organs (e.g. liver, brain, lungs and muscle) and have great potential in biomedical applications (e.g. vaccine development).

1.3.4. Immune response against adenoviruses

Despite the fact that first-generation adenoviral vectors are among the most used in gene therapy, they have a considerable toxicity profile (Raty *et al*., 2008). The immune response against FGAd involve both non-specific innate and adaptive mechanisms and consist of three overlapping phases (Brenner, 1999) (Figure 1.11). The first response, known as acute toxicity, is induced by the adenovirus capsid proteins and therefore is similar for both HDAd and FGAd vectors. It appears within minutes of the administration of the vector and it does not require viral gene expression since psoralen-inactivated UV Ad genomes do not show an attenuated acute toxicity (Dai *et al*., 1995; Seiler *et al*., 2007). Finally, this phase is characterized by an acute production of pro-inflammatory cytokines and chemokines as well as a widespread activation of macrophages, neutrophils and Kupffer cells in the liver (Otake *et al*., 1998).

The intermediate response, that occurs from several hours to one day after vector administration is characterized by side effects such as thrombocytopenia, periportal polymorphonuclear leukocyte infiltration and elevated liver enzymes (alanine and aspartate aminotransferases), which at certain doses can lead to dramatic effects such as tissue injury, multi-organ failure or even death (Morral *et al*., 2002). Moreover, detection of viral DNA by molecular sensors including the Toll-Like Receptor (TLR) family increases the expression of multiple pro-inflammatory cytokines (including IL-5, IL-6, IL-8, IL-12, TNFα, RANTES, IP-10, MIP-1b and MIP-2 among others), and also activates monocytes and resident macrophages (Seiler *et al*., 2007).

The third phase (delayed chronic toxicity) involves the adaptive immune response, and it occurs from several days to weeks after vector administration. This response is induced by the uptake of adenovirus by antigen-presenting cells (APCs), which process the adenoviral proteins or the adenoviral-encoded transgenes into oligopeptides and present them to the major histocompatibility complex (MHC) class-I molecules. Its successive binding to $CD8^+$ T cells leads to the generation of Ad-specific or transgene-product-specific cytotoxic T lymphocytes (CTLs) (Schagen *et al*., 2004). In addition, $CD4^+$ T cells are primed by APCs that present Ad-derived peptides on MHC-II and then stimulate B-lymphocytes, leading to the production of neutralizing antibodies.

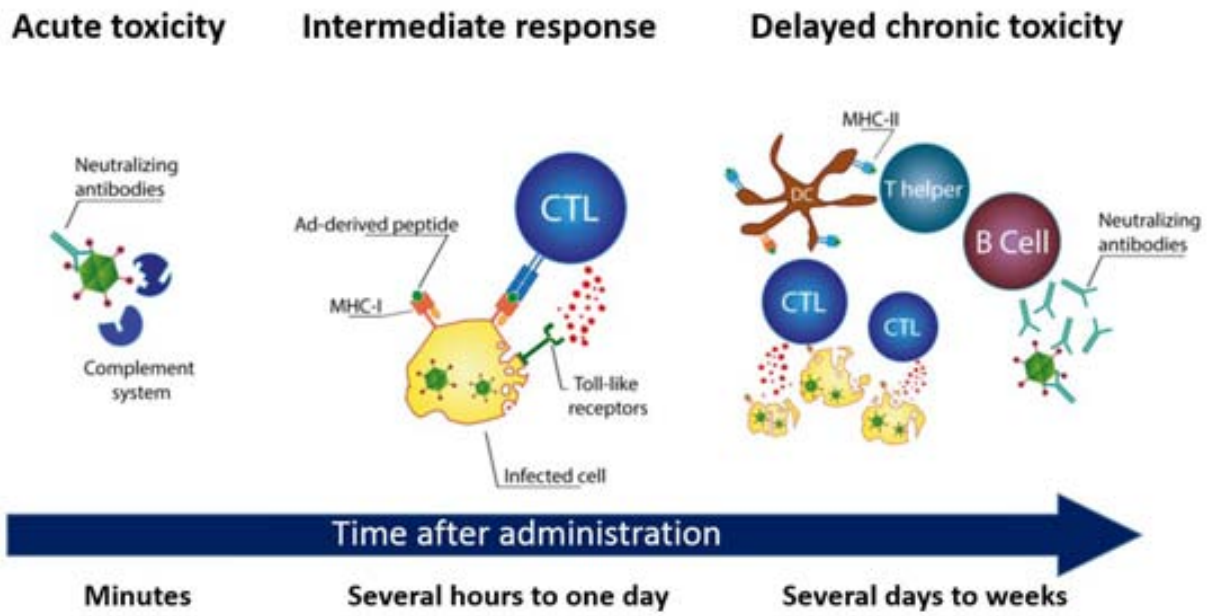

Figure 1.11. Immune response to Ad vectors. Activation of the innate immune system leads to the acute toxicity, which is generated within minutes after Ad infection, is mediated by the complement system, which is responsible for the induction of pro-inflammatory cytokines. Also, neutralizing antibodies against the Ad capsid present in patients that have been previously exposed to the Ad are important in this phase. The intermediate response generated between hours to a day after administration of the Ad vector is mediated by CTLs, which recognize Ad-derived peptides on MHC-I molecules. Activation of CTLs results in the lysis of infected cells. Also, the detection of viral DNA by TLRs leads to the generation of pro-inflammatory cytokines and the activation of monocytes and macrophages. Finally, APCs present Ad-derived peptides on the MHC-I, enhancing the cytotoxic activity of CTLs. In addition, T-helper lymphocytes primed by APCs that present Ad-derived peptides to MHC-II stimulate the production of neutralizing antibodies by B-lymphocytes.

HDAd vectors are devoid of viral genes, and therefore they elicit an attenuated adaptive immune response compared to FGAd vectors. In contrast, since host innate immune responses are induced by both HDAd and FGAd vectors in a similar manner (Muruve *et al*., 2004), a major limitation of HDAd vectors is their potential to activate a potent innate immune response. Thus, HDAd vectors also interact with bloodborne factors including C3 and C4b proteins, as well as clotting factors IX and X (Parker *et al*., 2007; Shayakhmetov *et al*., 2005; Zinn *et al*., 2004), in a non-linear toxic dose response (Tao *et al*., 2001; Seiler *et al*., 2007), indicating a key role for the innate immune sensing cells in the overall toxicity (Seiler *et al*., 2007). Additionally, primary macrophages can sense HDAd vectors via the Toll-like Receptor 9 (TLR9), which is essential for early detection of adenoviral infection (Seiler *et al*., 2007; Cerullo *et al*., 2007; Zhu *et al*., 2007). TLR9 is activated by viral dsDNA genomes (Cerullo *et al*., 2007) in a process mediated by MyD88 (Zhu *et al*., 2007), and it increases *IL-6*, *TNF*α and *IFN*β gene expression, which are key mediators of the acute response (Muruve *et al*., 2004). Nevertheless, the knowledge of all the signaling pathways and the interactions involved in Ad infection is still incomplete.

On the other hand, while encoded transgenes may or may not be immunogenic, residual expression of viral genes from first-generation adenoviral vectors is responsible for vector clearance within a few weeks of administration (Worgall *et al*., 1997; Yang *et al*., 1994). For that reason, different strategies to avoid innate and adaptive immune responses were rapidly developed. Strategies targeting the immune system, such as the use of immunosuppressive agents (cyclosporine A, cyclophosphamide, dexamethasone, FK506, Interleukin-12 and deoxypergualin) (Dai *et al*., 1995; Otake *et al*., 1998; Fang *et al*., 1995; Kaplan *et al*., 1997; Kuriyama *et al*., 2000), blockade of co-stimulatory interactions between APCs, T cells and B cells (Kay *et al*., 1995; Kay *et al*., 1997), antibodies to deplete CTLs (Poller *et al*., 1996), or macrophage depletion (Kuzmin *et al*., 1997; Stein *et al*., 1998; Wilson *et al*., 1998; Wolff *et al*., 1997) resulted in the impairment of the immune system, which made them unsuitable for use in future clinical trials. Similarly, other strategies such as oral tolerization (Ilan *et al*., 1998) and intrathymic administration of adenovirus (DeMatteo *et al*., 1997) also seemed promising, but their application have not progressed to clinical trials.

Since most adenoviral vectors are derived from human adenovirus type 5 (Ad5), and the great majority of the population have notable levels of neutralizing antibodies against them, vector uptake by target cells is prevented (Perreau *et al*., 2006; Wadell *et al*., 1972). To overcome vector neutralization, use of non-cross reacting serotypes (Mastrangeli *et al*., 1996; Morral *et al*., 1999), and vectors of non-human origin (such as ovine, canine, simian, chimpanzee and porcine adenoviruses) have been developed and show interesting results in mice (Lau *et al*., 2012). Thus, in contrast to human Ad5, CAV-2 vectors poorly transduced human monocyte-derived dendritic cells and therefore induce minimal upregulation of major histocompatibility complex class I/II and co-stimulatory molecules (CD40, CD80, and CD86) (Perreau *et al*., 2007). An alternative strategy based on a HDAd vector encoding the hyperactive transposase Sleeping Beauty achieved somatic integration of the therapeutic gene and stabilized transgene expression for up to three years in a canine model, thus circumventing the pre-existing immunity associated with vector readministration (Hausl *et al*., 2011).Similarly, modification of the physical and chemical properties of biological molecules by covalent attachment of polyethylene glycol, also known as PEGylation, has been widely tested to improve the stability, solubility, pharmacokinetic and immunological/toxicological profiles without compromising their bioactivity (Jain *et al*., 2008). Thus, PEGylated helper-dependent adenoviruses show a significantly reduced toxicity in mice (Mok *et al*., 2005), as well as in baboons, an animal

model, which has an immune system and pharmacokinetics phylogenetically similar to those in humans (Wonganan *et al*., 2011). In this study, baboons were intravenously injected with HDAd or PEGylated HDAd vectors expressing beta-galactosidase at $5 \cdot 10^{11}$ or $3 \cdot 10^{12}$ vp/kg. A three-fold reduction in IL-6 and a 50% reduction in IL-12 and serum transaminases were observed in animals injected with PEGylated HDAd vectors compared with the animals injected with non-PEGylated HDAd vectors. However, the use of PEGylated HDAd vectors in baboons did not seem as promising as it was in rodents, since hepatic transduction and viral half-life were reduced in plasma compared with those in rodents. These results suggest the presence of notable species-specific differences in the biodistribution and response to PEGylated HDAd vectors, probably related to differences in binding properties to coagulation factors, receptor density, and tissue architecture of the organs (Wonganan *et al*., 2011).

1.3.5. Helper-dependent adenovirus *in vivo*

1.3.5.1. Helper-dependent adenovirus as genetic vaccines

The use of helper dependent adenoviruses has minimized cellular toxicity, allowing a sustained high-level expression of the encoded transgenes in several animal models. A recent study has demonstrated that compared to FGAd, the administration of HDAd vector vaccines results in a lower anti-Ad T-cell response and higher levels of transgenic protein production in dendritic cells, and therefore a stronger cytotoxic T lymphocyte response against the transgene (Harui *et al*., 2004; Weaver *et al*., 2009). Thus, HDAd vectors have been successful in boosting anti-HIV immune responses in macaques (Weaver *et al*., 2009). However, since most humans have antibodies against Ad5, an adenovirus vaccine using this serotype may not be efficient. To overcome the preexisting immune response, Weaver and colleagues showed that serotype switching using HDAd serotypes 1, 2, and 6, clearly induce significant mucosal vaccine effects against HIV and therefore, that HDAd vectors are a robust platform for vaccination. Similarly, the ability of mucosally applied HDAd vaccines to induce systemic and local immunity against transgenes has also been examined by Fu and coworkers after intranasal administration to mice of HDAd vectors encoding an enhanced green fluorescent protein (GFP). As for systemic administration, a strong anti-immunogen-specific serum and mucosal antibody responses as well as lymphocyte proliferation responses were observed (Fu *et al*., 2010).

More recently, the efficacy of HDAd vectors to induce multispecific CTL responses has been demonstrated against the surface antigen of the hepatitis B virus (HBsAg). In contrast, FGAd vectors showed limited multispecificity because de novo expression of viral genes from FGAd vectors mainly induced CTLs against viral epitopes, while primed CTLs against one immunodominant epitope of HBsAg (Kron *et al*., 2011). Also, an HDAd vector genetic vaccine encoding the merozoite surface protein of *Plasmodium falciparum*, the causal agent of malaria tropica, has shown a good therapeutic potential, and it seems to act at two different stages in the parasite's infection cycle: in the liver and in the blood. As expected, in both cases HDAd vectors were more promising than FGAd vectors (Zong *et al*., 2011).

1.3.5.2. Helper-dependent adenovirus to the central nervous system

Adenoviral vectors hold great potential for brain-directed gene therapy because of their high efficiency to infect postmitotic cells (Persson *et al*., 2006) as well as to mediate long-term transgene expression. However, despite the apparent immune privilege of the CNS, in the case of pre-existing immunity against the vector, administration of FGAd into the brain will lead to a decrease in expression of the transgene 2 months after transduction, correlating with the disappearance of adenoviral DNA and chronic inflammation (Thomas *et al*., 2000; Zou *et al*., 2001). Interestingly, this immune response is significantly lower after HDAd vector administration, allowing higher levels of transgene expression than FGAd vectors and suggesting an evident therapeutic potential of HDAd vectors for gene therapy for brain disorders. In this regard, intratumoral administration of $5 \cdot 10^9$ vp of HDAd vectors encoding the conditionally cytotoxic herpes simplex type-1 thymidine kinase and the immunostimulatory cytokine FMS-like tyrosine kinase ligand 3 (*Flt3L*/*TK*) led to long-term survival (up to 1 year) of rats bearing intracranial orthotopic glioblastoma without systemic toxicity (Muhammad *et al*., 2010). Further experiments on distribution and immune response against this vector and the therapeutic transgenes in naïve rats indicated that $1 \cdot 10^9$ vp of this HDAd vector is the maximum tolerated dose that can be safely administered in the naïve brain parenchyma without adverse effects (Puntel *et al*., 2013). Notably, a Glioma Phase I Clinical Trial using *Flt3L*/*TK* HDAd vectors has been recently approved by the FDA (BB-IND 14574; NIH/OBA Protocol # 0907-990; OSU Protocol 10089) (Castro *et al*., 2012). No results are available yet.

To avoid pre-existing immunity and therefore vector neutralization, non-human adenoviral vectors have been used to achieve high transduction efficiency. Thus, stereotactic injection of canine HDAd vector expressing human N-sulfoglucosamine sulfohydrolase (*SGSH*) administered in mucopolysaccharidosis type IIIA (MPS-IIIA) mice enabled transgene expression for at least 8.5 months post-treatment in discrete areas of the brain (Lau *et al*., 2012).

Furthermore, the limited distribution of the HDAd vector after stereotactic injection (Huang *et al*., 2007; Huang *et al*., 2008) represents a major concern for the correction of diseases with global involvement, such as Alzheimer or Huntington disease. Interestingly, adenovirus vectors have also been administered into the CNS by lumbar puncture, which delivers the vector into the cerebrospinal fluid and allows the transduction of neuroepithelial cells. This method holds great promise to treat several neurological diseases, and it can be used to secrete therapeutic proteins into the cerebrospinal fluid and reach non-transduced cells, as shown by Butti and collaborators by lumbar puncture administration of HDAd vectors expressing anti-inflammatory cytokines in animal models of multiple sclerosis (Butti *et al*., 2008). Of note, injection of HDAd vectors by lumbar puncture allow at least three months transduction in non-human primates (Butti *et al*., 2008b) or up to 1 year in mice, with no chronic toxicity (Dindot *et al*., 2011).

1.3.5.3. Helper-dependent adenovirus to the muscle

Gene transfer of the skeletal muscle with HDAd vectors is very promising for the treatment of inherited skeletal muscle disorders, as well as for systemic gene therapy approaches where muscle is used as a protein production platform. Duchenne Muscular Dystrophy (DMD), a disease caused by genetic mutations in the dystrophin gene, has been considered a prime candidate for gene therapy due to the lack of effective treatments. The length of dystrophin cDNA (14 kb) precludes its cloning into most viral vectors. However, the high capacity of HDAd vectors (up to 37 kb) has opened up the possibility of treating DMD animal models (Dudley *et al*., 2004; Gilbert *et al*., 2003). Thus, *mdx* mice injected with HDAd vectors showed expression of dystrophin in neonate skeletal muscles for up to 1 year, which resulted in the mechanical stabilization of the sarcolemma by the restoration of the dystrophin-glycoprotein complex, as well as a reduction of muscle degeneration and amelioration of the physiological and

pathological indices of muscle disease (Dudley *et al*., 2004). Functional correction of the muscular contractility was also reported despite the loss of vector DNA copy number over time as well as the induction of a significant humoral response against the murine dystrophin protein (Dudley *et al*., 2004).

Notably, while immature or regenerating muscle can be effectively transduced by Ad vectors, adult skeletal muscle is only poorly transduced (Reay *et al*., 2008). Some authors suggest that this is caused by the small mass of immature muscle and because the basal lamina and other connective tissue are not yet formed (Huard *et al*., 1996), while others propose that the low Ad transduction in adult muscle correlates with a down-regulation of *CAR* during muscle development (Acsadi *et al*., 1994; Bilbao *et al*., 2003; Kass-Eisler *et al*., 1994). In any case, high levels of dystrophin expression seem to be required to reverse, at least partially, DMD pathology. Interestingly, Larochelle and collaborators injected AAV2 encoding *CAR* in adult *mdx* mice skeletal fibers and demonstrated that a moderate increase of CAR expression resulted in a significative increase of expression from Ad in skeletal muscle fibers (Larochelle *et al*., 2010), which could improve Ad-mediated DMD therapy and have a strong potential for non-regenerative skeletal muscle diseases.

Taking advantage of the immaturity of the fetal immune system, together with the robust CAR expression in the fetal skeletal muscle, Bilbao and colleagues analyzed the potential of HDAd vectors for *in utero* gene therapy for DMD. In this study, skeletal muscle fibers transduced before birth allowed the expression of the reporter protein for at least 5 months. However, despite the immaturity of the fetal immune system, antibodies against both the vector capsid and the transgene were developed (Bilbao *et al*., 2005).

Another strategy to treat DMD is the over-expression of utrophin, a functional homologue of dystrophin that is widely expressed during early development and is restricted to neuromuscular junctions in mature muscle. Interestingly, when HDAd vectors are administered to neonate *mdx* mice, the utrophin gene is expressed for up to 1 year, leading to a notable physiological improvement in young and adult animals. However, despite of the lack of antibodies and low cellular immunity, expression of utrophin decreased over time, probably because of the innate immune response as well as to the relatively short half-life of the protein (Deol *et al*., 2007). Importantly, later studies demonstrated that administration of

immunomodulatory molecules blocking the interaction between naïve T cells and APC cells allowed prolonged expression of the HDAd-encoded dystrophin (Jiang *et al*., 2004).

In DMD, the transduction of a critical number of fibers in multiple muscles is required, specially the diaphragm and other minor respiratory muscles, to avoid respiratory failure, which is the main cause of death in these patients (Matecki *et al*., 2004). Thus, laparotomy administration of HDAd encoding dystrophin in the diaphragm of *mdx* mice resulted in functional amelioration for at least 30 days (Matecki *et al*., 2004). Similarly, intraperitoneal injection of the vector in double knock-out mice for dystrophin and utrophin showed efficient transduction of the diaphragm, dystrophin expression for at least 9 weeks, and rescue from ventilatory impairment (Ishizaki *et al*., 2011). Of note, recent advances in vector development have shown that, in adult mice, intramuscular administration of chimeric HDAd5/3 vectors transduced the skeletal muscle significantly better than HDAd serotype 5, and long-term gene expression was observed for at least 1 year, suggesting the feasibility of these vectors for muscle-directed gene therapy (Guse *et al*., 2012, Figure 1.12).

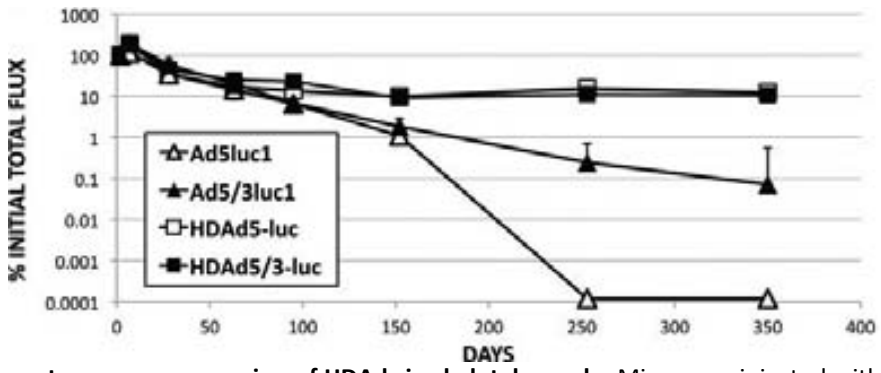

Figure 1.12. Long-term gene expression of HDAds in skeletal muscle. Mice were injected with FGAds (Ad5luc1 and Ad5/3luc1) or HDAds (HDAd5-luc and HDAd5/3luc). Over the course of almost 1 year, luciferase expression with FGAds decreased to less than 0.1% (Ad5/3luc1) while HDAds maintained 10% of initial expression over this time period. From (Guse *et al.,* 2012).

Organ	Disease	Species	Outcome	Reference
Liver	Hemophilia A	Mouse	Stable expression of factor VIII for more than 1 year in neonatal mice after injection of $5{\cdot}10^{12}$ vp of HDAd and subsequent readministration allowed by the operational tolerance to factor VIII	(Hu *et al.*, 2011)
		Dog	Significative improvement of the whole blood clotting time, plasma FVIII concentration, FVIII activity, and activated partial thromboplastin for 2 years after injection of $3{\cdot}10^{12}$ vp/kg of HDAd	(McCormack *et al.*, 2006)
		Human	No evidence of FVIII expression. Significant thrombocytopenia developed, forcing the trial to come to a halt	(White *et al.*, 2005)
	Hemophilia B	Mouse	Therapeutic hFIX levels for 45 weeks after intravenous administration of HDAd ($1{\cdot}10^{12}$ vp/kg)	(Brunetti-Pierri *et al.*, 2009)
		Dog	Decline of whole blood clotting time. Therapeutic levels of factor IX without spontaneous bleeds for at least 213 days after intravenous administration of HDAd ($3{\cdot}10^{12}$ vp/kg)	(Brunetti-Pierri *et al.*, 2005)
		Rhesus macaque	Therapeutic hFIX levels for 3 years after an intravenous administration of $1{\cdot}10^{12}$ and $1{\cdot}10^{11}$ vp/kg HDAd using a balloon occlusion catheter	(Brunetti-Pierri *et al.*, 2012)
	Ornithine transcarbamylase deficiency	Mouse	Metabolic correction of adult OTC-deficient mice, normalization of orotic aciduria and hepatic enzyme activity and absence of chronic hepatotoxicity for >6 months after an intravenous administration of $1{\cdot}10^{13}$ vp/kg of HDAd	(Mian *et al.*, 2004)
	Arginase deficiency	Mouse	Temporary correction of arginase activity and ammonia and amino acids levels and increased survival (from 14 to 27 days) of newborn mice after neonatal injection of $5{\cdot}10^{9}$ vp of HDAd	(Gau *et al.*, 2009)
	Propionic acidemia	Mouse	Moderately increased survival of mice (from 32 hours after birth until 50–70 hours after birth) after injection of $2.5{\cdot}10^{9}$ to 5×10^{10} vp of HDAd encoding the α and β subunits of propionyl-CoA carboxylase per neonate	(Hofherr *et al.*, 2009)
	Glycogen storage disease Ia	Mouse	Prolonged survival (average of 7 months) and long-term correction of G6Pase levels, body weight, glycemia, cholesterolemia and glycogen accumulation in the liver after the intravenous administration of 2 or $5{\cdot}10^{12}$ vp/kg of HDAd encoding *G6Pase* to 2-week-old G6Pase-KO mica	(Koeberl *et al.*, 2007)
		Dog	Prolonged survival (36 months) and reversion of hypoglycemia despite the persistence of long-term complications after neonatal administration of $2{\cdot}10^{12}$ vp HDAd5 and 22 months later $1{\cdot}10^{12}$ vp HDAd2 encoding for *G6Pase*	(Crane *et al.*, 2012)
	Crigler-Najjar syndrome	Rat	Correction of hyperbilirubinemia in the Gunn rat for 60 weeks using clinically relevant low HDAd doses of $5{\cdot}10^{11}$ vp/kg or $5{\cdot}10^{10}$ vp/kg when the vector is administered by hydrodynamic injection	(Dimmock *et al.*, 2011)
	Pompe disease	Mouse	Long-term correction and long-term hepatic secretion of hGAA after intravenous delivery of HDAd-*hGAA*, resulting in a complete reversal of cardiac glycogen storage and near-complete skeletal glycogen correction for at least 180 days after injection of $2.5{\cdot}10^{11}$ vp of HDAd	(Kiang *et al.*, 2006)
	ApoE deficiency	Mouse	Stable correction of hypercholesterolemia with negligible toxicity for at least 2.5 years after a single intravenous injection of $5{\cdot}10^{12}$ vp/kg of an HDAd carrying the *ApoE* gene	(Kim *et al.*, 2001)
	Familial hypercholesterolemia	Mouse	LDL cholesterol lowering and induction of regression of pre-existing atherosclerosis for at least 28 weeks after intravenous injection of $5{\cdot}10^{12}$ vp/kg HDAd containing the *LDLR* gene	(Li *et al.*, 2011)
	ApoA1 deficiency hypoalphalipoproteinemia	Mouse	Reduction in the development of atherosclerosis with the absence of significant toxicity for at least 2 years after a single intravenous injection of $4.5{\cdot}10^{12}$ vp/kg of an HDAd vector containing the human *APOA-I* gene	(Oka *et al.*, 2007)
	Gulonolactone oxidase deficiency	Mouse	Elevation of ascorbic acid levels in serum, urine and tissue for at least 23 days after intravenous administration of $2{\cdot}10^{11}$ vp of HDAd encoding for gulonolactone oxidase gene	(Li *et al.*, 2008)
	Chronic B hepatitis	Wood-chuck	Sustained viremia and WHV DNA reduction, loss of the e antigen and the surface antigen and improved liver histology in woodchucks with low viremia after intrahepatic injection of $2{\cdot}10^{10}$ IU of an HDAd encoding *IL12*	(Crettaz *et al.*, 2009)
	Type 1 diabetes	Mouse	Islet neogenesis and reversion of hyperglycemia in diabetic mice for at least 120 days after intravenous administration of 2 HDAd encoding Neurogenin3 ($5{\cdot}10^{11}$ vp) and Betacellulin ($1{\cdot}10^{11}$ vp)	(Li *et al.*, 2012)
	Type 2 diabetes	Mouse	Glucose homeostasis improvement without increasing insulin levels for at least 15 weeks after administration of $1{\cdot}10^{11}$ vp of a HDAd vector encoding exendin 4	(Samson *et al.*, 2008)

Table 1.4. Liver transduction of animal models for human diseases by helper-dependent adenovirus vectors.

Organ	Disease	Species	Outcome	Reference
CNS	Mucopolysaccharidosis type IIIA	Mouse	Expression of SGSH in discrete areas of the brain for at least 8.5 months. Injection of $2{\cdot}10^9$ pp after injection of an HDCAV-2.SGSH levels were insufficient to correct the neuropathology	(Lau *et al.*, 2012)
	Multiple sclerosis	Non-human primates	Long-term (3 months) infection of neuroepithelial cells after injection of $5{\cdot}10^8$ tu of HDAd by lumbar puncture into the cerebrospinal fluid. No signs of systemic or local toxicity were shown in monkeys bearing a pre-existing anti-adenoviral immunity	(Butti *et al.*, 2008)
		Mouse	One-year expression of GFP marker protein in neuroependymal and neuronal cells without chronic toxicity after injection of $1{\cdot}10^{12}$ vp/kg of HDAd by lumbar puncture	(Dindot *et al.*, 2011)
	Huntington disease	Mouse	Attenuation of aggregate formation 4 weeks after stereotactic injection of $1{\cdot}10^7$ IU of HDAd expressing a shRNA targeted to huntingtin. Limited effect due to vector distribution limited to a few millimeters from the needle track	(Huang *et al.*, 2007)
	Sandhoff neuropathy	Mouse	Reversion of gangliosidosis and amelioration of peripheral sensory dysfunction 8 weeks after a single injection of $1{\cdot}10^8$ vp of dorsal root ganglia-targeted HDAd encoding for Hexβ protein	(Terashima *et al.*, 2009)
	Glioblastoma	Rat	Long-term survival (1 year) after intratumoral injection of 5×10^{19} vp of HDAd encoding for *TK* and *Flt3L* without systemic toxicity in rats bearing large intracranial glioblastoma	(Puntel *et al.*, 2010)
Muscle	Duchenne muscular dystrophy	Mouse	Expression of dystrophin at the sarcolemma of >20% of total fibers in the injected diaphragm bundle for at least 30 days after injection of $5{\cdot}10^{10}$ vp of HDAd. Improved resistance to the abnormal force deficits induced by high-stress muscle contractions, despite the presence of mildly increased inflammation	(Matecki *et al.*, 2004)
		Mouse	One year gene expression of full-length dystrophin after a skeletal muscle injection of 10^9 vp of a 5/3 capsid-modified HDAd	(Guse *et al.*, 2012)
Vascular system	Hyperlipidemia	Rabbit	Improvement of endothelium-dependent vasodilation and atheroprotective effects in HDAd-infused arteries for more than 2 weeks by carotidal injection of an HDAd that leads to an over-expression of endothelial nitric oxide synthase	(Jiang *et al.*, 2012)
Lungs	Cystic fibrosis	Mouse	Transgene expression of a reporter gene human α-fetoprotein up to 15 weeks with absence of pulmonary inflammation after intranasal administration of the vector	(Toietta *et al.*, 2003)
		Rabbit	Extensive expression of a marker transgene from the trachea to terminal bronchioles for at least 5 days after administration of $5{\cdot}10^{11}$ vp encoding the *lacZ* reporter gene mixed with L-alpha-lysophosphatidylcholine using an intratracheal aerosolizer	(Koehler *et al.*, 2005)
		Non-human primates	High expression of the transgene from the trachea to terminal bronchioles	(Brunetti-Pierri *et al.*, 2009b)

Table 1.5. CNS, muscle, vascular system and lungs transduction of animal models for human diseases by helper-dependent adenovirus vectors.

1.3.5.4. Helper-dependent adenovirus to the liver

The liver is a very attractive target for gene therapy because it is affected in numerous genetic diseases and also plays an important role in many metabolic pathways. Thus, several diseases such as atherosclerosis, diabetes, Crigler–Najjar syndrome type I, glycogen storage disease type Ia, or hemophilia B, among others, have also been targeted with HDAd vectors, demonstrating their therapeutic potential in the majority of cases. A paradigmatic example comes from the studies performed in the Crigler–Najjar syndrome type I, which is a disease caused by mutations in the uridine diphospho-glucuronosyltransferase 1A1 gene (*UGT1A1)*, encoding a protein involved in the elimination of bilirubin. This deficiency results in high levels of non-conjugated bilirubin in serum and its accumulation in several organs, causing brain damage – and even neurological impairment and death – in non-treated patients (Jansen *et al*., 1999). Liver transplantation is the only cure available, and even though it provides a complete metabolic correction (Ozcay *et al*., 2009) it has some important drawbacks, such as rejection of the transplant and long-term morbidity associated with chronic immunosuppression (Meyburg *et al*., 2005). Interestingly, long-term correction of hyperbilirubinemia after administration of high doses ($\geq 3 \cdot 10^{12}$ vp/kg) of HDAd vectors was described in Gunn rats, a model of Crigler–Najjar syndrome type I (Toietta *et al*., 2005). However, these doses are likely to elicit a severe immune response in humans, as demonstrated with the death of a human patient due to the administration of $6 \cdot 10^{11}$ vp/kg (Raper *et al*., 2003). Interestingly, in a recent study, Dimmock and collaborators achieved correction of hyperbilirubinemia in the Gunn rat model using a more potent *UGT1A1* cassette and doses of $5 \cdot 10^{10}$ vp/kg after hydrodynamic injection (Dimmock *et al*., 2011).

Similarly, HDAd vectors encoding human α-1 anti-trypsin (*hAAT*) were intravenously injected in baboons and continuous hAAT expression was observed for more than 1-2 years. Interestingly no abnormalities in blood cell counts and liver enzymes were detected in any of the animals. In contrast, FGAd-treated baboons generated a cellular immune response directed against the transduced cells causing loss of hATT expression (Morral *et al*., 1999). Also, intravenous administration of an HDAd vector encoding the glucose-6-phosphatase gene on postnatal day 3 in a dog model of glycogen storage disease type Ia (GSD-Ia) resulted in the correction of the hypoglycemia and prolonged survival. After 6-22 months, vector-treated dogs developed hypoglycemia, anorexia and lethargy, suggesting that the HDAd-cG6Pase

serotype 5 vector had lost efficacy. Interestingly, a HDAd-cG6Pase serotype 2 vector was administered to two dogs, and hypoglycemia was reversed and prolonged survival in one GSD-Ia dog to 12 months of age and 36 months of age in another, though unfortunately, did not avoid the development of hepatic adenomas, which typically occur during adolescence in GSD-Ia and, on the other hand, are known not to be prevented by good metabolic control (Crane *et al*., 2012).

In addition, it has been hypothesized that liver fenestrations (size about 100 nm) may act as a structural barrier restricting the entrance of the adenovirus type 5 virion (80-120 nm) into the liver parenchyma (Lievens *et al*., 2004; Snoeys *et al*., 2007) (Figure 1.13).

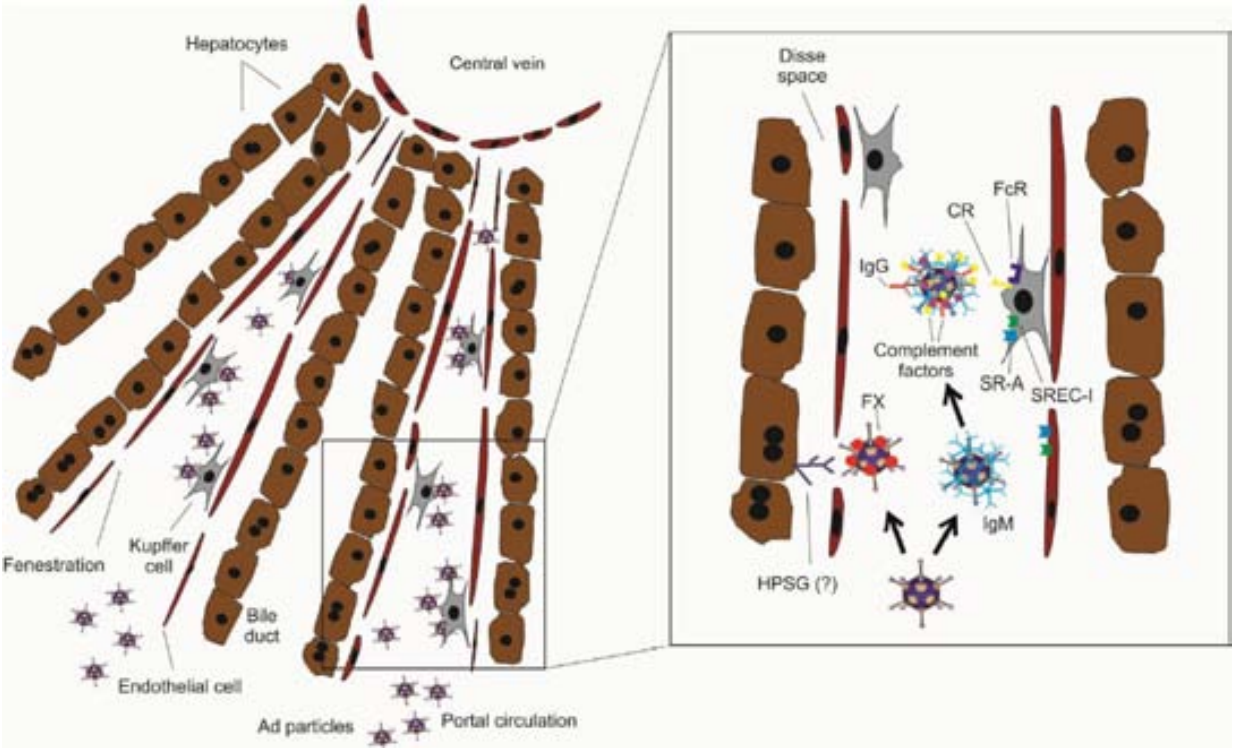

Figure 1.13. Schematic representation of the liver microarchitecture and the hurdles to efficient Ad vector-mediate hepatocyte gene therapy. Systemic delivery of Ad is hampered by binding of plasma proteins, Kupffer cell uptake, and limited permeability of endothelial cells. In the bloodstream, coagulation factor X (FX) binds with high affinity to the Ad capsid and protects from IgM and complement binding. Complement receptors bind to complement proteins bound to Ad particles. Vector particles opsonized by IgM, IgG, or complement factors are recognized by different receptors (FcR, CR) on Kupffer cells. Kupffer cells and endothelial cells also express SR-A and SREC-I scavenger receptors that bind to Ad5. The size of liver sinusoidal fenestrations affects the efficiency of Ad-mediated hepatocyte transduction. From (Piccolo and Brunetti-Pierri, 2014).

Several strategies have been applied to enlarge the fenestration size, including the use of the neuropeptide vasoactive intestinal peptide (VIP) (Vetrini *et al*., 2010), Na-decanoate (Lievens *et al*., 2004), and N-acetylcysteine (Snoeys *et al*., 2007), or by increasing the intrahepatic pressure during hydrodynamic administration of the vector (Brunetti-Pierri *et al*., 2005).

Interestingly, the use of VIP prior to HDAd vector administration not only increases liver transduction but also reduces splenic uptake of the HDAd and attenuates the HDAd vector-mediated innate immune response and hepatotoxicity (Snoeys *et al*., 2007). Of note, while the pharmacological approach will require further studies to determine its potential for human applications, hydrodynamic administration has already been discarded for this use, because the rapid injection of large volumes would not be indicated in humans. Nevertheless, a minimally invasive method based on two balloon occlusion catheters placed in the vena cava has been developed to mimic the high pressure achieved by hydrodynamic injection (Brunetti-Pierri *et al*., 2007), which allowed long-term transduction in non-human primates (964 days) after administration of HDAd vectors encoding α-fetoprotein (Brunetti-Pierri *et al*., 2009).

Other methods have also been used to confine the administered HDAd vectors into the liver and thus to reduce their diffusion to other organs, such as direct injection into the liver parenchyma (Crettaz *et al*., 2006), or surgical isolation of the liver followed by an intraportal injection of the virus (Brunetti-Pierri *et al*., 2006). In all cases, systemic vector dissemination was greatly reduced and high levels of transgene expression were achieved.

In addition to liver fenestrations, the presence of Kupffer cells makes predicting the efficiency of liver transduction difficult, since these cells have the capacity to sequester intravenously administered adenovirus, and play a very important role in the non-linear dose–response characteristic of liver transduction, where low virus doses lead to very low or undetectable levels of transgene expression, and high virus doses result in a very robust expression (Brunetti-Pierri *et al*., 2008). In this regard, the blockade of Kupffer scavenger receptor A (SR-A) and scavenger receptor of endothelial cells-I (SREC-1) prior to HDAd infection with antigen-binding specific fragments (Fabs) can be an interesting approach to increase hepatocyte transduction efficiency, allowing the use of lower doses of the vector and thus, lowering toxicity (Piccolo *et al*., 2013).

Lastly, neonatal gene therapy of the liver has also been studied to treat congenital diseases during early postnatal development. Initiating gene therapy in the neonatal period has advantages such as early gene expression, before the development of irreversible pathology, and the low or undetectable immune responses against the vector and the transgene as it has been described after neonatal administration of HDAd vectors encoding the clotting factor VIII in hemophilia A mouse models (Hu *et al*., 2011).

1.3.5.5. Helper-dependent adenovirus to the lung

Most of the gene therapy strategies in lung have been addressed to Cystic fibrosis (CF), which is the most common autosomal recessive disorder in caucasoids. The disease, characterized by chronic pulmonary infections, pancreatic enzyme insufficiency, and elevated electrolyte levels in sweat, is caused by mutations in the *CFTR* gene. As for other organs, administration of FGAd vectors into the airway of animal models induced innate, humoral and cellular immune responses, which limited transgene expression for 2-3 weeks. In contrast, administration of HDAds vectors carrying the *CFTR* gene driven by human cytokeratin 18 promoter caused no pulmonary inflammation and provided transgene expression for at least 15 weeks, protecting the lungs from opportunistic infections in mica (Koehler *et al*., 2003; Toietta *et al*., 2003). In addition, because cystic fibrosis is a chronic disease and the airway epithelium has a constant turnover, the treatment of CF by gene therapy requires repeated administrations of the vector (Burney *et al*., 2012). In this regard, Koehler and colleagues showed that in opposition to the initial administration of FGAd followed by a FGAd or HDAd vectors, readministration of moderate doses of HDAd vectors after a prior HDAd administration leads to a reduced immune response, suggesting that readministration of HDAd vectors for lung gene therapy may be feasible (Koehler *et al*., 2006). Similarly, immune response against HDAd vector readministration could be improved by rotating Ad serotypes (Parks *et al*., 1999), administering cyclophosphamide to temporary modulate the host's immune system (Cao *et al*., 2011), or by using PEGylated vectors (Croyle *et al*., 2001).

Notably, gene therapy strategies in the lung using adenoviral vectors have been hindered by the cellular structure of the epithelial airway, where the location of CAR receptors (the primary receptors of Ad5) on the basolateral surface – and therefore unavailable to the Ad vectors – is an important drawback for adenovirus transduction (Pickles *et al*., 2000; Pickles *et al*., 1998). Regarding this, different strategies to disrupt the tight-junctions such as the use of ethylenediamine tetra-acetic acid (EDTA), ethylene glycol tetra-acetic acid (EGTA), lysophosphatidycholine (LPC), and polycations prior to the Ad administration have had positive results (Chu *et al*., 2001; Kaplan *et al*., 1998; Koehler *et al*., 2005). However these strategies, usually based on two separate administrations are inefficient as they do not lead to homogenous distribution of the vector and the tight-junction opening agent. This has been recently improved by using an intratracheal nebulizer in a single administration, a delivery

method that is clinically relevant for humans and allows a high expression of the transgene from the trachea to terminal bronchioles in rabbits (Koehler *et al*., 2005), and non-human primates (Brunetti-Pierri *et al*., 2009b).

Lastly, the gene therapy studies on CF have been performed in animals with healthy airways instead of in the presence of thick deposition of mucus in the lungs, which inhibits Ad transduction (Perricone *et al*., 2000), and leads to multiple bacterial colonizations. Interestingly, the recently developed pig model for cystic fibrosis shares many features with human CF at anatomic, biochemical, and pato-physiological levels (Rogers *et al*., 2008; Welsh *et al*., 2009), and will allow to test gene therapy strategies using HDAd vectors in more clinical relevant conditions. This has a special relevance because, despite encouraging results, most preclinical studies have been performed in small animal models, and this makes the use of these strategies in humans difficult to predict. In this regard, the use of larger and more reliable animal models for each targeted disease will be crucial for the future use of these vectors in human trials.

1.4. HDAd PRODUCTION

1.4.1. Helper-dependent adenovirus production

Since HDAd vectors lack any viral coding region, proteins needed for its genome replication, capsid formation and packaging are provided *in trans* by coinfection of the HDAd vector with a helper adenovirus (helper-Ad). However, as both helper-Ad and HDAd vectors have the same capsid, as well as the same packaging efficiency, their production levels are similar, resulting in a large amount of helper vector contamination in the viral preparation. In order to lower the helper-Ad contamination, different production systems have been developed, all focusing on reducing the packaging of the helper genome. Most of the HDAd vectors preparations are currently produced using variants of the Cre/*loxP* recombination system (Parks *et al*., 1996). However, other strategies have recently been described – such as mutating the packaging signal of the helper-Ad to impair its packaging capacity (Palmer *et al*., 2003; Sato *et al.,* 2002; Soudais *et al*., 2004), or the insertion of an *attB*-ΦC31 sequence at the 5´ end of the packaging signal – which specifically delay the packaging process and the viral replicative cycle of the helper-Ad (Alba *et al*., 2007; Alba *et al*., 2011) (Figure 1.14).

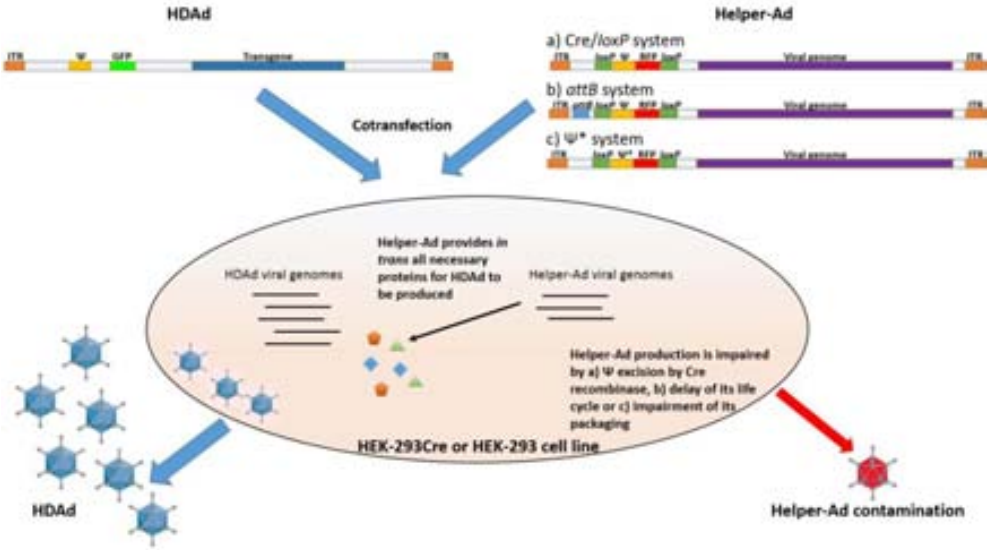

Figure 1.14. HDAd production systems. To produce HDAds, a HDAd is cotransfected altogether with a helper-Ad, which provides *in trans* the proteins required for HDAd production. To lower helper-Ad contamination, different strategies exist, such as the use of helper-Ad with a) a Ψ flanked by *loxP* sequences that mediate Ψ excision when using cells that express Cre recombinase, b) an *attB* sequence at 5' of Ψ that delays its viral life cycle or c) a mutated Ψ that impairs its packaging.

The classical Cre/*loxP* system is based on the specific excision of the packaging signal of the helper-Ad, flanked by *loxP* sequences, in cells expressing the Cre recombinase. In addition, this strategy may be combined with a physical separation on a final CsCl gradient ultracentrifugation step based on the different size of the virus genome, reducing the levels of helper-Ad contamination to a range of 1.0–0.1% (Parks *et al*., 1996).

Despite the success of this strategy, it also has some drawbacks, such as the toxicity of Cre recombinase (Loonstra *et al*., 2001). These problems have been addressed by the development of an improved system consisting of a suspension-adapted producer cell line expressing high levels of Cre recombinase, the use of a reverse Ψ in the Ad-helper vector, and a refined purification protocol (Palmer *et al*., 2003). With this system, large-scale production of $>1 \cdot 10^{13}$ highly infectious vector particles was easily achieved in spinner flasks with very low helper-Ad contamination levels (0.1–0.01%) (Palmer *et al*., 2003). However, this system still requires considerable time and effort to produce HDAd vectors. In this regard, a method consisting in the use of chamber cell factories with adherent cells was recently developed, in which comparable quantities of HDAd vector preparations were obtained with levels of contamination equivalent to those of the spinner flask approach, thus reducing technical complexity, effort and medium requirements (Suzuki *et al*., 2010).

Although major advances in cell system development have been achieved, it is important to note that all systems rely on the adoption of a CsCl gradient ultracentrifugation to lower the inevitable contamination with helper adenovirus, limiting the scalability of the manufacturing process and restricting its possible application in gene therapy protocols, where high-quality clinical-grade vectors need to be produced in large amounts under scalable good manufacturing process conditions (Lusky *et al*., 2005).

In order to scale up the HDAd vector productions, extensive optimization work is being performed nowadays. As volumetric productivity is limited by surface area, standard methods requiring adherent cell cultures are not suitable for large-scale productions, and therefore most of these methods are based on suspension cell cultures (Dormond *et al*., 2009b). Briefly, scalable methods consist of a first rescue step via transfection

followed by several amplification steps via coinfection of both helper-Ad and HDAd vectors on suspension-cell-culture bioreactors and downstream processing (Figure 1.15). The rescue step has been improved by adenofection, a transfection/infection method consisting in the use of the HDAd linearized plasmid linked to the helper-Ad with the aid of polyethylenimine (PEI) that outperforms prior protocols by producing higher HDAd vector yields (Dormond *et al*., 2009a). The amplification steps have also been widely studied, and the identification of the critical infection parameters to improve HDAd vectors yield and limit helper-Ad contamination, such as the optimal multiplicity of infection (MOI) of both HDAd and helper-Ad, the harvesting time, or the cell culture characteristics (cell density, media formulation, and vector production in fed-batch or in perfusion conditions) have been published (Dormond *et al*., 2009c).

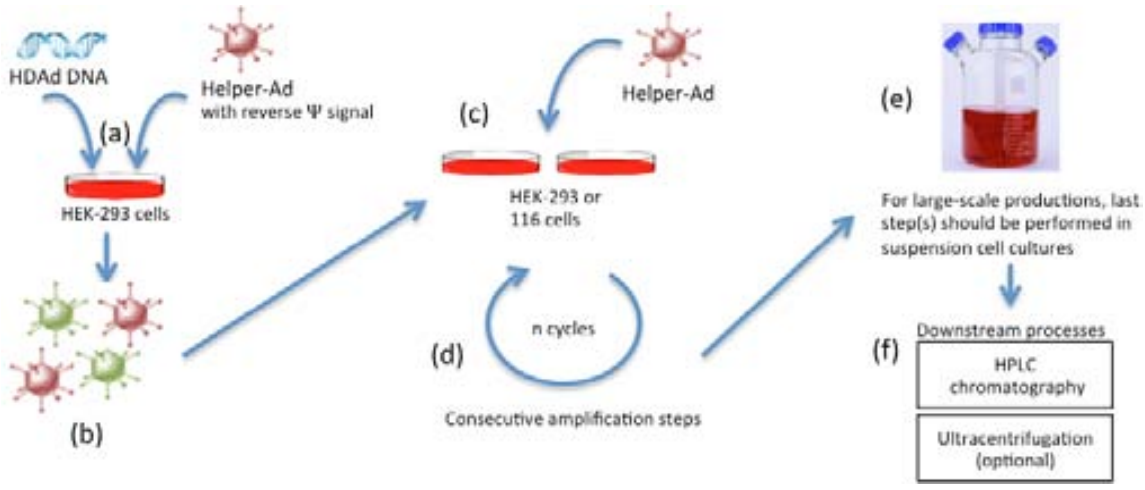

Figure 1.15. Production and purification of HDAd vectors. (a) Permissive HEK-293 cells are co-transduced with HDAd linearized genomes and Helper-Ad vectors carrying a reverse Ψ signal. To restrict and limit the packaging of Helper-Ad genomes, Helper-Ad vectors must have their Ψ sequences flanked by loxP or *attB* signals. **(b)** Initial HDAd viral stock. Both, HDAd and helper-Ad virions are present. **(c)** Amplification step in HEK-293 or 116 Cre-expressing cells. If required, supplementary Helper-Ad vectors can be added in this step. **(d)** Consecutive amplification steps to increase HDAd vector yields. In the classical Cre/*loxP* system, the loxP-flanked Ψ signal of the helper-Ad is excized when grown in Cre-expressing cells. In the *attB* system, helper-Ad vectors have a delayed packaging compared to HDAd vectors. In both systems, additional Helper-Ad vectors can be used if required. **(e)** For large-scale productions, the final steps must be performed in suspension cultures of HEK-293 or 116 cells. **(f)** Downstream processes. For small-scale productions, purification by ultracentrifugation in CsCl or iodixanol gradients is recommended. In large-scale productions HDAd vectors are purified by HPLC-chromatography. An additional ultracentrifugation step to remove empty viral capsids is recommended.

The last phase of vector manufacturing, known as downstream processing, includes the steps for recovering and purifying HDAd vectors, from the cell culture harvest to the

final product formulation. Unlike the non-scalable systems, where the final preparation is obtained after a CsCl ultracentrifugation, the scalable downstream process consists of methods such as membrane filtration or HPLC chromatography (Segura *et al*., 2008). The use of chromatographic steps allows a scalable clarification, capture and purification of the HDAd vectors, but unlike ultracentrifugation methods these systems cannot separate helper-Ad from HDAd vector particles. In this regard, an ultracentrifugation step has been included in a recent four-step downstream processing system consisting of: (1) release of viral vectors by concentration, cell lysis, DNA clearance and microfiltration; (2) capture of viral vectors by anion exchange chromatography; (3) removal of helper-Ad by ultracentrifugation; and (4) polishing and buffer exchange by size-exclusion chromatography, allowing an 80% recovery and a 10 x diminution of helper-Ad contamination from 2 to 0.2% (Dormond *et al*., 2011).

1.4.1.1. Differential amplification using attB/attP sequences from ΦC31

The Cre/*loxP* approach is the most used to produce HDAds. However, there are still residual levels of helper virus, probably due to an escape from Cre-mediated Ψ excision due to limiting Cre-levels (Ng *et al.*, 2002), the acquisition of Cre-resistant mutations and/or because of the reversibility of Cre reaction allowing reinsertion of the Ψ into the helper vector genome. Also, it has been described that high levels of Cre expression are toxic in mammalian cells as it induces chromosomal aberrations and increases the number of sister chromatid exchanges (Loonstra *et al.*, 2001; Ng *et al.*, 2002). To adress this toxicity and to reduce the levels of helper virus contamination, in our laboratory a number of helper-Ad vectors were generated with the packaging signal flanked by *attB* and *att*P sequences. Initially, the rationale was to excize the Ψ by the specific action of the ΦC31 recombinase, which specifically recognizes these sequences (Alba *et al.*, 2007). This recombinase is advantageous over the others because of the absence of reversible activity, allowing a more efficient excision of the packaging signal. Interestingly, the insertion of *attB*/*attP*-ΦC31 sequences flanking the packaging signal significantly lengthened the adenovirus cycle up to 60 hours (Figure 1.16) without reducing virus viability or production yield. This delay occurred in the absence of ΦC31

recombinase indicating that other mechanisms different from excision of packaging signal must be involved.

The reduction of the packaging efficiency of the helper adenovirus could impair its packaging without affecting helper-dependent adenovirus production. In this regard, at 36 hours post-coinfection helper-dependent adenovirus were efficiently produced, while production levels of helper *attB*/*attP*-modified adenovirus were 100–1000 times lower than controls (Alba *et al.*, 2007).

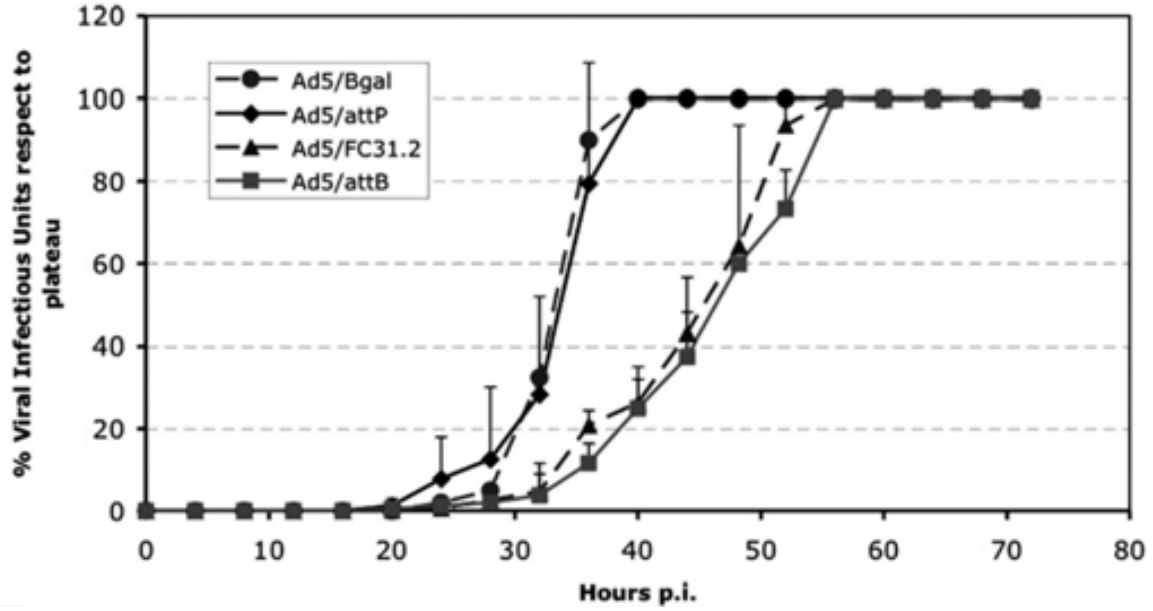

Figure 1.16. Viral cycle of *attB*/*attP*-modified and control Ads. A delay on the viral cycle can be observed in vectors with the *attB* sequence (Ad5/FC31.2 and Ad5/*attB*) but not in the control Ads (Ad5/*attP*, Ad5/βgal). From (Alba *et al*., 2007).

Unfortunately, in subsequent steps of amplification, helper-Ad contamination was greatly increased, due to homologous recombination between between the Ψ of HDAd and helper-Ad, generating a modified helper-Ad without the *attB* signal (Figure 1.17). This absence of *attB* in the helper virus leads to a 36-hour viral life cycle, thus generating high levels of helper vector contamination in HDAd amplification steps.

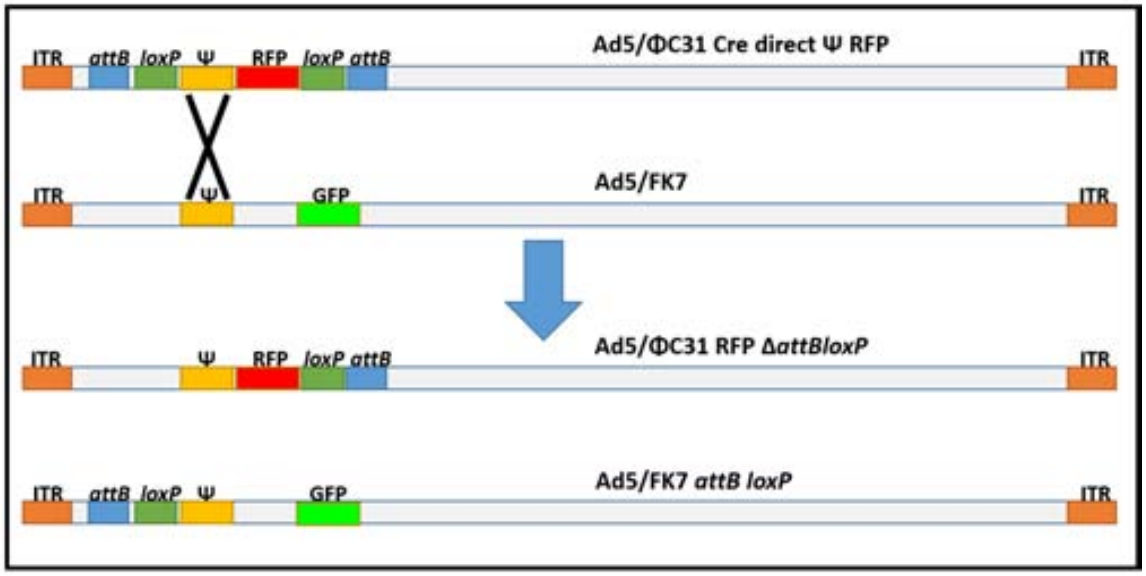

Figure 1.17. Recombination scheme between Ad5/ΦC31CreΨdir and FK7 by their direct packaging signal. This recombination generates Ad5/ΦC31 RFP Δ*attBloxP*, a helper-Ad without *attB* at 5' of the packaging signal, which therefore has a viral cycle similar to a FGAd and is capable of displacing the HDAd from the production.

An attractive strategy to solve the problem of homologous recombination between the packaging signal of the HDAd and the helper virus is the inversion of the packaging signal (Palmer *et al*, 2003). The inversion of Ψ does not prevent homologous recombination between Ψ, but if this occurs, the generated viral genome would have a size too large or too small to be able to efficiently package inside the capsid. Thus, the ability to solve this problem, and the results obtained 36 hours after co-infection of HDAd and helper-Ad suggest that the delay in the packaging of the genome of helper-Ad *attB* sequences is mediated by *attB* and indicates that the reversal of Ψ reduces the contamination of helper-Ad in HDAd productions and facilitate the process of scaling preparations for clinical level.

1.4.2. Canine adenovirus vectors serotype 2

Since most of adenoviral vectors are derived from the human adenovirus serotype 5 (Ad5) and the great majority of the population have notable levels of pre-existing neutralizing antibodies against them (Worgall *et al*., 1997; Yang *et al*., 1994) the development of vectors of non-human origin such as ovine, canine, simian, chimpanzee

and porcine adenoviruses have been used to overcome vector neutralization, showing interesting results in mice (Fang *et al*., 1995).

In this regard, canine adenovirus vectors serotype 2 (CAV-2) have the capacity to infect quiescent cells, particularly neurons (Soudais *et al.*, 2004). Theoretically, since neurons are quiescent cells, a single administration of CAV-2 to the CNS could lead to maintained transgene expression for long periods of time, maybe even for lifetime, without the need for readministering the vector. Moreover, it has been demonstrated that these vectors allow retrograde axonal transport (Soudais *et al.*, 2001) and efficiently infect glia cells and oligodendrocytes.

As seen in human adenoviral vectors, where HDAd vectors have a safer profile and higher expression than FGAd, helper-dependent canine vectors serotype 2 (HDCAV-2) perform better than their FG counterparts, as they improve the efficiency and duration of transgene expression mainly due to the elimination of the adaptive cell-mediated immune response in immunologically naïve animals (Bru *et al*., 2010). Thus, experiments in immunocompetent rats after striatal injections showed a long-term (>1 year), high-level transgene expression without immunosuppression, suggesting that the use of HDCAV-2 may be an interesting approach for the treatment of many neurodegenerative diseases (Soudais *et al*., 2004).

1.4.2.1. Helper-dependent Canine adenovirus vectors serotype 2 production

Like human HDAd vectors, HDCAV-2 vectors are amplified by the co-replication and preferential packaging via the expression of cre recombinase by DKCre cells, which renders the helper-CAV-2 packaging-defective (Bru *et al.,* 2010). However, in contrast of the highly-studied human HDAd production, HDCAV-2 production is yet to be optimized, as it renders low yields of HDCAV-2 and high levels of contamination. To this end, many different strategies have been used to improve it, such as the mutation of the packaging signal (Ψ*), which is often used in combination with the cre recombinase system to improve these modest productions. To improve these results, current production methods are based on tedious and complicated proceedments, which consist in multiple cycles of amplification of the vector in permissive DKZeo cells followed by the selection

and sorting of the infected cells by flow cytometry and Fluorescence-activated cell sorting (FACS) (E. Kremer, personal communication) (Figure 1.18).

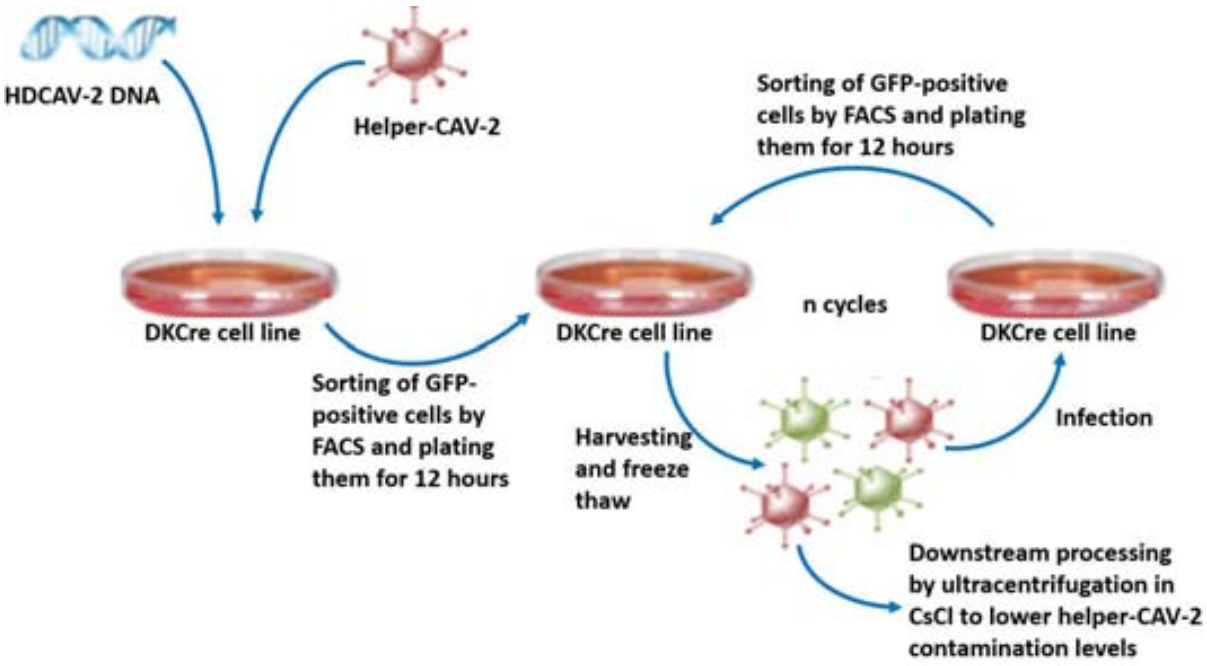

Figure 1.18. Amplification of HDCAV-2 using the FACS and cell sorter method. This strategy consists of an initial transfection of HDCAV-2 vector and infection with helper-CAV-2 followed by sorting of GFP-positive cells (which are infected by the HDCAV-2) by FACS. Usually, it involves six or more amplification steps in DKCre cells, as the production yields after each cycle is poor (1.5x to 2x HDCAV-2 enrichment per step). Finally, downstream processing is performed by ultracentrifugation in CsCl, which allows a partial separation of the HDAd from the helper-CAV-2 by the different density of these vectors, thus reducing helper-CAV-2 contamination levels.

As in the production of human HDAd, it is essential to optimize the production of HDCAV-2 vectors in order to be able to use them in research in animal models and ultimately in the clinic. Concerning this, it will be interesting to assess whether the inclusion of an *attB* sequence into helper-CAV-2 genome causes a delay in its viral life cycle, and therefore could improve HDCAV-2 production. In addition, the inclusion of two loxP sequences in each side of Ψ would open the possibility to use production canine cell lines that express Cre to further minimize helper-CAV-2 contaminants.

1.4.2.2. Helper-dependent Canine adenovirus vectors serotype 2 titration

The Maizel quantitation (Maizel *et al.,* 1968), which measures the number of physical particles by optical density at 260nm (OD_{260}) is a simple, inexpensive and quick titration method. However, it has two major limitations: 1) it cannot be used when the viral titer is lower than $3 \cdot 10^{11}$ PP/ml, 2) it cannot be used in non-purified samples due to contaminant interference. Altogether, these limitations make this titration method unsuitable for monitoring the virus yields of the amplification steps. Recently, these limitations were surpassed by the development in our laboratory of a CAV-2 titration strategy that relies on a qPCR assay with primers that amplify CAV-2 structural genes (Segura *et al*., 2009). This method is very useful for monitoring amplification steps, as it can titrate crude lysates and has a high sensitivity. However, some authors consider that these titration methods have a low biological relevance as, besides mature virions, the detection of physical particles also include defective virions and, if DNAse I is not used, naked DNA (Ma e*t al.,* 2001, Gallaher and Berk, 2013).

The use of biological titration methods, like the detection of reporter gene expression in transduced cells (i.e. β-galactosidase, GFP) provides an important information regarding the infectivity of a viral sample. Unfortunately, this assay can be associated with poor precision and high variability (Segura *et al*., 2010). To solve these issues, the tissue culture infectious dose ($TCID_{50}$) assay, based on the detection of cytopathic effect on infected permissive cells (DKZeo) was developed. However, even though this method improves the detection of transduced cells, it requires experience of the observer and time, as it takes nearly two weeks of virus culture for the cytopathic effect to appear.

To date, among all these titration methods, the detection of the reporter gene expression in transduced cells is the only option that can be used to quantify HDCAV-2 productions. This represents a major drawback for the optimization of these productions and its final titration in terms of variability and inaccuracy. In this regard, the development of a variant of the qPCR described by Segura*,* that could detect both vectors and in turn, be biologically relevant, would be very important in this aspect.

1.4.3. Chimeric adenoviruses

The viral surface proteins have great influence over the transduction efficacy, but also in the ability to cause immunological responses and to resist complement activation of viral vectors (Figure 1.19). Therefore, in order to influence these parameters, these proteins can be modified, replaced or removed depending on the characteristics of the pathology that is aimed to be targeted.

Since the interaction of the most used adenoviral vector, Ad5, to the target cells is through the binding to CAR, a protein that is distributed on the surface of many cell types, these vectors display a broad tropism. In order to restrict vector tropism and/or allow the use of adenoviral vectors in Ad5-refractory tissues, the use of adenoviral vectors other than Ad5 has been intended. However, in contrast of the production of Ad5, the production of these vectors is not optimized, rendering low titers. For this reason, efforts are made in generating chimeric vectors based on Ad5 with the fiber knob domain or the entire fiber genetically replaced with its structural counterpart from a different serotype.

In this regard, many chimeric vectors have been described, in some cases achieving high transduction levels in different Ad5 refractory cell types such as colon carcinoma (Silver *et al*., 2011), ovarian carcinoma (Rein *et al.,* 2011), prostate cancer (Murakami *et al*., 2010) and breast cancer (Stoff-khalili *et al*., 2007), among others. Furthermore, chimeric vectors have been recently generated to lower liver tropism and therefore increase tropism to other organs (Koski *et al.*, 2013).

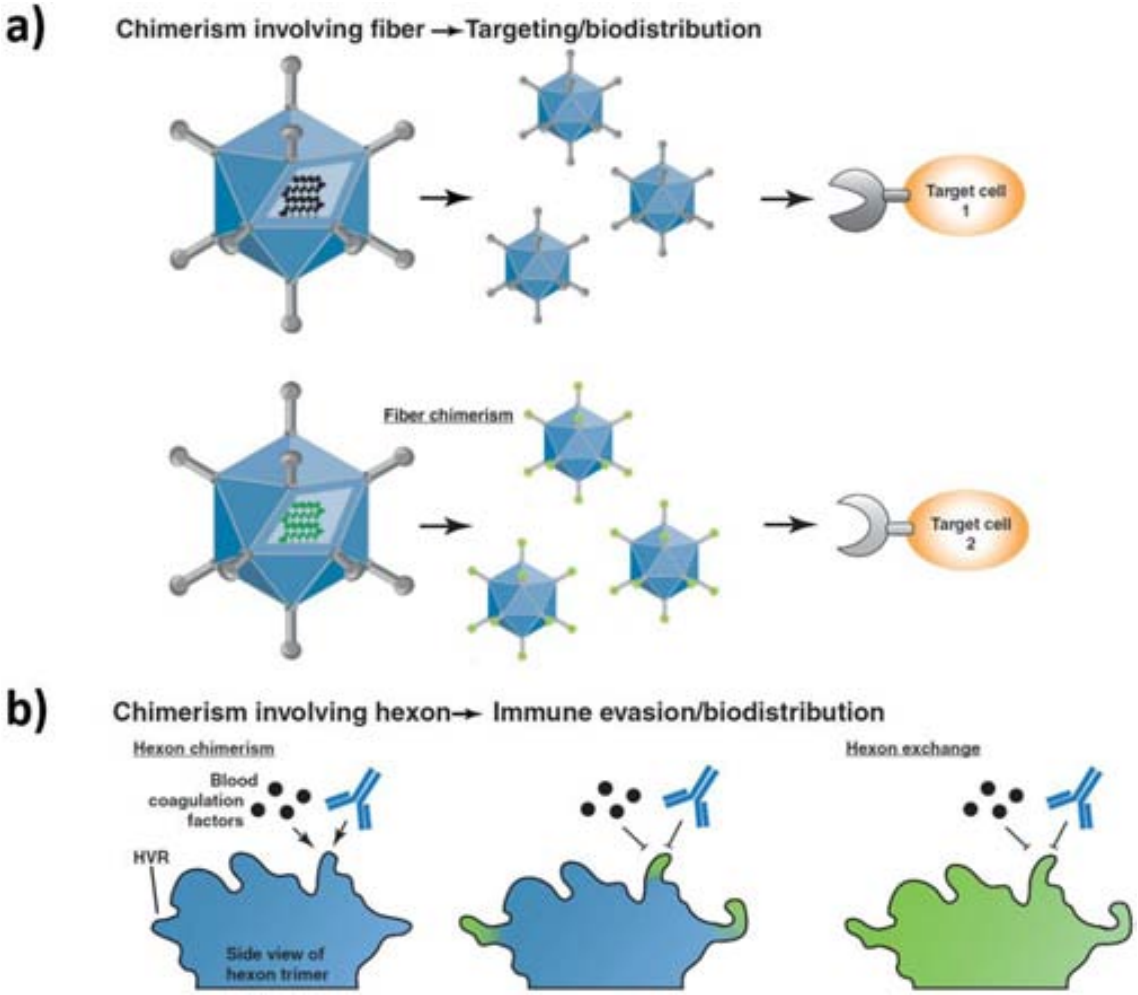

Figure 1.19. Chimerism of Ad vectors. a) For targeting and biodistribution purposes, the Ad fiber can be modified. The knob domain, responsible for primary receptor recognition, and the shaft can be exchanged individually or in combination (fiber chimerism). Also, the entire fiber protein can be exchanged. b) Evasion of pre-existing humoral immunity can be achieved by chimeric design or exchange of the major immunogenic determinants of the Ad capsid. Adapted from (Kauffmann and Nettelbeck, 2012)

1.4.3.1. Adenovirus 5/40S

Human adenovirus serotype 40 (Ad40) is an enteric adenovirus known for causing gastroenteritis in children. This virus contains two different types of fiber proteins, differentiated by their shaft region and their knob domain: the long fiber (F40L) that binds to CAR and the short fiber (F40S), responsible for the enteric tropism.

Because of this tropism, these vectors show great potential to target intestinal diseases such as Crohn's Disease, ulcerative colitis or celiac disease. However, the production of these vectors has been difficult as, even though they can be propagated in HEK-293 cells, their production lead to very low titers in comparison with other adenoviral serotypes

like Ad5. For this reason, these vectors are also known as “fastidious viruses”. In order to increase the production efficiency, Ad5/40S chimeric vectors (Ad5 capsid with the F40S protein, responsible for the enteric tropism of Ad40) were generated, allowing higher production titers (Miralles *et al*., 2012; Nakamura *et al*., 2003). However, since these vectors are first generation adenovirus, they encode for viral proteins and therefore still induce a strong immune response against the transduced cells (Shoggins *et al*., 2005). To adress this, our laboratory has developed a system for generating a HDAd5/F40S chimeric vector using a novel helper vector encoding for the F40S protein and with *attB* sequence.

Chapter 2

OBJECTIVES

The main objective of this thesis is to improve the production of helper-dependent adenoviruses of different serotypes and species (Ad5, Ad5/F40S and CAV-2) by using the *attB* system.

In order to reach this objective, the following specific objectives were considered:

1. Generation and characterization of a helper-Ad with a reverse Ψ (Ad5/ΦC31CreΨrev) to avoid the generation of RCA in HDAd productions.

2. Development and optimization of a HDAd production system using Ad5/ΦC31CreΨrev.

3. Generation and characterization of chimeric Ad5/ΦC31CreF40S helper-Ad.

4. Development of a HDAd production system using this helper-Ad to produce chimeric HDAds with the short Fiber protein of Ad40.

5. Generation and characterization of CAV-2/ΦC31CreΨ*, a CAV-helper vector with the *attB* sequence.

6. Development and optimization of a HDCAV-2 production system using CAV-2/ΦC31CreΨ*.

7. Determination of the factor that interacts with *attB* and is responsible for the delay of the viral life cycle of *attB*-vectors.

Chapter 3

MATERIALS

3.1. BACTERIAL STRAINS

TOP10^{R} INVITROGEN (used to amplify plasmids smaller than 10 Kb long)**:** F- mcrA Δ(mrr-hsdRMS-mcrBC) F80lacZΔM15 ΔlacX74 recA1 araD139 Δ(ara-leu)7697 galU galK rpsL (Str^{R}) endA1 nupG.

BJ5183^{R} STRATAGENE (used for the generation of the viral genome by homologous recombination): endA1 sbcBC recBC galK met thi-1 hsdR (Str^{R}).

3.2. PLASMIDS

pKP1.4ΔCMV: Plasmid containing the Ad genome except E1 region and part of E3 region.

6600/ΦC31CreΨrev: Shuttle plasmid containing the 5' region of the helper-Ad, including the Ψ flanked with *loxP* sequences, an *attB* at 5' of Ψ, and RFP gene.

pKP 1.4 ΔCMV F40S: Plasmid containing all the viral genes of a FGAd5 except for the Ad5 fiber protein gene, which is substituted by the short fiber protein of adenovirus 40.

pKP 1.4 ΔCMV ΦC31 F40S: Plasmid containing all the viral genes of a FGAd5 except for the Ad5 fiber protein gene, which is substituted by the short fiber protein of adenovirus 40, and an *attB* at 5' of Ψ.

3.3. VIRAL VECTORS

Ad5/ΦC31CreΨdir: Human helper-Ad with recognition sites for ΦC31 and Cre recombinases, direct Ψ and RFP gene.

Ad5/ΦC31CreΨrev: Human helper-Ad with recognition sites for ΦC31 and Cre recombinases, reverse Ψ and RFP gene.

Ad5/RFP: Human FGAd with the RFP gene.

Ad5/GFP: Human FGAd with the RFP gene.

FK7: Human HDAd with the GFP gene (MTA Stephan Kochanek).

Ad5/F40S: Human FGAd with the F40S and the GFP genes.

Ad5/ΦC31CreF40S: Human helper-Ad with recognition sites for ΦC31 and Cre recombinases, with the F40S and RFP genes.

CAV-2/RFP: Canine FGCAV-2 with the RFP gene.

CAV-2/ΦC31CreΨ*: Canine helper-CAV-2 with recognition sites for ΦC31 and Cre recombinases, mutated Ψ and the RFP gene.

RIGIE: Canine HDCAV-2 with the β-gluguronidase and GFP genes (Kindly provided by Eric Kremer).

HDmax: Canine HDCAV-2 with the GFP gene (Kindly provided by Eric Kremer).

LRRK2wt: Canine HDCAV-2 with the LRRK2wt and GFP genes (Kindly provided by Eric Kremer).

LRRK2*: Canine HDCAV-2 with the mutated LRRK2 and GFP genes (Kindly provided by Eric Kremer).

JBΔ5: Canine helper-CAV-2 with recognition sites for Cre recombinase, a mutated Ψ and the GFP gene (Kindly provided by Eric Kremer).

3.4. *IN VITRO* CELL LINES

HEK-293 cell line (ATCC® CRL-573™, Q-BIOgene, Montreal, Canada): Human embrionic kidney cells propagated in Dulbecco's Modified Eagle's Medium (DMEM, #E15-810, PAA laboratories) supplemented with 10% v/v Fetal Bovine Serum (FBS, PAA laboratories) and Penicillin (100 I.U/ml)/Streptomycin (100 I.U/ml) (PAA Laboratories) at 37^{o}C and 5% CO_2. They were used for adherence cultures.

HEK-293-F cell line: derivative of HEK-293 QBiogene adapted to be cultured in suspension with mild agitation (orbital shaker at 0.3 xg) in SFM II (medium Gibco Laboratories) supplemented with 0.5% v/v Fetal Bovine Serum (FBS), Penicillin (100 I.U/ml)/Streptomycin (100 I.U/ml), 1% v/v pluronics (Invitrogen Laboratories) and 4mM L-Glutamine (PAA laboratories) at 37^{o}C and 8% CO_2.

HEK-293Cre cell line: derivative of HEK-293 to express the Cre recombinase. These cells are propagated in Dulbecco's Modified Eagle's Medium (DMEM) supplemented with 10% v/v Fetal Bovine Serum (FBS) and Penicillin (100 I.U/ml)/Streptomycin (100 I.U/ml) at 37ºC and 5% CO_2. They were used for adherence cultures.

DKZeo cell line: Dog kidney cell line expressing the zeocin resistant protein. These cells are propagated in Dulbecco's Modified Eagle's Medium (DMEM) supplemented with 10% v/v Fetal Bovine Serum (FBS) and Penicillin (100 I.U/ml)/Streptomycin (100 I.U/ml) at 37ºC and 5% CO_2. They were used for adherence cultures.

DKZeoΦC31 cell line (clones 2 and 3): Dog kidney cell line expressing the zeocin resistant protein and ΦC31 recombinase. These cells are propagated in Dulbecco's Modified Eagle's Medium (DMEM) supplemented with 10% v/v Fetal Bovine Serum (FBS), Penicillin (100 I.U/ml)/Streptomycin (100 I.U/ml), 1% non-essential amino acids (PAA Laboratories) and 6µg/ml of hygromycin (PAA Laboratories) at 37ºC and 5% CO_2. They were used for adherence cultures.

DKCre cell line: Dog kidney cell line encoding for a zeocin resistant protein and Cre recombinase. These cells are propagated in Dulbecco's Modified Eagle's Medium (DMEM) supplemented with 10% v/v Fetal Bovine Serum (FBS), Penicillin (100 I.U/ml)/Streptomycin (100 I.U/ml) and 1% non-essential amino acids at 37ºC and 5% CO_2. They were used for adherence cultures.

3.5. EXPERIMENTAL ANIMALS

For *in vivo* experiments, 6-week old CD1 and C57BL/6 immunocompetent female mice were used (Harlan ibérica, Barcelona). All animals were kept under a pathogen-free area at Servei d´Estabuari of the Universitat Autònoma de Barcelona.

Mice were fed *ad libitum* with a standard diet (2018S Teklad Global, Harlan Laboratories; 17% calories from fat) and kept under a light-dark cycle of 12 hours (lights on at 8 a.m.).

Animal care and experimental procedures were performed in accordance with 86/609/EEC regarding the care and use of animals for experimental procedures and were approved by the Biosafety and the Ethics Committees of the Universitat Autònoma de Barcelona.

3.6. PRIMER LIST

Primer	Orientation	Sequence (5' to 3')
Helper-Ad Ψ	*Forward*	GAACACATGTAAGCGACGGATGTG
	Reverse	TCACTGCATTCTAGTTGTGGT
HDCAV-2 stuffer	*Forward*	TCTCTACCCGATGTGACC
	Reverse	GAACTCAGGGAGTCCAGAATGT
CAV-2 set 1	*Forward*	CGT GAA GCG CCG TAG ATG C
	Reverse	GAA CCA GGG CGG GAG ACA AGT ATT

Table 3.1. Sequences of the primers used.

Chapter 4

METHODS

4.1. MOLECULAR BIOLOGY METHODS

4.1.1. DNA quantification

DNA quantification was performed by UV absorption analysis at 260 nm (OD_{260}) with 2 µl of the sample using a spectrophotometer (NanoDrop ND-1000).

4.1.2. DNA purification

Purification of DNA from agarose gels was performed using the GENECLEAN Turbo Kit Q-BIOgene Kit (Cat. No. 1102#400) following the protocol supplied by the manufacturer.

4.1.3. DNA digestion with restriction enzymes

The enzymes used in this study were manufactured by Fermentas and New England Biolabs. Between 2 and 5 units of restriction enzyme were used to digest 1 µg of plasmid DNA in solution and temperature conditions specified by the manufacturer. The digestion time varied from 1-24 hours depending on different conditions (i.e. plasmid properties, amount of enzyme used). In case that DNA was needed for further manipulation, enzymes were inactivated at 65°C for 20 minutes.

4.1.4. DNA defosforilation and ligation

T4 DNA ligase (New England Biolabs) was used at 16°C between 4-18 hours, and was inactivated at 65°C for 20 minutes. CIP alkaline phosphatase (Alkaline Phosphatase, Calf Intestinal, New England Biolabs) was used at 37°C for 30 minutes. After this, enzymes were inactivated at 65°C for 20 minutes.

4.1.5. DNA electrophoresis in agarose gel

To analyze the restriction pattern of a plasmid digestion, DNA electrophoresis in agarose gels were performed. To prepare the gel, 1% or 2% agarose (w/v) (#50005 Seaken Iberlabo Agarose LE) in 1X TAE buffer (40 m*M* Tris-acetate pH=8.0, 0.1 m*M* EDTA) was melted (2% to analyze DNA fragments under 1000 bp and 1% for larger fragments). The mixture was heated (on a glass beaker) and let it to temper. Then, the sample was poured into the gel tray (MAX FILL gel trays and buckets, BioRad) and a comb suitable for the cargo volume was placed. Once the gel polymerized, the comb was removed, and 1X TAE buffer (40 m*M* Tris-acetate pH=8.0, 0.1 m*M* EDTA) was added until it exceeded the gel 1mm. Next, the samples were loaded into the wells with 1X loading buffer mixed with a dye (10X loading buffer: 50% glycerol, 100 m*M* EDTA pH=8.0, 1% SDS, 0.1% Bromophenol Blue/0.1 Xylene Cyanol FF and dilute in milliQ water). An electric current of 70-100 V was then applied for the amount of time required for the optimal separation of the DNA bands (Sources of Power Pac Basic electrophoresis, BioRad). The gel was removed from the gel tray and immersed in an ethidium bromide solution (TAE 1% + 100 µg/ml EtBr), incubated for 10 minutes and observed under UV light using a UV light-coupled camera (Syngene IMAGING SYSTEM) and GeneSnap Visualization and imaging software (Syngene).

4.1.6. Polymerase chain reaction

The polymerase chain reaction (PCR) is a rapid procedure for *in vitro* enzymatic amplification of a specific segment of DNA using two oligonucleotides (or primers) complementarily hybridizing to the ends of the sequence to be amplified. The enzyme *Taq* polymerase incorporates nucleotides needed until the end of the DNA strand and thus amplify the region of interest. This process is repeated until 30-35 cycles are completed.

For this work, we used the following reagents and conditions:

Reagents:

20-50 pmol of each oligonucleotide used.

5 µl *Taq* polymerase buffer.

4 µl $MgCl_2$ (25 m*M*).

0.4 µl dNTPs (25 m*M*)

0.3 µl *Taq* polymerase (5 U/µl).

50 ng of DNA of interest.

Final volume: 50 µl of milliQ water.

Thermocycler (Eppendorf Mastercycler Gradient) amplification conditions:

95°C for 5 minutes.

30-35 cycles consisting in 94°C for 30 seconds, 54°C for 30 seconds, 74°C for 1 minute.

74°C for 2 minutes.

25°C for 5 minutes.

Store at 4°C or frozen at -20°C.

Amplification conditions vary depending on the number of Kb (1 minute/Kb), the amount of the starting DNA (10 ng to 100 ng of plasmid or genomic DNA), or the sequence of the oligonucleotides used (binding temperature to the template strand).

4.1.7. Southern blot

Southern blotting is the transfer of DNA fragments from an electrophoresis gel to a membrane support. The transfer and the subsequent treatment results in immobilization of the DNA fragments, so the membrane carries a semipermanent reproduction of the banding pattern of the gel. After immobilization, the DNA can be subjected to hybridization analysis, enabling the identification of bands with sequence similarity to a labeled probe.

For this experiment, we used an specific prove for the canine Ad-helper 5'ITR (present in both pJB19 and pTJB19ΦC31CreGFP):

5'-GGACAAAGAGGTGTGGCTTAAATTTGGGTGTTGCAAGGGGCGGGGTCATGGGACGGTC AG-3'

4.1.7.1. Extraction of genome DNA from DKZeo cells

DKZeo cells were lysed by 3 freeze/though cycles, thus allowing the release of the viral genomes to the medium. 100 µl of crude lysate were mixed with 7 µl 10% SDS, 3 µl 0.5 M EDTA and 40 µl of proteinase K (10 mg/ml) (Roche, #3115879001) and incubated for 3 hours in a 55ºC water bath. Subsequently, samples were heated for 5 minutes at 95ºC. Then, 50 µl milliQ water, 100 µl 7.5 *M* ammonium acetate and 300 µl phenol/chloroform/isoamyl alcohol (25:24:1) (isoamyl phenol chloroform AMRESCO #2810) were added and the samples, which were centrifuged for 7 minutes at 11750 xg. The upper phase was transferred to a new 1.5 ml Eppendorf tube discarding the interphase. Then, 600 µl 100% ethanol were added and, samples incubated for 30 minutes at -80ºC. After the incubation, samples were centrifuged for 15 minutes at 8160 xg and washed with 70% ethanol. Finally, the pellet was resuspended in 40 µl of milliQ water.

4.1.7.2. Electrophoresis and gel treatment

An electrophoresis gel was loaded with 7 µg of digested DNA per lane and the electrophoresis was performed until the bromophenol blue was at 4 cms to the end of the gel. Then, DNA was stained with ethidium bromide and visualized with ultraviolet light exposure, to assess if the DNA digestion was successful. Subsequently, the gel had to be treated to allow a good DNA transference to the membrane by denaturing it for its further hybridization with the marked probe. To do this, the gel was incubated first for 15 minutes with HCl (3 ml HCl in 147 ml of distilled water) and later, 45 minutes in alkaline solution with 5 *M* NaOH, 1.5 *M* NaCl (105 ml of distilled water, 3 g of NaOH, 45 ml of 5 *M* NaCl) to denature the DNA. Then, the gel was neutralized with 20X SSC (3 *M*

NaCl, 0.3 *M* sodium citrate pH=7.4) for 45 minutes, allowing DNA to acquire again negative charge.

4.1.7.3. Transfer of DNA to the membrane

Downward capillary transfer involves transferring DNA to a positively charged membrane (Roche Diagnostics Corp., Indianapolis, IN; #1417240) in a high ionic strength buffer (10X SSC). The transfer was performed with filter papers (GB002 and GB004, Shleicher & Schueller, Keene, New Hampshire) that allow the buffer to pass through. The transfer process last between 14 and 18 hours. Once completed, the membrane was irradiated with ultraviolet light, following the *optimal crosslink* program from UV-*stratalinker* 1800 (Stratagene, La Jolla, CA) to bind the DNA to the membrane.

4.1.7.4. Hybridization and revealed

The membrane was then pre-hybridized with a hybridization solution (Amersham Biosciences #RPN3680) for 15 minutes at 55^{o}C with gentle agitation. Subsequently the probe was labelled using Alk Phos Direct Amersham Biosciences kit (#RPN3680) and then added to the membrane and left overnight at 55^{o}C with gentle agitation (hybridization oven ProblotTM Jr., Labnet). Once this step was complete, the membrane was washed to remove traces of non-attached probe. Two 10-minute washes were performed at 55^{o}C with primary wash solution and two more washes with secondary wash solution were done for 5 minutes at room temperature. To reveal the membrane, CDP-Star reagent was added upon the membrane for 5 minutes. Finally, the film (high performance chemiluminescence film HyperfilmTM ECL, Amersham Biosciences) was exposed for two hours and developed with a film imaging processor (FUJIFILM FPM 100-A).

4.1.8. Electrophoretic Mobility Shift Assay (EMSA)

The DNA-binding assay using non-denaturing polyacrylamide gel electrophoresis (PAGE) provides a simple, rapid, and extremely sensitive method for detecting sequence-specific DNA-binding proteins. Proteins that bind specifically to an end-labeled DNA

fragment retard the mobility of the fragment during electrophoresis, resulting in discrete bands corresponding to the protein-DNA complexes. The assay can be used to test the binding of purified proteins or of uncharacterized factors found in crude extracts.

4.1.8.1. Preparation of nuclear extracts

Nuclear extracts prepared from HEK-293 or DKZeo cells were obtained from 15-cm plates at 75% confluence. 100 ml of 1X PBS with 250 n*M* PMSF (phenylmethasulphonylfluoride) was prepared and cooled in ice. Cells were dislodged from the plates adding 2.5 ml of PBS-PMSF and centrifuged for 10 minutes at 320 xg and 4^{o}C. The precipitate was resuspended in 7.5 ml PBS-PMSF and centrifuged again at the previous conditions. After this centrifugation, the packed cell volume (PCV) of the precipitated cells was estimated. Then, cells were resuspended in buffer A (10 m*M* HEPES pH=7.5, 10 m*M* KCl and 1.5 m*M* $MgCl_2$ in milliQ water) with protease inhibitors to a final volume of 5 times the original PCV. Cellular samples were incubated one hour on ice and transferred into a glass mortar, where it was homogenized using a pestle. Samples were then transferred into a new tube and centrifuged for 5 minutes at 600 xg and 4^{o}C. The supernatant was removed and the pellet was resuspended in 1 ml of buffer A. Samples were again centrifuged under the same conditions and the supernatant was removed. Pellet was resuspended in 3 PCV volumes of buffer B (20 m*M* HEPES pH=7.5, 20% glycerol, 450 m*M* NaCl, 1.5 m*M* $MgCl_2$ and 0.2 m*M* EDTA in milliQ water), transferred into a new tube, incubated on ice for one hour and centrifuged for 30 minutes at 16000 xg and 4^{o}C. Finally the supernatant (containing nuclear extracts) was transferred to a cryotube and stored at -80^{o}C. Samples were quantified by the BCA method (bicinchonic acid) following the protocol provided by the manufacturer (BCATM, #23227 Pierce Protein assay kit).

4.1.8.2. EMSA assay

Three µg of nuclear extracts were incubated for 30 minutes at 37°C with 2.6 ml of 5X Binding buffer (LightShift Chemiluminescent EMSA Kit, #20148X, Pierce), 1 µl salmon sperm or poly-dIdC (poly-deoxyinosic-deoxycytidylic acid), 1 µl of biotin-labeled wild type-*attB* or mutant *attB* oligonucleotides and milliQ water, until the sample reached a volume of 10 µl. The non-denaturing polyacrylamide gel was prepared (38.8 ml distilled water, 2.5 ml 10X TBE pH=8.3, 5.6 ml acrylamide, 2.8 ml bis-acrylamide (Acryl/Bis AMRESCO #2810), 300 µl APS and 40 µl of TEMED) and samples loaded with 1.5 µl of loading buffer (0.25% bromophenol blue, 0.25% xylene cyanol and 30% glycerol). Samples were separated for 90 minutes at 120 V, and transferred to a positively charged membrane (Roche Diagnostics Corp, Indianapolis, IN; #1417240) using the transblot (#Transblot SD semi-dry transfer, BIO-RAD) for 45 minutes at 25 V. The membrane was previously pretreated with methanol 10 for minutes, 5 minutes with milliQ water and 10 minutes with transfer buffer (5X TT). Once the transference was performed, the membrane was irradiated with ultraviolet light with UV-*stratalinker* to covalently bind the biotin-labeled DNA to the membrane. Subsequently, the membrane was treated with blocking buffer (LightShift Chemiluminescent EMSA Kit, #20148X, Pierce) and incubated with a peroxidase-streptavidin conjugate, washed with washing buffer (LightShift Chemiluminescent EMSA Kit, #20148X, Pierce) and incubated with luminol (LightShift Chemiluminescent EMSA Kit, #20148X, Pierce) following the protocol provided by the manufacturer. Finally, the film (high performance chemiluminescence film HyperfilmTM ECL, Amersham) was exposed to the membrane for 1 to 30 minutes, varying the time as needed for optimal detection, and developed with a film imaging processor (FUJIFILM FPM 100-A). To confirm observations, the experiment was repeated in three independent analysis.

The sequences of the oligonucleotides used are:

*attB*wt (wild type):

5'ACCGGTCCGCGGTGCGGGTGCCAGGGCGTGCCCTTGGGCTCCCCGGGCGCGTACTCCAC3'.

*attB** oligonucleotide (mutant):

5’-ACCGGTGGGCACGCGCGCACCTGGCGCACCGCGTCGGCGCACCTGCGCACCTGGCACCA 3’.

4.1.9. Detection of *attB*-interacting proteins using streptavidin columns

As a strategy to purify the proteins that interact with biotinylated *attB*wt or *attB** oligomers, we used a streptavidin column (#20357 High Capacity Streptavidin Agarose Resin, PIERCE). This method is based on the tight complex that biotin forms with streptavidin and it can be used to elute the protein in a small volume (i.e., as high a concentration) as possible. To do this, we followed the manufacturer´s protocol (http://www.piercenet.com/instructions/2160187.pdf) and analyzed the eluted samples by the MALDI-TOF mass spectrometry of Servei de Seqüenciació de Proteïnes (IBB, Universitat Autònoma de Barcelona).

4.1.10. Fast Protein Liquid Chromatography (FPLC)

To fraction HEK-293 nuclear extracts, chromatography purification was conducted on an ÄKTA Explorer 100 (GE Healthcare) low-pressure liquid chromatography system. The system is controlled by a UNICORN software. Absorbance at 280 nm and 260 nm was measured on-line. Sepharose 6FF gel was packed into an XK 16/70 column (GE Healthcare) to a final volume of 130 ml. Nuclear extracts from ten 15-cm plates of HEK-293 cells were loaded. Isocratic elution was carried out in PBS buffer at pH=7.4, and at a flow rate of 2 ml/minute (60 cm/hour) and fractioned samples of 2 ml were transferred to cryotubes and stored at -80^{o}C.

4.1.11. Biacore assays

Biacore assays were performed in The Biocentre (University of Reading, UK) using Biacore Surface Plasmon Resonance technology (BIACORE 3000, GE Healthcare). Technical manipulations were done by experience personnel of The Biocentre.

4.2. BACTERIAL MANIPULATION TECHNIQUES

4.2.1. Preparation of chemically competent bacteria cells

Chemically competent bacteria cells have the ability to take up DNA by transformation. In our laboratory, *E. coli* competent cells were prepared following the rubidium salts method. First, buffers TFB1 and TFB2 had to be prepared:

Working solution, pH 5.8	Amount per liter
100 m*M* RbCl	*12.1 g*
50m*M* $MnCl_2$	*9.9 g*
30 m*M* potassium acetate	*2.9 g*
10 m*M* $CaCl_2$	*1.1 g*
15% glycerol	15 ml

Table 4.1. *Buffer TFB1*

Working solution, pH 6.8	Amount per liter
100 m*M* MOPS	*2.1 g*
50m*M* RbCl	*1.2 g*
75 m*M* $CaCl_2$	*8.3 g*
15% glycerol	15 ml

Table 4.2. *Buffer TFB2*

Once the buffers were prepared, a trace of *E. coli* cells was removed from the glycerol stock vial with a sterile toothpick or inoculating loop, and streaked it out on LB-agar plates. Then, LB-agar plates were incubated at 37°C overnight. The following day, a single colony was picked and 10 ml LB medium was inoculated and let grow overnight at 37°C. Next day, 1 ml overnight culture was added to 100 ml prewarmed LB medium containing ampicillin in a 500 ml flask, which was then placed at the shaker at 37°C until an OD_{600} of 0.5 was reached (approximately 90–120 min). Subsequently, the culture was cooled on ice for 5 min and transferred to a sterile centrifuge tube. Then, cells were

collected by centrifugation at low speed for 5 minutes at 4000 x*g and* 4°C and the supernatant was discarded carefully, always keeping the cells on ice. The cells were then gently resuspended with cold TFB1 buffer (at 4°C, using 30 ml of TFB1 for a 100 ml culture) and the suspension was kept on ice for an additional 90 min. After, the cells were collected by centrifugation (5 min, 4000 x*g* and 4°C) and the the supernatant was carefully discarded. Always keep the cells on ice. Finally, the cells were carefully resuspended in 4 ml ice-cold TFB2 buffer and aliquots of 100–200 µl in sterile microcentrifuge tubes were prepared and stored at -80°C.

4.2.2. Plasmidic DNA obtention

4.2.2.1. Plasmidic DNA minipreparations

Chemically competent cells were transformed by heat shock protocol as described by Chartier *et al.* 1996. To obtain plasmidic DNA in low quantities (5-15 µg) DNA minipreparations were performed by the alkaline lysis procedure. To this end, a single bacterial colony was inoculated with three ml of sterile LB medium and left overnight at 37°C (441 Shaker, Thermo electron corporation, Marietta, OH) to allow its growth to saturation. Then, the culture was centrifuged for 1 minute at 11750 xg in a 1.5 ml Eppendorf tube. The supernatant was eliminated and the cellular precipitate was resuspended in 200 µl of the resuspension buffer (50 m*M* Tris-HCl pH=8.0, 10 m*M* EDTA, 100 µg/ml RNAseA). Subsequently, 400 µl of the lysis buffer (200 m*M* NaOH, 1% SDS (w/v)) was added and the solution was gently mixed. Then, 400 µl of the protein precipitation buffer (3 *M* potassium acetate at pH=5.5) was added and the samples were stirred until the precipitate was homogeneous. Then, samples were incubated for 10 minutes on ice and centrifuged 10 minutes at 11750 xg. Next, the supernatant was transferred to a new tube and 550 µl of isopropanol was added. After this, samples were incubated for 10 minutes at room temperature and later centrifuged at 11750 xg for 10 minutes. Finally, samples were washed with 70% ethanol and resuspended in 30 µl of milliQ water.

4.2.2.2. Plasmidic DNA maxipreparations

To obtain large amounts of high-quality plasmid DNA (250-1000 mg), DNA maxipreparations were performed using the kit "Phoenix Maxiprep Kit" from Q-BIOgene (#2075-300) or the "Plasmid Maxi Kit" from Qiagen (#12163) in 200 to 500 ml cultures depending on the plasmid (high or low copy number per cell). The preparations were performed according to the manufacturer's protocol.

4.2.3. Homologous recombination

Chemically competent *E.coli* BJ5183 cells were mixed with 50 ng of each linearized plasmid to be recombined and were transformed by heat shock. Positive clones were verified by enzymatic digestion and then transformed into *E.coli* TOP10 cells, because they allow a higher yield of plasmid DNA and therefore, the recombination can be better verified. Of note, it is important to maintain plasmids obtained by homologous recombination at -20°C (or -80°C if possible) because, since these plasmids have a high molecular weight, they are easily degraded at 4°C.

4.3. *IN VITRO* CULTURES

4.3.1. Subculture of adherent cells

Cells were subcultured to a new plate before 90% confluence is reached. To do this, the medium was removed and cells washed with 1X saline solution (50 g of potassium chloride, 20 g of sodium chloride and distilled water until 500 ml). Then, 10 ml of 1X saline solution were added to the plates and they were incubated at room temperature for 5-10 minutes. For DKZeo, DKCre and DKZeoΦC31 cells, 5 ml of trypsin (PAA Laboratories) were used instead of saline solution to ensure a complete cell dislodgement. Cells were then harvested and centrifuged for 5 minutes at 140 xg for human cells and at 320 xg for canine cells. The supernatant was discarded and cells were resuspended in growth medium (DMEM + 10% FBS + 1% penicillin/streptomycin). Once resuspended, a fraction of the total medium with cells was added on a new plate and fresh growth medium was added to complete the optimal volume (growth medium vary depending on the used cell lines as is described in Materials, 3.4. *In vitro* cell lines).

4.3.2. Subculture of suspension cells

HEK-293-F cells were grown in 125 ml shake flasks (25 ml working volume) with mild agitation (orbital shaker at 0.3 xg). Since these cells are very sensible to their confluence and the lack of fresh medium, they required a close control of their concentration. Counting of these cells was performed by the trypan blue exclusion test of cell viability, consisting in counting cells that do not take up the dye in a Neubauer chamber. Then, the concentration of cells per ml was calculated using the following formula:

$$[\text{cells/ml}] = \text{number of viable cells} \cdot \text{dilution factor} \cdot 10^4$$

Due to the high growth rate of these cells, they were subcultured every 2 to 3 days, when they reached $2 \cdot 10^6$ cells/ml. To do so, cells were first concentrated by centrifuging the culture at 180 xg for 5 minutes and later seeded at a density of $5 \cdot 10^5$ cells/ml in fresh SFM II medium supplemented with FBS, Penicillin/Streptomycin, pluronics and L-Glutamine.

4.4. ADENOVIRUS MANIPULATION TECHNIQUES

4.4.1. Preparation of the adenoviral genome to transfect HEK-293 cells

The adenoviral plasmids were linearized to remove the origin of replication and ampicillin resistant gene. 100 µg of DNA were digested with 50 U of *PacI* or *PmeI* in a final volume of 200 µl for 14-16 hours. Then, DNA was precipitated with 20 ml of 3 *M* potassium acetate pH=5.2 and 550 µl of cold absolute ethanol and incubated 30 minutes at -80°C. Later, samples were centrifuged at 16000 xg and 4°C and the supernatant was discarded. DNA pellet was washed with 70% ethanol and dried for 15 minutes. Finally, plasmids were resuspended in milliQ water or TE (10 m*M* Tris-HCl/1 m*M* EDTA, pH=8).

4.4.2. Adenovirus transfection

HEK-293, HEK-293Cre, DKZeo, DKCre and DKZeo-ΦC31 cells (clones 2 and 3) were transfected with linear *PacI* or *PmeI*-digested plasmids containing adenoviral genomes using polyethylenimine (PEI, 25 kDa, Aldrich, #40,872, St. Louis, MO, USA). To do this, a PEI/DNA complex was prepared on two Eppendorf tubes separately. To transfect 10^6 cells, 6 µg of viral DNA was added to a final volume of 150 µl of 150 m*M* NaCl in a first tube, and 6.8 µl of 10 m*M* PEI was added in a final volume of 150µl of 150 m*M* NaCl and in a second tube. Once both components were prepared separately, PEI-NaCl solution was added dropwise to the DNA-NaCl solution, and was incubated for 30 minutes at room temperature. Then, 700 µl of culture medium (DMEM + 2% FBS) was added and the solution was gently mixed. Subsequently, the media from the cells was aspirated and the mixed solution was cautiously added on a single well of a 6-well plate at 70% confluence. Then, cells were incubated for 4 hours at 37°C and 5% CO_2. After incubation, the transfection mix with culture medium was aspirated and 2 ml of fresh growth medium (DMEM + 10% FBS) was added to the cells. The initial transfection step was not harvested until viral foci were observed (between 36 and 72 hours post-transfection). Once the cells were collected, three freeze/thaw cycles were performed and samples

were centrifuged for 5 minutes at 2250 xg. Finally, the cellular pellet was discarded and the supernatant (crude lysate) was used for the next step of amplification.

4.4.3. Adenovirus amplification

4.4.3.1. FGAd amplification

Virus stocks were sequentially amplified, first, in a single 10-cm plate, after in two 15-cm plates and finally in twenty 15-cm plates (except for CAV-2/ΦC31CreΨ* production which, because of its low productivity, needed a fourth step of amplification of one-hundred 15-cm plates). In each step, cells were harvested when cytopathic effect appeared on infected cells. The harvesting time varied depending on the characteristics of the vector to amplify: thus, 36 hours per amplification step for FGAds without *attB*, 60 hours for Ad5/ΦC31CreΨdir and Ad5/F40S, 72 hours for CAV-2/ΦC31CreΨ* and 78 hours for Ad5/ΦC31CreΨrev.

Of note, every time cells were collected after each step of amplification, the cell pellet was concentrated to a final volume of 18-20 ml, and three freeze/thaw rounds were performed to liberate virus particles. Then, samples were centrifuged for 5 minutes at 2250 xg and finally, the cellular pellet was discarded and the supernatant (crude lysate) was used for the next step of amplification or, in case that the lysate was obtained from the final amplification step, for the further ultracentrifugation in CsCl gradient.

4.4.3.2. HDAd amplification in suspension cells

$2 \cdot 10^6$ HEK-293-F cells were harvested at a final concentration of 10^6 cells/ml in 6 wells-plates in Free Style medium (Gibco Laboratories) supplemented with 0,5% v/v Fetal Bovine Serum (FBS), Penicillin (100 I.U/ml)/Streptomycin (100 I.U/ml) and 1% v/v pluronics. Cells were infected with a MOI=5 of helper-Ad and a MOI of HDAd that varied depending on the experiment performed. Twenty hours post-infection, medium was changed for fresh Free Style medium in order to eliminate helper excess. Finally, after a

specific time points for each experiment, fluorescent cells were detected and quantified by fluorescence microscopy (NIKON Inverted Microscope ECLIPSE TS100/TS100-F) in order to determine the percentage of infected cells. GFP was detected in HDAd-infected cells and RFP was detected in helper-Ad-infected cells.

4.4.4. Adenovirus purification

4.4.4.1. Ammonium sulphate precipitation

In case that the recovery of viruses present in the culture medium of the last step of amplification was needed (usually in virus produced at low yields), an ammonium sulphate precipitation was performed. To do this, ammonium sulphate (9.69 g for each 40 ml of culture medium) was added to the medium and softly agitated for 3 hours at room temperature. After this, medium was centrifuged for 15 minutes at 570 xg, the supernatant was discarded and the precipitate was resuspended in 20 ml 1X PBS Ca^{2+}/Mg^{2+}.

4.4.4.2. Viral purification

To concentrate the adenovirus productions, two serial centrifugations on CsCl gradient were performed, using the crude lysate from the last amplification step and, if applicable, the viruses precipitated with ammonium sulphate and resuspended in PBS Ca^{2+}/Mg^{2+}.

The first ultracentrifugation is performed with a step CsCl gradient formed by 10 ml δ=1.25 g/ml CsCl and 10ml δ=1.40g/ml CsCl (Beckman Centrifuge tubes polyallomer, #331374). The viral fraction was carefully added to fill completely the centrifuge tube, which was subsequently ultracentrifuged for 1 hour and 42 minutes at 170000 xg and 18°C in a Beckman SW32 rotor. As a result of this ultracentrifugation, several bands could be observed on the tube, varying in position and density depending on whether they correspond to empty viral capsids, full mature capsids or cell debris, which in turn depends on the characteristics of the production (high or low yields, viral life cycle of the vector length, harvesting time). Four ml of the viral band corresponding to mature

virions were aspirated with an hypodermic needle (B.braun 100 Sterican 1.20X40mm 18Gx 1.5''), and added on top of the second CsCl gradient (isopycnic gradient), formed by 4 ml δ=1.34 g/ml CsCl (which is approximately the density of a mature virion). The isopycnic CsCl gradient was then ultracentrifuged for 18 hours at 284000 xg and 18°C in a Beckman SW40 rotor. Usually, two bands are observed after this ultracentrifugation: a superior band corresponding to empty capsids and an inferior band corresponding to fully mature viral capsids. After the ultracentrifugation, fully mature viral capsids were aspirated with a hypodermic needle and subsequently purified from CsCl by molecular exclusion cromatography in a sephadex column (PD-10 desalting columns, Amersham Biosciences, Uppsala, Sweden). Viral eluted samples (F2-F9) were collected in 500 µl fractions and were conserved in Phosphate Buffered Saline buffer supplemented with Ca^{2+} and Mg^{2+} (Dubelcco DPBS + Ca^{2+} and Mg^{2+}) and with 10% sterile glycerol.

Notably, a third centrifugation step similar to the second centrifugation was performed when the separation of HDAd from helper-Ad by the different density of their bands was required.

4.4.5. Adenovirus titration

4.4.5.1. Physical particles titration

Viral samples were diluted 1/20 with lysis buffer (Tris-EDTA, 0.1% SDS), incubated for 10 minutes at 56°C and optical density was read with a Biophotometer at 260 nm. Viral physical particles per ml were determined by using the optical density, the dilution factor, and a conversion factor of $1.1 \cdot 10^{12}$ using the following formula:

$$[PP/ml] = \text{dilution factor} \cdot D.O._{260} \cdot 1.1 \cdot 10^{12}$$

4.4.5.2. End-point titration

Adenoviral infection units were titrated by end-point dilutions from 10^{-3} to 10^{-10} for the most concentrated purified viral fractions (previous approximated viral titration of all viral fractions). Each dilution was done in triplicate and 2 replicates were performed for each triplicate, in order to diminish variability. Adherence HEK-293 or DKZeo cells at 80%

confluence were infected in 96 wells-plates with 100 µl of each dilution (dilutions were done in DMEM medium supplemented with 2% v/v Fetal Bovine Serum (FBS) and Penicillin (100 I.U/ml)/Streptomycin (100 I.U/ml). Infected cells were visualized by fluorescence microscopy (NIKON Inverted Microscope ECLIPSE TS100/TS100-F) before two viral cycles were completed (this is analized at 48 hours post-infection for Ad5/RFP, Ad5/GFP, CAV-2/RFP, HDAd (FK7) and HDCAV-2 (RIGIE, HDmax, LRRK2 and LRRK2*) and 110 hours post-infection for helper-Ad or helper-CAV with the *attB* sequence).

Since all vectors expressed the either GFP or the RFP genes, the titration was performed by counting cells expressing GFP/RFP in a fluorescence microscope. Infection units per ml were calculated taken into account the dilution of the last well infected and the volume of viral sample used for the infection using the following formula:

$$[IU/ml] = \text{dilution factor}^{-1} / \text{ infected viral volume per well}$$

4.4.5.3. HDAd titration in suspension cells

$2 \cdot 10^6$ HEK293-F cells were harvested at a final concentration of 10^6 cells/ml in 6 wells plates in Free Style medium (Gibco Laboratories) supplemented with 0.5% v/v Fetal Bovine Serum (FBS), Penicillin (100 I.U/ml)/Streptomycin (100 I.U/ml) and 1% v/v pluronic. Cells were infected with a known volume of viral preparation and, 40h post-infection, infected cells were quantified by fluorescence microscopy (NIKON Inverted Microscope ECLIPSE TS100/TS100-F). GFP accounted for HDAd-infected cells and RFP detection for helper-Ad-infected cells. Infection units per ml were calculated as with the number of infected cells per well and the volume of viral sample used for the infection using the following formula:

$$[IU/ml] = \text{number of infected cells per well} / \text{infected viral volume per well}$$

4.4.5.4. Quantification of infective CAV-2 by $TCID_{50}$ assay

The amount of CAV-2 replication-competent particles in the DKZeo permissive cell line was measured by the tissue culture infectious dose at 50% assay ($TCID_{50}$). The method was adapted from the assay described in the Adeno-X Expression System User Manual

(PT3414-1; Clontech, Mountain View, CA). In brief, DKZeo cells ($2 \cdot 10^4$ cells/well) were infected with serial dilutions of virus from 10^{-3} to 10^{-10} across rows of a 96-well plate. Each well was checked for cytopathic effect (CPE) 10 days after infection and scored as positive or negative. The number of infectious units (IU) per milliliter was calculated using the following formula based on the Spearman-Kärber method:

Titer (IU/ml) = $10^{(x+0.8)}$, where x is the sum of the fractions of CPE-positive wells in each row.

4.4.5.5. Titration of CAV-2 by Flow Cytometry

10^6 DKZeo cells were infected (n=3) with different dilutions of the viral samples obtained from the cell-sorting process with HDCAV-2 vectors (RIGIE and HDmax). In parallel, 10^6 DKZeo non-infected cells were used as a negative control. Infected and non-infected cells were recovered at 36 hours post-infection. Medium was recovered and saline buffer (50 g of potassium chloride, 20 g of sodium chloride and distilled water until 500 ml) was added to harvest the cells. After centrifugation, cells were first resuspended in PBS and then in 4% paraformaldehyde. Finally, GFP expression of infected cells was analyzed by flow cytometry (FACSCanto) at *Servei de Citometria* of IBB-UAB (Universitat Autònoma de Barcelona).

4.4.5.6. Titration of CAV-2 samples by qPCR

To titrate CAV-2 samples from amplification steps or purified preparations, we developed a method consisting of the infection of suspension HEK-293-F cells followed by the extraction of the viral genomes from the infected cells and a qPCR analysis of these samples. To do this, 10^6 HEK-293-F cells were infected with 1 µl of the viral sample and after 24 hours, viral genomes were extracted as previously described (4.1.7.1.). Then, 10 ng of cellular extracts were used for the qPCR analysis, in the following conditions:

Initial denaturing step at 95°C for 3 minutes, followed by 40 cycles consisting in 95°C for 10 seconds, 58°C for 10 seconds, and 72°C for 30 seconds. Each sample was analyzed in triplicate.

4.4.6. Adenovirus characterization

4.4.6.1. Determination of the viral life cycle

HEK-293 or DKZeo cells (when using canine vectors) at 70 to 80% confluency were infected (with Ad5/RFP, Ad5/F40s, CAV-2/RFP and Ad5/ΦC31CreΨdir, Ad5/ΦC31CreΨrev or Ad5/ΦC31CreF40s) at MOI=5, in a 24-well plate. Cells were harvested (pellet and supernatant) every 4 hours, up to 72 hours. Three freeze/thaw rounds were performed to liberate virus particles and the number of IU/cell at each time point calculated by end-point dilution assay. Viral life cycle was defined as the process from virus entry into the cell to formation of infective virus particles. End of viral life cycle was defined as the time when the IU/cell number reached a plateau (values do not increase or even decrease compared to values of previous time points), after a period of maintained exponential amplification of at least 12 hours. To avoid the effects of a second amplification cycle, once the end of a viral life cycle was defined for a given vector, further time points were considered as plateau.

4.4.6.2. Co-infection assays

HEK-293 cells were infected with Ad5/ΦC31CreΨdir, Ad5/ΦC31CreΨrev, Ad5/GFP or Ad5/RFP in a 6-well plate at 5 IU/cell for single infection. For co-infection experiments *att*B*/att*P-modified Ads (Ad5/ΦC31CreΨdir and Ad5/ΦC31CreΨrev) were co-infected with control FGAd (Ad5/GFP or Ad5/RFP) at 5 IU/cell per virus. At 36 hours post-infection, viruses were harvested and further titered by end-point dilution assay using fluorescence microscope.

4.5. *IN VIVO* TECHNIQUES

4.5.1. Tail-vein injections

Systemic administration of HDAd (FK7) and FGAd (Ad5/GFP) was performed via tail-vein injection to six-week old CD1 female mice (Harlan ibérica). First, in order to vasodilate their veins to facilitate the administration, mice were exposed for 10 minutes to near-infrared light. Then, still irradiating with the infrared light, mice were anesthetized by intraperitoneal injection of ketamine (10 mg/kg of body weight; Imalgene 500; Rhône-Merieux) and xylazine (1 mg/kg of body weight; Rompun; Bayer). Subsequently, we administered $1 \cdot 10^{12}$pp of FK7 or Ad5/GFP in a 10 µl total volume, using a Hamilton syringe (Hamilton Bonaduz Ag, Switzerland). Mock-injected control animals were injected with 10 µl of PBS. A total of 18 mice were injected (n=2).

4.5.2. Joint injections

Joint-administration of AAV2, AAV5, AAV8, AAV9, AAV10, CAV-2, Ad5, Ad40, and Ad52 vectors was performed using six-week old C57BL/6 female mice (Harlan ibérica).

Mice were first anesthetized by intraperitoneal injection of ketamine (10 mg/kg of body weight; Imalgene 500; Rhône-Merieux) and xylazine (1 mg/kg of body weight; Rompun; Bayer). Two microliters of the vector preparation (with 10^9vg for all vectors except of AAV2, which had $6 \cdot 10^8$vg) were loaded into a Hamilton syringe (Hamilton Bonaduz Ag, Switzerland) and injected to mice joints. The needle was slowly withdrawn a minute after injection. Mock-injected control animals were injected with 2 µl of PBS. A total of 10 animals were injected, one injection for each knee joint (n=2).

4.5.3. Sample obtaining and processing

To obtain liver and knee joint samples, mice were killed using a CO_2 chamber. Liver samples were extracted from CD1 mice after a subcostal incision of the right hypochondrium and were stored in a sterile tube at -80°C for further processing.

Samples were fixed in 4% paraformaldehyde, embedded in optimal cutting temperature using OCT, and frozen. Cryostrate sections were observed using confocal microscopy (Servei de microscòpia, Universitat Autònoma de Barcelona).

Knee joints from C57BL/6 mice were cut using surgery scissors and were stored in a sterile tube with 2% paraformaldehyde. Samples were decalcified in 0.5 *M* EDTA (pH 7.5) solution, and embedded in paraffin (HE) wax for histology observation using confocal microscopy (Servei de microscòpia, Universitat Autònoma de Barcelona).

4.6. STATISTICAL ANALYSIS

Statistical analysis was performed using the Student's t-test.

Chapter 5

RESULTS

5.1. OPTIMIZATION OF HDAd PRODUCTION USING THE *attB*-ΦC31 TECHNOLOGY

5.1.1. Generation of the Ad5/ΦC31CreΨrev plasmid by homologous recombination

The generation of replication-competent adenovirus (RCA) by the recombination between helper-Ad and HDAd through their packaging signal during the production of HDAd using the *attB*-ΦC31 technology has been previously described in our laboratory (Alba *et al*., 2007). Since these newly generated RCA contain all the viral genes required for their amplification in HEK-293 cells, and in addition they also have a viral cycle similar to first-generation adenoviruses, they displace the HDAd during the amplification process, thus limiting the ability to produce HDAd. To solve this issue, we created the Ad5/ΦC31CreΨrev genome which, due to its reverse packaging signal is unable to generate RCA, as the recombination between both viral genomes (Ad5/ΦC31CreΨrev and HDAd) would lead to the generation of a genome without any viral gene as well as a size too small to be efficiently packaged. This helper-Ad was generated by homologous recombination between 6600/ΦC31CreΨrev (a shuttle plasmid previously created in the laboratory) and pKP1.4ΔCMV (Figure 5.1).

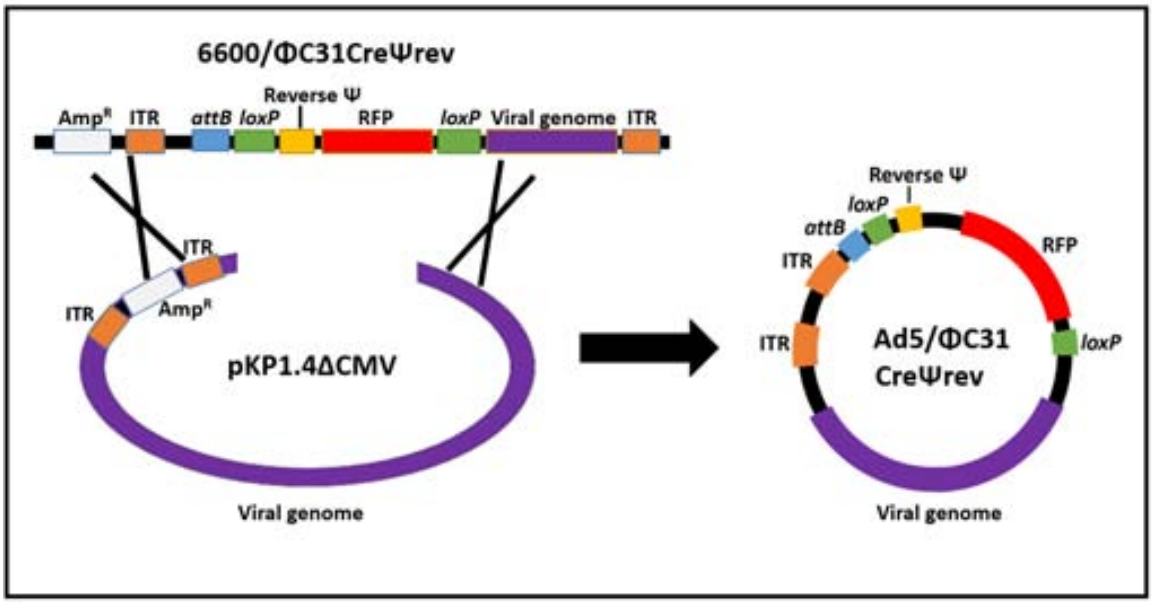

Figure 5.1. Recombination strategy for the generation of the Ad5/ΦC31CreΨrev genome.

The comparison between the observed (Figure 5.2) and the expected bands for the parental and recombinant plasmids (Table 5.1) indicated that the recombination was effective, and therefore the Ad5/ΦC31CreΨrev genome was successfully generated.

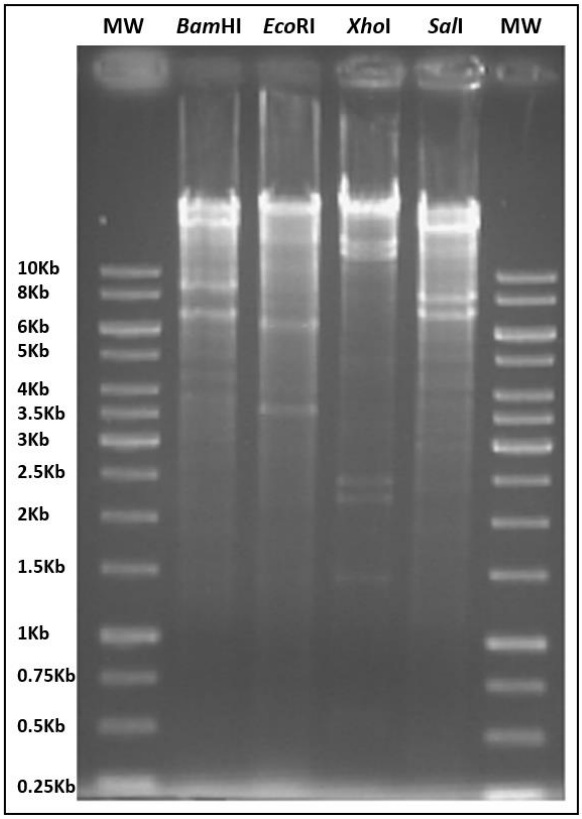

Figure 5.2. Comprobation electrophoresis for the generation of the Ad5/ΦC31CreΨrev genome.

pKPΔCMV				6600/ΦC31CreΨrev				Ad5/ΦC31CreΨrev			
***Bam*HI**	***Eco*RI**	***Xho*I**	***Sal*I**	***Bam*HI**	***Eco*RI**	***Xho*I**	***Sal*I**	***Bam*HI**	***Eco*RI**	***Xho*I**	***Sal*I**
18.9 Kb	24.7 Kb	14.5 Kb	19.2 Kb	6.6 Kb	6.6 Kb	6.1 Kb	6.6 Kb	18.9 Kb	24.7 Kb	14.5 Kb	19.3 Kb
7.2 Kb	6.1 Kb	13.8 Kb	6.9 Kb			523pb		8.8 Kb	6.1 Kb	12.7Kb	7.8 Kb
6.7 Kb	2 Kb	2.5 Kb	6.4 Kb					6.7 Kb	3.6 Kb	2.5 Kb	6.9 Kb
		1.4 Kb	375 pb							2.2 Kb	375 pb
		591 pb								1.4 Kb	
										591 pb	
										523 pb	

Table 5.1. Expected band lengths for the enzymatic digestions of parental and recombinant plasmids.

5.1.2. Production and purification of Ad5/ΦC31CreΨrev virus

Once generated, the Ad5/ΦC31CreΨrev genome was digested by *Pac*I (Figure 5.3) to linearize the viral genome, leaving the ITR regions exposed on both ends. The linearized plasmid was then transfected to a six-well plate of HEK-293 cells. 24 hours later, cells

were analyzed with a fluorescence microscope to assess whether they were correctly transfected and the vector expressed the RFP protein (Figure 5.4). 120 hours later, cells showed cytopathic effect and 3 freeze/thaw cycles were performed to release virions. Later, 50µl of the lysate were used to infect a 10-cm plate with HEK-293 cells and 120 hours later, the three freeze/thaw cycles were repeated. The total lysate was then used to infect twenty 15-cm plates. At 70 hours post-infection these cells showed no sign of cytopathic effect. However, since we expected the viral cycle to be near to 60 hours, the cellular fraction was collected and three freeze/thaw cycles were performed. Subsequently, two CsCl gradient ultracentrifugations were performed, showing two faint bands corresponding to the fraction of mature virions and virions in maturation process (Figure 5.5). The absence of cytopathic effect at 70 hours post-infection could suggest that the viral cycle of this vector could be slower than the similar *attB*-carrying vectors tested before, which ranged between 56 and 60 hours (Alba *et al*., 2007). Also, the low intensity of the obtained bands after the CsCl ultracentrifugation and the band corresponding to the non-mature virions being as intense as the band corresponding to the mature virions, supported this hypothesis.

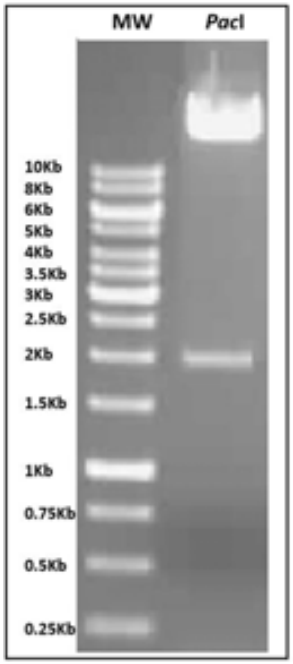

Figure 5.3. linearization of Ad5/ΦC31CreΨrev genome.

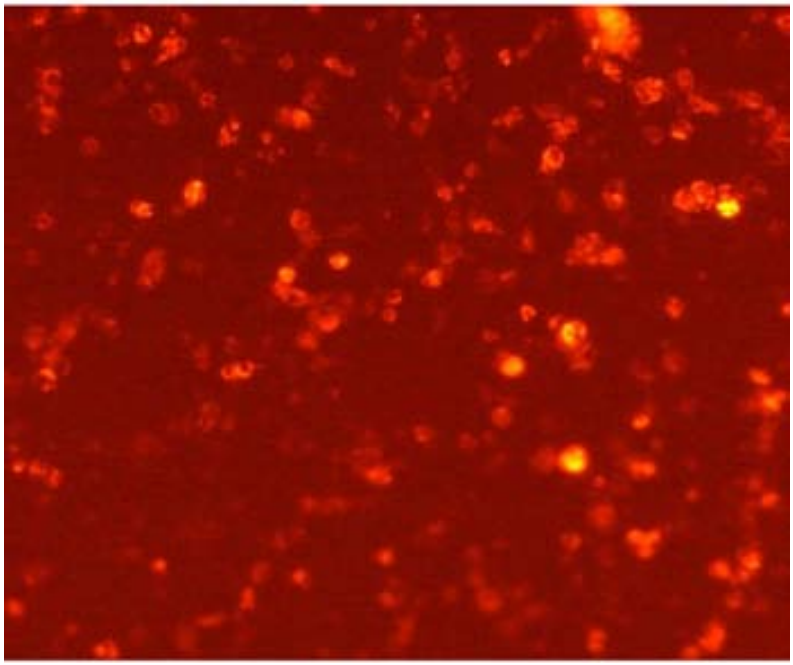

Figure 5.4. Ad5/ΦC31Ψrev RFP expression in HEK-293 cells. Image obtained by fluorescence microscopy.

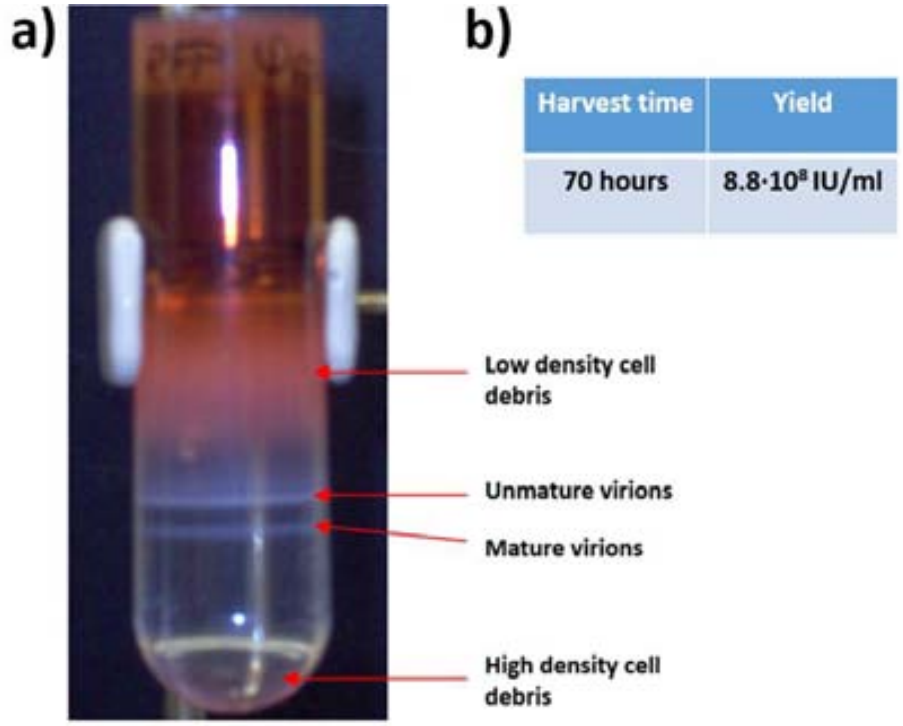

Figure 5.5. Production of Ad5/ΦC31CreΨrev. a) Viral bands after the first CsCl ultracentrifugation. b) Harvest time and production yield.

5.1.3. Production and purification of Ad5/ΦC31CreΨdir virus

To better characterize the properties of Ad5/ΦC31CreΨrev in terms of the length of its viral life cycle and its capacity to amplify HDAd, we used Ad5/ΦC31CreΨdir vector as a control, which differs only in the orientation of the packaging signal (direct). To this end, the Ad5/ΦC31CreΨdir plasmid was first digested by *Pac*I and then transfected to a six-well plate with HEK-293 cells. Once the transfection was confirmed by detecting RFP expression, two more amplification steps, consisting of the infection of a single 10-cm plate followed by an infection of twenty 15-cm plates, were performed. In agreement with the published results (Alba *et al*., 2007), the cytopathic effect appeared at 60 hours post-infection.

5.1.4. Analysis of the infective capacity of the Ad5/ΦC31CreΨrev in HEK-293 cells over time

In order to determine the pattern of RFP expression over time, HEK-293 cells were infected with a MOI=2 of Ad5/RFP, Ad5/ΦC31CreΨdir and Ad5/ΦC31CreΨrev, and were analyzed by fluorescence microscopy at different times post-infection. As observed in Figure 5.6, there is an important delay on RFP expression in Ad5/ΦC31CreΨdir and Ad5/ΦC31CreΨrev compared to Ad5/RFP. Also, Ad5/ΦC31CreΨrev showed a slightly delayed protein expression when compared to Ad5/ΦC31CreΨdir. These results are in agreement with the poor productivity of Ad5/ΦC31CreΨrev at 70 hours post-infection.

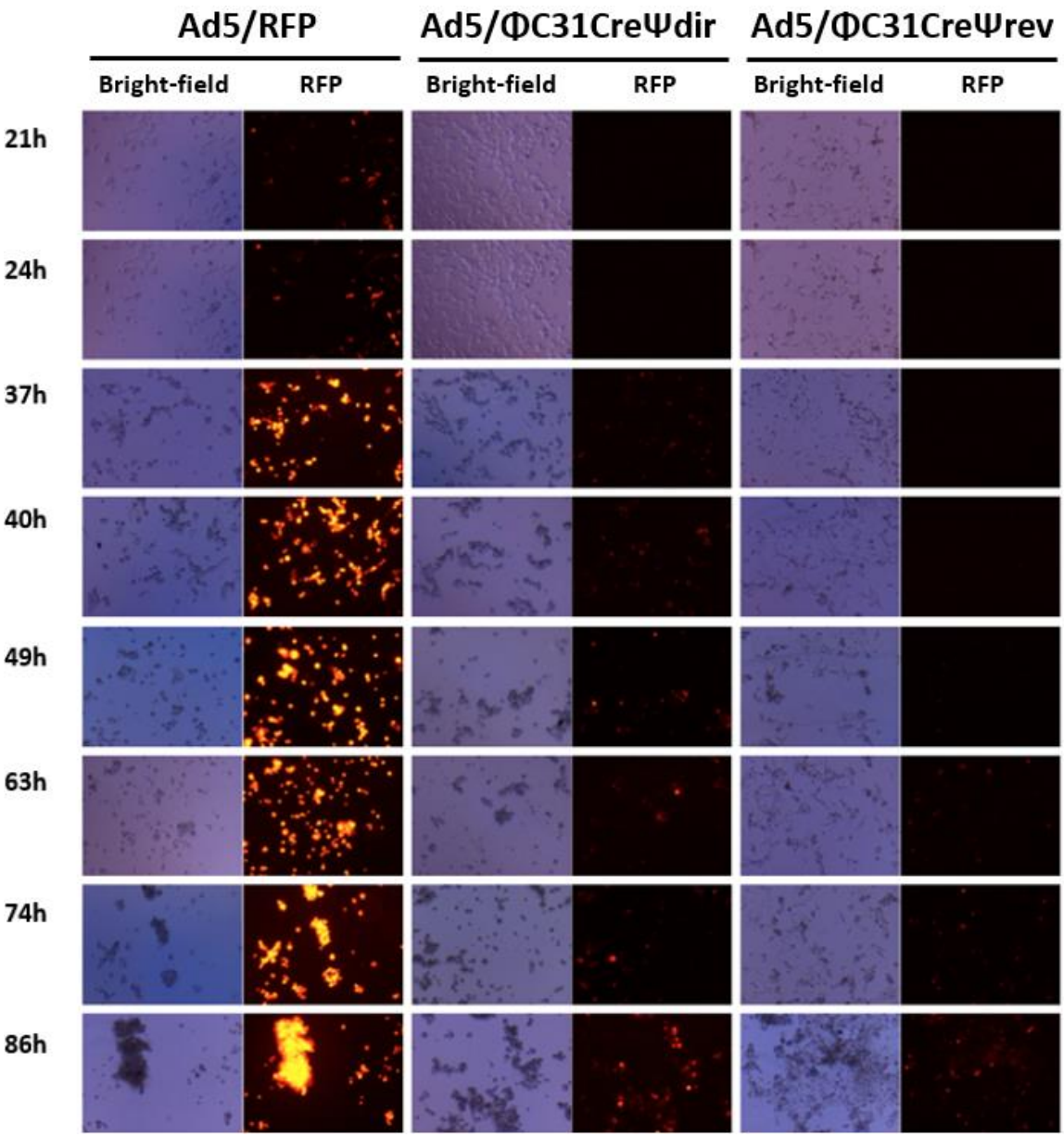

Figure 5.6. RFP expression at different times in human HEK-293 cells infected with Ad5/RFP (FGAd) and helper-Ad Ad5/ΦC31Ψdir and Ad5/ΦC31Ψrev. Cells were infected with a MOI=2.

5.1.5. Determination of the viral life cycle of Ad5/RFP, Ad5/ΦC31CreΨdir and Ad5/ΦC31CreΨrev vectors

In order to optimize HDAd production by taking advantage of the differential amplification between helper-Ad and HDAd, it was essential to determine the precise time needed to complete the viral life cycle. To this end, HEK-293 cells were infected with Ad5/RFP, Ad5/ΦC31CreΨdir and Ad5/ΦC31CreΨrev at MOI=5 and the samples obtained at different times post-infection were titrated.

A clear delay of the viral life cycle of Ad5/ΦC31CreΨrev can be observed when compared to Ad5/RFP (Figure 5.7). While Ad5/RFP shows a cycle of approximately 40 hours, Ad5/ΦC31CreΨrev has a viral life cycle similar to Ad5/ΦC31CreΨdir or slightly slower, with an increase of viral production starting at 60 hours post-infection and reaching its maximum at between 72 and 96 hours post-infection. After these results, the harvesting time of Ψ reverse vectors was set up at 78/80 hours post-infection, which allowed a 7-fold increase in the total productivity (from $8.8 \cdot 10^8$IU/ml to $6.4 \cdot 10^9$IU/ml).

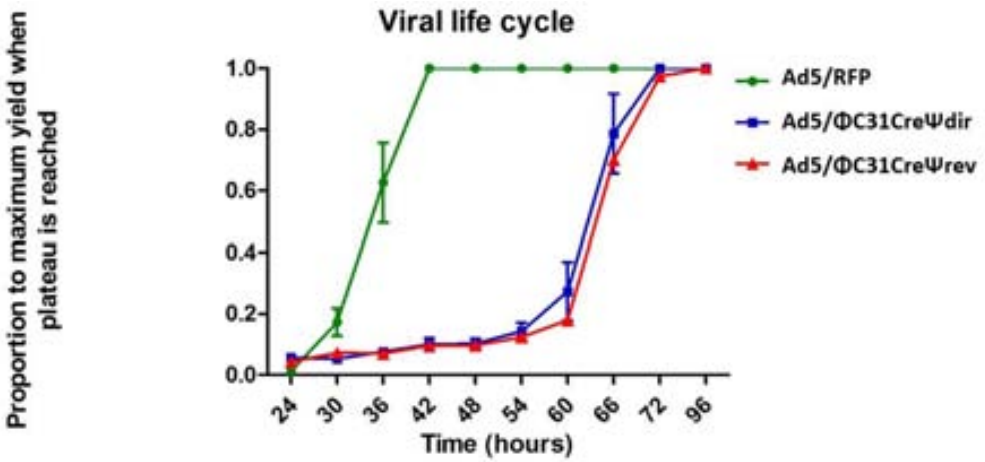

Figure 5.7. Viral life cycle of Ad5/RFP, Ad5/ΦC31CreΨdir and Ad5/ΦC31CreΨrev. Cells were infected with a MOI=5.

5.1.6. Amplification of helper-adenovirus in coinfection with control adenovirus

Once the virus was produced and the viral life cycle determined, we considered important to assess if the contribution of viral proteins by a FGAd could affect the viral cycle of the helper-Ad with the *attB* sequence. To this end, we performed an experiment

consisting of the infection of $1 \cdot 10^6$ HEK-293 cells with a MOI=5 of a) Ad5/ΦC31CreΨdir, Ad5/ΦC31CreΨrev, Ad5/GFP or Ad5/RFP alone, and b) helper-Ad (Ad5/RFP, Ad5/ΦC31CreΨdir and Ad5/ΦC31CreΨrev) coinfected with Ad5/GFP (MOI=5 each virus). Samples were analyzed at 40 hours post-infection.

As seen in Figure 5.8, when administered individually to the cells, both Ad5/ΦC31CreΨdir and Ad5/ΦC31CreΨrev viruses are poorly amplified, about two logarithms lower than control adenoviruses (Ad5/GFP, Ad5/RFP). When coinfected, production levels of all the vectors are statistically similar than when they are infected individually. However, after coinfection, *attB*-carrying vectors are not able to increase their productivity even in the presence of control non-*attB* FGAd vectors. Therefore, these data indicate that: a) the production titers of *attB*-helper adenovirus cannot be normalized by the supply of viral proteins expressed by control adenoviruses, and b) that control adenoviruses are not affected by the coinfection with the *attB*-helper viruses and thus, the differences observed in the production titers must be due to differences in their viral genome. These results correlate with previous experiments by Dr. Alba where the coinfection of Ad5/ΦC31CreΨdir with control non-*attB* FGAd vectors was studied, and suggest that the inversion of the packaging signal does not affect the amplification properties of helper-Ad.

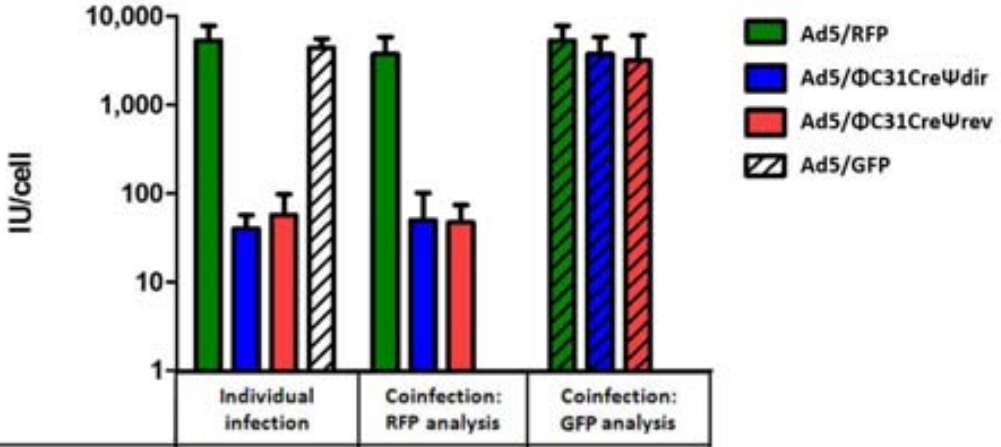

	Individual infection	Coinfection: RFP analysis	Coinfection: GFP analysis
Ad5/RFP	5310	3742	5310
Ad5/ΦC31CreΨdir	40	50	3760
Ad5/ΦC31CreΨrev	57	47	3170
Ad5/GFP	4380		

Figure 5.8. Coinfection experiments of Ad5/ΦC31CreΨdir, Ad5/ΦC31CreΨrev and Ad5/RFP with Ad5/GFP. Ad5/GFP titration is represented in dashed bars.

5.1.7. HDAd amplification using Ad5/ΦC31CreΨrev or Ad5/ΦC31CreΨdir as helper-Ads

After producing and characterizing the helper adenovirus Ad5/ΦC31CreΨrev, the next step was to produce a HDAd vector. To do this, we used the pFK7 plasmid, kindly provided by Florian Kreppel (University of Ulm), which corresponds to a HDAd encoding for the GFP protein (Figure 5.9a). To amplify this vector, the plasmid was linearized after digestion with *Pme*I (Figure 5.9b).

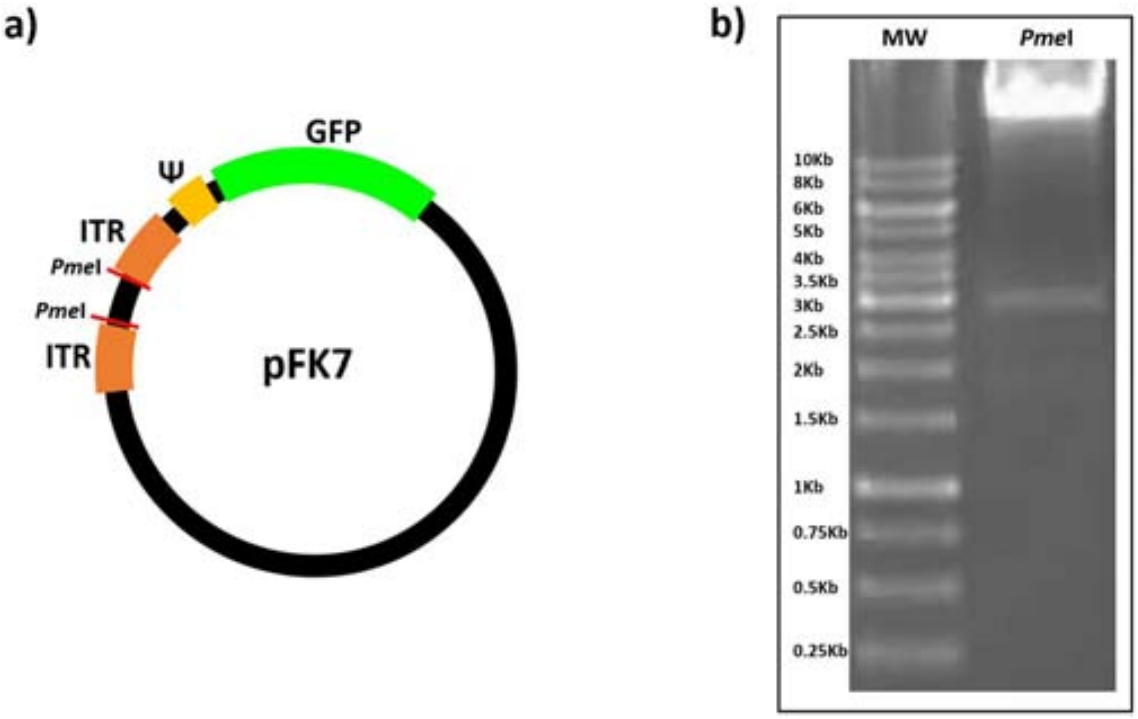

Figure 5.9. Digestion of pFK7 by *PmeI.* a) Scheme of pFK7. b) Electrophoresis analysis.

Consecutively, we transfected six-well plate wells with 3µg of this plasmid altogether with 3µg of linearized Ad5/ΦC31CreΨrev or Ad5/ΦC31CreΨdir plasmids. Transfected cells were harvested 5 days later. Titration of the samples indicated that high levels of HDAd were produced in both experiments, with a very low helper contamination (Figure 5.10). HDAd titration results were surprisingly high, but corresponded with the observation of the producer cells at 48 hours post-infection, that showed an intense expression of GFP in the totality of the cells, and a very low presence of RFP protein (nearly no cells with RFP expression). However, since these high production levels are infrequent, several transfections in parallel and selection of the best samples were needed to reproduce them.

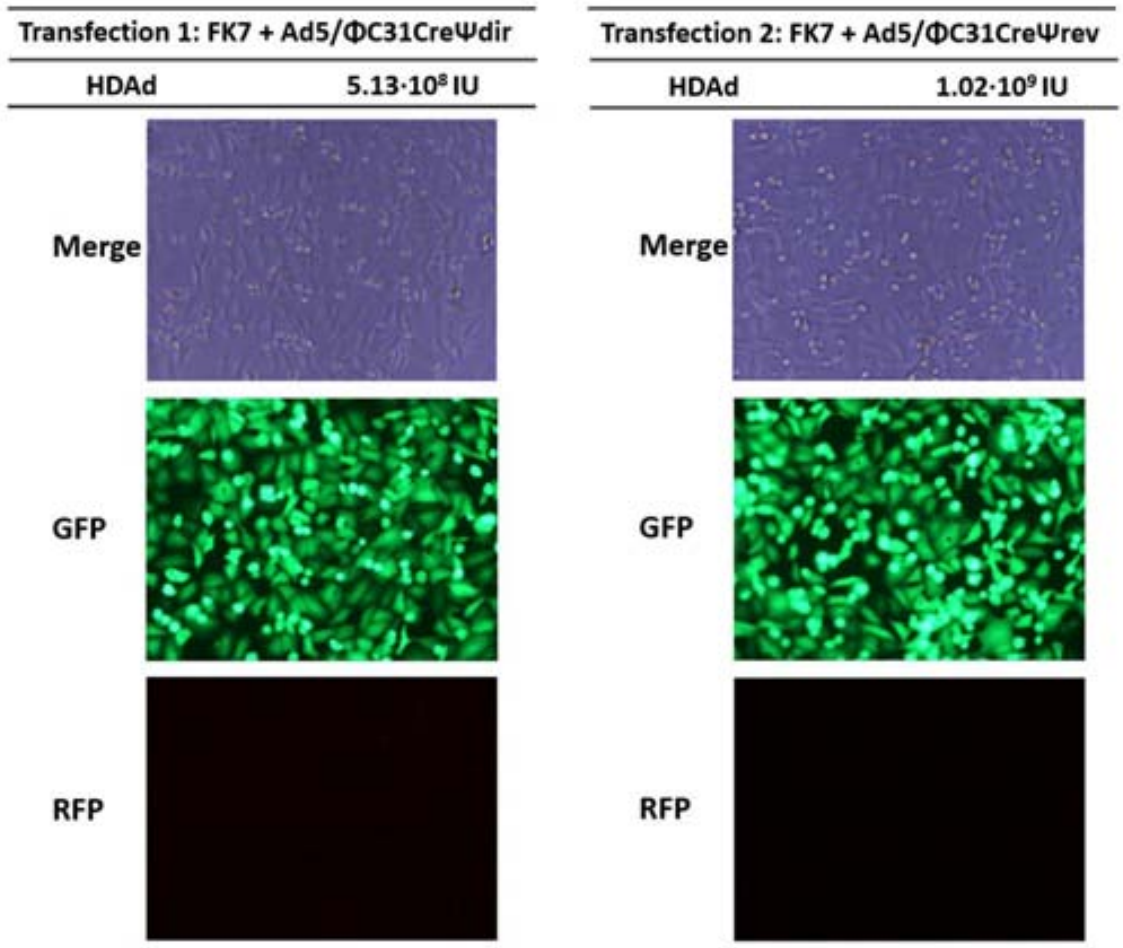

Figure 5.10. First step of helper-dependent adenovirus production. Tables above show results from a transfection of 3µg of both helper-dependent plasmid pFK7 (encoding GFP) and helper plasmid Ad5/Φ31Cre (direct or reverse Ψ) in a 6 well plaque using HEK-293 adherent cells. Images below taken by fluorescence microscopy show the infected HEK-293 cells.

After the first step of HDAd amplification was optimized, we considered that we had enough HDAd to scale to a final step of amplification. Then, we wanted to assess the possibility to perform the last amplification step in suspension cells, as they are easy to manipulate and, in contrast to adherence cells, allow the scalability of the procedure. To do this, we infected HEK-293 cells in suspension, with three different MOIs of helper-Ad (MOI=10, MOI=2 or MOI=0.5) and two different harvesting times (40 or 120 hours post-infection). We used a MOI=5 of FK7 in all the conditions, as we considered that this parameter had already been deeply studied (Dormond *et al*., 2009b).

As observed in Figure 5.11, when suspension cells were used, the best condition was to harvest the virus at 40 hours post-infection, with an initial inoculum of MOI=0.5 of the helper-Ad, regardless of the *attB*-helper-Ad used. Fluorescence microscopy images of this titration can be observed in Figure 5.12.

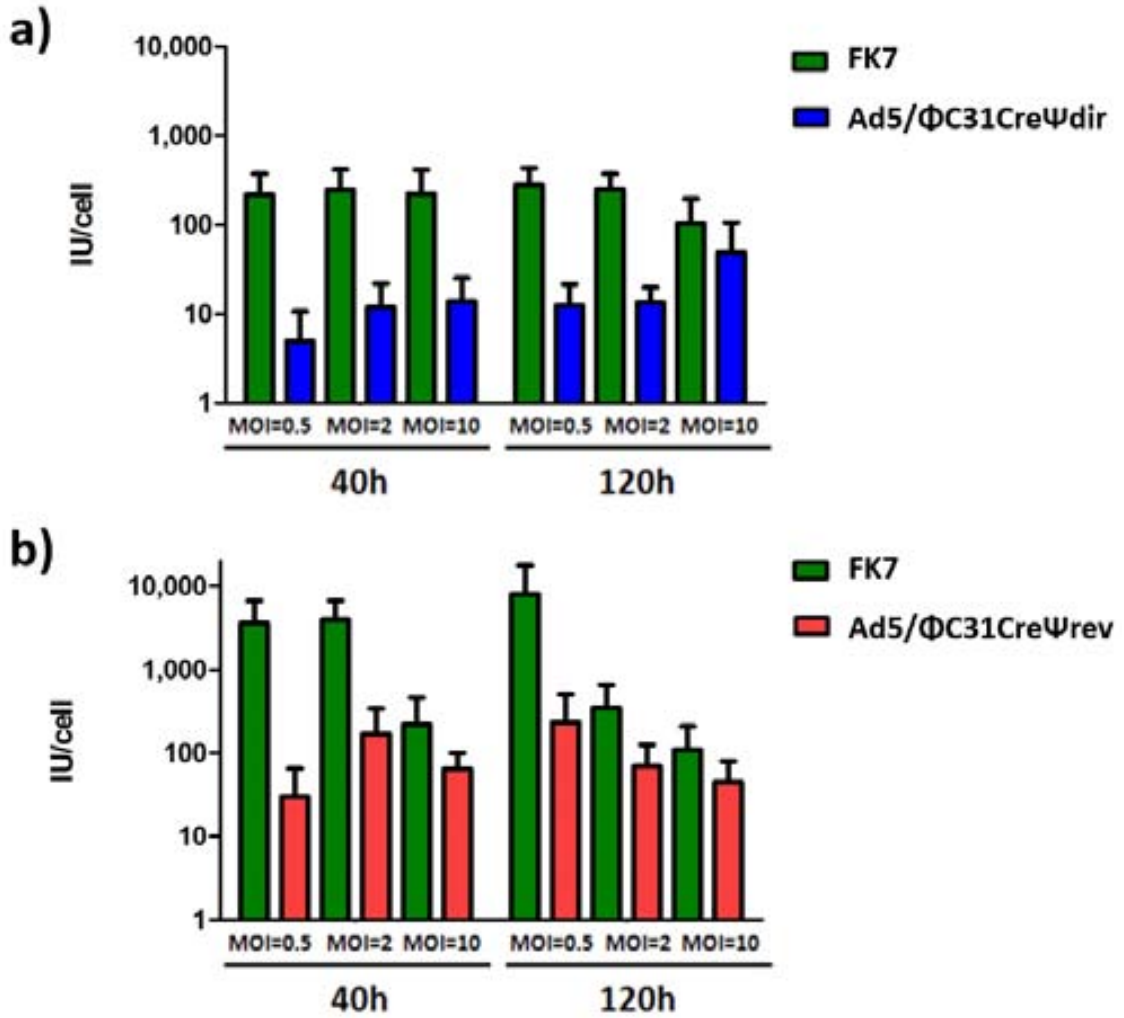

Figure 5.11. Optimization of the last amplification step in HEK-293 suspension cells. A MOI=5 of FK7 and a MOI=0.5, MOI=2 or MOI=10 of a) Ad5/ΦC31CreΨdir or b) Ad5/ΦC31CreΨrev were used. Cells were harvested at 40 or 120 hours post-infection.

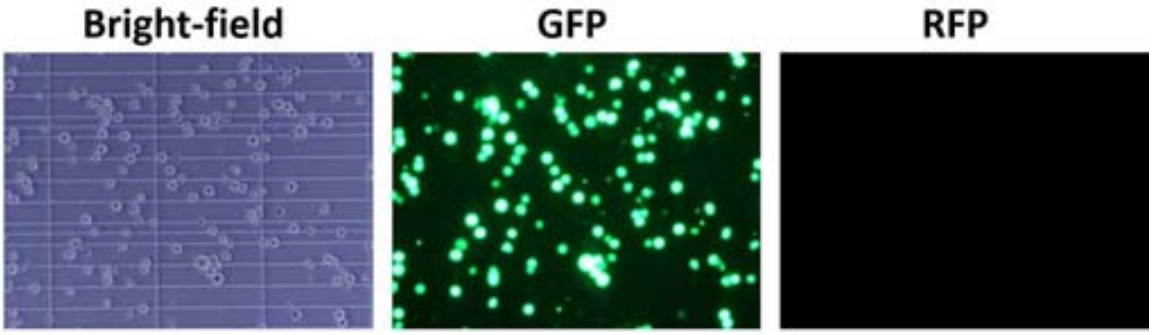

Figure 5.12. Titration of FK7 and Ad5/ΦC31CreΨrev in suspension cells (condition MOI=0.5 of helper-Ad and harvesting time at 40 hours post-infection).

In addition, we also performed a similar experiment but in HEK-293 adherent cells, to observe how they compare to suspension cells.

For this experiment, two different MOIs of helper-Ad (MOI=2 or MOI=0.5) and three different harvesting times were tested (36, 40 or 120 hours post-infection). Results indicate that the optimal condition was to add a MOI=0.5 of the helper-Ad and harvest the vector at 36 hours post-infection (Figure 5.13).

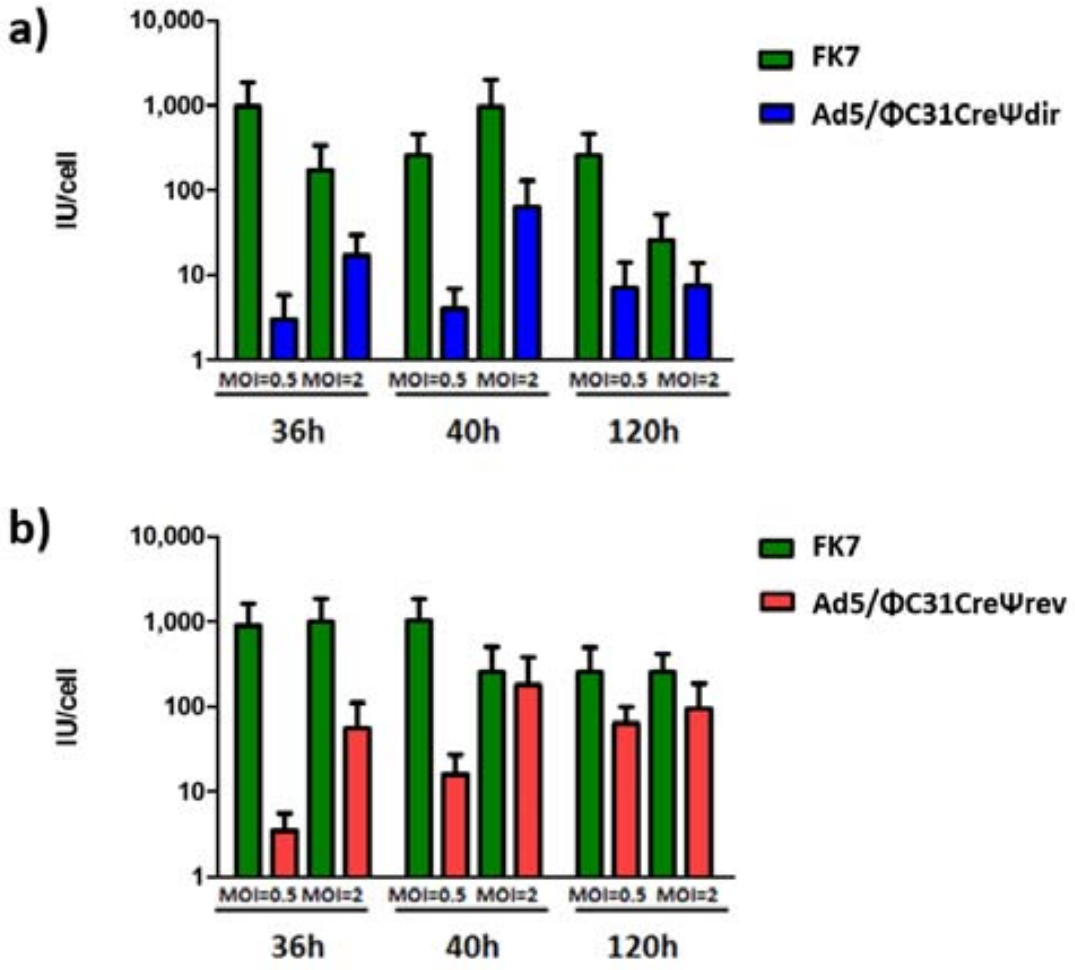

Figure 5.13. Optimization of the last amplification step in HEK-293 adherent cells. A MOI=5 of FK7 and a MOI=0.5 or MOI=2 of a) Ad5/ΦC31CreΨdir or b) Ad5/ΦC31CreΨrev was used, and cells were harvested at 36, 40 or 120 hours post-infection.

Overall, these results indicate that a) the viral yields are higher in HEK-293 suspension cells and b) viral yields decrease at long harvesting times, possibly due to cellular death or reinfection of cells with the newly generated adenovirus particles.

After this analysis, the last amplification step was performed using two flasks with 200ml of suspension HEK-293 cells (concentrated at 10^6 cells/ml) (Figure 5.14). Cells were infected with a MOI=5 of FK7 and a MOI=0.5 of the helper-adenovirus (Ad5/ΦC31CreΨrev or Ad5/ΦC31CreΨdir). Also, as a control, a third flask with 200ml of suspension HEK-293 cells was infected with a MOI=5 of FK7 and a MOI=0.5 of Ad5/RFP.

This last step of HDAd amplification in suspension cultures led to high levels of HDAd production with very low levels of helper contamination, indicating that the use of helper-Ad with the *attB* sequence and a reverse Ψ is a good strategy to produce HDAds.

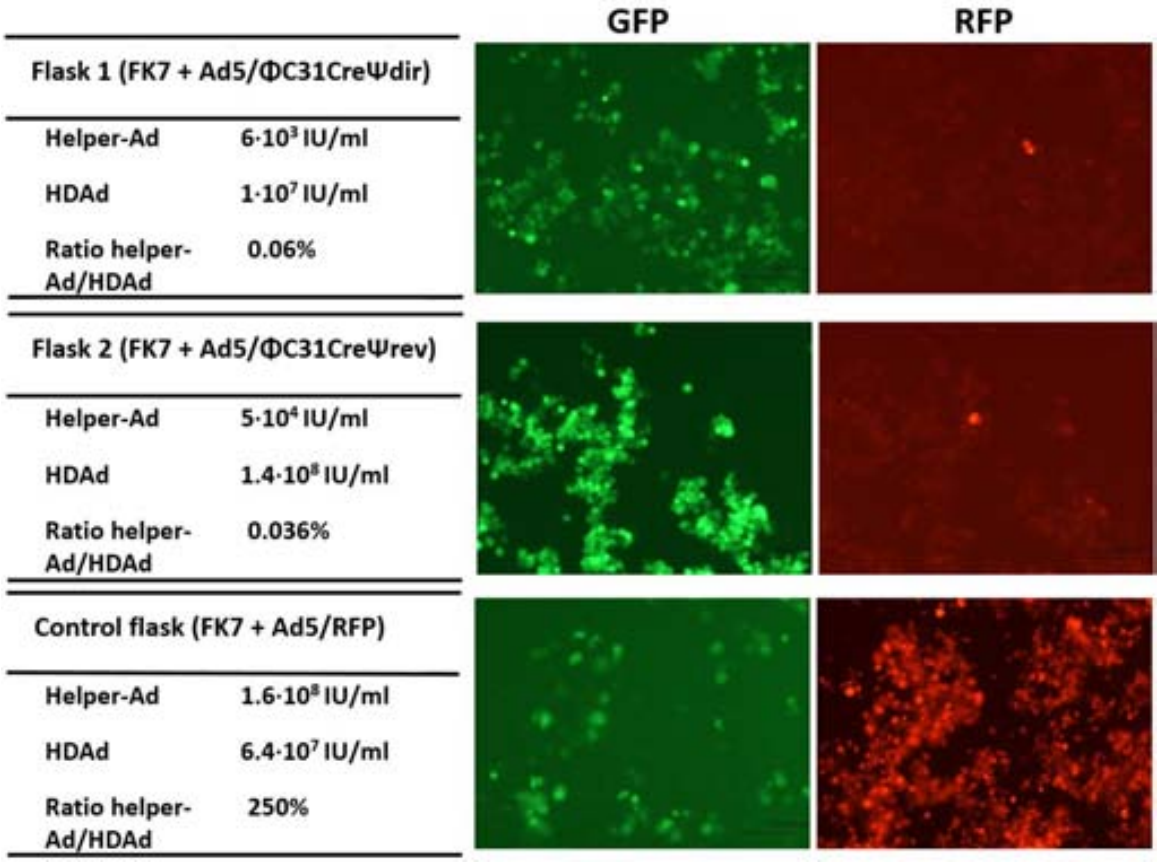

Figure 5.14. Second step of helper-dependent adenovirus production. On the left side, results from coinfection using MOI=5 of helper-dependent plasmid pFK7 (from the first production step) and a MOI=0.5 of helper plasmid Ad5/ΦC31Cre (direct or reverse Ψ) and Ad5/RFP (control flask) using 200 ml of HEK-293 suspension cells (total of 200 million cells per flask). End-point titration was analyzed at 96 hours post-infection. On the right side, fluorescence microscope images of suspension HEK-293 cells reflected the difference between both viruses, except in the control flask, where the helper-Ad titer is higher.

5.1.8. RCA detection analysis

After the final step of the amplification process, we assessed whether the recombination between the direct packaging signal of Ad5/ΦC31CreΨdir and FK7 had occurred, thus resulting in the generation of recombinant contaminant particles with the viral genome and a cell cycle similar to a first generation adenovirus. To this end, viral DNA was extracted from the crude lysate. Also, a PCR was performed using primers that bind at 5' and 3' of the packaging signal of both helper adenoviruses (Figure 5.15). No signs of recombination were observed, neither for Ad5/ΦC31CreΨrev or Ad5/ΦC31CreΨdir.

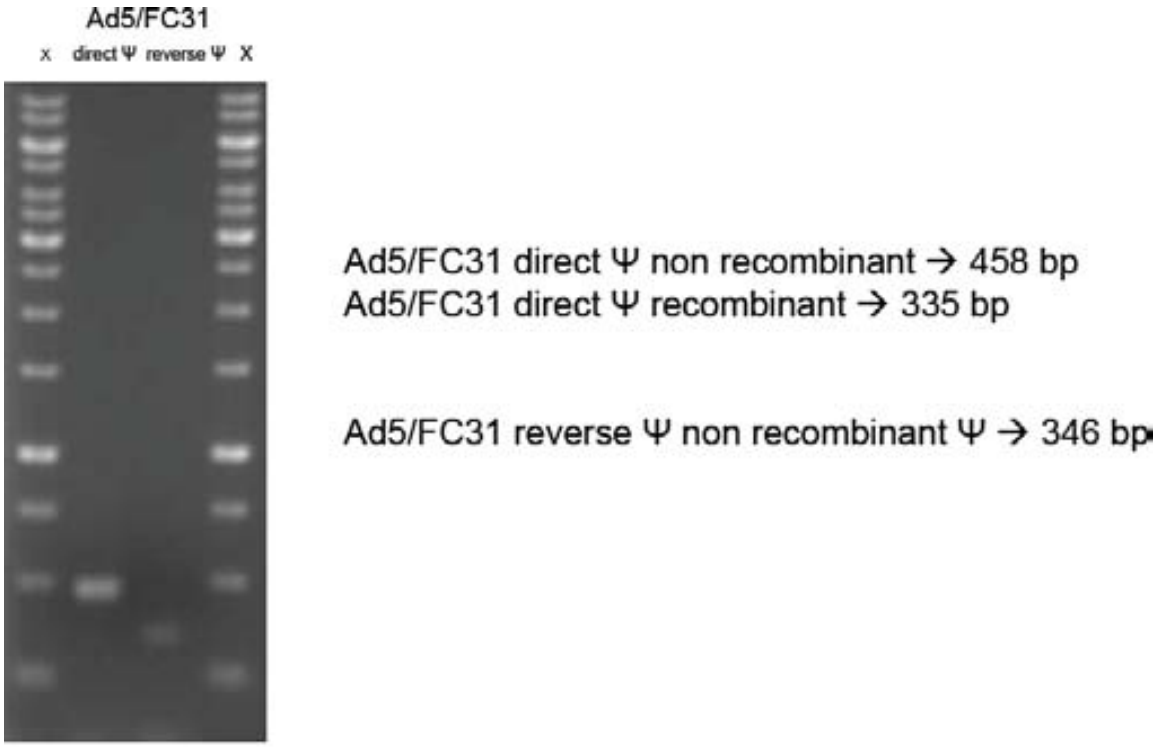

Figure 5.15. Electrophoresis of the DNA fragments obtained in the PCR to check the generation of RCA particles by recombination.

5.1.9. Intravenous injection of FK7 and Ad5/GFP to mice

In order to observe the infection capacity of the vectors *in vivo* and the ability to persist and express the transgene in liver, we intravenously injected $1 \cdot 10^{12}$ pp of HDAd/GFP (FK7) or FGAd (Ad5/GFP) via tail vein to 6 weeks old mice and analyzed GFP expression in liver at different times (1, 4 and 32 weeks post-injection). As seen in Figure 5.16, while the GFP expression on FGAd-injected mice decreases between one and four weeks post-injection, HDAd-injected mice show a sustained GFP expression until the end of the experiment (32 weeks post-injection). This suggests that, as expected, the levels of contaminating helper-Ad were sufficiently low to not induce cellular immune response against the transduced hepatocytes.

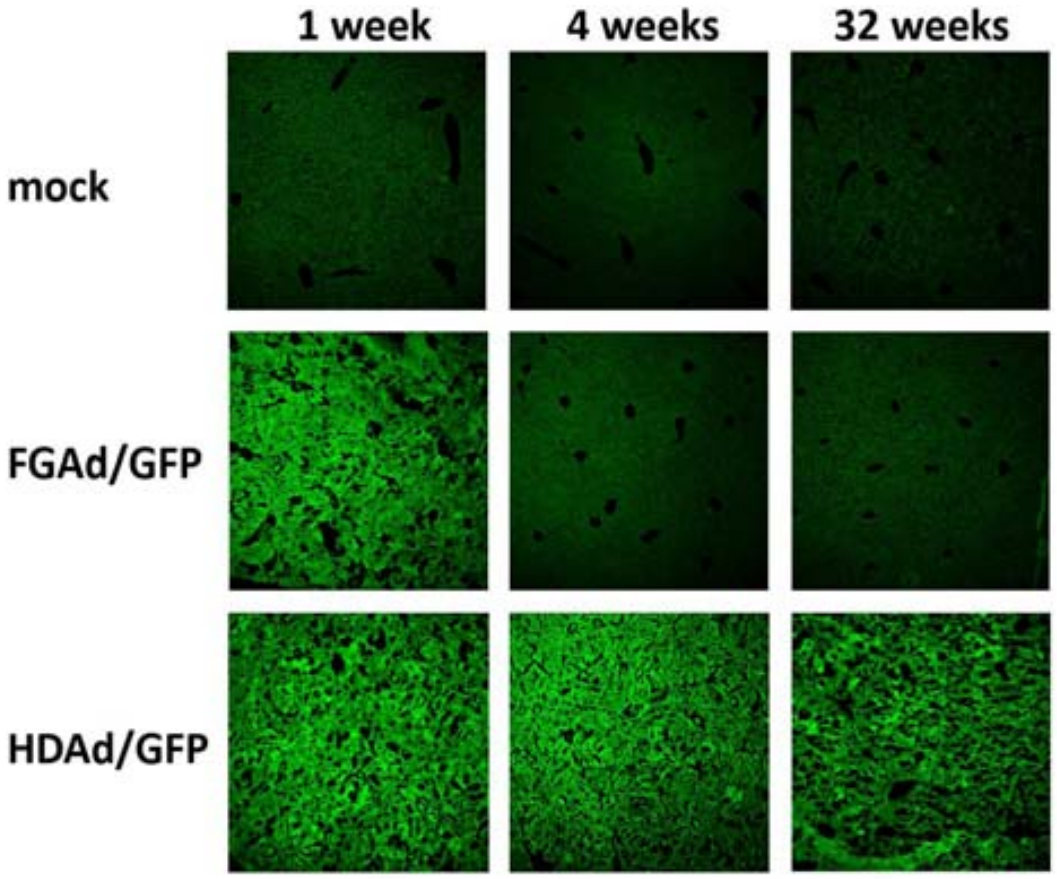

Figure 5.16. Fluorescence imaging of liver samples corresponding to mice injected with FGAd/GFP, HDAd/GFP or PBS (mock).

5.2. GENERATION AND PRODUCTION OF CHIMERIC HDAd5/F40S

5.2.1. Generation of pKP1.4ΔCMVF40S and pKP1.4 ΔCMVΦC31CreF40S

To assess whether the inclusion of the *attB* sequence could be also used to produce other human helper-dependent vectors, such as chimeric Ad5/F40S vectors, the pKP1.4ΔCMVΦC31CreF40S genome was generated. This helper-adenovirus encodes the gene of the short fiber protein of adenovirus 40, and it also has an *attB* sequence a 5' and two *loxP* sequences flanking the packaging signal. In order to analyze this vector in terms of length of its viral cycle and production capacity, we also generated a first-generation chimeric vector, pKP1.4ΔCMVF40S, which contains all the viral genes of a FGAd5 except for the Ad5 fiber protein gene, which is substituted by the short fiber protein of adenovirus 40 (Figure 5.17).

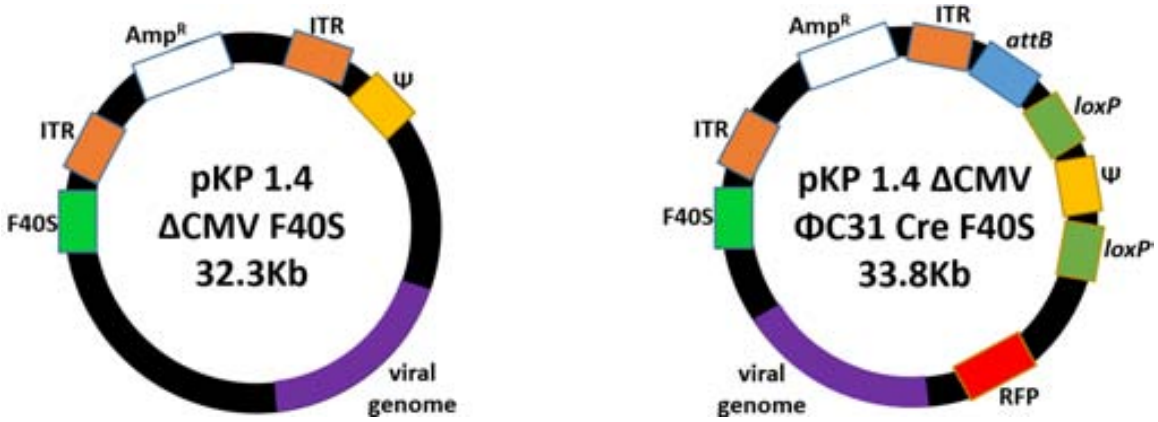

Figure 5.17. Graphic scheme of pKP1.4ΔCMVF40S and pKP1.4ΔCMVΦC31CreF40S. These plasmids were generated by enzymatic ligation and homologous recombination.

5.2.2. Determination of the viral life cycle of Ad5/ΦC31CreF40S

As for standard HDAd5 production, the viral life cycle of the chimeric Ad5/ΦC31CreF40S was determined to facilitate the optimization of the production. Also, this experiment is important to assess whether the viral life cycle delay mediated by the inclusion of *attB* is specific of Ad5 helper-Ad constructs, or it could be also applied to other adenovirus vectors. To this end, HEK-293 cells were infected with Ad5/RFP, Ad5/F40S and

Ad5/ΦC31CreF40S at MOI=5, and samples were harvested at different times post-infection.

A modest delay of the viral life cycle of Ad5/ΦC31CreF40S was observed when compared to Ad5/F40S (Figure 5.18). While Ad5/F40S has a viral life cycle of approximately 52 hours, Ad5/ΦC31CreF40S reaches its maximum production at approximately 56 hours post-infection. This suggests that its potential as vector is lower than helper-Ad5, and that probably, a combination of the *attB* and Cre-loxP strategies is needed to lower helper-Ad contamination.

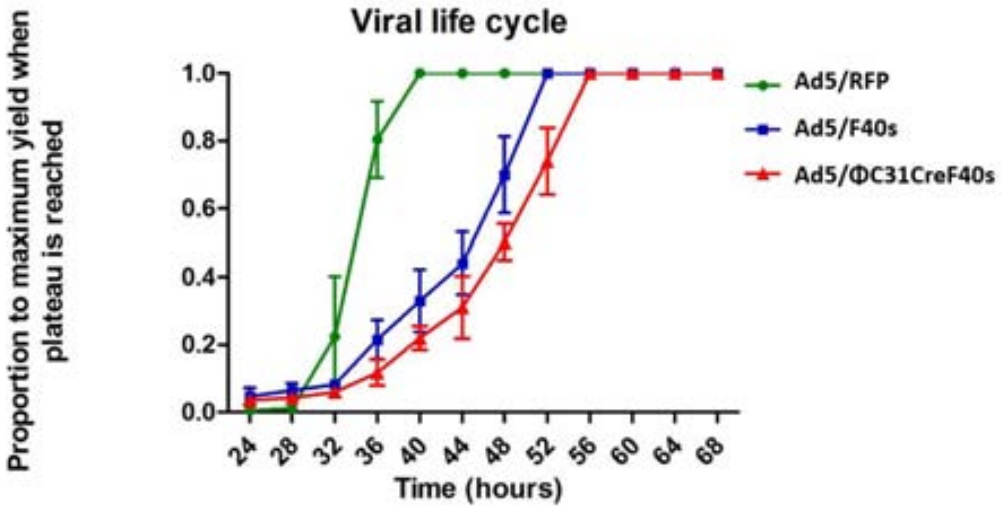

Figure 5.18. Viral life cycle of Ad5/ΦC31CreF40S. Ad5/RFP and Ad5/F40S are used as controls. Cells were infected with a MOI=5.

Since the production of Ad5/ΦC31CreF40S resulted in very low yields ($8.2 \cdot 10^8$ IU per twenty 15cm-plate production) we tested whether a) the use of polybrene, a polymer used to enhance viral infectivity, could increase its productivity and b) whether this would change the viral life cycle of this vector. To do this, HEK-293 cells were infected with Ad5/RFP, Ad5/F40S and Ad5/ΦC31CreF40S with or without polybrene at MOI=5, and samples were harvested at different times post-infection.

As observed in Figure 5.19a, comparison of the viral productivity per cell in the optimal harvesting times (40 hours for Ad5/RFP, 52 hours for Ad5/F40S and 56 hours for Ad5/ΦC31CreF40S with or without polybrene) indicated that while Ad5/ΦC31CreF40S yields are 3 logarithms below Ad5/RFP and 1.5 logarithm below Ad5/F40S, the addition to polybrene leads to a moderate increase in its yields (1.8-fold). Figure 5.19b shows

that the use of polybrene does not significativelly affect the viral life cycle of Ad5/ΦC31CreF40S and therefore, its use was reccomendable.

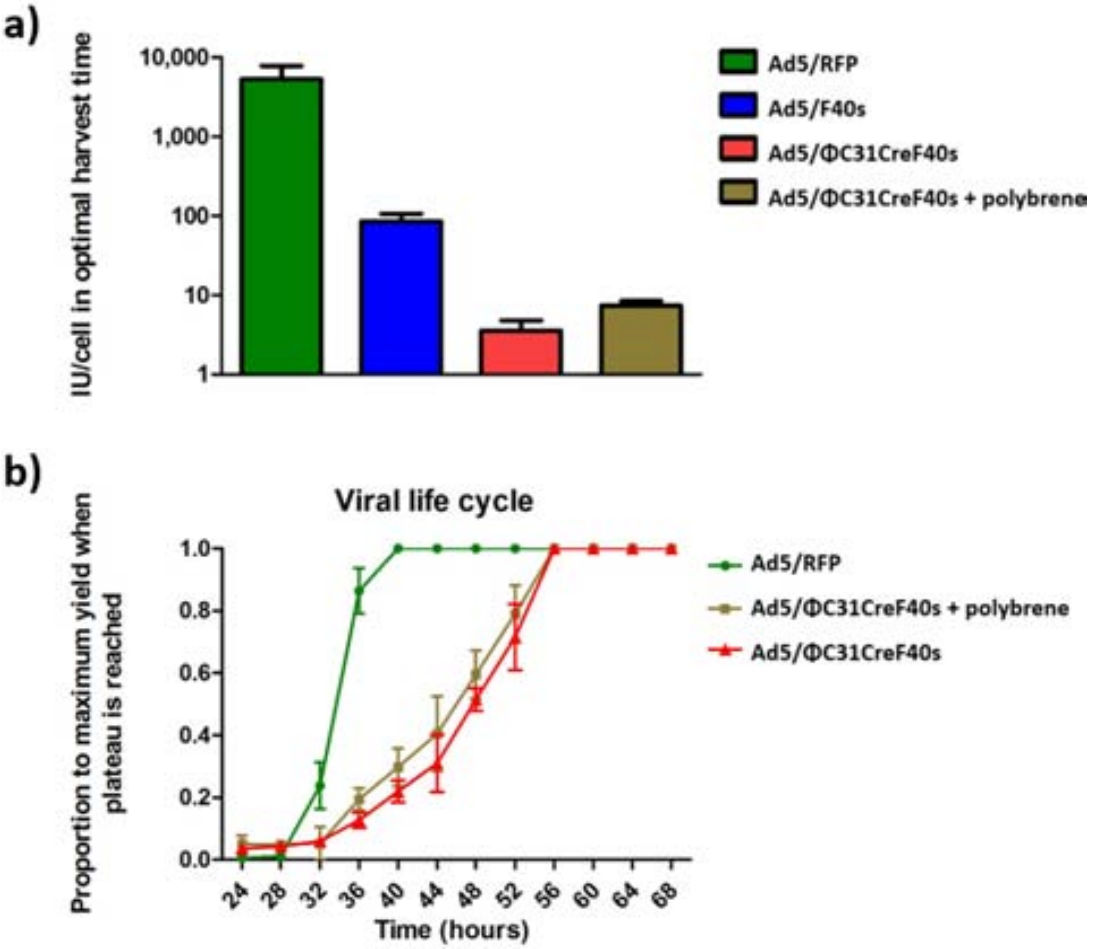

Figure 5.19. Use of polybrene to enhance Ad5/ΦC31CreF40S production yields. a) Comparison of the productivity of Ad5/RFP, Ad5/F40S and Ad5/ΦC31CreF40S (with or without polybrene) in optimal harvest time conditions and MOI=5 in HEK-293 cells. b) Viral life cycle of Ad5/ΦC31CreF40S + polybrene. Ad5/RFP and Ad5/ΦC31CreF40S without polybrene are used as controls.

5.2.3. HDAd production using Ad5/ΦC31CreF40S

Testing of different conditions to achieve maximum HDAd yelds and lower contamination indicated that the optimal conditions were to harvest the amplification steps at 60 hours post-infection. Since in intermediate steps, which were performed in parallel, the presence of helper-Ad contamination was not detrimental (as it did not overpass HDAd levels), we performed them using HEK-293 cells. In these amplification steps, at least 70% of GFP-expressing cells and 10-20% RFP-expressing cells were achieved. In case that RFP expression was low, samples were supplemented with a

MOI=1 of Ad5/ΦC31CreF40S. Finally, to test whether the use of cells that express the Cre recombinase could lower the helper-Ad contamination, the last amplification step was performed using HEK-293 cells or HEK-293Cre cells. Results in Figure 5.20 show that, the use of HEK-293Cre cells allow higher HDAd yields than HEK-293 cells (*$8{\cdot}10^8$ IU vs $1{\cdot}10^8$ IU respectively) and lead to lower helper-Ad contamination levels ($8{\cdot}10^6$ IU vs $2{\cdot}10^7$ IU respectively). Notably, the IU:pp ratio is low (1:500 to 1:2000).*

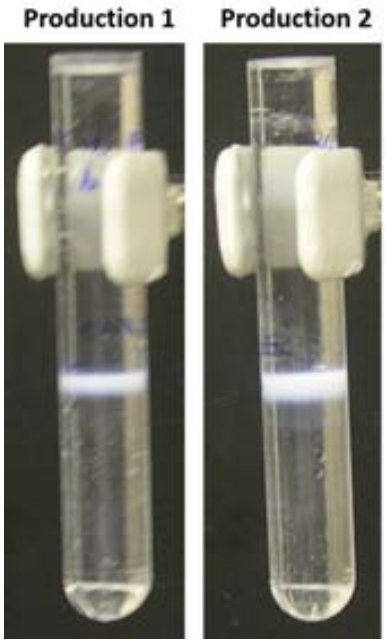

	Cells used	HDAd	Helper-Ad	Ratio Helper-Ad:HDAd
Production 1	HEK-293	$1{\cdot}10^8$ IU	$2{\cdot}10^7$ IU	1:5
Production 2	HEK-293Cre	$8{\cdot}10^8$ IU	$8{\cdot}10^6$ IU	1:100

***Figure 5.20. HDAd last amplification step using* Ad5/ΦC31CreF40S chimeric helper-Ad.**

5.3. OPTIMIZATION OF HDCAV-2 PRODUCTION USING *att*B-ΦC31 TECHNOLOGY

5.3.1. Generation and production of CAV-2/ΦC31CreΨ*

In contrast to human HDAd, the production of HDCAV-2 vectors is very inefficient. Usually, these productions rely on a synergy between a non-lethal mutation in Ψ (Ψ*) altogether with a Cre/*loxP*-mediated excision of Ψ*, which impairs the helper-CAV-2 amplification. However, the procedure is not optimized and between 6-10 amplification steps are needed, each one of them including cell sorting. On the other hand, given the success of the inclusion of the *attB* sequence in human helper-Ad to produce HDAd, we considered that the use of a helper-CAV-2 vector with the *attB* sequence could improve the efficiency of the current production protocol. For this reason, we generated CAV-2/ΦC31CreΨ*, a helper-CAV-2 with the *attB* sequence as well as a mutated packaging signal (Ψ*) and RFP gene surrounded by 2 *loxP* sequences (Figure 5.21).

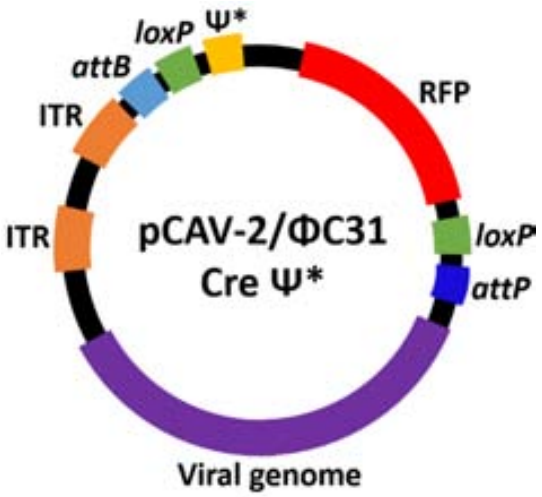

Figure 5.21. Plasmid representation of pCAV-2/ΦC31CreΨ*.

The production of the CAV-2/ΦC31CreΨ* helper-Ad (Figure 5.22) consisted initially of three steps of amplification in canine DKZeo cells (one 10-cm, three 15-cm and twenty 15-cm plates). In all steps, cells were harvested at 60 hours post-infection. However,

titration of the vector after the CsCl ultracentrifugation was very poor (2 ml at $2 \cdot 10^6$ IU/ml) and insufficient for our purposes.

Figure 5.22. Production of CAV-2/ΦC31CreΨ* helper vector. a) First production, amplification in 3 steps and harvest at 60 hours post-infection. Physical particles could not be calculated because the titer was lower than the spectrometer detection limit.

5.3.2. Determination of the viral life cycle of CAV-2/ΦC31CreΨ*

To be considered a good helper-Ad, the CAV-2/ΦC31CreΨ* vector should be able to efficiently amplify HDCAV-2 to high yields while maintaining its own production low. To determine if the inclusion of the *attB* sequence had an effect on the viral life cycle of CAV-2 viruses, an experiment to determine the viral life cycle was performed. As observed in Figure 5.23, the CAV-2/ΦC31 Cre Ψ* vector showed a delayed cycle (around 66 hours), while the FG CAV-2 vector (CAV-2/RFP) reached its peak around 54 hours post-infection, indicating that the inclusion of this sequence has the capacity of delaying the viral cycle also in CAV-2 vectors.

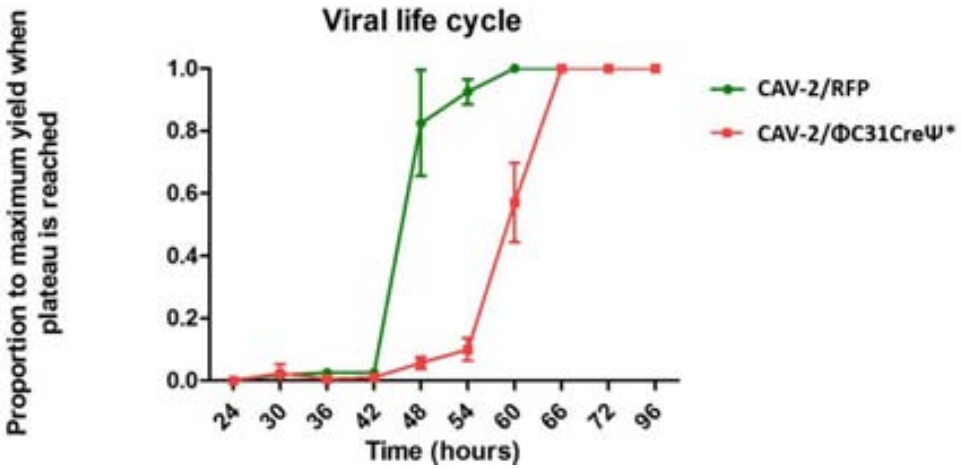

Figure 5.23. Viral life cycle of CAV-2/ΦC31CreΨ* helper vector. Cells were infected with a MOI=5.

5.3.3. Optimization of CAV-2/ΦC31CreΨ* production

To increase the production yields, a new strategy was performed, including an additional step of amplification (100x15-cms plates) and harvest at 72 hours instead of 60 hours (Figure 5.24). After CsCl ultracentrifugation, titration showed that despite of a slightly inefficient production, a clear improvement was observed (3 ml at $5 \cdot 10^8$ IU/ml), which should be sufficient for further characterization experiments of this vector. Notably, these results are consistent with the determination of the viral life cycle of these vectors at around 66 hours, as harvesting at 72 instead of 60 hours post-infection allowed a viral life cycle to complete, thus leading to a 50-fold increase in viral productivity.

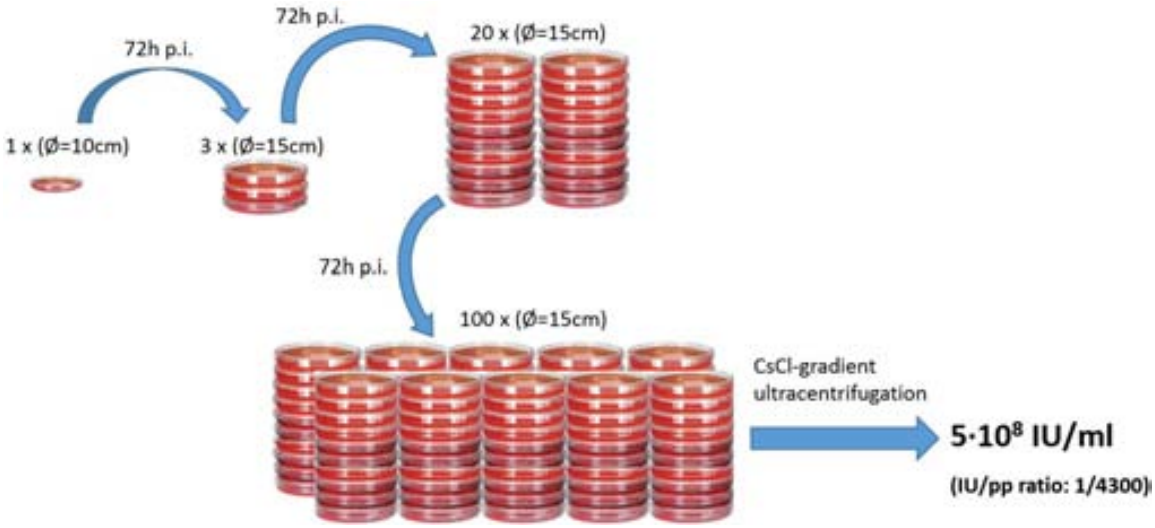

Figure 5.24. Optimized production of CAV-2/ΦC31CreΨ* helper vector. Second production of CAV-2/ΦC31CreΨ* helper vector, including a 4rth step of amplification with 100 x 15-cms plates. Harvest was performed at 72 hours post-infection.

5.3.4. Amplification of HDCAV-2 using CAV-2/ΦC31CreΨ* as a helper-CAV-2

To assess whether CAV-2/ΦC31CreΨ* helper-CAV-2 could be eligible for the production of HDCAV-2, we tested if it could efficiently amplify these vectors. To this end, DKZeo cells were transfected in a 6-well plate with 3µg of the linearized CAV-2/ΦC31 Cre Ψ* helper plus 3µg of the linearized GUSB, LRRK2*wt* or LRRK2* plasmids, which were generated at the CNRS of Montpellier and sent to our laboratory within the objectives of the European Brain-CAV project (FP7).

As seen in Figure 5.25, only few DKZeo cells were transfected, which is consistent with the very low transfection efficiency of DK cells. Since the presence of both helper-CAV-2 and HDCAV-2 genomes in the cells is required to amplify HDCAV-2, and there were only few cells transfected with both plasmids, the production titers of HDCAV-2 were too low to successfully scale the amplification steps (Table 5.2).

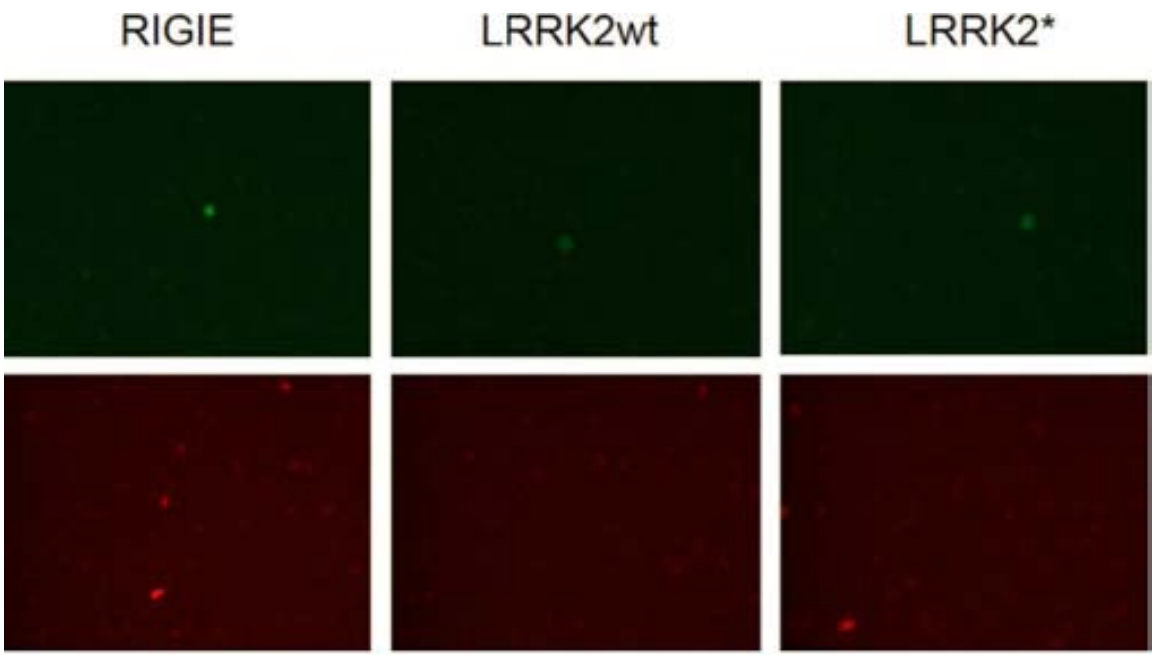

Figure 5.25. Observation of DKZeo cells at 36 hours post-transfection by fluorescence microscopy. GFP-positive cells indicate transfection by RIGIE, LRRK2*wt* or LRRK2*. RFP-positive cells indicate transfection by CAV-2/ΦC31CreΨ*.

RIGIE production		LRRK2wt production		LRRK2* production	
HDCAV-2	**Helper-CAV-2**	**HDCAV-2**	**Helper-CAV-2**	**HDCAV-2**	**Helper-CAV-2**
$2 \cdot 10^3$IU/ml	$8 \cdot 10^4$IU/ml	$1 \cdot 10^3$IU/ml	$6.5 \cdot 10^4$IU/ml	$4 \cdot 10^3$IU/ml	$2.1 \cdot 10^5$IU/ml

Table 5.2. Titration results of the double transfection step.

After this non-successful double transfection strategy, we wanted to assess if a single transfection of HDCAV-2 followed by an infection by the helper-CAV-2 would facilitate HDCAV-2 amplification, by ensuring that most or all transfected cells would be infected by the helper-CAV-2 and therefore would be able to amplify HDCAV-2.

To this end, DKZeo cells were transfected in a 6-well plate with 3µg of the linearized CAV-2/ΦC31CreΨ* helper plus 3µg of the linearized GUSB, LRRK2*wt* or LRRK2* plasmids and infected with three different MOIs of CAV-2/ΦC31CreΨ* helper-Ad (MOI=0.5, MOI=2 and MOI=5). Cells were harvested at 44 or 88 hours post-infection. The highest titers of HDCAV-2 were obtained when the cells were infected with a MOI=2 of helper-CAV-2 and cells were harvested at 44 hours post-infection (Table 5.3).

In this experiment, HDCAV-2 titers were higher than when the double transfection protocol was used. However, they were still too low for further amplification steps, as the volume required to reach a sufficient MOI of HDCAV-2 which would largely exceed the plate capacity. In this regard, despite exhaustive conditions were tested, none of them could increase HDAd production yields and lower helper-Ad contamination.

RIGIE production		**LRRK2wt production**		**LRRK2* production**	
HDCAV-2	**Helper-CAV-2**	**HDCAV-2**	**Helper-CAV-2**	**HDCAV-2**	**Helper-CAV-2**
$3 \cdot 10^4$IU/ml	$1.5 \cdot 10^6$IU/ml	$1.7 \cdot 10^4$IU/ml	$4 \cdot 10^6$IU/ml	$8.8 \cdot 10^3$IU/ml	$3.2 \cdot 10^6$IU/ml

Table 5.3. Titration results of the infection + transfection step. Cells were transfected with 6µg of HDCAV-2 linearized plasmid and infected with a MOI=2 of helper-CAV-2. Cells were harvested at 44 hours post-infection.

Overall, these low production yields confirmed that the combination of a mutated packaging signal and the presence of *attB* on this vector genome leads to a difficult production as well as to its incapability as a helper vector of HDCAV-2.

5.3.5. Comprobation of the ΦC31 recombinase activity of DKZeo-ΦC31 cells

In parallel, we assessed whether Ψ* excision by ΦC31, a recombinase that specifically excises the DNA fragment between the *attB* and *attP* sites, could be a good strategy to reduce CAV-2/ΦC31CreΨ* contamination levels in HDCAV-2 productions. To do this DKZeo-ΦC31 (clones 2 and 3), two DKZeo-modified cell lines that constitutively express ΦC31 recombinase were generated in our laboratory.

To evaluate their ΦC31 recombinase activity, 15-cm plates containing these cell lines were transfected in duplicated with pTJB19ΦC31CreGFP (shuttle plasmid containing the *attB* sequences) and pJB19 (control shuttle plasmid with CAV-2 genome but without *attB* sequences). Forty-eight hours later, the viral genomes were extracted as described in Methods, 4.1.7. Subsequently, after linearizing the plasmids with *Xmn*I, a Southern blot was performed, using a specific probe for the canine Ad-helper 5'ITR (present in both plasmids).

The entire pTJB19ΦC31CreGFP plasmid has 5808bp. In case an excision mediated by the ΦC31 recombinase occurred, a 3710bp band would appear. The control pJB19 plasmid is 2600 pb long.

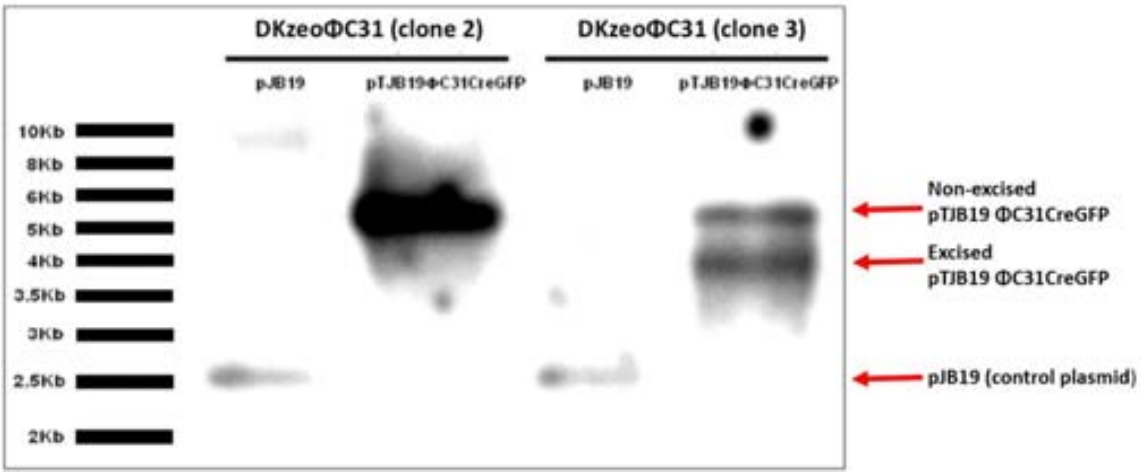

Figure 5.26. Southern blot against the ITR region of pJB19 and pTJB19ΦC31CreGFP plasmids. A 3710 pb band corresponding to the excised pTJB19ΦC31CreGFP plasmid can be observed on the DNA samples extracted from DKZeo ΦC31 (clone 3) cells but not on the ones extracted from DKZeo ΦC31 (clone 2) cells.

As observed in Figure 5.26, there is an absence of recombinase activity 48 hours post-transfection in DKZeo ΦC31 (clone 2) cells, but indicates that there is recombinase activity in DKZeo ΦC31 (clone 3). However, the analyzed activity (57%) does not allow an efficient or complete excision of Ψ and therefore, the use of these cells to amplify HDCAV-2 was discarded.

5.3.6. HDCAV-2 amplification using coinfection with helper-CAV-2 JBΔ5 and FACS + cell sorter

After discarding CAV-2/ΦC31 Cre Ψ* helper-CAV-2 to amplify HDCAV-2 as well as DKZeo-ΦC31 cells, we checked the potential of another helper-CAV-2 vector (JBΔ5) for HDCAV-2 production. This vector expresses the β-galactosidase as a reporter protein, and its production is impaired by its mutated packaging signal and the *loxP* sites located at 3' and 5' of it (Figure 5.27).

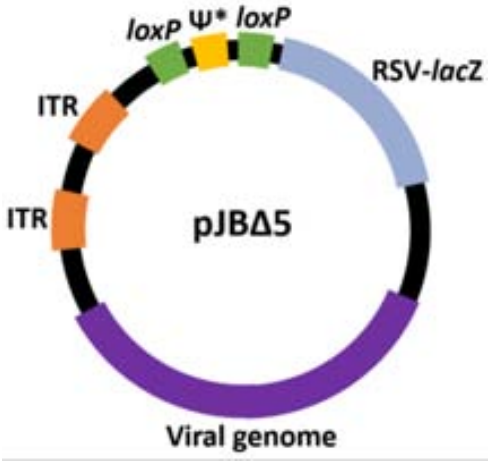

Figure 5.27. Scheme of pJBΔ5.

Initially, pJBΔ5 was used by the laboratory of Dr Kremer to amplify the HDCAV-2 vectors named RIGIE and HDmax, carrying the GUSB:GFP and GFP genes respectively. However, the methodology used was very inefficient and time consuming, and involved several (6 to 10) steps consisting of: a) infection in DKCre cells and b) cells sorting of the GFP expressing cells (Figure 5.28).

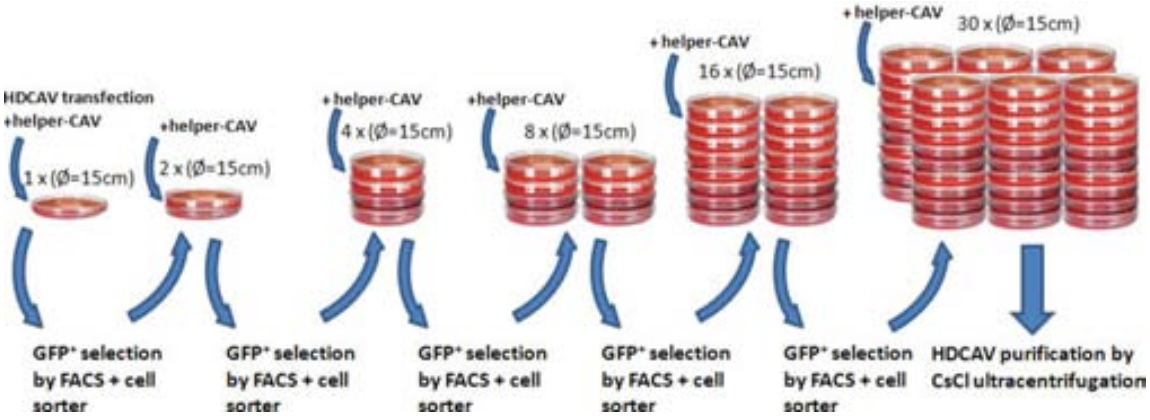

Figure 5.28. Amplification of HDCAV-2 using the FACS and cell sorter method. This strategy often involves 6 to 10 amplification steps as the production yields after each cycle is poor (1.5x to 2x HDCAV-2 enrichment per step). If required, a MOI=5 of helper-CAV-2 is added at the beginning of each step of amplification.

The main drawbacks of this strategy was that the overall process was very tedious, as the FACS + cell sorting required a notable amount of time and, HD-CAV-2 were only enriched 1.5 to 2-fold per step, therefore requiring an important number of steps to obtain a reasonable viral amplification. In addition, toxicity of the infected DKCre cells through the process was very high.

To set up this method in our laboratory, 15-cm plates of DKCre cells were infected with a MOI=5 of RIGIE or HDmax vector and a MOI=5 of helper-CAV-2 JBΔ5. At 24 hours post-infection medium was discarded and cells were trypsinized and resuspended in 1X PBS, and immediately after cells were sorted to separate the cells infected with the HDCAV-2 (GFP positive) from those that were not. Due to the natural tendency to aggregate and adhere of DKCre cells, the cell sorting process was very tedious (it took nearly 4 hours to process a single 15-cm plate), as the sorter was continuously blocked. Overall, cell sorting detected a total of 781288 events, only 33080 of them were GFP positive and therefore sorted separately from the rest. Sorted cells were then plated with growth medium (DMEM with 2% FBS and 1% non-essential amino acids), incubated for 12 hours more and harvested. Notably, these cells showed an absence of GFP expression and a lytic aspect, indicating that the process could have been too aggressive for them (Figure 5.29). Notably, this idea was supported by the absence GFP-positive cells when the crude lysate was titrated by end-point titration.

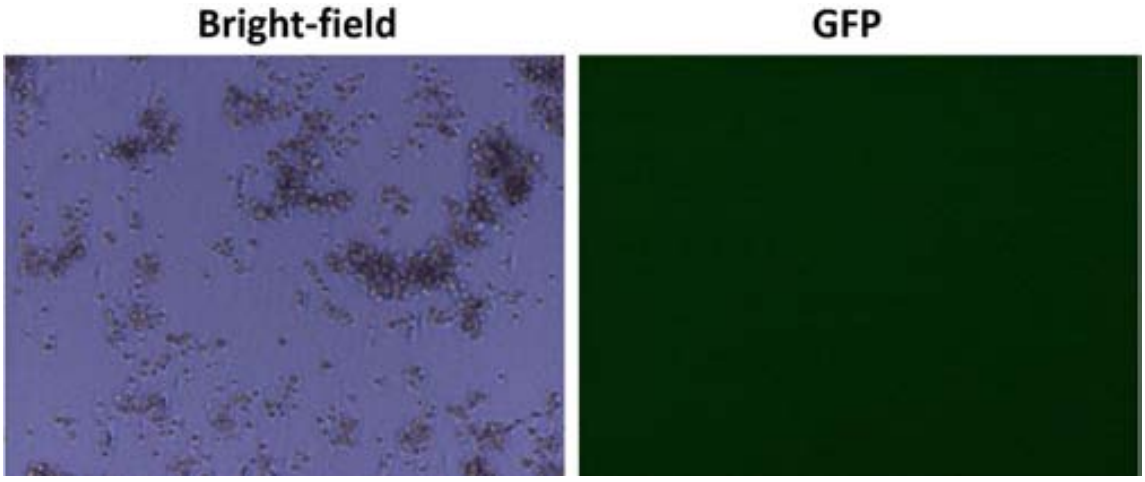

Figure 5.29. DKCre cells after the sorting process. Microscopy imaging show a lytic aspect of the sorted cells, without any detectable presence of GFP expression.

However, we wanted to assess the possibility that these cells amplified the vectors, but its GFP expression was too low to be detected by a fluorescence microscope.

To answer this, DKZeo cells were infected with viral samples obtained from the cell-sorting process and 36 hours later, cells were trypsinized and analyzed by FACS (Figure 5.30). As observed in the titration, no GFP-expressing cells were detected. This, together with the lytic aspect that DKCre cells had after cell sorting (Figure 5.29) suggests that sorted GFP expressing cells had probably died during cell sorting and/or could not amplify the vectors due to the aggressive conditions of this procedure.

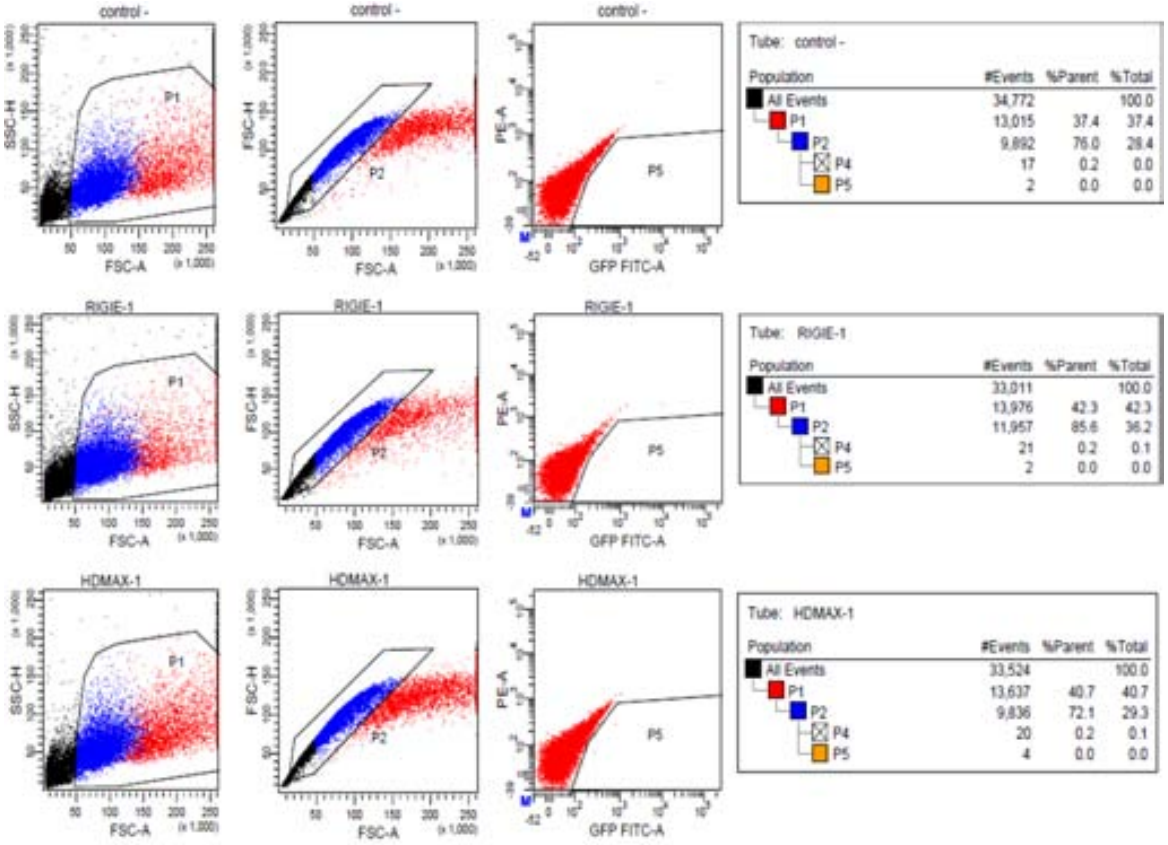

Figure 5.30. FACS analysis of trypsinized non-infected DKZeo cells (control -) or infected with RIGIE or HDmax.

Given the poor outcome of this procedure as well as not being a scalable method we discarded its optimization. Instead, we decided to amplify HDCAV-2 vectors focusing on the optimization of each individual amplification, as done for human HDAd vectors.

5.3.7. HDCAV-2 titration

In order to develop an optimized strategy for the amplification of HDCAV-2 vectors, we decided to develop a precise titration method from crude lysate samples since we had observed wide variability depending on the assays.

In the end-pont dilution assay at low dilutions, more than one infective unit is expected to infect each cell. At higher dilutions, the number of infected cells decrease to reach one I.U. per cell, which is generally accepted to happen when the number of infected cells is between 5% to 10% of the total number of cells. From this point and for subsequent dilutions, the number of positive cells tends to linearly correlate with the dilution from this point. For example, if there is 1000 positive cells in a well and the following dilution is 1/10, we would expect the next well to have around 100 positive cells, and then 10 and 1 for the next dilutions.

This can be observed when titrating purified CAV-2 and Ad vectors (Figure 5.31a), and also when titrating crude lysates of Ad5, but surprisingly this is not observed when titrating crude lysates of CAV-2 vectors (Figure 5.31b). Fortunately this is not crucial to titrate FGCAV-2 vectors, since the amplification is well set up and optimized and titration of intermediate amplification steps is not needed. However, this is a critical issue for HD-CAV-2 vectors where the titration of intermediate steps to evaluate the conditions to be used in following steps must be done. Unfortunately, no linearity in the end-point dilutions assays for crude lysates of HDCAV-2 was observed. Thus, as seen in Figure 5.31b, at 36 hours post-infection the number of cells expressing the reported gene did not correlate with the dilutions performed, which avoided an accurate titration.

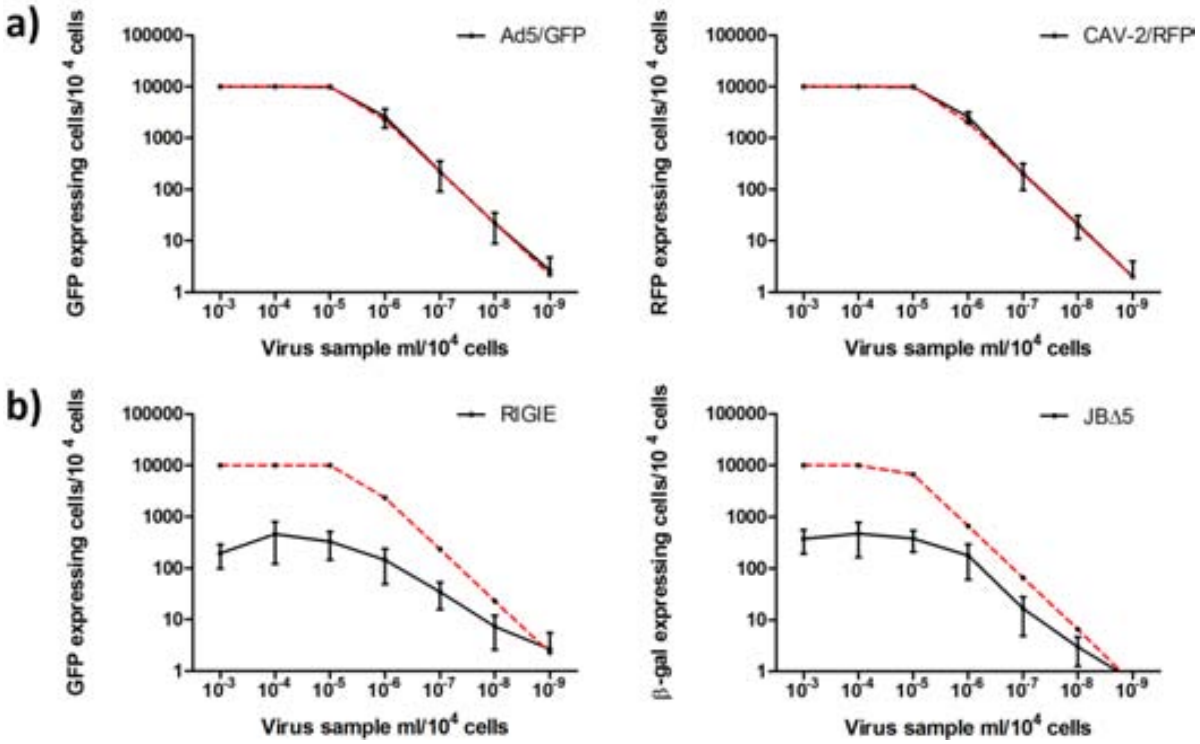

	10^{-3}ml	10^{-4} ml	10^{-5} ml	10^{-6} ml	10^{-7} ml	10^{-8} ml	10^{-9} ml	Titration
Ad5/GFP	S	S	S	2610	335	22	2.3	$2.2 \cdot 10^{9}$ IU/ml
CAV-2/RFP	S	S	S	2550	200	21	2	$2 \cdot 10^{9}$ IU/ml
RIGIE	195	462	329	145	34	7	2.6	$3.2 \cdot 10^{8}$ IU/ml?
JBΔ5	378	473	381	178	16	3	0.6	$1.6 \cdot 10^{8}$ IU/ml?

Figure 5.31. Titration results of RIGIE and JBΔ5 in a) purified vectors Ad5/GFP and CAV-2/RFP or b) crude lysate of RIGIE and JBΔ5 amplification steps. Dotted lines correspond to the expected titration pattern considering the highest dilution counting. S: saturation (between 80 to 100% GFP-positive cells).

While for the titration of control Ad (Ad5/GFP and Ad5/RFP), the final titration results could be obtained by a simple multiplication of the number of cells per well per its dilution factor, the titration of CAV-2 vectors would immensely vary depending on the dilution point considered.

Because of their poor precision and high variability (Segura *et al.,* 2010), CAV-2 titrations are usually performed using other titration methods that do not rely on the detection of the reporter gene expression by fluorescence microscopy, like the detection of physical particles by absorbance at 260nm, qPCR or $TCID_{50}$ titration. However, the detection of pp by absorbance at 260nm cannot be used to titer crude lysates. We also discarded qPCR because we were interested in titrating the infective particles present in a sample,

in order to define the conditions for the following amplification steps. Therefore, we focused on the $TCID_{50}$ titration. In addition, to facilitate comparison we first analyzed crude lysate samples of FGCAV-2 vectors (as JBΔ5). As observed in table 5.4, the end-point dilution analysis of crude lysate samples clearly underestimates titration by at least one if not two logarithms, while values from purified vectors for an end-point $TCID_{50}$ analysis are at the same range.

	End-point dilution	$TCID_{50}$	pp by optical density
JBΔ5 (crude lysate)	$1.6 \cdot 10^8$ IU/ml	$1.9 \cdot 10^{10}$ IU/ml	n/a
JBΔ5 (purified virus)	$8.5 \cdot 10^9$ IU/ml	$2.3 \cdot 10^{10}$ IU/ml	$1.7 \cdot 10^{12}$ pp/ml

Table 5.4. Comparison between titration of JBΔ5 from crude lysate or purified virus by end-point dilution and $TCID_{50}$ analysis.

It is important to mention that, even though we were aware that titration by the observation of the reporter gene was highly inaccurate, there was no alternative to it at that point, since $TCID_{50}$ can only titrate helper-CAV-2, but not HDCAV-2 vectors as they do not replicate neither cause cytopathic effect. Therefore, the development of an alternative strategy to titer the infectivity of these vectors was highly desirable.

5.3.8. Determination of viral titers by qPCR in purified samples

In order to precisely quantify the infective titers of both, HDCAV-2 and helper-CAV-2 vectors in both crude lysate samples and purified viral batches, a qPCR-based titration method was also developed. Usually, qPCR methods quantify the vector genomes of samples pretreated with DNAse I, but this detects both infective and non-infective virions. To avoid this, the viral samples were used to infect HEK-293 suspension cells, which do not allow the replication of CAV-2 genomes, and 24 hours later the vector genomes found in the cellular extracts were quantified. This approach seems to be more relevant since titration reflects the infectivity of the viral sample.

First, a set of primers (CAV-2 set 1) amplifying a small genomic fragment of CAV-2 pVI-hexon at the 5' end of the CAV-2 viral genome and previously designed in our laboratory

(Segura *et al*., 2010) was used to quantify helper-CAV-2 genomes. Then, a second set of primers (designed in this work) amplifying a fragment of the DNA stuffer region that is common in both RIGIE and HDmax HDCAV-2 vectors was also used (Table 5.5).

Primer	Orientation	Sequence (5' to 3')	Amplicon size (bp)
CAV-2 set 1	*Forward*	CGT GAA GCG CCG TAG ATG C	185
	Reverse	GAA CCA GGG CGG GAG ACA AGT ATT	
HDCAV-2 stuffer	*Forward*	TCTCTACCCGATGTGACC	217
	Reverse	GAACTCAGGGAGTCCAGAATGT	

Table 5.5. Primer sequences tested.

Once the primers were established, it was important to test if they could be used to amplify viral DNA from 1) purified virus prepations, 2) cellular extracts from infected HEK-293 suspension cells (Figure 5.32).

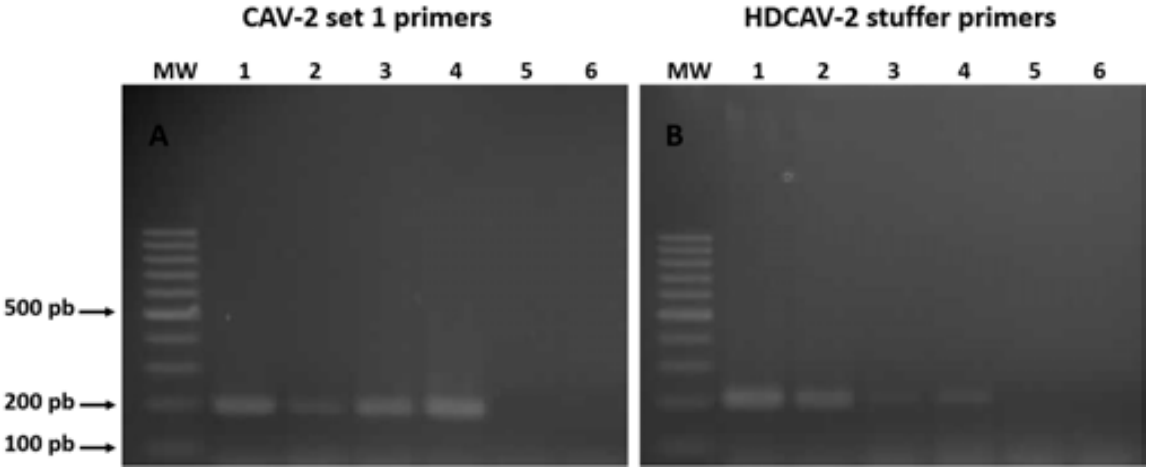

Figure 5.32. Agarose DNA electrophoresis showing the amplicons obtained by PCR. Results were obtained using two different sets of primers (HDCAV-2 stuffer and CAV-2 set 1) and samples from different origin: 1) crude lysate from RIGIE amplification step, 2) crude lysate from HDmax amplification step, 3) cellular extracts from RIGIE amplification step, 4) cellular extracts from HDmax amplification step, 5) non-infected cellular extracts and 6) negative control.

To assess if these primers could be used to amplify by qPCR samples from cellular extracts using the SYBR green polymerase, a qPCR amplification experiment using 120ng of infected cellular extracts/reaction and HDCAV-2 stuffer or CAV-2 set 1 primers was performed. However, results showed a total absence of DNA amplification for both

primer sets and all replicates. Then, we wanted to determine if there was an element in the cellular extracts that interfered the qPCR reaction and, in that case, to set the optimal conditions for qPCR amplification using cellular extracts. To do this, we performed an experiment consisting of a qPCR assay using 1ng or 0.24pg of a plasmid coding for the E1-deleted CAV-2 vector genome (pJB19) spiked in different dilutions of non-infected cellular extracts ranging from 120 to 0.94 ng (Table 5.6).

Results indicate that in the process of extracting cellular extracts there is a factor that interferes with the qPCR reaction, totally inhibiting the qPCR reaction when 120 or 60 ng of cellular extracts are added per reaction. Also, it is important to mention that when the amount of cellular extracts per reaction is 15 ng or less no inhibition of the qPCR is observed.

Condition	**0.24 pg of pJB19 plasmid**	**1 ng of pJB19 plasmid**
120 ng of cellular extracts	0 Ct	0 Ct
60 ng of cellular extracts	0 Ct	0 Ct
15 ng of cellular extracts	21.25 Ct	14.41 Ct
3.75 ng of cellular extracts	21.41 Ct	14.78 Ct
0.94 ng of cellular extracts	22.19 Ct	17.11 Ct
Without cellular extracts	21.66 Ct	14.69 Ct

Table 5.6. qPCR assay results using 0.24 pg or 1 ng of *pJB19* plasmid and different dilutions of non-infected cellular extracts. Ct = Threshold cycle.

Then, we generated a standard curve to quantify FGCAV-2 vectors with precision. Cellular extracts from HEK-293 suspension cells infected with different dilutions of JBΔ5 were analyzed by qPCR using the CAV-2 set 1 primers (Figure 5.33).

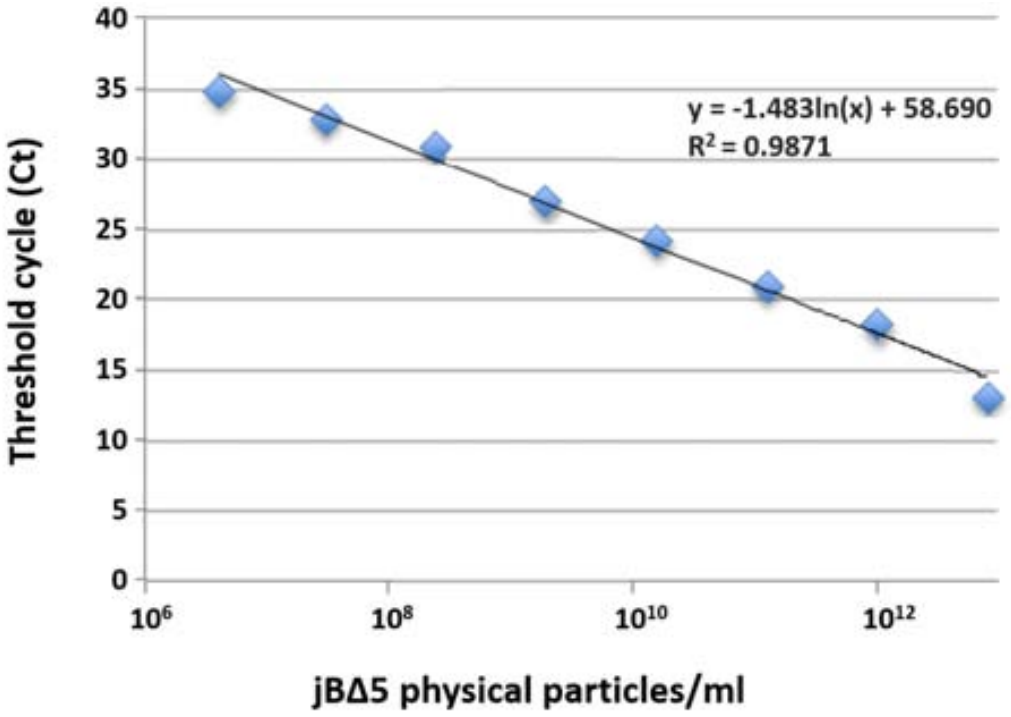

Figure 5.33. JBΔ5 standard curve linearity and sensitivity. The curve was generated by qPCR quantitation using cellular extracts from HEK-293 suspension cells infected with 1 µl of a 8-fold dilution series of JBΔ5, ranging from $3.8 \cdot 10^6$ pp/ml to $8 \cdot 10^{12}$ pp/ml.

Also, even though a calibration curve cannot be obtained for a HDCAV-2 because of the absence of a pure and properly titrated sample of this vector, the generation of DNA primers specific to the stuffer region of HDCAV-2 allowed the comparison between HDCAV-2 productions in terms of which production has a higher concentration of HDCAV-2.

5.3.9. Optimized amplification of HDCAV-2 vectors

Since we only had access to a few microliters of RIGIE and HDmax viruses in crude lysate, we performed the first amplification step in a single well of a 24-well plate, infecting DKCre cells with a MOI=5 of RIGIE or HDmax and a MOI=5 of JBΔ5.

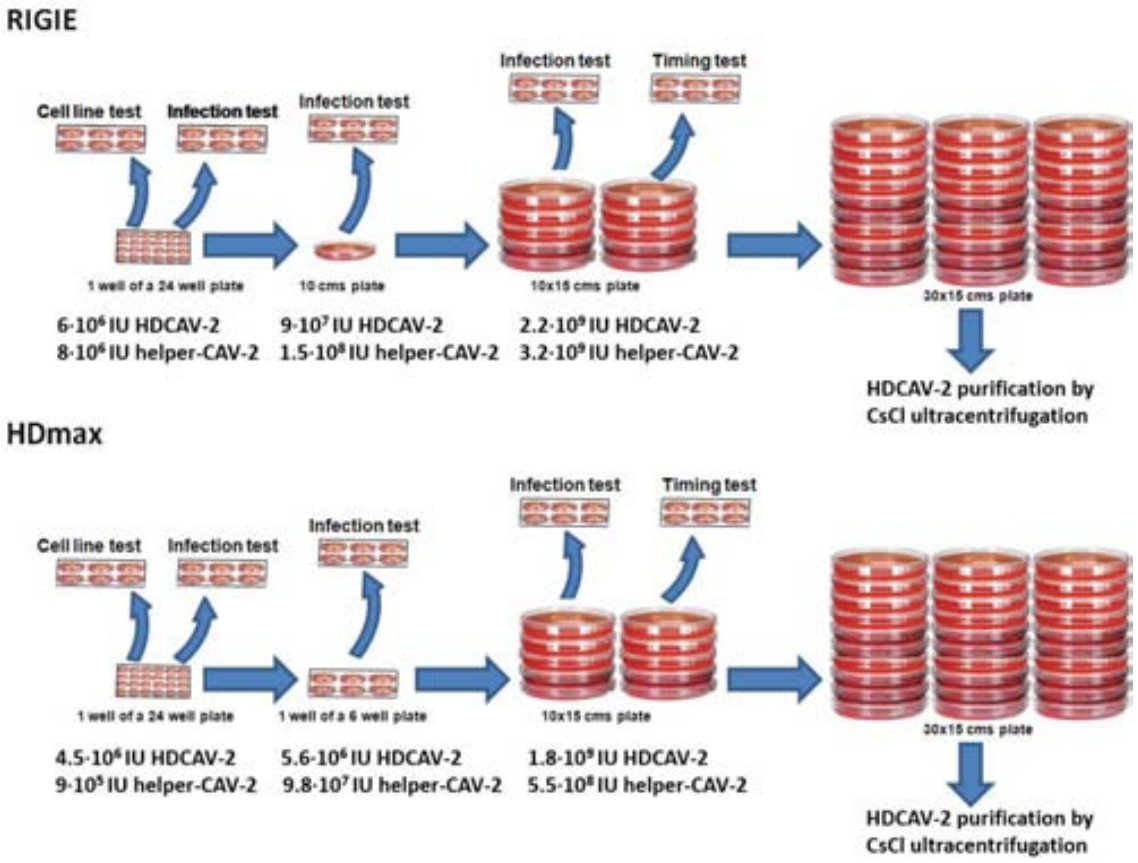

Figure 5.34. Overview of RIGIE and HDmax amplification. Since conventional end-point titration by microscopy was not a reliable method, before each step of amplification an infection test was done with different dilutions of the viral production and the optimal condition was determined by the newly generated qPCR titration method. Also, an experiment to assess which cell line produced better yields was performed after the first step of amplification and an experiment to assess if production times lower than 36 hours could improve the HDCAV-2/helper-CAV-2 ratio was performed before the last step of amplification.

After the first amplification step we wanted to assess if the use of DKCre instead of DKZeo cells could improve HDCAV-2 production by increasing HDCAV-2 yields and/or lowering the helper-CAV-2 contamination.

For the amplification of the RIGIE vector, results of this analysis indicated that, while the yields of HDCAV-2 were similar, the levels of helper-CAV-2 were slightly lower when

DKCre cells were used (Figure 5.35). For the amplification of HDmax vector, the values were similar for both cells.

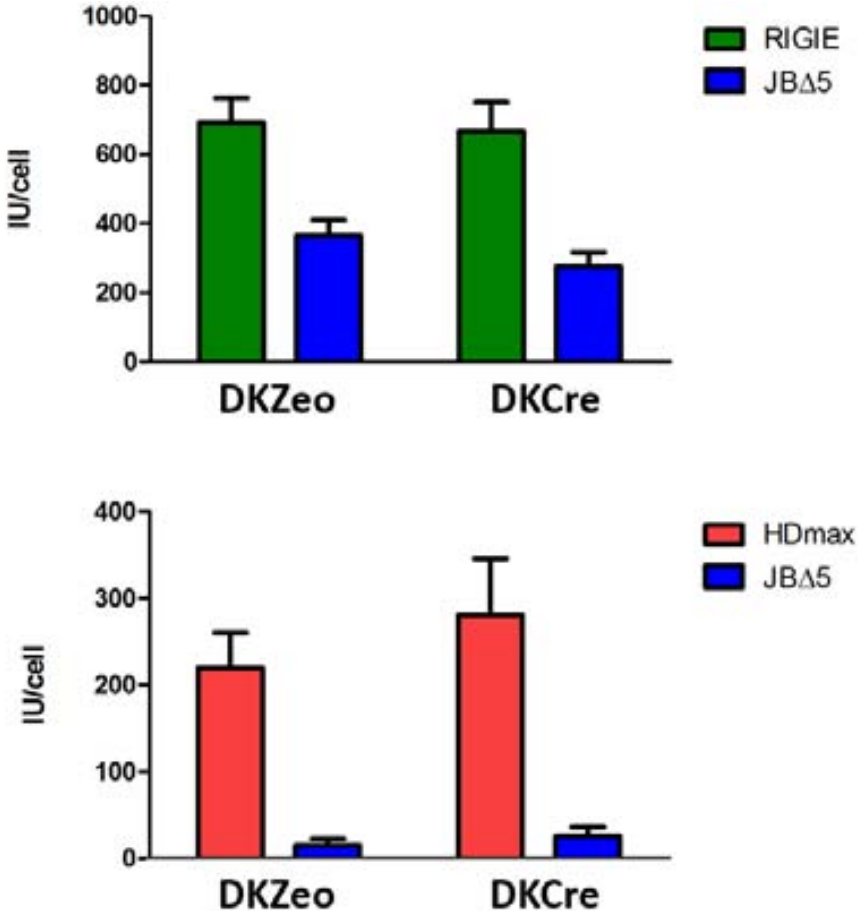

Figure 5.35. Comparison between DKZeo and DKCre cell lines for the production of RIGIE and HDmax.

Overall, after this experiment we decided to use DKCre instead of DKZeo for the amplification of these HDCAV-2 vectors, as these results indicated that these cells could perform slightly better for their production.

To optimize the production of the canine HDCAV-2 in terms of production yields and helper-CAV-2 contamination it was also very important to determine the optimal harvest time. To do this, an experiment comparing the viral production at stopping the experiment at different times post-infection was performed in DKCre cells (Figure 5.36).

Results indicate that for both RIGIE and HDmax productions, the optimal harvesting time is at 36 hours post-infection and its shortening leads to lower yields of HDAd vector and more notably, this does not reflect into an improvement of the HDCAV-2/helper-CAV-2 ratio. Also, harvesting times longer than 36 hours resulted in an increase of helper-CAV-

2 contamination without a significant increase of HDCAV-2 yields. Therefore, shorter or longer harvesting times were discarded and the last step of amplification was stopped at 36 hours post-infection.

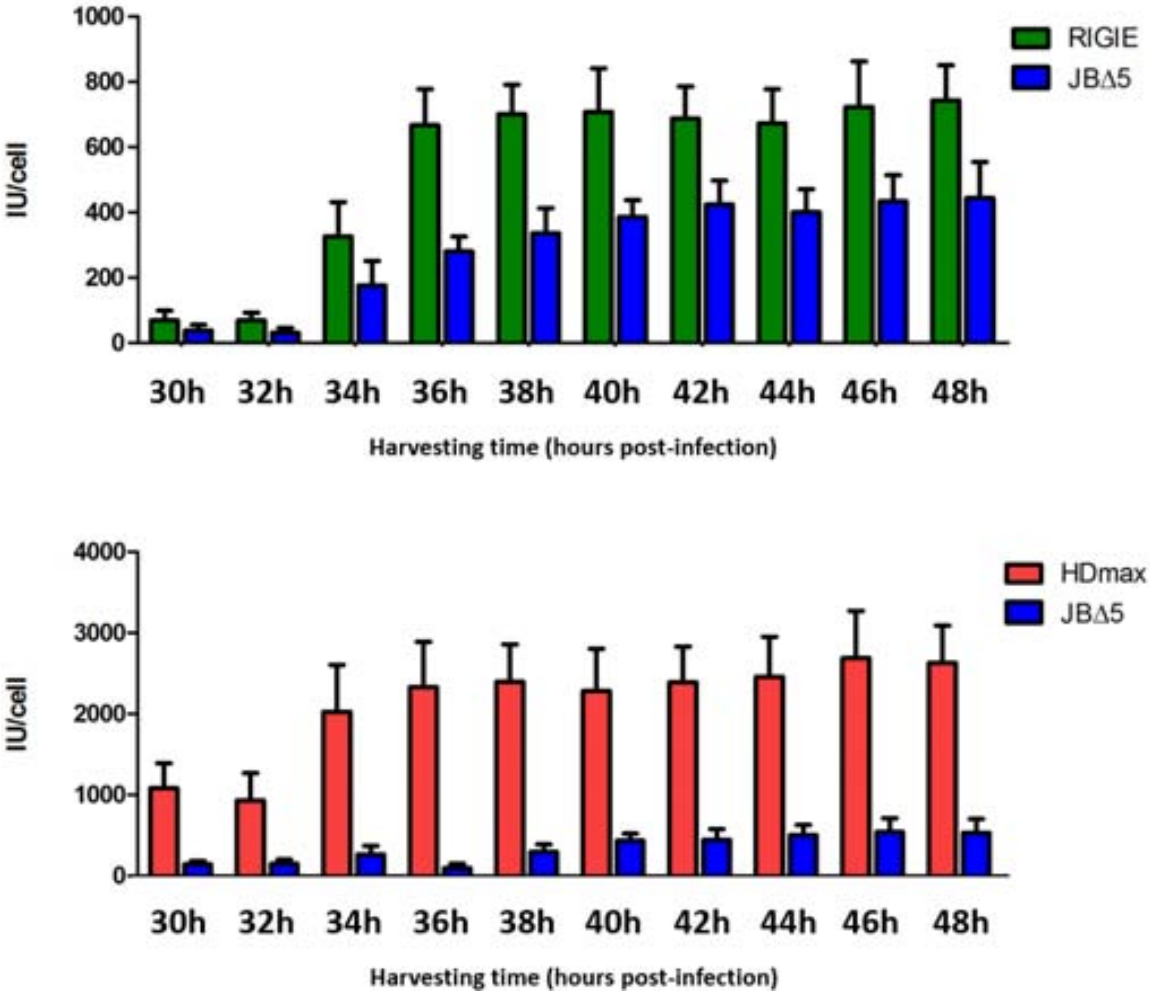

Figure 5.36. Comparison between different harvesting times for RIGIE and HDmax amplification.

5.3.10. Virus purification by triple ultracentrifugation in CsCl gradient

After the harvest of the infected cells in the last amplification step, samples were ultracentrifuged in CsCl gradient, first in a discontinuous gradient and second in an isopycnic gradient (see in materials and methods). Since HDCAV-2 and helper-CAV-2 vectors have different genome size and therefore should have different density,

theoretically it could be possible to differentiate the bands in the isopycnic gradient. Since only one band was observed after the second gradient, a third ultracentrifugation step was performed using the same conditions (in density, time and g's) than the second step. This last ultracentrifugation step displayed two close bands, which likely corresponded to the helper-Ad and HDAd vectors.

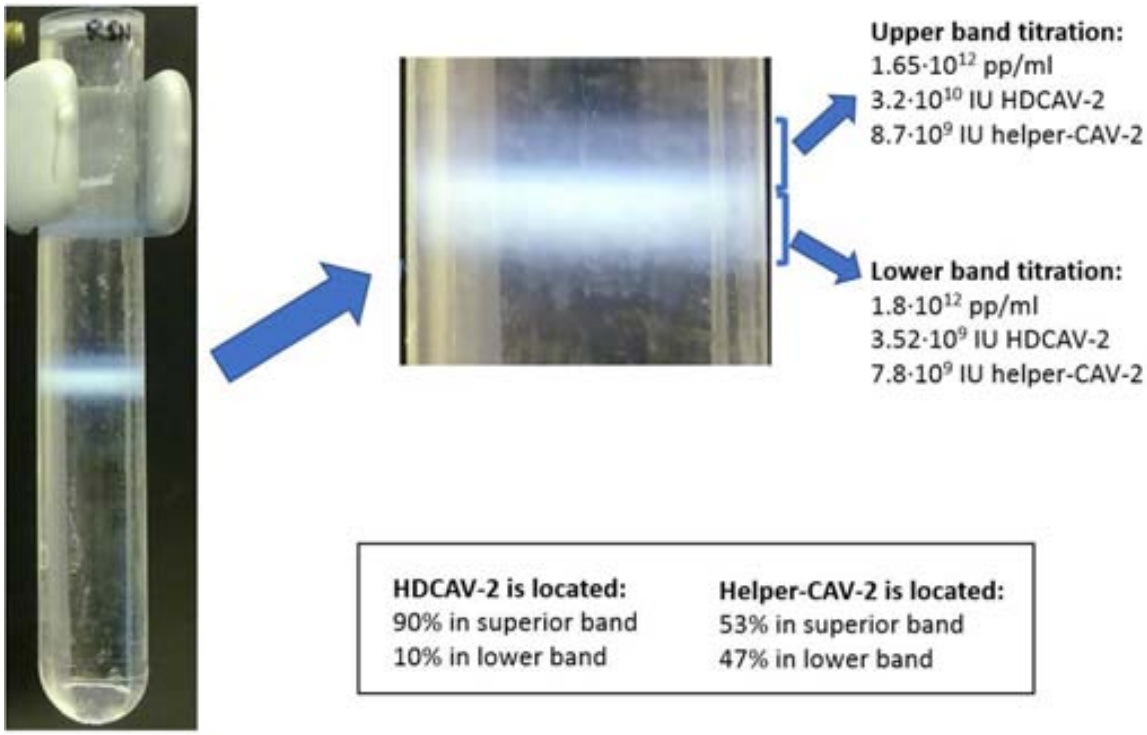

Figure 5.37. Third gradient of CsCl ultracentrifugation, band separation and titration of the RIGIE vector production from a 30 x 15-cms plate amplification.

As observed in Figure 5.37, both bands have different vector composition and thus 90% of the HDCAV-2 vector (RIGIE) was detected in the upper band, but only 10% of it in the lower band. On the other hand, helper-CAV-2 (JBΔ5) was detected at similar levels 53% vs 47% in the upper and lower bands respectively. Similar results were also obtained for HDmax vector production, with 94% of the HDCAV-2 vector detected in the upper band versus only 6% in the lower band and 63% of helper-CAV-2 in the upper band versus 37% in the lower (Figure 5.38).

In summary, a third ultracentrifugation step clearly helps to reduce the contamination of helper-CAV-2 vectors, even though the band-extracting technique was not specialy accurate. To improve this, a fourth ultracentrifugation step could be helpful to further

separate the bands. However, we discarded this as continuous expositions to CsCl reduce the overall infectivity of the adenovirus.

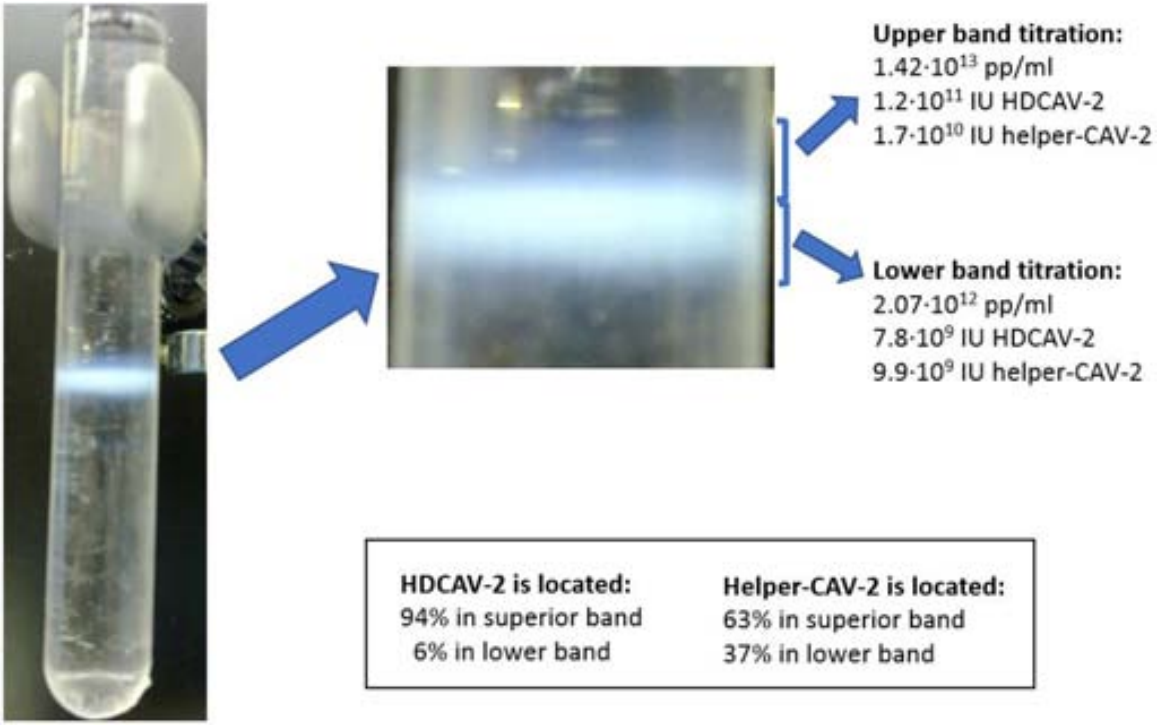

Figure 5.38. Second gradient of CsCl ultracentrifugation, band separation and titration of the RIGIE vector production from a 30 x 15-cms plate amplification.

5.3.11. Intraarticular injection of viral vectors

RIGIE vector encodes for the beta-glucuronidase, a lysosomal enzyme that is either lacking or misfunctional in mucopolysaccharidosis patients. It has been described that enzyme replacement therapy, consisting in the systemic administration of the enzyme, allows partial correction of the disease. However, some structures such the hydrocephalic membrane in central nervous system and the synovial membrane in joints prevent the access of the enzyme to these tissues, thus rendering these tissues without an effective treatment (Rohrbach and Clarke, 2007). Since the injection of this vector in SNC was already being studied by a laboratory collaborator, we decided to focus on the articular pathology of these diseases. Before starting with a proper treatment in mice models, we first wanted to assess whether the direct vector administration to mice joints was feasible and which vectors could efficiently infect the synovial tissue. To do this, different viral vectors were injected into mice knee joints ($6 \cdot 10^8$ pp to 10^9 pp in 2 µl of final volume per joint, 2 joints each virus). Mice were sacrificed at 2 weeks post-injection and articular tissue was observed by a fluorescence microscope to detect GFP expression.

- $6 \cdot 10^8$ vg AAV2 GFP
- 10^9 vg AAV5 GFP
- 10^9 vg AAV8 GFP
- 10^9 vg AAV9 GFP
- 10^9 vg AAV10 GFP
- 10^9 pp CAV-2 GFP
- 10^9 pp Ad5 GFP
- 10^9 pp Ad40 GFP
- 10^9 pp Ad52 GFP

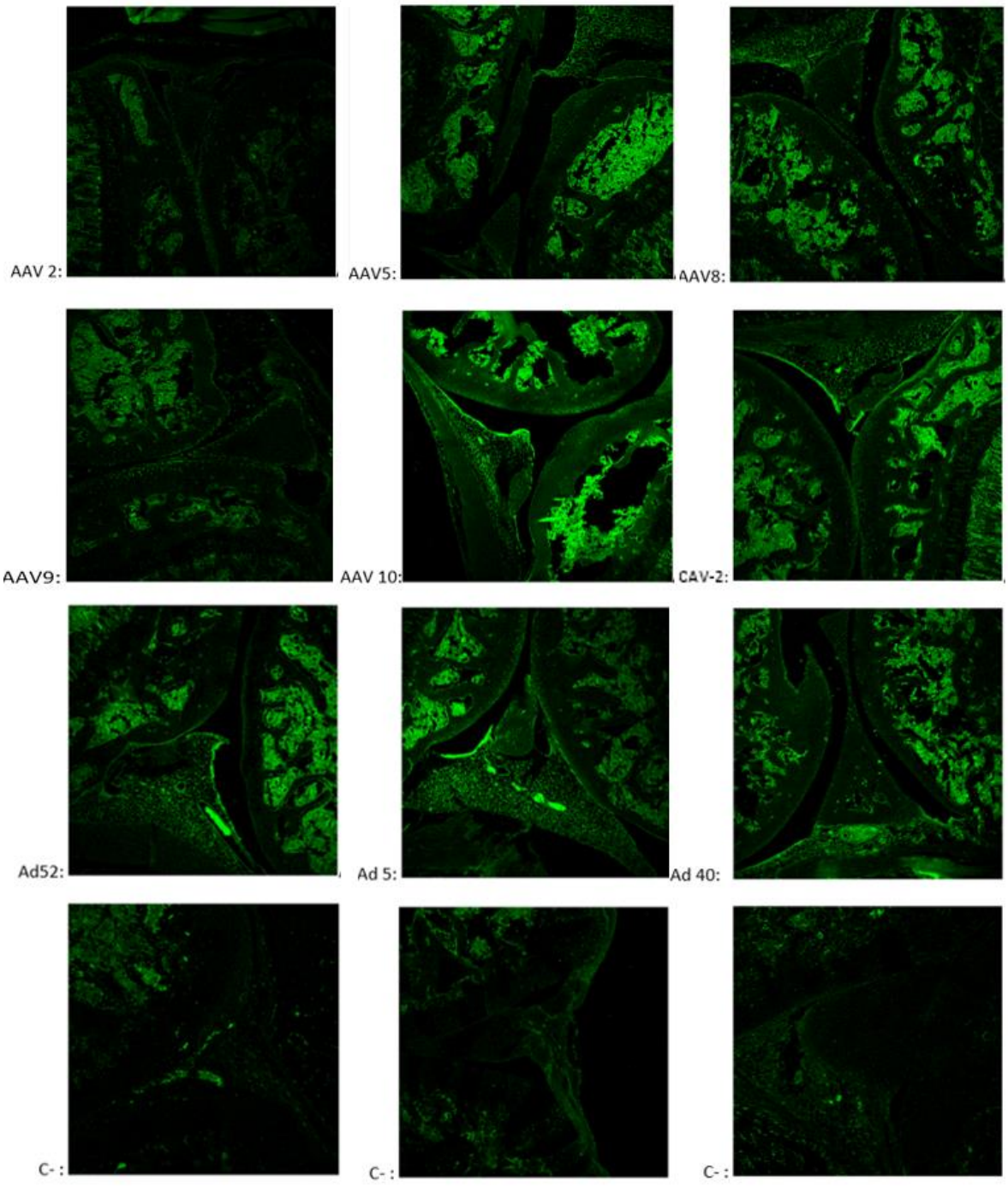

Figure 5.39. Fluorescence imaging of articular tissue injected with different GFP-expressing vectors.

As observed in Figure 5.39, Images show differences between the samples corresponding to knees injected with saline buffer (C-) and the samples corresponding to the knees injected with viral vectors. However, the presence of background signal and the low number of samples suggest that further injections should be tested before deciding whether RIGIE could be a vector to be tested in animal models for MPS VII to target the articular pathology of this disease.

5.4. DETERMINATION OF THE NUCLEAR PROTEIN THAT INTERACTS WITH THE *attB* SEQUENCE *IN VITRO*

5.4.1. A nuclear protein interacts with the *attB* sequence *in vitro*

Ad-helper vectors with the *attB* sequence 5' of the packaging signal having a delayed viral cycle lead to the hypothesis that a cellular factor could be interacting with the *attB* sequence, thus impairing the formation of the packaging complex with the packaging signal. In order to test this hypothesis, an electrophoretic mobility shift assay (EMSA) was performed to detect specific interactions mediated by nuclear protein(s). In addition to the wild type *attB* sequence, we also tested a mutant *attB* sequence encoding the same nucleotide composition as the wild type *att*B but in a different order (described on Methods 4.1.18).

Results clearly show that *in vitro*, the wild type *attB* sequence (but not the mutant *attB*) interacts with a nuclear protein from HEK-293 cells (Figure 5.40).

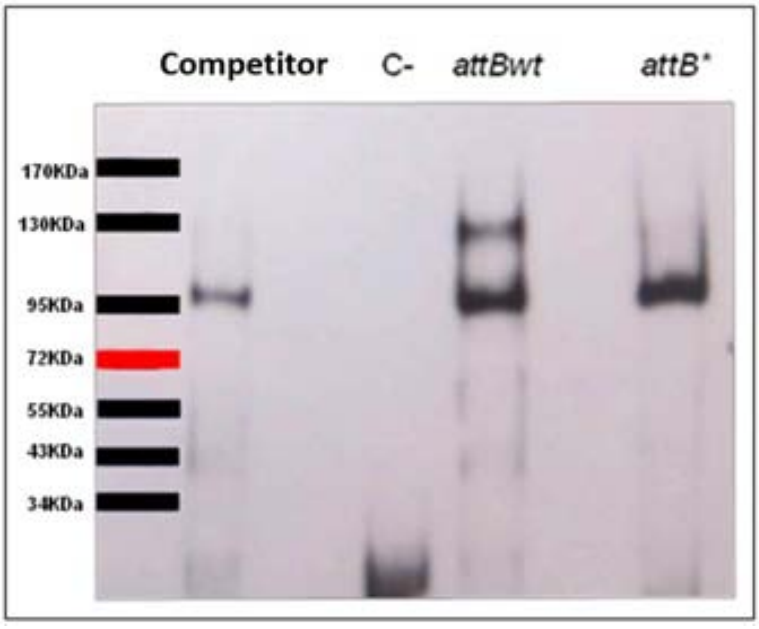

Figure 5.40. Enzyme electrophoretic mobility shift assay using HEK-293 cell nuclear extracts. Competitor: HEK-293 cell nuclear extracts incubated with the *attB*wt sequence together with poly-dIdC and unlabeled *attB*wt as specific competitor. C-: *attB*wt sequence without nuclear extracts. *attB*wt: Nuclear extracts from HEK-293 cells incubated with a wild type *attB* sequence and poly-dIdC. *attB**: Nuclear extracts from HEK-293 cells incubated with a mutant *attB* sequence and poly-dIdC.

In order to test whether this interaction was specific for the HEK-293 cell line, we also tested the interaction between the *attB* sequence and protein extracts from canine DKZeo cells. The band-shift was also observed in DKZeo cells (Figure 5.41), indicating that this interaction was not unique for HEK-293 cells. However, the band-shift in DKZeo cells appeared to be less intense than in HEK-293 cells, suggesting different levels of expression for this nuclear factor between both cell types.

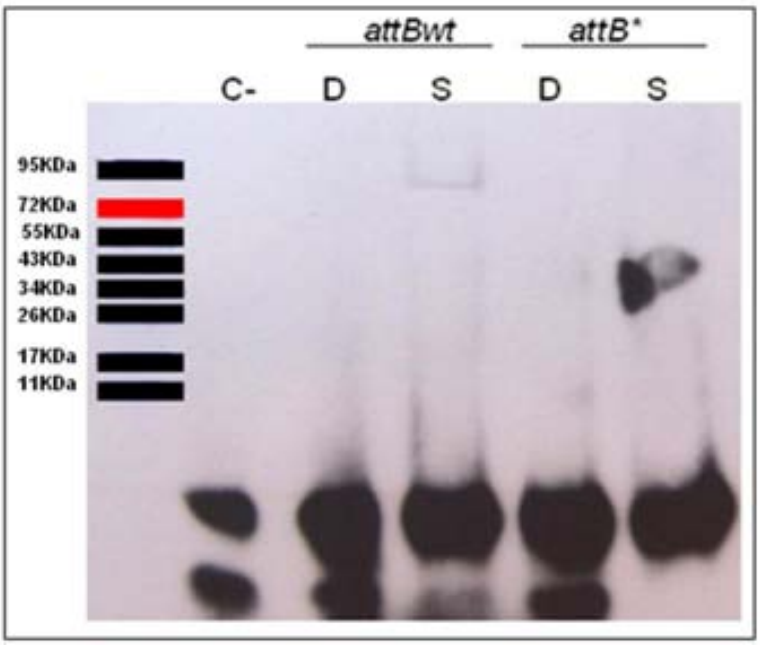

Figure 5.41. Enzyme electrophoretic mobility shift assay using DKZeo cell nuclear extracts. C-: *attB*wt sequence without nuclear extracts. *attB*wt: Nuclear extracts from DKZeo cells incubated with a wild type *attB* sequence and poly-dIdC (D) or sperm salmon DNA (S). *attB**: Nuclear extracts from DKZeo cells incubated with a mutant *attB* sequence and poly-dIdC (D) o sperm salmon DNA (S).

5.4.2. Determination of the protein or proteins that interact with the *attB* sequence

To identify the interacting protein(s), an EMSA assay was performed in duplicate (Figure 5.42). The first half was processed as described before. The precise location of the band corresponding to the *attBwt* interaction was then measured and equivalent fragment of the other half membrane was cut and further analyzed by mass spectrometry.

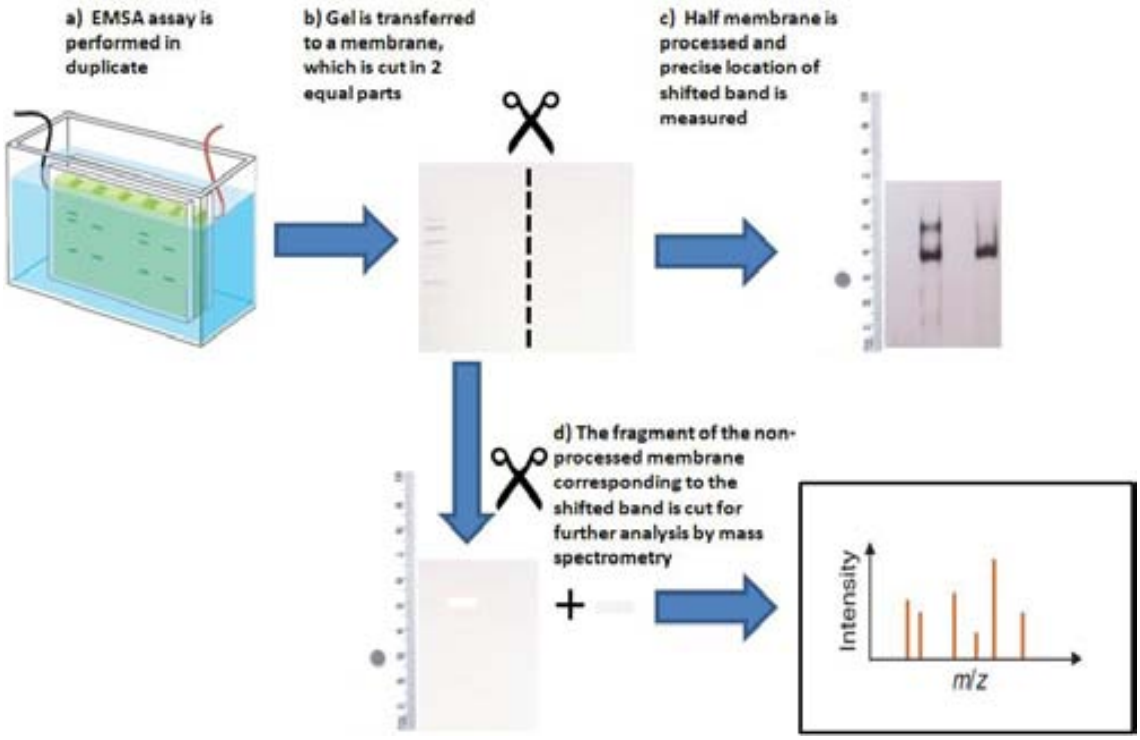

Figure 5.42. Determination of the protein or proteins that interact with the *attBwt* biotinylated oligomers by mass spectrometry analysis of the shifted band from an EMSA assay.

Results of this experiment showed an important presence of histones H1.2, H1.3 and H1.4, altogether with several Keratin proteins (Figure 5.43 and Table 5.7). However, these results show that this strategy is far from being specific, as in the section of the membrane analyzed not only the interacting protein is expected to be present but also all the proteins migrating at the same location. Moreover, the presence of highly abundant proteins like histones could be expected with this analysis and the detection of several forms of keratins can be considered as merely contamination while processing the samples.

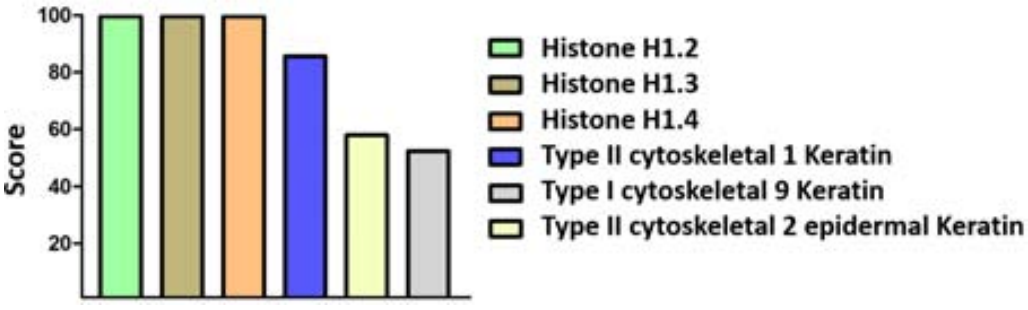

Figure 5.43. Proteins detected by mass spectrometry corresponding to the area on the shifted band from an EMSA assay. Proteins with a score below 50 are not shown.

Accession	Coverage	# Peptides	# AAs	MW [kDa]	calc. pI	Score	Description
04264	23,91	15	644	66,0	8,12	85,69	Keratin, type II cytoskeletal 1
35908	14,71	9	639	65,4	8,00	52,41	Keratin, type II cytoskeletal 2 epidermal
16403	13,62	8	213	21,4	10,93	99,55	Histone H1.2
16402	13,12	8	221	22,3	11,02	99,55	Histone H1.3
10412	13,24	8	219	21,9	11,03	99,55	Histone H1.4
35527	24,24	8	623	62,0	5,24	57,96	Keratin, type I cytoskeletal 9
13645	13,18	6	584	58,8	5,16	35,00	Keratin, type I cytoskeletal 10
02538	4,26	6	564	60,0	8,00	24,94	Keratin, type II cytoskeletal 6A
95678	4,36	6	551	59,5	7,74	22,75	Keratin, type II cytoskeletal 75
5XKE5	4,49	6	535	57,8	7,20	28,71	Keratin, type II cytoskeletal 79
67809	30,25	5	324	35,9	9,88	27,26	Nuclease-sensitive element-binding protein 1
02539	7,44	4	215	21,8	10,99	43,54	Histone H1.1
22492	7,73	4	207	22,0	11,71	41,46	Histone H1t
81605	22,73	3	110	11,3	6,54	11,39	Dermcidin
38159	6,65	3	391	42,3	10,05	12,72	Heterogeneous nuclear ribonucleoprotein G
13647	5,59	3	590	62,3	7,74	12,67	Keratin, type II cytoskeletal 5
09651	12,63	3	372	38,8	9,23	14,54	Heterogeneous nuclear ribonucleoprotein A1
09651-2	14,69	3	320	34,2	9,23	14,54	Isoform A1-A of Heterogeneous nuclear ribonucleoprotein A1
09651-3	17,60	3	267	29,4	9,14	14,54	Isoform 2 of Heterogeneous nuclear ribonucleoprotein A1
23246	5,80	3	707	76,1	9,44	16,01	Splicing factor, proline- and glutamine-rich
23246-2	6,13	3	669	72,2	9,23	16,01	Isoform F of Splicing factor, proline- and glutamine-rich
16989	10,22	2	372	40,1	9,77	14,08	DNA-binding protein A
16989-2	12,54	2	303	31,9	9,66	11,84	Isoform 2 of DNA-binding protein A
86YZ3	3,54	2	2850	282,2	10,04	14,77	Hornerin
11142	4,33	2	646	70,9	5,52	11,26	Heat shock cognate 71 kDa protein
11142-2	5,68	2	493	53,5	5,86	7,60	Isoform HSC54 of Heat shock cognate 71 kDa protein
04259	3,90	2	564	60,0	8,00	10,36	Keratin, type II cytoskeletal 6B
62750	14,74	2	156	17,7	10,45	18,67	60S ribosomal protein L23a
05387	42,61	2	115	11,7	4,54	16,31	60S acidic ribosomal protein P2
62241	11,54	2	208	24,2	10,32	5,77	40S ribosomal protein S8
13148	7,25	2	414	44,7	6,19	7,40	TAR DNA-binding protein 43
60174	10,04	2	249	26,7	6,90	6,40	Triosephosphate isomerase
06753-2	10,08	2	248	29,0	4,78	9,32	Isoform TM30nm of Tropomyosin alpha-3 chain
62988	38,16	2	76	8,6	7,25	8,60	Ubiquitin

Table 5.7. Proteins detected by mass spectrometry corresponding to the area on the shifted band from an EMSA assay.

As an alternative, we applied another strategy consisting in the use of streptavidin resins that have the capacity to bind to the biotinylated oligomers (Figure 5.44). In this approach, *attBwt* and *attB** were first incubated with HEK-293 cellular extracts and were then added into a column with streptavidin resin. Once the biotinylated oligomers were bound to the streptavidin, the column was washed to eliminate the proteins that do not interact with the biotinylated oligomers. Then, the complexes were eluted from the column using an extraction step with 8M guanidine-HCl at pH=1.5, that breaks the streptavidin-biotin interaction. Finally, samples were analyzed by mass spectrometry.

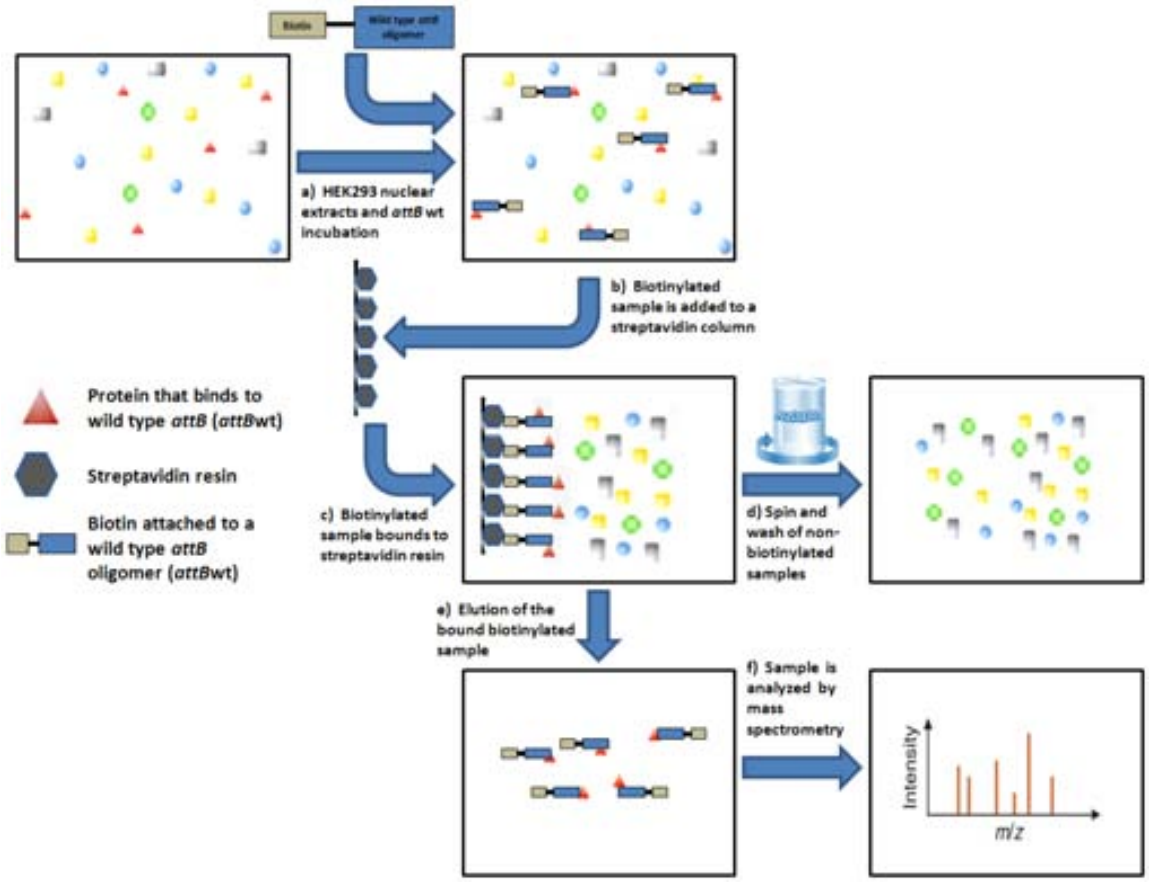

Figure 5.44. Determination of the protein(s) that interact with the *attB* oligomer using a column with streptavidin resin.

This experiment still provided a large list of potential interacting proteins (Figure 5.45 and Tables 5.8 and 5.9). The presence of different forms of Keratins and Hornerin is usually seen in these experiments and it is considered a contamination of the samples. Also, these results didn´t show any specific interaction with an important score. Histone H1.2, which was present in the previous experiment, is also present here in both *attBwt* and *attB** result list, indicating that this interaction, if exists, it is not specific for the *attBwt* sequence.

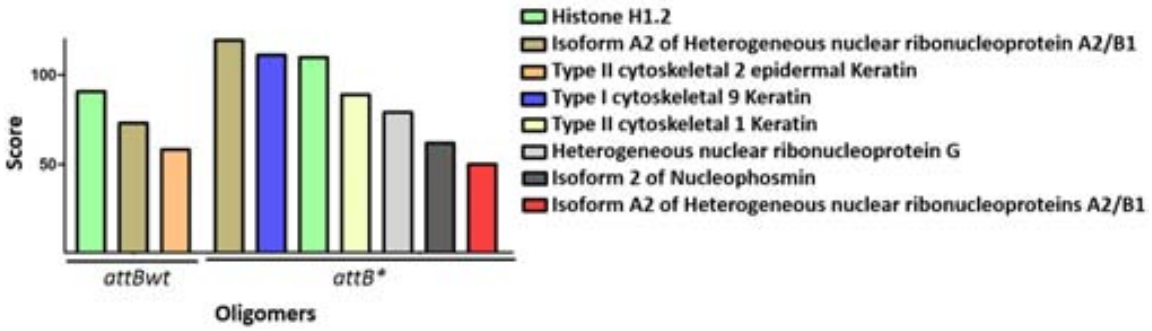

Figure 5.45. Proteins detected by mass spectrometry from proteins bound to the streptavidin resin. Proteins with a score below 50 are not shown.

Accession	Coverage	# Peptides	# AAs	MW [kDa]	calc. pI	Score	Description
P16403	19,72	11	213	21,4	10,93	90,70	Histone H1.2 OS=Homo sapiens
P22626-2	17,60	10	341	36,0	8,65	73,14	Isoform A2 of Heterogeneous nuclear ribonucleoproteins A2/B1
P35908	15,65	7	639	65,4	8,00	58,40	Keratin, type II cytoskeletal 2 epidermal
P06748-2	18,49	6	265	29,4	4,61	47,06	Isoform 2 of Nucleophosmin
P04264	5,59	7	644	66,0	8,12	46,15	Keratin, type II cytoskeletal 1
Q86YZ3	4,70	4	2850	282,2	10,04	38,48	Hornerin
P13645	11,30	6	584	58,8	5,21	36,51	Keratin, type I cytoskeletal 10
P35527	11,24	4	623	62,0	5,24	36,39	Keratin, type I cytoskeletal 9
P09651-3	12,73	4	267	29,4	9,14	33,87	Isoform 2 of Heterogeneous nuclear ribonucleoprotein A1
P62750	10,90	3	156	17,7	10,45	30,44	60S ribosomal protein L23a
P38159	7,67	4	391	42,3	10,05	26,80	Heterogeneous nuclear ribonucleoprotein G
P19338	8,31	5	710	76,6	4,70	24,96	Nucleolin
P47914	13,21	3	159	17,7	11,66	18,71	60S ribosomal protein L29
P23246	4,38	3	707	76,1	9,44	15,34	Splicing factor, proline- and glutamine-rich
Q13151	12,46	2	305	30,8	9,29	7,40	Heterogeneous nuclear ribonucleoprotein A0

Table 5.8. Proteins detected by mass spectrometry from proteins bound to the streptavidin resin when the *attBwt* oligomer is used.

Accession	Coverage	# Peptides	# AAs	MW [kDa]	calc. pI	Score	Description
P22626-2	28,15	18	341	36,0	8,65	119,32	Isoform A2 of Heterogeneous nuclear ribonucleoproteins A2/B1
P35527	33,71	18	623	62,0	5,24	111,25	Keratin, type I cytoskeletal 9
P16403	19,72	8	213	21,4	10,93	109,82	Histone H1.2
P04264	19,57	16	644	66,0	8,12	89,02	Keratin, type II cytoskeletal 1
P38159	21,99	13	391	42,3	10,05	79,10	Heterogeneous nuclear ribonucleoprotein G
P06748-2	18,87	10	265	29,4	4,61	62,62	Isoform 2 of Nucleophosmin
P09651-3	17,23	7	267	29,4	9,14	50,24	Isoform 2 of Heterogeneous nuclear ribonucleoprotein A1
Q00839	12,61	7	825	90,5	6,00	48,97	Heterogeneous nuclear ribonucleoprotein U
P35908	6,57	5	639	65,4	8,00	38,71	Keratin, type II cytoskeletal 2 epidermal
P19338	11,69	7	710	76,6	4,70	38,25	Nucleolin
P13645	11,30	6	584	58,8	5,21	37,48	Keratin, type I cytoskeletal 10
Q99729-3	10,53	3	285	30,6	7,91	27,05	Isoform 3 of Heterogeneous nuclear ribonucleoprotein A/B
Q86V81	18,29	3	257	26,9	11,15	22,81	THO complex subunit 4
Q13151	12,46	5	305	30,8	9,29	22,79	Heterogeneous nuclear ribonucleoprotein A0
0Q96KK5	28,91	3	128	13,9	10,89	17,85	Histone H2A type 1-H
Q86YZ3	1,96	3	2850	282,2	10,04	17,14	Hornerin
P69905	21,83	4	142	15,2	8,68	13,72	Hemoglobin subunit alpha
P07305	10,82	2	194	20,9	10,84	12,24	Histone H1.0
P07437	6,53	2	444	49,6	4,89	11,18	Tubulin beta chain
P61978-3	9,55	2	440	48,5	5,54	10,73	Isoform 3 of Heterogeneous nuclear ribonucleoprotein K
P23246	4,38	2	707	76,1	9,44	9,35	Splicing factor, proline- and glutamine-rich

Table 5.9. Proteins detected by mass spectrometry from proteins bound to the streptavidin resin when the *attBwt* oligomer is used.

In order to find a more efficient way to detect the interacting protein which is specific for the *attBwt* sequence we focused on Biacore, a product specialized in measuring protein-protein but also DNA-protein interactions and binding affinity. This technology is based on Surface Plasmon Resonance (SPR), an optical phenomenon that allows detection of unlabeled interactants in real time. SPR occurs when polarized light strikes an electrically conducting surface at the interface between two media. This generates electron charge density waves called plasmons, reducing the intensity of reflected light at a specific angle known as the resonance angle, in proportion to the mass on a sensor surface. The SPR-based biosensors can be used in determination of active concentration as well as characterization of molecular interactions in terms of both affinity and chemical kinetics. Also, they can be used to concentrate the interacting factor allowing its final determination with mass spectrometry. A simple interaction experiment involves the immobilization of a molecule (ligand) on the sensor chip surface and the injection of a series of concentrations of its potential interacting partner (analyte) across the surface. During the course of the interaction, polarized light is directed toward the sensor surface and the angle of minimum intensity reflected light is detected. This angle changes as molecules bind and dissociate and the interaction profile is thus recorded in real time. Changes in the index of refraction at the surface are detected by the hardware and recorded as resonance units (RU) in the control software. Curves are generated from the RU trace and are evaluated by fitting algorithms which compare the raw data to well-defined binding models. These fits allow determination of a variety of thermodynamic constants, including the apparent affinity of the binding interaction.

The first step of the experiment was the immobilization of the biotinylated *attBwt* (Figure 5.46) or *attB** (Figure 5.47) oligomers (ligands) to a streptavidin sensor chip. Continuously, several buffer injections were performed to assess the stability of the interaction, indicating that the immobilization of the ligands to the chip as satisfactory, as it shows an increase of 1100 RU for *attBwt* and 1063 RU for *attB**, which corresponds to a 60% of the maximum capacity indicated by the manufacturer.

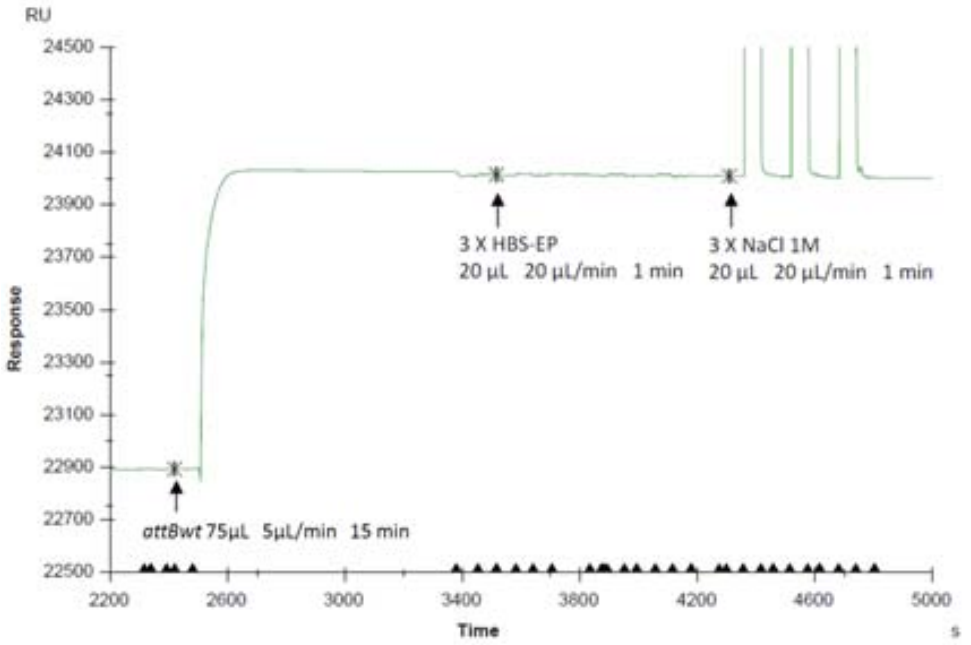

Figure 5.46. Sensogram corresponding to the *attBwt* immobilization to the streptavidin chip.

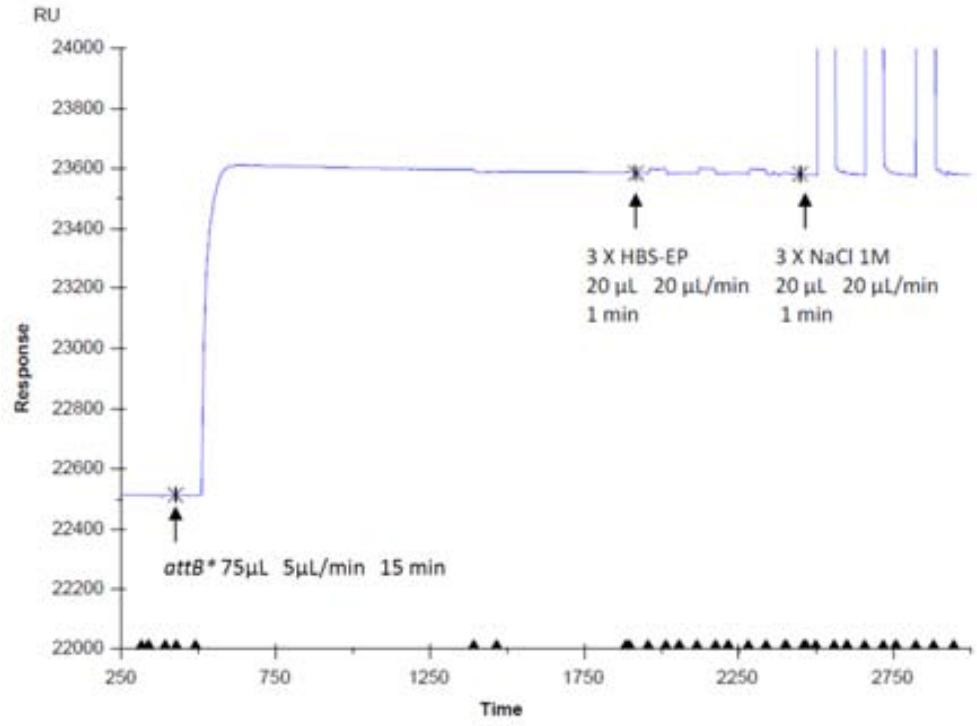

Figure 5.47. Sensogram corresponding to the *attB immobilization to the streptavidin chip.**

Once the ligands were immobilized, we proceeded to study the interaction with the HEK-293 nuclear extracts. The first conclusion is that the association and dissociation kinetic is similar for both ligands, but with a slightly higher affinity for the *attBwt* oligomer (Figure 5.48).

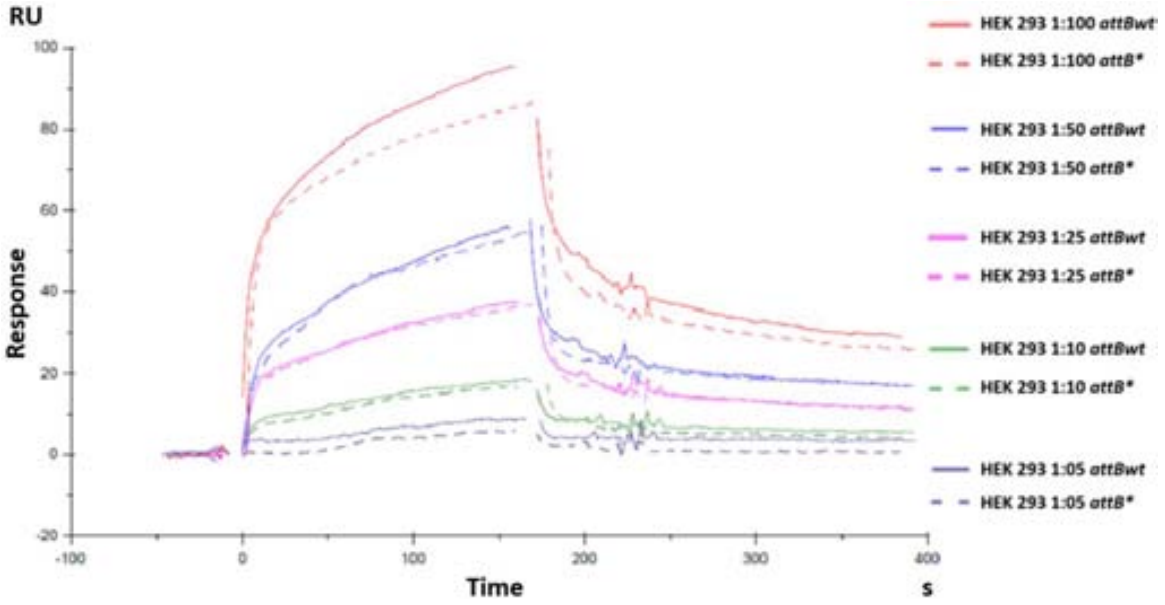

Figure 5.48. Study of the interaction between HEK-293 cell extracts with different concentrations of the *attBwt* or *attB oligomers.** Results indicate a slightly higher affinity of the HEK-293 nuclear extracts with the *attBwt* biotinylated oligomer, when compared to the *attB*.*

By using different buffer injections, the proteins interacting with the *attBwt* or *attB** ligand were recuperated and they were later studied by mass spectrometry (Figure 5.49 and Tables 5.10 and 5.11).

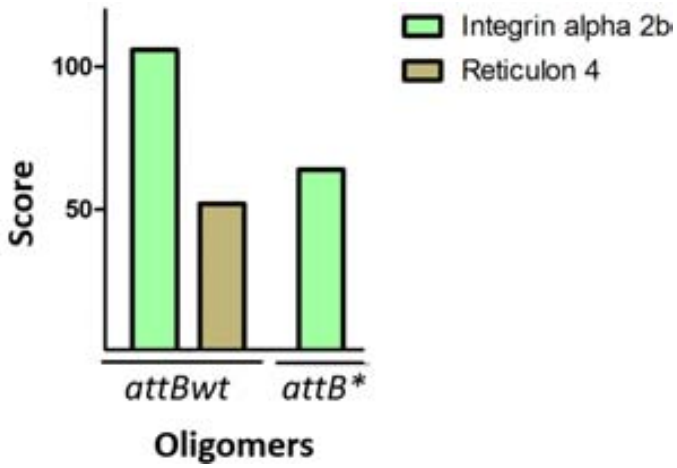

Figure 5.49. Biacore hits using *attBwt* or *attB biotinylated oligomers.**

Accession	Coverage (hit protein cover)	# Peptides (hit number)	Prot matches	MW [kDa]	calc. pI	Score	Description
190068	3,4	5	9	114387	5,21	106	Platelet glycoprotein IIb
386753	3,4	5	9	114488	5,21	106	Platelet glycoprotein IIb
88758615	3,4	5	9	114446	5,21	106	Integrin alpha 2b preproprotein
119571979	3,7	5	9	104210	5,41	106	Integrin, alpha 2b, isoform CRA_a
119571980	3,4	5	9	114420	5,21	106	Integrin, alpha 2b, isoform CRA_b
119571982	3,3	5	9	115132	5,24	106	Integrin, alpha 2b, isoform CRA_d
189067516	3,4	5	9	114462	5,21	106	Unnamed protein product
221046816	3,6	5	9	105384	5,3	106	Chain A of Integrin Aiibb3
9408096	2,5	8	2	130260	4,43	52	Nogo-A protein
11878278	3,1	8	2	106693	4,42	52	Nogo-A protein short form
13377628	3	8	2	108755	4,52	52	Testis specific reticulon 5 protein
24431935	2,5	8	2	130250	4,43	52	Reticulon 4 isoform A
40788974	2,4	8	2	134892	4,51	52	KIAA0886 protein
47519562	3	8	2	108782	4,52	52	Reticulon 4 isoform E
119620531	3,4	8	2	98702	4,56	52	Reticulon 4, isoform CRA_g
119620534	2,6	8	2	128295	4,43	52	Reticulon 4, isoform CRA_h

Table 5.10. Biacore hits using *attBwt* biotinylated oligomers.

Accession	Coverage (hit protein cover)	# Peptides (hit number)	Prot matches	MW [kDa]	calc. pI	Score	Description
190068	1,9	11	5	114387	5,21	64	Platelet glycoprotein IIb
386753	1,9	11	5	114488	5,21	64	Platelet glycoprotein IIb
799326	2,6	11	5	82414	5,92	64	Glycoprotein IIb
1093618	2,6	11	5	82515	6,01	64	Glycoprotein receptor GPIIb
1708571	3,3	11	5	66708	5,45	64	Platelet glycoprotein IIb
62088684	3,6	11	5	59818	5,68	64	Integrin alpha-IIb precursor variant
88758615	1,9	11	5	114446	5,21	64	Integrin alpha 2b preproprotein
112351374	11,6	11	5	18759	4,75	64	Integrin subunit aIIb
119571979	2,1	11	5	104210	5,41	64	Integrin, alpha 2b, isoform CRA_a
119571980	1,9	11	5	114420	5,21	64	Integrin, alpha 2b, isoform CRA_b
119571981	2,3	11	5	93400	5,33	64	Integrin, alpha 2b, isoform CRA_c
119571982	1,9	11	5	115132	5,24	64	Integrin, alpha 2b, isoform CRA_d
189067516	1,9	11	5	114462	5,21	64	Unnamed protein product
221046816	2,1	11	5	105384	5,3	64	Chain A of Integrin Aiibb3

Table 5.11. Biacore hits using *attB biotinylated oligomers.**

Results corresponding to the *attBwt* interaction indicate that integrin alpha 2b (also known as platelet glycoprotein IIb) could be the candidate protein interacting with *attBwt*. However, we discard this hypothesis for its high score in the *attB** results. On the other hand, we found only one specific protein (Reticulon 4, also known as Nogo), but its low score discarded it as potential candidate for the interaction.

Since we wanted to get rid of the inespecificity observed when analyzing HEK-293 nuclear extracts we separated these extracts in fractions of different molecular weight by separating them using a FPLC chromatography in a sepharose gel (Figure 5.50).

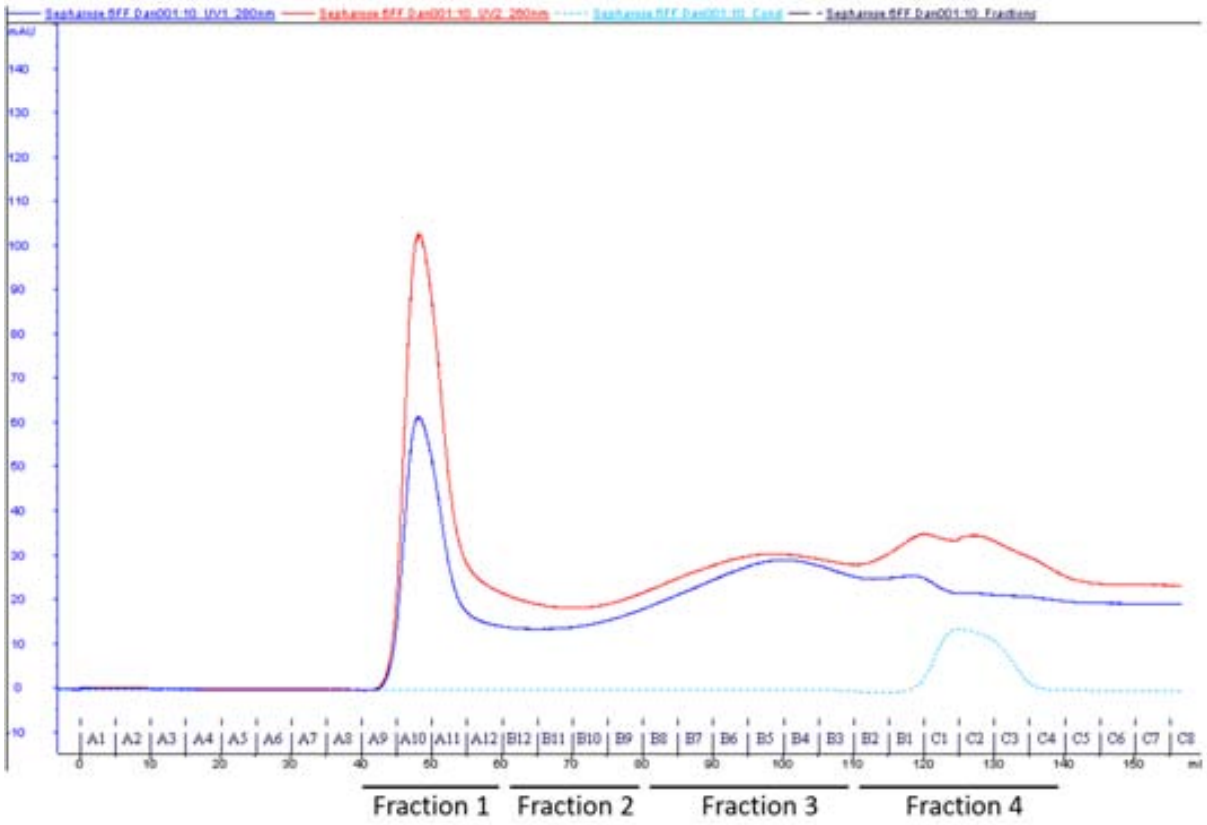

Figure 5.50. Spectrometry graph corresponding on the separation of HEK 293 nuclear extracts by molecular exclusion FPLC chromatography with a sephadex column. Samples were later separated into 4 different groups for further EMSA and BIACORE analysis.

Once all samples were collected, we repeated the EMSA experiment using different fractions of the nuclear extracts. No sign of interaction between the *attBwt* oligomers and the nuclear extract from fractions 1, 2 and 4 were observed, but a shifted band could be observed on the last 3 samples of fraction 3 (Figure 5.51), indicating that the interacting protein was present there.

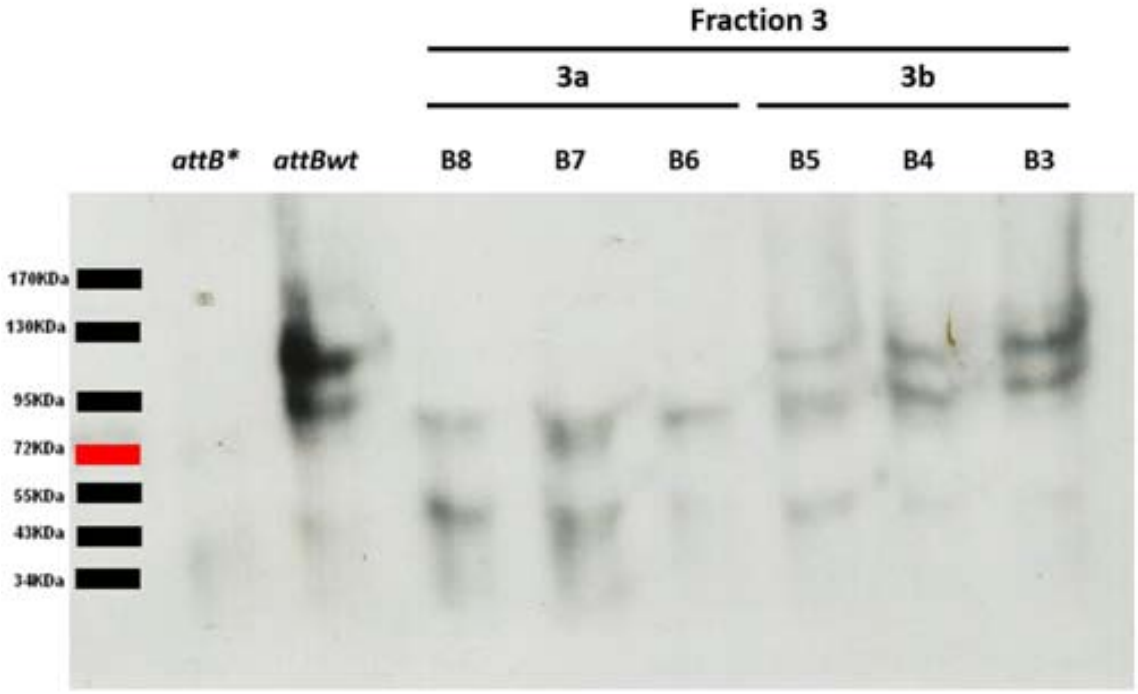

Figure 5.51. Enzyme electrophoretic mobility shift assay using the 3rd fraction of the HEK-293 nuclear extracts separated by sepharose chromatography. *attB**: Total nuclear extracts from HEK-293 cells incubated with a mutant *attB* sequence and poly-dIdC. attBwt: Total nuclear extracts from HEK-293 cells incubated with a wild type *attB* sequence and poly-dIdC. Fraction 3 (B8, B7, B6, B5, B4, B3): Nuclear extracts from HEK-293 cells (corresponding to the separation by sepharose chromatography) incubated with a wild type *attB* sequence and poly-dIdC.

After the nuclear extracts were separated and the fraction with the protein responsible for the interaction with attBwt sequence was determined (3b), we repeated the biacore experiment with the a*ttBwt* oligomer with the fractions 1, 2, 3a (corresponding to the subfractions B6, B7 and B8), 3b (corresponding to the subfractions B3, B4 and B5) or 4 (Figure 5.52 and Tables 5.12 and 5.13).

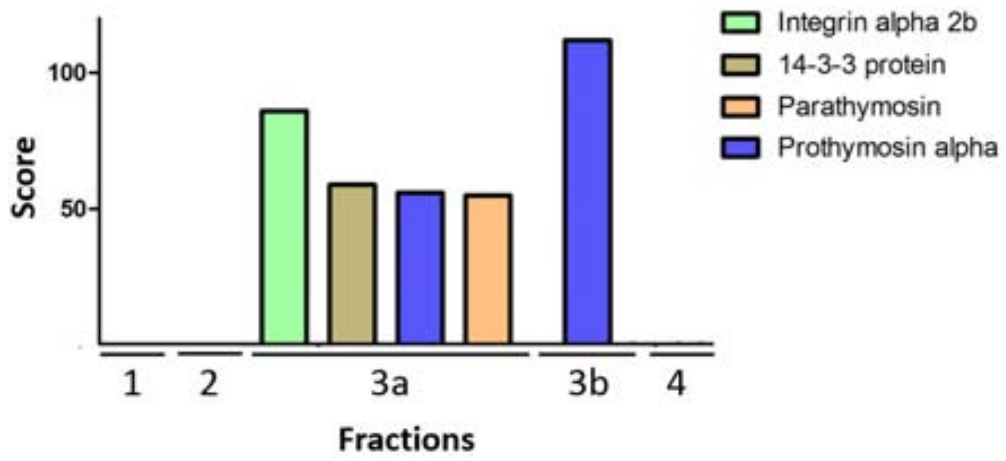

Figure 5.52. Biacore hits using different fractions of the HEK-293 nuclear extracts separated by sepharose chromatography and *attBwt* biotinylated oligomers.

Accession	Coverage (hit protein cover)	# Peptides (hit number)	Prot matches	MW [kDa]	calc. pI	Score	Description
190068	1,9	5	1	114387	5,21	86	Platelet glycoprotein IIb
386753	1,9	5	1	114488	5,21	86	Platelet glycoprotein IIb
799326	2,6	5	1	82414	5,92	86	Glycoprotein IIb
1093618	2,6	5	1	82515	6,01	86	Glycoprotein receptor GPIIb
1708571	3,3	5	1	66708	5,45	86	Platelet glycoprotein IIb
62088684	3,6	5	1	59818	5,68	86	Integrin alpha-IIb precursor variant
88758615	1,9	5	1	114446	5,21	86	Integrin alpha 2b preproprotein
112351374	11,6	5	1	18759	4,75	86	Integrin subunit aIIb
119571979	2,1	5	1	104210	5,41	86	Integrin, alpha 2b, isoform CRA_a
119571980	1,9	5	1	114420	5,21	86	Integrin, alpha 2b, isoform CRA_b
119571981	2,3	5	1	93400	5,33	86	Integrin, alpha 2b, isoform CRA_c
119571982	1,9	5	1	115132	5,24	86	Integrin, alpha 2b, isoform CRA_d
221046816	2,1	5	1	105384	5,3	86	Chain A of Integrin Aiibb3
112696	5,7	6	1	28010	4,77	59	14-3-3 protein zeta/delta (KCIP-1)
253706	5,7	6	1	27810	4,73	59	14-3-3 protein zeta chain
1051270	5,7	6	1	27955	4,73	59	14-3-3 zeta isoform
4262000	20,3	6	1	8009	8,16	59	14-3-3 protein/cytosolic phospholipase A2
4507953	5,7	6	1	27899	4,73	59	Tyrosine 3/tryptophan 5 - monooxygenase activation protein, zeta polypeptide
83754467	5,4	6	1	29413	4,97	59	Chain A, Molecular Basis For The Recognition Of Phosphorylated And Phosphoacetylated Histone H3 By 14-3-3
161172138	6,1	6	1	26439	5	59	Chain A, Phosphorylation Independent Interactions Between 14-3-3 And Exoenzyme S
192988247	5,7	6	1	28043	4,73	59	Chain A, 14-3-3 Protein Zeta In Complex With Thr758 Phosphorylated Integrin Beta2 Peptide
107540	24,1	7	1	6281	3,95	56	Prothymosin alpha homolog
206378	16,1	7	1	9527	3,84	56	Prothymosin-alpha
206380	16,1	7	1	9529	3,69	56	Prothymosin-alpha
209475	50	7	1	3064	4,25	56	Thymosin (partial)
307350	12,8	7	1	11952	3,65	56	Prothymosin alpha
307352	19,2	7	1	8156	3,72	56	Prothymosin alpha
307354	12,7	7	1	12040	3,64	56	Prothymosin alpha
553793	15,9	7	1	9533	3,6	56	Prothymosin alpha
4261582	93,3	7	1	1555	4,03	56	Prothymosin alpha
18490877	12,7	7	1	12009	3,71	56	Prothymosin, alpha
27657705	12,7	7	1	12037	3,7	56	Prothymosin alpha
119591379	16,3	7	1	9906	10,96	56	Prothymosin, alpha isoform CRA_b
151101404	12,7	7	1	12067	3,69	56	Prothymosin, alpha isoform 2
151101407	12,6	7	1	12196	3,69	56	Prothymosin, alpha isoform 1
158515409	12,7	7	1	12065	3,7	56	Prothymosin alpha isoform 1
226474	10,9	8	1	11421	4,15	55	Zn binding protein
46276863	10,8	8	1	11523	4,14	55	Parathymosin
59800148	10,8	8	1	11450	4,09	55	Parathymosin

Table 5.12. Biacore hits using fraction 3a and *attBwt* biotinylated oligomers.

Accession	Coverage (hit protein cover)	# Peptides (hit number)	Prot matches	MW [kDa]	calc. pI	Score	Description
190198	25,7	1	4	11980	3,7	112	Prothymosin alpha
307350	25,7	1	4	11952	3,65	112	Prothymosin alpha
307354	25,5	1	4	12040	3,64	112	Prothymosin alpha
18490877	25,5	1	4	12009	3,71	112	Prothymosin, alpha
27657705	25,5	1	4	12037	3,7	112	Prothymosin alpha protein
151101404	25,5	1	4	12067	3,69	112	Prothymosin, alpha isoform 2
151101407	25,2	1	4	12196	3,69	112	Prothymosin, alpha isoform 1

Table 5.13. Biacore hits using fraction 3b and *attBwt* biotinylated oligomers.

As expected, no hits were obtained for fractions 1, 2 or 4, suggesting that the interacting protein or proteins were not present in these fractions.

Prothymosin alpha, a nuclear protein that may mediate immune function by conferring resistance to certain opportunistic infections, has a significant hit in the 3a and is the only hit in 3b samples, where it also has a high score (Figure 5.53). This corresponds with the previous EMSA experiment where a shifted band was observed in the 3b samples.

Sequence coverage (in red) = 25 %

1 M**SDAAVDTSS EITTK**DLQEK KEVVEEAENG RDAPANGNAN EENGEQEADN
51 EVDEEEEEGG EEEEEEEGDG EEEDGDEDEE AETATGKR**AA EDDEDDDVDT**
101 **KK**QKTDEDD

Figure 5.53. Sequence coverage of prothymosin alpha. The peptides detected (in red) were found in several different prothymosin alpha forms which vary slightly in sequence.

5.4.3. Determination of the effects of prothymosin alpha overexpression or inhibition on the production yields of Ad with the *attB* sequence

Since the specific interaction between prothymosin alpha and the *attB* oligomers was found *in vitro*, the conditions of this interaction were far from the physiological conditions in HEK-293 cells. Therefore, before concluding that the interaction between this protein and *attB* not only existed but also caused the delay of the viral cell cycle of Ad with the *attB* sequence, it was necessary to test whether the overexpression or inhibition of this protein has an effect on this cycle. To do this, we generated three plasmids, one containing the GFP cDNA (which was used as a control), another containing prothymosin alpha cDNA and another containing the shRNA against this protein mRNA. Then, we transfected HEK-293 cells with these plasmids and after four hours, infected them with Ad5/ΦC31CreΨrev or Ad5/RFP. Analysis of the viral yields at different times post-infection showed that the overexpression or inhibition of prothymosin alpha did not result in a modification of the viral life cycle (Figure 5.54). Therefore, this assays suggest that while the interaction between *attB* and prothymosin alpha may occur *in vitro,* either is not present in the Ad5-a*ttB* infected cells or it is not

responsible for the delayed cycle of these vectors and thus that other factor must be responsable for the delay in the viral life cycle observed for a*ttB*-vectors.

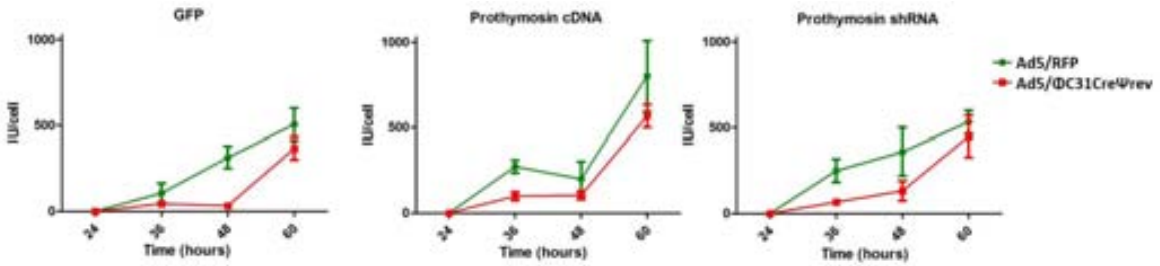

Figure 5.54. Effects of Prothymosin alpha overexpression and inhibition in Ad5 with the attB sequence. Ad5/RFP vs Ad5/ΦC31CreΨrev productivity per cell at 24, 36, 48 and 60 hours post-infection in HEK-293 cells transfected with plasmids containing a) GFP cDNA, b) Prothymosin alpha cDNA and c) Prothymosin alpha shRNA. Time=0h is the time when cells were infected.

Chapter 6

DISCUSSION

6.1. PRODUCTION OF HDAd5 VECTORS USING THE *attB* SYSTEM

Helper-dependent adenovirus vectors are excellent candidates for gene therapy due to their reduced capacity to induce cellular immune responses and their ability to direct stable transgene expression for up to 2 years (Morral *et al.,* 1999). Despite these advantages, their production presents two important problems: a) contamination with helper-Ad, and b) low titer preparations. During the last decade, optimization of the Cre-*lox*P system has been done by combining the excision of Ψ (using a Cre expressing cell line) with the physical separation of helper and HDAd virions by density in CsCl ultracentrifugation. This has improved the reduction of helper-Ad contamination levels from 10% down to 0.1%-0.01% (Palmer *et al.,* 2003). Additional strategies to optimize the excision of Ψ mediated by Cre recombinase must consider the compromise required between recombination activity and cell toxicity, i.e. low Cre levels limit efficient excision of Ψ, while high Cre levels become cytotoxic and affect proliferation of adenovirus-producing Cre cell lines (Ng *et al.,* 2002). Of note, alternative packaging domain excision-based methods using recombinases such as FLPe has not resolved this issue (Ng *et al.,* 2001; Umana *et al.,* 2001).

To address the limitations of the existing systems, Alba *et al.,* previously reported a non-excision method based on the differential packaging efficiency between helper Ad and HDAd genomes mediated by the *attB* sequence of bacteriophage ΦC31 inserted between the ITR and the packaging domain in the helper-Ad genome (Alba *et al.,* 2007).

Further experiments showed that helper-Ad packaging process was impaired, featuring a delay on their viral cycle, which was extended up to 56–60 hours. As a consequence of this, production yield of Ads with the *attB* sequence (in IU/cell) was significantly reduced (>99%) at 36 hours. Surprisingly, though *attB* and *attP* sites are sequences recognized by ΦC31 recombinase, differential packaging takes place in the absence of recombinase indicating that mechanism(s) other than recombination are involved. Interestingly, since *attB*-ΦC31 technology is not dependent on the action of recombinases, the generation of new recombinase-based cell lines can be avoided. In addition, since the *attB* strategy

is not associated with the use of ultracentrifugation in CsCl and therefore can be used in scalable procedures.

Unfortunately, attempts to produce HDAd at large scale using this recently described *attB*-ΦC31 technology in our laboratory were partially unsuccessful because of the generation of recombinant adenovirus by the recombination of both vectors by their packaging signal. When this recombination occurs, an *attB*-free helper-vector containing viral genes and with a viral cycle equal to first-generation adenoviruses is generated, thus displacing HDAd from the production.

The inversion of the helper-Ad packaging signal has been previously described as a good strategy to avoid the generation of recombinant adenoviruses, as the recombination between both vectors can only generate a vector that is too small in size to be packaged. To this end, we generated and produced Ad5/ΦC31CreΨrev, a helper-Ad with the *attB* signal and with the packaging signal in a reverse position.

Once the Ad5/ΦC31CreΨrev was produced, its viral life cycle was assessed to determine whether it was also delayed as well as to determine if it would efficiently amplify HDAd vectors. In addition, the accurate determination of the helper-Ad viral life cycle is important to set the optimal harvest time.

As observed for other *attB*-Ad5 vectors, Ad5/ΦC31CreΨrev has a delayed viral life cycle, which is longer than the 36-48 hours of FGAd5 vectors, although slightly longer than Ad5/ΦC31CreΨdir (Alba *et al*., 2007). This would explain the absence of cytopathic effect at 70 hours post-infection observed in the production of Ad5/ΦC31CreΨrev, as well as the presence of a band of non-mature virions as intense as the band of mature virions after CsCl ultracentrifugations when the virus was harvested at 70 hours post-infection. The substancial difference between the viral life cycles of FGAd and Ad5/ΦC31CreΨrev suggest a strong potential for these helper-Ad to produce high-quality HDAd preparations.

Further characterization of Ad5/ΦC31CreΨrev in comparison with control FGAd without the *attB* sequence showed that the production yields of this vector were notably lower (1.5 to 2.5 logarithms below). This is consistent with the observed differences in viral cycle among these vectors, where FGAd reach their production peak at 40 hours post-

infection and helper-Ad with the *attB* sequence reach it at 72 hours. Moreover, coinfection experiments showed that the production titers of these helper-Ad are not normalized by the aport of viral proteins *in trans* from FGAd, suggesting that the observed differences in production titers are due to differences in their viral genome. Of note, these results were similar for helper-Ad with direct and reverse Ψ, indicating that Ψ reversion does not affect these properties of Ad5/ΦC31CreΨrev.

Once Ad5/ΦC31CreΨrev was characterized, we assessed whether it could be used to produce HDAd efficiently. The transfection of pFK7 together with Ad5/ΦC31CreΨdir or Ad5/ΦC31CreΨrev linearized plasmids in 6-well plates was very efficient, resulting in high yields of HDAd and negligible levels of helper-Ad contamination. Optimization of the last amplification step indicated that the optimal conditions were to amplify HDAd in suspension HEK-293 cells with a MOI=0.5 of helper-Ad and harvest at 36 hours post-infection. This optimization was performed infecting the cells with a MOI=5 of HDAd, as other authors (Dormond, *et al.,* 2009c) had already widely studied this parameter. The last step of HDAd amplification resulted in high yields of HDAd ($1.36 \cdot 10^8$ IU/ml) with very low levels of helper-Ad contamination (0.036%). These helper-Ad contamination levels were in the same range that the lowest published, which are 0.01%-0.02% (Palmer *et al.,* 2003). However, it is important to mention that results from other authors were obtained using the classical Cre-based methodology, which is accomplished by recombination-mediated excision of the packaging signal of helper-Ad followed by further separation of helper-Ad from HDAd by the minimal density difference between them using a last step of ultracentrifugation in CsCl. In this regard, our amplification method in suspension cells is less time-consuming and avoids the current limitations associated with this method, since it does not require physical removal of contaminating helper virions by ultracentrifugation, and allows the use of scalable downstream methods, such as HPLC purification. Concerning this, scalability is especially important when HDAd preparations for clinical trials or large animals is desired, as large quantities of HDAd are needed. Other methods, like the production in cell factories (Suzuki *et al.,* 2010), have similar helper-Ad contamination rates (0.038% vs 0.036%). However, even though these methods have an scalable amplification, they require a last step of ultracentrifugation in CsCl, which does not permit the scalability of the whole production

process. The comparison with similar scalable methods using suspension cells with recombinase activity (Dormond *et al.,* 2009a) shows similar HDAd yields ($1.44 \cdot 10^8$ IU/ml vs $1.36 \cdot 10^8$ IU/ml) but slightly higher helper-Ad contamination rates (0.265% vs 0.036%). Interestingly, since *attB*-ΦC31 technology is not dependent on the action of recombinases, the use of recombinase-based cell lines can be avoided. However, since these helper-Ad have the *loxP* sites on both sides of Ψ, these cell lines could be easily used in case a further reduction of the helper-Ad contamination levels is required.

In previous HDAd amplification experiments at our laboratory using *attB*-helper-Ad vectors with the Ψ in direct orientation, both HDAd and *attB*-helper-Ad vectors were able to recombine through their packaging signal. Since the only internal region of the viral genome that is common to both, HDAd and helper-Ad is Ψ, the recombination between both Ψ generates a new FGAd vector expressing RFP but without the *attB* sequence, and therefore with a normal viral life cycle of 36 hours. When this occurs, these new recombinant FGAd vectors rapidly displace initial HDAd and a*ttB*-helper vectors and the amplification process must be cancelled.

However, because the number of RFP-expressing cells was very low, we could discard the presence of an important amount of newly-generated replication-competent adenoviruses. On the other hand, it is important to take into consideration that RCA particles need 2 or 3 amplification steps to overgrow the HDAd and helper-Ad vectors. Therefore, since our optimized protocol is based on one step of transfection followed by one or two steps of amplification, we performed a qPCR test to assess if RCA particles had been generated. This test showed that, in contrast with the previous HDAd productions using helper-Ad with direct Ψ, the use of helper-Ad with Ψ in reverse orientation did not allow recombination between both HDAd and helper-adenovirus vectors.

As expected, and in contraposition to the administration of $5 \cdot 10^{11}$pp of control FGAd to 6-week old mice via tail-vein injection, which resulted in the loss of transgene expression between 1 to 4 weeks post-injection, the adminisration of the produced HDAd led to a high long-term expression of the transgene until the end of the experiment (32 weeks after administration). These results indicated that HDAd vectors produced using the

attB-ΦC31 technology could efficiently infect liver parenchyma and maintain its transgene expression for long periods of time.

These data are consistent with many previous experiments of systemic Ad administration, where a high and long-term expression of the HDAd infected cells *in vivo* is reported, in contraposition with the short-term expression after FGAd administration (Brunetti-Pierri *et al*., 2006; Brunetti-Pierri *et al*., 2009c; Brunetti-Pierri *et al*., 2007; Kim *et al*., 2001; Morral *et al*., 1999; Toietta *et al*., 2005). While both vectors elicit acute toxicity (induced by the Ad capsid proteins), leading to a production of pro-inflammatory cytokines and chemokines and a widespread activation of macrophages, neutrophils and Kupffer cells in the liver (Otake *et al*., 1998), HDAd elicit an attenuated adaptative immune response compared to FGAd vectors. This response is induced by the uptake of Ad by antigen-presenting cells (APCs), which ultimately activates $CD8^+$ T cells, leading to the generation of Ad-specific or transgene-product-specific cytotoxic T lymphocytes (CTLs) (Schagen *et al*., 2004) that cause the transgene expression differences observed between these vectors (Yang *et al.,* 1994a, Yang *et al.,* 1994b*).* Notably, this indicates that, despite the high administered dose, the levels of helper-Ad contamination in HDAd preparations are too low to induce the cellular immune response against the transduced cells.

6.2. GENERATION AND PRODUCTION OF CHIMERIC HDAd5/F40S

The absence of vectors that selectively target the intestine has prevented the use of gene therapy strategies for intestinal diseases. The production *in vitro* of vectors with intestinal tropism, like the Human Adenovirus 40 serotype (Ad40), an enteric adenovirus of the subgroup F is extremely inefficient, resulting in low titers in comparison to other adenoviral serotypes (Sherwood *et al*., 2007; Tiemessen *et al*., 1994). In this regard, recent experiments at our laboratory indicated that a chimeric Ad5 carrying the short fiber protein of Ad40 can be produced and efficiently infect the colon (preferentially enteroendocrine cells and macrophages) and to a lesser extent, the small intestine when intrarectally administered (Rodriguez *et al*., 2013).

In order to test whether HDAd carrying the F40S protein can be produced by using the *att*B-ΦC31 production system, Ad5/ΦC31CreF40S, a helper-Ad encoding the gene of the short fiber protein of adenovirus 40, with an *attB* sequence and 2 *loxP* sequences flanking the packaging signal, was generated.

Initial characterization experiments using Ad5/ΦC31CreF40S showed a modest delay compared to Ad5/F40S, reaching its maximum production at approximately 56 hours post-infection instead of 52 hours. Production of this vector alone was very tedious, requiring multiple amplification steps, time and effort. Moreover, its productivity was very low $1.1 \cdot 10^{11}$ pp total vs $2 \cdot 10^{12}$pp total.

For this reason, we performed an experiment to determine the productivity of this vector as well as and other control Ads (Ad5/RFP, Ad5/F40S) in optimal conditions. Also, the Ad5/ΦC31CreF40S infection combined with polybrene, a cationic polymer used to increase its efficiency of infection, was tested. Results confirmed that the productivity of Ad5/ΦC31CreF40S was very low (3.5 IU/cell), more than a logarithm less than the productivity of Ad5/F40S (85 IU/cell) and more than three logarithms less than Ad5/RFP (5310 IU/cell). Moreover, these results also indicated that the use of polybrene improved the Ad5/ΦC31CreF40S yields, doubling its productivity (from 3.5 to 7.4 IU/cells). Notably, the use of polybrene to enhance Ad5/ΦC31CreF40S yields did not

affect the viral cycle of this vector and, therefore, its use was compatible with the amplification of chimeric HDAd using the *attB*-based methodology.

The production of chimeric HDAd using this strategy led to modest levels of HDAd yields ($8 \cdot 10^8$ IU) and a reasonably low helper-Ad contamination levels (1%). However, a last step of amplification using HEK-293Cre cells was required to achieve this yield, because HDAd yields were lower ($1 \cdot 10^8$ IU) and helper-Ad contamination was higher (17%) when HEK-293 cells were used.

Overall, these results are interesting as, even though a few other chimeric HDAd such as HDAd5/3 (Guse *et al.,* 2012) or HDAd5/35 (Wang *et al.,* 2008; Balamotis *et al.,* 2004) have been produced, the production of HDAd5/40 has not been described yet elsewhere. However, further optimization of this strategy will be required, as the low titers obtained for the HDAd5/40 batches would only be useful for small experiments in animal models that do not require high doses or clinical-grade preparations.

6.3. OPTIMIZATION OF HDCAV-2 PRODUCTION USING *attB*-ΦC31 TECHNOLOGY

Canine adenovirus serotype 2 (CAV-2) vectors, altogether with vectors of ovine, porcine, bovine or simian origin have been generated to circumvent the humoral immune response caused by neutralizing antibodies against human adenoviruses. Since most humans have not been exposed to these non-human viruses, the development of these vectors is an interesting strategy to lower this immune response and, in turn, increase target cell transduction and lower biosafety concerns. Notably, the development of CAV-2 vectors is specially interesting when infection of the CNS is intended, as these vectors have a good neuronal tropism as well as the capacity to infect quiescent cells (Soudais *et al.*, 2004). As it occurs in HDAd when compared to their FGAd counterparts, the generation of HDCAV-2 has several advantages over FGCAV-2, including a longer transgene expression due to the lower cell-immune response against the infected cells. Unfortunately the current HDCAV-2 production protocol, based on Cre-*LoxP* system combined with the impairment of the helper-CAV-2 by mutations in its packaging signal, is very inefficient and tedious and leads to low HDCAV-2 yields and significant helper-CAV-2 contamination (1 to 10%), which in the end makes the use of these vectors in the clinic not feasible.

To improve current production methods, we assessed if the successful optimization of the HDAd production using helper-Ad with the *attB* sequence could be reproduced also for the production of HDCAV-2 vectors. To this end, we generated CAV-2/ΦC31CreΨ*, a helper-CAV-2 with the *attB* sequence, a mutated packaging signal and RFP gene surrounded by 2 *loxP* sequences. However, the production of CAV-2/ΦC31CreΨ* yielded only discrete amounts of vector ($2 \cdot 10^9$ IU total) and productivity was also very low (1 IU/cell), even when very permissive conditions were used (harvesting at 72 hours post-infection and 100 fifteen-cm plaques). To amplify HDCAV-2 using the *attB*-ΦC31 technology, helper-CAV-2 should have a delayed viral cycle compared to HDCAV-2 to lower the helper-CAV-2 contamination, as well as the capacity to provide sufficient proteins *in trans* so HDCAV-2 can be efficiently produced. The determination of the viral

cycle indicated that while the control FGCAV-2 vector (CAV-2/RFP) reached its peak around 54 hours post-infection, the CAV-2/ΦC31CreΨ* vector showed a delayed viral cycle (around 66 hours). We hypothesized that, even though this 12-hour difference is not as high as the 24-hour observed for HDAd, it could be sufficient to allow an efficient production of HDCAV-2 with relatively low levels of mature helper-CAV-2.

However, all attempts to produce HDCAV-2 using this helper-CAV-2 failed and none of the many conditions tested (double transfection; transfection + infection strategy; different MOI; etc.) worked efficiently. In addition, and in parallel to the experiments with the *attB*-CAV-2 vectors, we generated DKZeo-ΦC31 cell line as a complementary procedure to optimize HDCAV-2 production. Thus, instead of the Cre recombinase, which is toxic for the cells (Silver *et al.,* 2001) and has a bidirectional activity that impairs its efficiency (Alba et al., 2005), DKZeo-ΦC31 cells constitutively express the ΦC31 recombinase, which has a low toxicity and unidirectional recombinase activity (Groth *et al.,* 2000). However, analysis of the recombinase activity of these cells when transfecting with a plasmid with *attB* and *attP* signals showed the excission of only 57% of the total plasmids, too low to be used in HDCAV-2 productions. This, together with the inefficient amplification, led us to discard, at least for the moment, the use of *attB*-vectors for the production of HDCAV-2 vectors.

In summary, these results confirmed what was suspected after the low titers obtained during the helper-CAV-2 amplification; this is, that the combination of a mutated packaging signal and the presence of *attB* on its genome leads to its inefficient production and its inability to provide enough proteins in *trans* to allow the suficient amplification of HDCAV-2. A future strategy to adress this problem could be to generate a helper-CAV-2 vector with the *attB* sequence but carrying a non-mutated wild-type Ψ signal. This should permit higher production yields of the helper-CAV-2 vector, which in turn would lead to higher HDCAV-2 yields. Indeed, helper-CAV-2 contamination levels may also be higher, and the optimization of the production protocol should therefore be performed as it has been described in this work for HDAd5 and HDAd5/F40S vectors.

In contraposition to Ad5 vectors, titration of CAV-2 vectors is complex and it is often associated with poor precision and high variability (Segura *et al*., 2010). To adress this problem, other methods such as the tissue culture infectious dose ($TCID_{50}$) assay, or the

development of qPCR strategies to detect CAV-2 have been developed. However, these titration systems have some limitations, like the inability to detect HDCAV-2 in the $TCID_{50}$ procedure, or the low biological relevance of analyzing purified vector samples by qPCR. To solve these issues we set up a new titration method consisting of the analysis by qPCR of DNA samples from infected cells. As opposed to qPCR methods that detect viral DNA from mature and non-mature virions, since the DNA samples for this titration are obtained from infected cells, this analysis only detects infective virions and, therefore, titration results using this method are biologically relevant.

As an alternative to amplify HDCAV-2, we used JBΔ5, a canine helper-adenovirus with a mutated packaging signal that leads to its impaired packaging. In addition, it is also surrounded by two *loxP* sequences that allow the specific excission of the packaging signal when HDCAV-2 amplifications are performed using Cre expressing cells, like DKCre cells. The reported procedure to amplify HDCAV-2 is based on cell sorting to select HDCAV-2-infected cells and it is very tedious and unefficient. Therefore, we optimized a cell-sorting-free procedure to amplify HDCAV-2 and determined that the optimal harvesting time to obtain higher yields of HDCAV-2 with less helper-CAV-2 contamination was at 36 hours post-infection. Since the titration of CAV-2 by observation of the marker protein expression was highly inaccurate, each amplification step was titrated by the recenlty-generated qPCR-based titrating method. Lastly, since helper-CAV-2 and HDCAV-2 vectors have a different genome size, we could improve the helper-CAV-2 contamination by partially removing helper-CAV-2 from the final preparation after a third ultracentrifugation with CsCl gradient. After all these improvements we were able to obtain viral batches of up to $1.42 \cdot 10^{13}$ pp/ml ($1.2 \cdot 10^{11}$ IU of HDCAV-2) and a helper-CAV-2 contamination of 12.4%. Therefore, even though we improved the method for HDCAV-2 production in terms of simplicity and effectivity, the helper-CAV-2 contamination was still too high compared to the helper-CAV-2 contamination found in HDAd productions, and thus more optimization experiments are required.

Mucopolysaccharidoses are a group of lysosomal storage diseases characterized by metabolic disorders caused by the absence or malfunctioning of glycosaminoglycans. These diseases lead to several disorders, affecting nervous system and bone

development and leading to a degenerative joint disease (Simonaro *et al.,* 2008). As a potential strategy to treat the articular pathology of MPS in mice models we wanted to assess wether we could efficiently administer viral vectors to ankle joint articular tissue and which viral vector or vectors could be optimal to infect this tissue. After proper training first in dead mice using chinese ink and afterwards in vivo, we could obtain the expertise to administer viral vectors to mice joints. Later on, a series of different GFP-encoding viral vectors were administered into mice joints, and animals were analyzed by immunochemistry. Unfortunately, none of the vectors tested (inculiding CAV-2) allowed efficient transgene expression. However, since high background levels were observed, more experiments must be performed to finally accept or discard the vectors tested as efficient viral vectors to treat the degenerative joint disease in MPSVII.

6.4. DETERMINATION OF THE NUCLEAR PROTEIN THAT INTERACTS WITH THE *attB* SEQUENCE *IN VITRO*

To predict by which mechanism the presence of *attB* in the genome of adenoviruses delays their viral cycle, we performed an EMSA assay using biotin-labeled *attB* or reorganized *attB* (*attB**) oligomers and nuclear extracts from HEK-293 or DKZeo cells. Results indicated that the wild type *attB* sequence (but not the mutant *attB*) interacts with a nuclear protein from both HEK-293 and DKZeo cells *in vitro*. The band-shift in appeared to be more intense when HEK-293 instead of DKZeo cells were used, suggesting different levels of expression for this nuclear factor between both cell types.

These results suggest a mechanism where the *attB* sequence interferes with virus assembly and could be related to the binding of a nuclear protein to this sequence. Due to the proximity of *attB* site to Ψ, efficient interaction between packaging complex proteins and Ψ would be affected by the binding of the unknown nuclear factor to *attB*, therefore causing the delayed viral cycle of Ad with this sequence in both HEK-293 and DKZeo cells.

Since we hypothesized that the knowledge of this protein would allow the generation of a cell line that, by overexpressing this protein, could enhance the performance of HDAd production using the *attB*-ΦC31 method in the future, we wanted to determine the nature of this factor. Because EMSA assays indicated a higher presence of the interacting protein in HEK-293 nuclear extracts than in DKZeo nuclear extracts, we used these extracts for the multiple approaches that were performed for its determination.

At first, we intended to detect the interacting factor/protein by cutting the shifted band from the EMSA assays. Unfortunatelly this experiment was unsuccessful as the mass spectrometry analysis did not provide a specific proteic candidate. Instead, this analysis resulted in a large number of hits, which could correspond to proteins that are not necessarily interacting with *attB* but were present in the selected fraction only because their molecular weight and conformation placed them at that level when the EMSA assay was performed.

To set a more specific idea about what protein could be interacting with the *attB* sequence, we used streptavidin resins that specifically bind biotinylated oligomers. However, this experiment did not provide the specifity that was expected, as it resulted in a long list of proteins that happened to interact not only with the *attB* but also with the *attB** sequence, thus indicating high background levels.

As a third and last approach, we used the biacore system, based on surface plasmon resonance and specialized in measuring protein-protein or DNA-protein interactions and binding affinity. First, association and dissociation kinetic analysis between HEK-293 nuclear extracts and *attB* or *attB** oligomers indicated a similar kinetic for both ligands, but with a slightly higher affinity for the *attBwt* oligomer. However, these experiments did not show important differences between the bound proteins when *attBwt* or *attB** oligomers were used.

In order to obtain more specific results, we separated nuclear extracts from HEK-293 cells in different fractions by FPLC chromatography and performed an EMSA assay using these fractions separately in different lanes. The observation of the lanes with shifted bands allowed the determination of the fractions with the most *attB*-interacting protein.

Then, a biacore analysis with different fractions of the HEK-293 nuclear extracts was analyzed. As expected, no signs of specific interaction were indicated on the fractions where a band-shift could not be observed in the EMSA assay. More importantly, the analysis of the fraction where the band shift appeared (3b) generated a high score (112) for prothymosin alpha, by detecting the 25% of its total aminoacidic sequence, thus indicating that this could be the interacting protein. However, since these analysis do not reproduce the physiological conditions present in HEK-293 or DKZeo cells, we could not conclude that the interaction of prothymosin alpha with *attB* observed in the Biacore analysis also occurred in these cells, therefore causing the delay of the viral life cycle of *attB*-Ad.

To test whether prothymosin alpha was responsible for this delay, we generated two plasmids, one carrying the prothymosin alpha cDNA, and the other carrying a shRNA against the prothymosin alpha. By transfecting these plasmids in HEK-293 cells together with Ad5-*attB* or Ad5 vectors without the *attB* sequence we were able to assess if

overexpression and specially inhibition of prothymosin alpha expression would affect the viral cycle of these vectors. Unfortunately, no significative differences were observed, thus indicating that this protein must not be the one responsible for the delay observed in *attB*-carrying Ad vectors.

Chapter 7

CONCLUSIONS

1. Ad5/ΦC31CreΨrev was generated. Its characterization shows that Ad5/ΦC31CreΨrev has a delayed viral life cycle of 72 hours.

2. The production of HDAd was optimized using HEK-293 suspension cells and Ad5/ΦC31CreΨrev as helper-Ad. In these conditions, high yields of HDAd ($1.36 \cdot 10^8$ IU/ml) and very low levels of helper-Ad contamination (0.036%) were obtained. Notably, this production method is scalable, as it does not require physical removal of helper virions by ultracentrifugation.

3. The use of Ad5/ΦC31CreΨrev as a helper-Ad does not permit the recombination between the helper-Ad and the HDAd genomes and therefore, it avoids the generation of RCA in HDAd productions.

4. In agreement with other HDAd production procedures, systemic administration of HDAd vectors produced using *attB*-ΦC31 technology also leads to a long-last high transgene expression in mice liver, even when high doses are administered.

5. Ad5/ΦC31CreF40S has a delayed viral life cycle of 56 hours. However, since the viral delay respect to Ad5/F40S helper-Ad is only of few hours, this method requires numerous steps of amplification.

6. The use of the *attB* system allows the production of HDAd/F40S vectors with low helper-Ad contamination levels and low yields of chimeric HDAds.

7. CAV-2/ΦC31CreΨ* was successfully generated and amplified, and the inclusion of *attB* in CAV-2 leads to a delayed viral life cycle of 66 hours. However, the production of HDCAV-2 using CAV-2/ΦC31CreΨ* as a helper-CAV-2 is not recommended, as this vector is unable to amplify efficiently HDCAV-2 vectors.

8. Biologically relevant titration of CAV-2 from crude lysate and purified preparations can be achieved by a newly developed titration method consisting on the analysis by qPCR of DNA samples from infected cell nucleus.

9. The optimization of each amplification step and a final removal of helper virions by ultracentrifugation allows the production of HDCAV-2 vectors RIGIE and HDmax using JBΔ5 helper-CAV-2 vectors more efficiently than the current described method based on cell sorting. However, more optimization is required to improve the production yields as well as to reduce more the helper-Ad contamination levels.

10. There is a nuclear protein that interacts with the *attB* sequence and leads to the delay of the viral life cycle of *attB*-vectors. Biacore analysis suggested that this protein could be prothymosin alpha. However, further attempts to verify this possibility using overexpression of this protein or its specific inhibition by shRNA in HEK-293 did not lead to differences in the life viral cycle of *attB*-vectors, suggesting that prothymosin alpha is not the protein responsible for the delay.

Chapter 8

BIBLIOGRAPHY

A

Acsadi G, Jani A, Massie B, Simoneau M, Holland P, Blaschuk K*, et al.* A differential efficiency of adenovirus-mediated in vivo gene transfer into skeletal muscle cells of different maturity. Hum Mol Genet 1994; 3: 579-84.

Akusjärvi G, Aleström P, Pettersson M, Lager M, Jörnvall H, Pettersson U. The gene for the adenovirus 2 hexon polypeptide. J Biol Chem. 1984; 259:13976-9.

Alba R, Bradshaw AC, Parker AL, Bhella D, Waddington SN, Nicklin SA, *et al*. Identification of coagulation factor (F)X binding sites on the adenovirus serotype 5 hexon: effect of mutagenesis on FX interactions and gene transfer. Blood. 2009; 114:965-71.

Alba R, Cots D, Ostapchuk P, Bosch A, Hearing P, Chillon M. Altering the Ad5 packaging domain affects the maturation of the Ad particles. PLoS One 2011; 6: e19564.

Alba R, Hearing P, Bosch A, Chillon M. Differential amplification of adenovirus vectors by flanking the packaging signal with attB/attP-PhiC31 sequences: implications for helper-dependent adenovirus production. Virology 2007; 367: 51-8.

Amalfitano A, Begy CR, Chamberlain JS. Improved adenovirus packaging cell lines to support the growth of replication-defective gene-delivery vectors. Proc Natl Acad Sci U S A. 1996; 93:3352-6.

Amalfitano A, Hauser MA, Hu H, Serra D, Begy CR, Chamberlain JS. Production and characterization of improved adenovirus vectors with the E1, E2b, and E3 genes deleted. J Virol. 1998; 72:926-33.

Aoki K, Benkö M, Davison AJ, Echavarria M, Erdman DD, Harrach B, *et al*; Members of the Adenovirus Research Community. Toward an integrated human adenovirus designation system that utilizes molecular and serological data and serves both clinical and fundamental virology. J Virol. 2011; 85:5703-4.

Armentano D, Zabner J, Sacks C, Sookdeo CC, Smith MP, St George JA, *et al*. Effect of the E4 region on the persistence of transgene expression from adenovirus vectors. J Virol. 1997; 71:2408-16.

B

Balamotis MA1, Huang K, Mitani K. Efficient delivery and stable gene expression in a hematopoietic cell line using a chimeric serotype 35 fiber pseudotyped helper-dependent adenoviral vector. Virology. 2004; 324:229-37.

Benihoud K, Yeh P, Perricaudet M. Adenovirus vectors for gene delivery. Curr Opin Biotechnol. 1999; 10:440-7. Review.

Bergelson JM, Cunningham JA, Droguett G, Kurt-Jones EA, Krithivas A, Hong JS, *et al*. Isolation of a common receptor for Coxsackie B viruses and adenoviruses 2 and 5. Science. 1997; 275:1320-3.

Bett AJ, Prevec L, Graham FL. Packaging capacity and stability of human adenovirus type 5 vectors. J Virol. 1993; 67:5911-21.

Bilbao R, Reay DP, Wu E, Zheng H, Biermann V, Kochanek S*, et al.* Comparison of high-capacity and first-generation adenoviral vector gene delivery to murine muscle in utero. Gene therapy 2005; 12: 39-47.

Bilbao R, Srinivasan S, Reay D, Goldberg L, Hughes T, Roelvink PW*, et al.* Binding of adenoviral fiber knob to the coxsackievirus-adenovirus receptor is crucial for transduction of fetal muscle. Hum Gene Ther 2003; 14: 645-9.

Blackford AN, Patel RN, Forrester NA, Theil K, Groitl P, Stewart GS, *et al*. Adenovirus 12 E4orf6 inhibits ATR activation by promoting TOPBP1 degradation. Proc Natl Acad Sci U S A. 2010; 107:12251-6.

Blaese RM, Culver KW, Miller AD, Carter CS, Fleisher T, Clerici M, *et al*. T lymphocyte-directed gene therapy for ADA- SCID: initial trial results after 4 years. Science. 1995; 270:475-80.

Bowles DE, McPhee SW, Li C, Gray SJ, Samulski JJ, Camp AS, *et al*. Phase 1 gene therapy for Duchenne muscular dystrophy using a translational optimized AAV vector. Mol Ther. 2012; 20:443-55.

Bremner KH, Scherer J, Yi J, Vershinin M, Gross SP, Vallee RB. Adenovirus transport via direct interaction of cytoplasmic dynein with the viral capsid hexon subunit. Cell Host Microbe. 2009; 6:523-35.

Brenner M. Gene transfer by adenovectors. Blood 1999; 94: 3965-7.

Brough DE, Lizonova A, Hsu C, Kulesa VA, Kovesdi I. A gene transfer vector-cell line system for complete functional complementation of adenovirus early regions E1 and E4. J Virol. 1996; 70:6497-501.

Brunetti-Pierri N, Grove NC, Zuo Y, Edwards R, Palmer D, Cerullo V*, et al.* Bioengineered factor IX molecules with increased catalytic activity improve the therapeutic index of gene therapy vectors for hemophilia B. Hum Gene Ther 2009a; 20: 479-85.

Brunetti-Pierri N, Liou A, Patel P, Palmer D, Grove N, Finegold M*, et al.* Balloon catheter delivery of helper-dependent adenoviral vector results in sustained, therapeutic hFIX expression in rhesus macaques. Mol Ther 2012; 20: 1863-70.

Brunetti-Pierri N, Nichols TC, McCorquodale S, Merricks E, Palmer DJ, Beaudet AL*, et al.* Sustained phenotypic correction of canine hemophilia B after systemic administration of helper-dependent adenoviral vector. Hum Gene Ther 2005a; 16: 811-20.

Brunetti-Pierri N, Ng T, Iannitti DA, Palmer DJ, Beaudet AL, Finegold MJ*, et al.* Improved hepatic transduction, reduced systemic vector dissemination, and long-term transgene expression by delivering helper-dependent adenoviral vectors into the surgically isolated liver of nonhuman primates. Hum Gene Ther 2006; 17: 391-404.

Brunetti-Pierri N, Ng P. Progress and prospects: gene therapy for genetic diseases with helper-dependent adenoviral vectors. Gene therapy 2008; 15: 553-60.

Brunetti-Pierri N, Ng P. Progress towards liver and lung-directed gene therapy with helper-dependent adenoviral vectors. Current gene therapy 2009b; 9: 329-40.

Brunetti-Pierri N, Palmer DJ, Mane V, Finegold M, Beaudet AL, Ng P. Increased hepatic transduction with reduced systemic dissemination and proinflammatory cytokines following hydrodynamic injection of helper-dependent adenoviral vectors. Mol Ther 2005b; 12: 99-106.

Brunetti-Pierri N, Stapleton GE, Law M, Breinholt J, Palmer DJ, Zuo Y*, et al.* Efficient, long-term hepatic gene transfer using clinically relevant HDAd doses by balloon occlusion catheter delivery in nonhuman primates. Mol Ther 2009c; 17: 327-33.

Brunetti-Pierri N, Stapleton GE, Palmer DJ, Zuo Y, Mane VP, Finegold MJ*, et al.* Pseudo-hydrodynamic delivery of helper-dependent adenoviral vectors into non-human primates for liver-directed gene therapy. Mol Ther 2007; 15: 732-40.

Bru T, Salinas S, Kremer EJ. An update on canine adenovirus type 2 and its vectors. Viruses. 2010; 2:2134-53.

Burney TJ, Davies JC. Gene therapy for the treatment of cystic fibrosis. Appl Clin Genet 2012; 5: 29-36.

Butti E, Bergami A, Recchia A, Brambilla E, Del Carro U, Amadio S*, et al.* IL4 gene delivery to the CNS recruits regulatory T cells and induces clinical recovery in mouse models of multiple sclerosis. Gene therapy 2008; 15: 504-15.

Butti E, Bergami A, Recchia A, Brambilla E, Franciotta D, Cattalini A*, et al.* Absence of an intrathecal immune reaction to a helper-dependent adenoviral vector delivered into the cerebrospinal fluid of non-human primates. Gene therapy 2008b; 15: 233-8.

C

Cannon P, June C. Chemokine receptor 5 knockout strategies. Curr Opin HIV AIDS. 2011; 6:74-9. Review.

Cao H, Yang T, Li XF, Wu J, Duan C, Coates AL*, et al.* Readministration of helper-dependent adenoviral vectors to mouse airway mediated via transient immunosuppression. Gene therapy 2011; 18: 173-81.

Cartier N, Hacein-Bey-Abina S, Bartholomae CC, Veres G, Schmidt M, Kutschera I, *et al*. Hematopoietic stem cell gene therapy with a lentiviral vector in X-linked adrenoleukodystrophy. Science. 2009; 326:818-23.

Castro M, Xiong W, Puntel M, Farrokhi C, Kroeger KM, Pechnick RN*, et al.* Safety Profile of Gutless Adenovirus Vectors Delivered into the Normal Brain Parenchyma: Implications for a Glioma Phase I Clinical Trial. Human gene therapy methods 2012.

Cavazzana-Calvo M, Payen E, Negre O, Wang G, Hehir K, Fusil F, *et al*. Transfusion independence and HMGA2 activation after gene therapy of human β-thalassaemia. Nature. 2010; 467:318-22.

Cerullo V, Seiler MP, Mane V, Brunetti-Pierri N, Clarke C, Bertin TK*, et al.* Toll-like receptor 9 triggers an innate immune response to helper-dependent adenoviral vectors. Mol Ther 2007; 15: 378-85.

Chardonnet Y, Dales S. Early events in the interaction of adenoviruses with HeLa cells. I. Penetration of type 5 and intracellular release of the DNA genome. Virology. 1970; 40:462-77.

Chartier C, Degryse E, Gantzer M, Dieterle A, Pavirani A, Mehtali M. Efficient generation of recombinant adenovirus vectors by homologous recombination in Escherichia coli. J Virol. 1996; 70:4805-10.

Chen D, Maa YF, Haynes JR. Needle-free epidermal powder immunization. Expert Rev Vaccines. 2002; 1:265-76. Review.

Christensen JB, Ewing SG, Imperiale MJ. Identification and characterization of a DNA binding domain on the adenovirus IVa2 protein. Virology. 2012; 433:124-30.

Chung J, Rossi JJ, Jung U. Current progress and challenges in HIV gene therapy. Future Virol. 2011; 6:1319-1328.

Chu Q, St George JA, Lukason M, Cheng SH, Scheule RK, Eastman SJ. EGTA enhancement of adenovirus-mediated gene transfer to mouse tracheal epithelium in vivo. Hum Gene Ther 2001; 12: 455-67.

Ciuffi A. Mechanisms governing lentivirus integration site selection. Curr Gene Ther. 2008; 8:419-29. Review.

Coura R dos Santos, Nardi NB. The state of the art of adeno-associated virus-based vectors in gene therapy. Virol J. 2007; 4:99. Review.

Crane B, Luo X, Demaster A, Williams KD, Kozink DM, Zhang P*, et al.* Rescue administration of a helper-dependent adenovirus vector with long-term efficacy in dogs with glycogen storage disease type Ia. Gene therapy 2012; 19: 443-52.

Crettaz J, Berraondo P, Mauleon I, Ochoa-Callejero L, Shankar V, Barajas M*, et al.* Intrahepatic injection of adenovirus reduces inflammation and increases gene transfer and therapeutic effect in mice. Hepatology 2006; 44: 623-32.

Crettaz J, Otano I, Ochoa-Callejero L, Benito A, Paneda A, Aurrekoetxea I*, et al.* Treatment of chronic viral hepatitis in woodchucks by prolonged intrahepatic expression of interleukin-12. Journal of virology 2009; 83: 2663-74.

Croyle MA, Chirmule N, Zhang Y, Wilson JM. "Stealth" adenoviruses blunt cell-mediated and humoral immune responses against the virus and allow for significant gene expression upon readministration in the lung. Journal of virology 2001; 75: 4792-801.

Cupelli K, Stehle T. Viral attachment strategies: the many faces of adenoviruses. Curr Opin Virol. 2011; 1:84-91. Review.

D

Dai Y, Schwarz EM, Gu D, Zhang WW, Sarvetnick N, Verma IM. Cellular and humoral immune responses to adenoviral vectors containing factor IX gene: tolerization of factor

IX and vector antigens allows for long-term expression. Proceedings of the National Academy of Sciences of the United States of America 1995; 92: 1401-5.

Danthinne X, Imperiale MJ. Production of first generation adenovirus vectors: a review. Gene Ther. 2000; 7:1707-14. Review.

Davidson BL, Breakefield XO. Viral vectors for gene delivery to the nervous system. Nat Rev Neurosci. 2003; 4:353-64. Review.

Dechecchi MC, Melotti P, Bonizzato A, Santacatterina M, Chilosi M, Cabrini G. Heparan sulfate glycosaminoglycans are receptors sufficient to mediate the initial binding of adenovirus types 2 and 5. J Virol. 2001; 75:8772-80.

DeMatteo RP, Chu G, Ahn M, Chang E, Barker CF, Markmann JF. Long-lasting adenovirus transgene expression in mice through neonatal intrathymic tolerance induction without the use of immunosuppression. Journal of virology 1997; 71: 5330-5.

Deol JR, Danialou G, Larochelle N, Bourget M, Moon JS, Liu AB*, et al.* Successful compensation for dystrophin deficiency by a helper-dependent adenovirus expressing full-length utrophin. Mol Ther 2007; 15: 1767-74.

Dimmock D, Brunetti-Pierri N, Palmer DJ, Beaudet AL, Ng P. Correction of hyperbilirubinemia in gunn rats using clinically relevant low doses of helper-dependent adenoviral vectors. Hum Gene Ther 2011; 22: 483-8.

Dindot S, Piccolo P, Grove N, Palmer D, Brunetti-Pierri N. Intrathecal injection of helper-dependent adenoviral vectors results in long-term transgene expression in neuroependymal cells and neurons. Hum Gene Ther 2011; 22: 745-51.

Dormond E, Kamen AA. Manufacturing of adenovirus vectors: production and purification of helper dependent adenovirus. Methods Mol Biol 2011; 737: 139-56.

Dormond E, Meneses-Acosta A, Jacob D, Durocher Y, Gilbert R, Perrier M*, et al.* An efficient and scalable process for helper-dependent adenoviral vector production using polyethylenimine-adenofection. Biotechnol Bioeng 2009a; 102: 800-10.

Dormond E, Perrier M, Kamen A. From the first to the third generation adenoviral vector: what parameters are governing the production yield? Biotechnol Adv 2009b; 27: 133-44.

Dormond E, Perrier M, Kamen A. Identification of critical infection parameters to control helper-dependent adenoviral vector production. J Biotechnol 2009c; 142: 142-50.

Dropulić B. Lentiviral vectors: their molecular design, safety, and use in laboratory and preclinical research. Hum Gene Ther. 2011; 22:649-57. Review.

Dudley RW, Lu Y, Gilbert R, Matecki S, Nalbantoglu J, Petrof BJ*, et al.* Sustained improvement of muscle function one year after full-length dystrophin gene transfer into mdx mice by a gutted helper-dependent adenoviral vector. Hum Gene Ther 2004; 15: 145-56.

E

Eberling JL, Jagust WJ, Christine CW, Starr P, Larson P, Bankiewicz KS, *et al.* Results from a phase I safety trial of hAADC gene therapy for Parkinson disease. Neurology. 2008; 70:1980-3.

Enders JF, Bell JA, Dingle JH, Francis T Jr, Hilleman MR, Huebner RJ, *et al*. Adenoviruses: group name proposed for new respiratory-tract viruses. Science. 1956; 124:119-20.

F

Fabry CM, Rosa-Calatrava M, Conway JF, Zubieta C, Cusack S, Ruigrok RW, *et al*. A quasi-atomic model of human adenovirus type 5 capsid. EMBO J. 2005; 24:1645-54.

Fallaux FJ, Bout A, van der Velde I, van den Wollenberg DJ, Hehir KM, Keegan J, *et al*. New helper cells and matched early region 1-deleted adenovirus vectors prevent generation of replication-competent adenoviruses. Hum Gene Ther. 1998; 9:1909-17.

Fallaux FJ, Kranenburg O, Cramer SJ, Houweling A, Van Ormondt H, Hoeben RC, *et al*. Characterization of 911: a new helper cell line for the titration and propagation of early region 1-deleted adenoviral vectors. Hum Gene Ther. 1996; 7:215-22.

Fang B, Eisensmith RC, Wang H, Kay MA, Cross RE, Landen CN, *et al.* Gene therapy for hemophilia B: host immunosuppression prolongs the therapeutic effect of adenovirus-mediated factor IX expression. Hum Gene Ther 1995; 6: 1039-44.

Franich NR, Fitzsimons HL, Fong DM, Klugmann M, During MJ, Young D. AAV vector-mediated RNAi of mutant huntingtin expression is neuroprotective in a novel genetic rat model of Huntington's disease. Mol Ther. 2008; 16:947-56.

Fu YH, He JS, Zheng XX, Wang XB, Xie C, Shi CX, *et al.* Intranasal vaccination with a helper-dependent adenoviral vector enhances transgene-specific immune responses in BALB/c mice. Biochem Biophys Res Commun 2010; 391: 857-61.

G

Gallaher SD, Berk AJ. A rapid Q-PCR titration protocol for adenovirus and helper-dependent adenovirus vectors that produces biologically relevant results. J Virol Methods. 2013; 192:28-38.

Gastaldelli M, Imelli N, Boucke K, Amstutz B, Meier O, Greber UF. Infectious adenovirus type 2 transport through early but not late endosomes. Traffic. 2008; 9:2265-78.

Gau CL, Rosenblatt RA, Cerullo V, Lay FD, Dow AC, Livesay J, *et al.* Short-term correction of arginase deficiency in a neonatal murine model with a helper-dependent adenoviral vector. Mol Ther 2009; 17: 1155-63.

Gilbert R, Dudley RW, Liu AB, Petrof BJ, Nalbantoglu J, Karpati G. Prolonged dystrophin expression and functional correction of mdx mouse muscle following gene transfer with

a helper-dependent (gutted) adenovirus-encoding murine dystrophin. Hum Mol Genet 2003; 12: 1287-99.

Ginsberg HS, Pereira HG, Valentine RC, Wilcox WC. A proposed terminology for the adenovirus antigens and virion morphological subunits. Virology. 1966; 28:782-3.

Gräble M, Hearing P. Adenovirus type 5 packaging domain is composed of a repeated element that is functionally redundant. J Virol. 1990; 64:2047-56.

Graham FL, Smiley J, Russell WC, Nairn R. Characteristics of a human cell line transformed by DNA from human adenovirus type 5. J Gen Virol. 1977; 36:59-74.

Grieger JC, Samulski RJ. Adeno-associated virus vectorology, manufacturing, and clinical applications. Methods Enzymol 2012; 507: 229-54.

Groth AC, Olivares EC, Thyagarajan B, Calos MP. A phage integrase directs efficient site-specific integration in human cells. Proc Natl Acad Sci U S A. 2000; 97:5995-6000.

Guse K, Suzuki M, Sule G, Bertin TK, Tyynismaa H, Ahola-Erkkila S*, et al.* Capsid-modified adenoviral vectors for improved muscle-directed gene therapy. Hum Gene Ther 2012; 23: 1065-70.

Gustin KE, Lutz P, Imperiale MJ. Interaction of the adenovirus L1 52/55-kilodalton protein with the IVa2 gene product during infection. J Virol. 1996; 70:6463-7.

H

Hacein-Bey-Abina S, Von Kalle C, Schmidt M, McCormack MP, Wulffraat N, Leboulch P, *et al*. LMO2-associated clonal T cell proliferation in two patients after gene therapy for SCID-X1. Science. 2003; 302:415-9.

Hajjar, Zsebo K, Deckelbaum L, Thompson C, Rudy J, Yaroshinsky A, *et al.* Design of a phase 1/2 trial of intracoronary administration of AAV1/SERCA2a in patients with heart failure. J Card Fail. 2008; 14:355-67.

Harada JN, Shevchenko A, Shevchenko A, Pallas DC, Berk AJ. Analysis of the adenovirus E1B-55K-anchored proteome reveals its link to ubiquitination machinery. J Virol. 2002; 76:9194-206.

Harui A, Roth MD, Kiertscher SM, Mitani K, Basak SK. Vaccination with helper-dependent adenovirus enhances the generation of transgene-specific CTL. Gene therapy 2004; 11: 1617-26.

Hausl M, Zhang W, Voigtlander R, Muther N, Rauschhuber C, Ehrhardt A. Development of adenovirus hybrid vectors for Sleeping Beauty transposition in large mammals. Current gene therapy 2011; 11: 363-74.

Hearing P, Samulski RJ, Wishart WL, Shenk T. Identification of a repeated sequence element required for efficient encapsidation of the adenovirus type 5 chromosome. J

Virol. 1987; 61:2555-8.

Hearing P, Shenk T. The adenovirus type 5 E1A transcriptional control region contains a duplicated enhancer element. Cell. 1983; 33:695-703.

Hofherr SE, Senac JS, Chen CY, Palmer DJ, Ng P, Barry MA. Short-term rescue of neonatal lethality in a mouse model of propionic acidemia by gene therapy. Hum Gene Ther 2009; 20: 169-80.

Hong SS, Karayan L, Tournier J, Curiel DT, Boulanger PA. Adenovirus type 5 fiber knob binds to MHC class I alpha2 domain at the surface of human epithelial and B lymphoblastoid cells. EMBO J. 1997; 16:2294-306.

Horwitz, M. S. Adenoviruses. B. N. Fields and D. M. Knipe (ed.), Virology. Raven Press, New York. 1990. p. 1723–1740.

Hu C, Cela RG, Suzuki M, Lee B, Lipshutz GS. Neonatal helper-dependent adenoviral vector gene therapy mediates correction of hemophilia A and tolerance to human factor VIII. Proceedings of the National Academy of Sciences of the United States of America 2011; 108: 2082-7.

Huang B, Schiefer J, Sass C, Kosinski CM, Kochanek S. Inducing huntingtin inclusion formation in primary neuronal cell culture and in vivo by high-capacity adenoviral vectors expressing truncated and full-length huntingtin with polyglutamine expansion. J Gene Med 2008; 10: 269-79.

Huang B, Schiefer J, Sass C, Landwehrmeyer GB, Kosinski CM, Kochanek S. High-capacity adenoviral vector-mediated reduction of huntingtin aggregate load in vitro and in vivo. Hum Gene Ther 2007; 18: 303-11.

Huard J, Feero WG, Watkins SC, Hoffman EP, Rosenblatt DJ, Glorioso JC. The basal lamina is a physical barrier to herpes simplex virus-mediated gene delivery to mature muscle fibers. Journal of virology 1996; 70: 8117-23.

I

Ilan Y, Sauter B, Chowdhury NR, Reddy BV, Thummala NR, Droguett G*, et al.* Oral tolerization to adenoviral proteins permits repeated adenovirus-mediated gene therapy in rats with pre-existing immunity to adenoviruses. Hepatology 1998; 27: 1368-76.

Ishizaki M, Maeda Y, Kawano R, Suga T, Uchida Y, Uchino K*, et al.* Rescue from respiratory dysfunction by transduction of full-length dystrophin to diaphragm via the peritoneal cavity in utrophin/dystrophin double knockout mice. Mol Ther 2011; 19: 1230-5.

J

Jain A, Jain SK. PEGylation: an approach for drug delivery. A review. Crit Rev Ther Drug Carrier Syst 2008; 25: 403-47.

Jansen PL. Diagnosis and management of Crigler-Najjar syndrome. Eur J Pediatr 1999; 158 Suppl 2: S89-94.

Jiang B, Du L, Flynn R, Dronadula N, Zhang J, Kim F*, et al.* Overexpression of endothelial nitric oxide synthase improves endothelium-dependent vasodilation in arteries infused with helper-dependent adenovirus. Hum Gene Ther 2012; 23: 1166-75.

Jiang Z, Schiedner G, van Rooijen N, Liu CC, Kochanek S, Clemens PR. Sustained muscle expression of dystrophin from a high-capacity adenoviral vector with systemic gene transfer of T cell costimulatory blockade. Mol Ther 2004; 10: 688-96.

Józkowicz A, Dulak J. Helper-dependent adenoviral vectors in experimental gene therapy. Acta Biochim Pol. 2005; 52:589-99. Review.

K

Kampik D, Ali RR, Larkin DF. Experimental gene transfer to the corneal endothelium. Exp Eye Res. 2012; 95:54-9. Review.

Kaplan JM, Pennington SE, St George JA, Woodworth LA, Fasbender A, Marshall J*, et al.* Potentiation of gene transfer to the mouse lung by complexes of adenovirus vector and polycations improves therapeutic potential. Hum Gene Ther 1998; 9: 1469-79.

Kaplan JM, Smith AE. Transient immunosuppression with deoxyspergualin improves longevity of transgene expression and ability to readminister adenoviral vector to the mouse lung. Hum Gene Ther 1997; 8: 1095-104.

Kass-Eisler A, Falck-Pedersen E, Elfenbein DH, Alvira M, Buttrick PM, Leinwand LA. The impact of developmental stage, route of administration and the immune system on adenovirus-mediated gene transfer. Gene therapy 1994; 1: 395-402.

Kaufmann JK, Nettelbeck DM. Virus chimeras for gene therapy, vaccination, and oncolysis: adenoviruses and beyond. Trends Mol Med. 2012 Jul; 18:365-76. Review.

Kay MA, Glorioso JC, Naldini L. Viral vectors for gene therapy: the art of turning infectious agents into vehicles of therapeutics. Nat Med. 2001; 7:33-40. Review.

Kay MA, Holterman AX, Meuse L, Gown A, Ochs HD, Linsley PS*, et al.* Long-term hepatic adenovirus-mediated gene expression in mice following CTLA4Ig administration. Nat Genet 1995; 11: 191-7.

Kay MA, Meuse L, Gown AM, Linsley P, Hollenbaugh D, Aruffo A*, et al.* Transient immunomodulation with anti-CD40 ligand antibody and CTLA4Ig enhances persistence and secondary adenovirus-mediated gene transfer into mouse liver. Proceedings of the National Academy of Sciences of the United States of America 1997; 94: 4686-91.

Kiang A, Hartman ZC, Liao S, Xu F, Serra D, Palmer DJ*, et al.* Fully deleted adenovirus persistently expressing GAA accomplishes long-term skeletal muscle glycogen correction in tolerant and nontolerant GSD-II mice. Mol Ther 2006; 13: 127-34.

Kim IH, Jozkowicz A, Piedra PA, Oka K, Chan L. Lifetime correction of genetic deficiency in mice with a single injection of helper-dependent adenoviral vector. Proceedings of the National Academy of Sciences of the United States of America 2001; 98: 13282-7.

Kochanek S. High-capacity adenoviral vectors for gene transfer and somatic gene therapy. Hum Gene Ther 1999; 10: 2451-9.

Koeberl DD, Sun B, Bird A, Chen YT, Oka K, Chan L. Efficacy of helper-dependent adenovirus vector-mediated gene therapy in murine glycogen storage disease type Ia. Mol Ther 2007; 15: 1253-8.

Koehler DR, Sajjan U, Chow YH, Martin B, Kent G, Tanswell AK*, et al.* Protection of Cftr knockout mice from acute lung infection by a helper-dependent adenoviral vector expressing Cftr in airway epithelia. Proceedings of the National Academy of Sciences of the United States of America 2003; 100: 15364-9.

Koehler DR, Frndova H, Leung K, Louca E, Palmer D, Ng P*, et al.* Aerosol delivery of an enhanced helper-dependent adenovirus formulation to rabbit lung using an intratracheal catheter. J Gene Med 2005; 7: 1409-20.

Koehler DR, Martin B, Corey M, Palmer D, Ng P, Tanswell AK*, et al.* Readministration of helper-dependent adenovirus to mouse lung. Gene therapy 2006; 13: 773-80.

Kohn DB. Update on gene therapy for immunodeficiencies. Clin Immunol. 2010; 135:247-54. Review.

Koski A, Karli E, Kipar A, Escutenaire S, Kanerva A, Hemminki A. Mutation of the fiber shaft heparan sulphate binding site of a 5/3 chimeric adenovirus reduces liver tropism. PLoS One. 2013; 8:e60032.

Kron MW, Engler T, Schmidt E, Schirmbeck R, Kochanek S, Kreppel F. High-capacity adenoviral vectors circumvent the limitations of DeltaE1 and DeltaE1/DeltaE3 adenovirus vectors to induce multispecific transgene product-directed CD8 T-cell responses. J Gene Med 2011; 13: 648-57.

Kuriyama S, Tominaga K, Mitoro A, Tsujinoue H, Nakatani T, Yamazaki M*, et al.* Immunomodulation with FK506 around the time of intravenous re-administration of an adenoviral vector facilitates gene transfer into primed rat liver. Int J Cancer 2000; 85: 839-44.

Kuzmin AI, Finegold MJ, Eisensmith RC. Macrophage depletion increases the safety, efficacy and persistence of adenovirus-mediated gene transfer in vivo. Gene therapy 1997; 4: 309-16.

L

Lam AP, Dean DA. Progress and prospects: nuclear import of nonviral vectors. Gene Ther. 2010; 17:439-47. Review.

Larochelle N, Teng Q, Gilbert R, Deol JR, Karpati G, Holland PC*, et al.* Modulation of coxsackie and adenovirus receptor expression for gene transfer to normal and dystrophic skeletal muscle. J Gene Med 2010; 12: 266-75.

Lau AA, Rozaklis T, Ibanes S, Luck AJ, Beard H, Hassiotis S*, et al.* Helper-dependent canine adenovirus vector-mediated transgene expression in a neurodegenerative lysosomal storage disorder. Gene 2012; 491: 53-7.

Leopold PL, Crystal RG. Intracellular trafficking of adenovirus: many means to many ends. Adv Drug Deliv Rev. 2007; 59:810-21. Review.

Li R, Chao H, Ko KW, Cormier S, Dieker C, Nour EA*, et al.* Gene Therapy Targeting LDL Cholesterol but not HDL Cholesterol Induces Regression of Advanced Atherosclerosis in a Mouse Model of Familial Hypercholesterolemia. J Genet Syndr Gene Ther 2011; 2: 106.

Li R, Oka K, Yechoor V. Neo-islet formation in liver of diabetic mice by helper-dependent adenoviral vector-mediated gene transfer. J Vis Exp 2012.

Li Y, Shi CX, Mossman KL, Rosenfeld J, Boo YC, Schellhorn HE. Restoration of vitamin C synthesis in transgenic Gulo-/- mice by helper-dependent adenovirus-based expression of gulonolactone oxidase. Hum Gene Ther 2008; 19: 1349-58.

Lievens J, Snoeys J, Vekemans K, Van Linthout S, de Zanger R, Collen D*, et al.* The size of sinusoidal fenestrae is a critical determinant of hepatocyte transduction after adenoviral gene transfer. Gene therapy 2004; 11: 1523-31.

Lochmüller H, Jani A, Huard J, Prescott S, Simoneau M, Massie B, *et al*. Emergence of early region 1-containing replication-competent adenovirus in stocks of replication-defective adenovirus recombinants (delta E1 + delta E3) during multiple passages in 293 cells. Hum Gene Ther. 1994; 5:1485-91.

Loonstra A, Vooijs M, Beverloo HB, Allak BA, van Drunen E, Kanaar R*, et al.* Growth inhibition and DNA damage induced by Cre recombinase in mammalian cells. Proceedings of the National Academy of Sciences of the United States of America 2001; 98: 9209-14.

Lusky M. Good manufacturing practice production of adenoviral vectors for clinical trials. Hum Gene Ther 2005; 16: 281-91.

M

Ma L, Bluyssen HA, De Raeymaeker M, Laurysens V, van der Beek N, Pavliska H, *et al*. Rapid determination of adenoviral vector titers by quantitative real-time PCR. J Virol Methods. 2001; 93:181-8.

Maier O, Galan DL, Wodrich H, Wiethoff CM. An N-terminal domain of adenovirus protein VI fragments membranes by inducing positive membrane curvature. Virology. 2010; 402:11-9.

Maizel JV Jr, White DO, Scharff MD. The polypeptides of adenovirus. I. Evidence for multiple protein components in the virion and a comparison of types 2, 7A, and 12. Virology. 1968; 36:115-25.

Mastrangeli A, Harvey BG, Yao J, Wolff G, Kovesdi I, Crystal RG*, et al.* "Sero-switch" adenovirus-mediated in vivo gene transfer: circumvention of anti-adenovirus humoral immune defenses against repeat adenovirus vector administration by changing the adenovirus serotype. Hum Gene Ther 1996; 7: 79-87.

Matecki S, Dudley RW, Divangahi M, Gilbert R, Nalbantoglu J, Karpati G*, et al.* Therapeutic gene transfer to dystrophic diaphragm by an adenoviral vector deleted of all viral genes. Am J Physiol Lung Cell Mol Physiol 2004; 287: L569-76.

McCormack WM, Jr., Seiler MP, Bertin TK, Ubhayakar K, Palmer DJ, Ng P*, et al.* Helper-dependent adenoviral gene therapy mediates long-term correction of the clotting defect in the canine hemophilia A model. J Thromb Haemost 2006; 4: 1218-25.

Meier O, Greber UF. Adenovirus endocytosis. J Gene Med. 2004; 6:S152-63. Review.

Meyburg J, Hoffmann GF. Liver transplantation for inborn errors of metabolism. Transplantation 2005; 80: S135-7.

Mian A, McCormack WM, Jr., Mane V, Kleppe S, Ng P, Finegold M*, et al.* Long-term correction of ornithine transcarbamylase deficiency by WPRE-mediated overexpression using a helper-dependent adenovirus. Mol Ther 2004; 10: 492-9.

Miralles M, Segura MM, Puig M, Bosch A, Chillon M. Efficient Amplification of Chimeric Adenovirus 5/40S Vectors Carrying the Short Fiber Protein of Ad40 in Suspension Cell Cultures. PLoS One. 2012; 7:e42073.

Mok H, Palmer DJ, Ng P, Barry MA. Evaluation of polyethylene glycol modification of first-generation and helper-dependent adenoviral vectors to reduce innate immune responses. Mol Ther 2005; 11: 66-79.

Morral N, O'Neal W, Rice K, Leland M, Kaplan J, Piedra PA*, et al.* Administration of helper-dependent adenoviral vectors and sequential delivery of different vector serotype for long-term liver-directed gene transfer in baboons. Proceedings of the National Academy of Sciences of the United States of America 1999; 96: 12816-21.

Morral N, O'Neal WK, Rice K, Leland MM, Piedra PA, Aguilar-Cordova E*, et al.* Lethal toxicity, severe endothelial injury, and a threshold effect with high doses of an adenoviral vector in baboons. Hum Gene Ther 2002; 13: 143-54.

Moyer CL, Wiethoff CM, Maier O, Smith JG, Nemerow GR. Functional genetic and biophysical analyses of membrane disruption by human adenovirus. J Virol. 2011; 85:2631-41.

Muhammad AK, Puntel M, Candolfi M, Salem A, Yagiz K, Farrokhi C*, et al.* Study of the efficacy, biodistribution, and safety profile of therapeutic gutless adenovirus vectors as a prelude to a phase I clinical trial for glioblastoma. Clin Pharmacol Ther 2010; 88: 204-13.

Murakami M, Ugai H, Belousova N, Pereboev A, Dent P, Fisher PB, *et al*. Chimeric adenoviral vectors incorporating a fiber of human adenovirus 3 efficiently mediate gene

transfer into prostate cancer cells. Prostate. 2010; 70:362-76.

Muramatsu S, Fujimoto K, Kato S, Mizukami H, Asari S, Ikeguchi K, *et al.* A phase I study of aromatic L-amino acid decarboxylase gene therapy for Parkinson's disease. Mol Ther. 2010; 18:1731-5.

Muruve DA. The innate immune response to adenovirus vectors. Hum Gene Ther 2004; 15: 1157-66.

N

Nakamura T, Sato K, Hamada H. Reduction of Natural Adenovirus Tropism to the Liver by both Ablation of Fiber-Coxsackievirus and Adenovirus Receptor Interaction and Use of Replaceable Short Fiber. J Virol. 2003; 77: 2512–2521.

Nathwani AC, Tuddenham EG, Rangarajan S, Rosales C, McIntosh J, Linch DC, *et al*. Adenovirus-associated virus vector-mediated gene transfer in hemophilia B. N Engl J Med. 2011; 365:2357-65.

Nicol CG, Graham D, Miller WH, White SJ, Smith TA, Nicklin SA, *et al*. Effect of adenovirus serotype 5 fiber and penton modifications on in vivo tropism in rats. Mol Ther. 2004; 10:344-54.

Ng P, Beauchamp C, Evelegh C, Parks R, Graham FL. Development of a FLP/frt system for generating helper-dependent adenoviral vectors. Mol Ther. 2001; 3:809–815.

Ng P, Evelegh C, Cummings D, Graham FL. Cre levels limit packaging signal excision efficiency in the Cre/loxP helper-dependent adenoviral vector system. J Virol. 2002; 76:4181-9.

O

Oka K, Belalcazar LM, Dieker C, Nour EA, Nuno-Gonzalez P, Paul A*, et al.* Sustained phenotypic correction in a mouse model of hypoalphalipoproteinemia with a helper-dependent adenovirus vector. Gene therapy 2007; 14: 191-202.

Orre RS, Cotter MA 2nd, Subramanian C, Robertson ES. Prothymosin alpha functions as a cellular oncoprotein by inducing transformation of rodent fibroblasts in vitro. J Biol Chem. 2001; 276:1794-9.

Ostapchuk P, Anderson ME, Chandrasekhar S, Hearing P. The L4 22-kilodalton protein plays a role in packaging of the adenovirus genome. J Virol. 2006; 80:6973-81.

Ostapchuk P, Hearing P. Control of adenovirus packaging. J Cell Biochem. 2005; 96:25-35.

Ostapchuk P, Yang J, Auffarth E, Hearing P. Functional interaction of the adenovirus IVa2 protein with adenovirus type 5 packaging sequences. J Virol. 2005; 79:2831-8.

Otake K, Ennist DL, Harrod K, Trapnell BC. Nonspecific inflammation inhibits adenovirus-mediated pulmonary gene transfer and expression independent of specific acquired immune responses. Hum Gene Ther 1998; 9: 2207-22.

Ozcay F, Alehan F, Sevmis S, Karakayali H, Moray G, Torgay A*, et al.* Living related liver transplantation in Crigler-Najjar syndrome type 1. Transplant Proc 2009; 41: 2875-7.

P

Palmer D, Ng P. Improved system for helper-dependent adenoviral vector production. Mol Ther 2003; 8: 846-52.

Parker AL, McVey JH, Doctor JH, Lopez-Franco O, Waddington SN, Havenga MJ*, et al.* Influence of coagulation factor zymogens on the infectivity of adenoviruses pseudotyped with fibers from subgroup D. J Virol 2007; 81: 3627-31.

Parker AL, Waddington SN, Nicol CG, Shayakhmetov DM, Buckley SM, Denby L, *et al*. Multiple vitamin K-dependent coagulation zymogens promote adenovirus-mediated gene delivery to hepatocytes. Blood. 2006; 108:2554-61.

Parks RJ, Chen L, Anton M, Sankar U, Rudnicki MA, Graham FL. A helper-dependent adenovirus vector system: removal of helper virus by Cre-mediated excision of the viral packaging signal. Proceedings of the National Academy of Sciences of the United States of America 1996; 93: 13565-70.

Parks R, Evelegh C, Graham F. Use of helper-dependent adenoviral vectors of alternative serotypes permits repeat vector administration. Gene therapy 1999; 6: 1565-73.

Parks RJ, Graham FL. A helper-dependent system for adenovirus vector production helps define a lower limit for efficient DNA packaging. J Virol. 1997; 71:3293-8.

Perez-Romero P, Tyler RE, Abend JR, Dus M, Imperiale MJ. Analysis of the interaction of the adenovirus L1 52/55-kilodalton and IVa2 proteins with the packaging sequence in vivo and in vitro. J Virol. 2005; 79:2366-74.

Perreau M, Kremer EJ. The conundrum between immunological memory to adenovirus and their use as vectors in clinical gene therapy. Mol Biotechnol 2006; 34: 247-56.

Perreau M, Mennechet F, Serratrice N, Glasgow JN, Curiel DT, Wodrich H*, et al.* Contrasting effects of human, canine, and hybrid adenovirus vectors on the phenotypical and functional maturation of human dendritic cells: implications for clinical efficacy. J Virol 2007; 81: 3272-84.

Perricone MA, Rees DD, Sacks CR, Smith KA, Kaplan JM, St George JA. Inhibitory effect of cystic fibrosis sputum on adenovirus-mediated gene transfer in cultured epithelial cells. Hum Gene Ther 2000; 11: 1997-2008.

Persson A, Fan X, Widegren B, Englund E. Cell type- and region-dependent coxsackie adenovirus receptor expression in the central nervous system. J Neurooncol 2006; 78: 1-6.

Piccolo P and Brunetti-Pierri N. Challenges and Prospects for Helper-Dependent Adenoviral Vector-Mediated Gene Therapy. Biomedicines 2014; 2:132-148.

Piccolo P, Vetrini F, Mithbaokar P, Grove NC, Bertin T, Palmer D*, et al.* SR-A and SREC-I are Kupffer and endothelial cell receptors for helper-dependent adenoviral vectors. Mol Ther 2013; 21: 767-74.

Pickles RJ, Fahrner JA, Petrella JM, Boucher RC, Bergelson JM. Retargeting the coxsackievirus and adenovirus receptor to the apical surface of polarized epithelial cells reveals the glycocalyx as a barrier to adenovirus-mediated gene transfer. Journal of virology 2000; 74: 6050-7.

Pickles RJ, McCarty D, Matsui H, Hart PJ, Randell SH, Boucher RC. Limited entry of adenovirus vectors into well-differentiated airway epithelium is responsible for inefficient gene transfer. Journal of virology 1998; 72: 6014-23.

Poller W, Schneider-Rasp S, Liebert U, Merklein F, Thalheimer P, Haack A*, et al.* Stabilization of transgene expression by incorporation of E3 region genes into an adenoviral factor IX vector and by transient anti-CD4 treatment of the host. Gene therapy 1996; 3: 521-30.

Porteus MH, Connelly JP, Pruett SM. A look to future directions in gene therapy research for monogenic diseases. PLoS Genet. 2006; 2:e133. Review.

Puntel M, A KMG, Farrokhi C, Vanderveen N, Paran C, Appelhans A*, et al.* Safety profile, efficacy, and biodistribution of a bicistronic high-capacity adenovirus vector encoding a combined immunostimulation and cytotoxic gene therapy as a prelude to a phase I clinical trial for glioblastoma. Toxicol Appl Pharmacol 2013; 268: 318-30.

Puntel M, Muhammad AK, Candolfi M, Salem A, Yagiz K, Farrokhi C*, et al.* A novel bicistronic high-capacity gutless adenovirus vector that drives constitutive expression of herpes simplex virus type 1 thymidine kinase and tet-inducible expression of Flt3L for glioma therapeutics. Journal of virology 2010; 84: 6007-17.

R

Raper SE, Chirmule N, Lee FS, Wivel NA, Bagg A, Gao GP*, et al.* Fatal systemic inflammatory response syndrome in a ornithine transcarbamylase deficient patient following adenoviral gene transfer. Mol Genet Metab 2003; 80: 148-58.

Raty JK, Lesch HP, Wirth T, Yla-Herttuala S. Improving safety of gene therapy. Curr Drug Saf 2008; 3: 46-53.

Reay DP, Bilbao R, Koppanati BM, Cai L, O'Day TL, Jiang Z*, et al.* Full-length dystrophin gene transfer to the mdx mouse in utero. Gene therapy 2008; 15: 531-6.

Rein DT, Volkmer A, Beyer IM, Curiel DT, Janni W, Dragoi A, *et al*. Treatment of chemotherapy resistant ovarian cancer with a MDR1 targeted oncolytic adenovirus. Gynecol Oncol. 2011; 123:138-46.

Rodríguez E, Romero C, Río A, Miralles M, Raventós A, Planells L, *et al.* Short-fiber protein of ad40 confers enteric tropism and protection against acidic gastrointestinal conditions. Hum Gene Ther Methods. 2013 Aug; 24:195-204.

Rogers CS, Stoltz DA, Meyerholz DK, Ostedgaard LS, Rokhlina T, Taft PJ*, et al.* Disruption of the CFTR gene produces a model of cystic fibrosis in newborn pigs. Science 2008; 321: 1837-41.

Rohrbach M, Clarke JT. Treatment of lysosomal storage disorders: progress with enzyme replacement therapy. Drugs. 2007; 67:2697-716.

Russell WC. Update on adenovirus and its vectors. J Gen Virol. 2000; 81:2573-604. Review.

Rux JJ, Burnett RM. Adenovirus structure. Hum Gene Ther. 2004; 15:1167-76. Review.

S

Samson SL, Gonzalez EV, Yechoor V, Bajaj M, Oka K, Chan L. Gene therapy for diabetes: metabolic effects of helper-dependent adenoviral exendin 4 expression in a diet-induced obesity mouse model. Mol Ther 2008; 16: 1805-12.

Saphire AC, Guan T, Schirmer EC, Nemerow GR, Gerace L. Nuclear import of adenovirus DNA in vitro involves the nuclear protein import pathway and hsc70. J Biol Chem. 2000; 275:4298-304.

Sato M, Suzuki S, Kubo S, Mitani K. Replication and packaging of helper-dependent adenoviral vectors. Gene therapy 2002; 9: 472-6.

Schagen FH, Ossevoort M, Toes RE, Hoeben RC. Immune responses against adenoviral vectors and their transgene products: a review of strategies for evasion. Crit Rev Oncol Hematol 2004; 50: 51-70.

Schiedner G, Hertel S, Kochanek S. Efficient transformation of primary human amniocytes by E1 functions of Ad5: generation of new cell lines for adenoviral vector production. Hum Gene Ther. 2000; 11:2105-16.

Schmid SI, Hearing P. Cellular components interact with adenovirus type 5 minimal DNA packaging domains. J Virol. 1998; 72:6339-47.

Schoggins JW, Nociari M, Philpott N, Falck-Pedersen E. Influence of fiber detargeting on adenovirus-mediated innate and adaptive immune activation. J Virol. 2005; 79:11627-37.

Segura MM, Alba R, Bosch A, Chillon M. Advances in helper-dependent adenoviral vector research. Current gene therapy 2008; 8:222-35.

Segura MM, Monfar M, Puig M, Mennechet F, Ibanes S, Chillón M. A real-time PCR assay for quantification of canine adenoviral vectors. J Virol Methods. 2010; 163:129-36.

Seto D, Chodosh J, Brister JR, Jones MS; Members of the Adenovirus Research Community. Using the whole-genome sequence to characterize and name human adenoviruses. J Virol. 2011; 85:5701-2.

Seiler MP, Cerullo V, Lee B. Immune response to helper dependent adenoviral mediated liver gene therapy: challenges and prospects. Current gene therapy 2007; 7: 297-305.

Shayakhmetov DM, Gaggar A, Ni S, Li ZY, Lieber A. Adenovirus binding to blood factors results in liver cell infection and hepatotoxicity. J Virol 2005; 79: 7478-91.

Sherwood V, Burgert HG, Chen YH, Sanghera S, Katafigiotis S, *et al*., Improved growth of enteric adenovirus type 40 in a modified cell line that can no longer respond to interferon stimulation. J Gen Virol. 2007; 88:71-76.

Shinagawa M, Iida Y, Matsuda A, Tsukiyama T, Sato G. Phylogenetic relationships between adenoviruses as inferred from nucleotide sequences of inverted terminal repeats. Gene. 1987; 55:85-93.

Silver DP, Livingston DM. Self-excising retroviral vectors encoding the Cre recombinase overcome Cre-mediated cellular toxicity. Mol Cell. 2001; 8:233-43.

Silver J, Mei YF. Transduction and oncolytic profile of a potent replication-competent adenovirus 11p vector (RCAd11pGFP) in colon carcinoma cells. PLoS One. 2011; 6:e17532.

Simonaro CM, D'Angelo M, He X, Eliyahu E, Shtraizent N, Haskins ME, *et al.* Mechanism of glycosaminoglycan-mediated bone and joint disease: implications for the mucopolysaccharidoses and other connective tissue diseases. Am J Pathol. 2008; 172:112-22.

Simonelli F, Maguire AM, Testa F, Pierce EA, Mingozzi F, Bennicelli JL, *et al.* Gene therapy for Leber's congenital amaurosis is safe and effective through 1.5 years after vector administration. Mol Ther. 2010; 18:643-50.

Snoeys J, Lievens J, Wisse E, Jacobs F, Duimel H, Collen D*, et al.* Species differences in transgene DNA uptake in hepatocytes after adenoviral transfer correlate with the size of endothelial fenestrae. Gene therapy 2007; 14: 604-12.

Soudais C, Laplace-Builhe C, Kissa K, Kremer EJ. Preferential transduction of neurons by canine adenovirus vectors and their efficient retrograde transport in vivo. FASEB J. 2001; 15:2283-5.

Soudais C, Skander N, Kremer EJ. Long-term in vivo transduction of neurons throughout the rat CNS using novel helper-dependent CAV-2 vectors. FASEB J 2004; 18: 391-3.

Stein CS, Pemberton JL, van Rooijen N, Davidson BL. Effects of macrophage depletion and anti-CD40 ligand on transgene expression and redosing with recombinant adenovirus. Gene therapy 1998; 5: 431-9.

Stephen SL, Montini E, Sivanandam VG, Al-Dhalimy M, Kestler HA, Finegold M*, et al.* Chromosomal integration of adenoviral vector DNA in vivo. Journal of virology 2010; 84: 9987-94.

Stephen SL, Sivanandam VG, Kochanek S. Homologous and heterologous recombination between adenovirus vector DNA and chromosomal DNA. J Gene Med. 2008; 10:1176-89.

Stoff-Khalili MA, Rivera AA, Stoff A, Michael Mathis J, Rocconi RP, Matthews QL, *et al*. Combining high selectivity of replication via CXCR4 promoter with fiber chimerism for effective adenoviral oncolysis in breast cancer. Int J Cancer. 2007; 120:935-41.

Strunze S, Engelke MF, Wang IH, Puntener D, Boucke K, Schleich S, *et al*. Kinesin-1-mediated capsid disassembly and disruption of the nuclear pore complex promote virus infection. Cell Host Microbe. 2011.

Smith JG, Cassany A, Gerace L, Ralston R, Nemerow GR. Neutralizing antibody blocks adenovirus infection by arresting microtubule-dependent cytoplasmic transport. J Virol. 2008; 82:6492-500.

Smith JG, Silvestry M, Lindert S, Lu W, Nemerow GR, Stewart PL. Insight into the mechanisms of adenovirus capsid disassembly from studies of defensin neutralization. PLoS Pathog. 2010; 6:e1000959.

Suomalainen M, Nakano MY, Keller S, Boucke K, Stidwill RP, Greber UF. Microtubule-dependent plus- and minus end-directed motilities are competing processes for nuclear targeting of adenovirus. J Cell Biol. 1999; 144:657-72.

Suzuki M, Cela R, Clarke C, Bertin TK, Mourino S, Lee B. Large-scale production of high-quality helper-dependent adenoviral vectors using adherent cells in cell factories. Hum Gene Ther 2010; 21: 120-6.

T

Tao N, Gao GP, Parr M, Johnston J, Baradet T, Wilson JM*, et al.* Sequestration of adenoviral vector by Kupffer cells leads to a nonlinear dose response of transduction in liver. Mol Ther 2001; 3: 28-35.

Tardieu M, Zerah M, Husson B, de Bournonville S, Deiva K, Adamsbaum C, *et al.* Intracerebral administration of AAV rh.10 carrying human SGSH and SUMF1 cDNAs in children with MPSIIIA disease: results of a phase I/II trial. Hum Gene Ther. 2014. *Ahead of print.*

Terashima T, Oka K, Kritz AB, Kojima H, Baker AH, Chan L. DRG-targeted helper-dependent adenoviruses mediate selective gene delivery for therapeutic rescue of sensory neuronopathies in mice. J Clin Invest 2009; 119: 2100-112.

Thomas CE, Schiedner G, Kochanek S, Castro MG, Lowenstein PR. Peripheral infection with adenovirus causes unexpected long-term brain inflammation in animals injected intracranially with first-generation, but not with high-capacity, adenovirus vectors: toward realistic long-term neurological gene therapy for chronic diseases. Proceedings of the National Academy of Sciences of the United States of America 2000; 97: 7482-7.

Tiemessen CT, Kidd AH. Adenovirus type 40 and 41 growth in vitro: host range diversity reflected by differences in patterns of DNA replication. J Virol. 1994; 68:1239–1244.

Toietta G, Koehler DR, Finegold MJ, Lee B, Hu J, Beaudet AL. Reduced inflammation and improved airway expression using helper-dependent adenoviral vectors with a K18 promoter. Mol Ther 2003; 7: 649-58.

Toietta G, Mane VP, Norona WS, Finegold MJ, Ng P, McDonagh AF*, et al.* Lifelong elimination of hyperbilirubinemia in the Gunn rat with a single injection of helper-dependent adenoviral vector. Proceedings of the National Academy of Sciences of the United States of America 2005; 102: 3930-5.

Tomko RP, Xu R, Philipson L. HCAR and MCAR: the human and mouse cellular receptors for subgroup C adenoviruses and group B coxsackieviruses. Proc Natl Acad Sci U S A. 1997; 94:3352-6.

Trotman LC, Mosberger N, Fornerod M, Stidwill RP, Greber UF. Import of adenovirus DNA involves the nuclear pore complex receptor CAN/Nup214 and histone H1. Nat Cell Biol. 2001; 3:1092-100.

U

Umana P, Gerdes CA, Stone D, Davis JR, Ward D, Castro MG, *et al*. Efficient FLPe recombinase enables scalable production of helper-dependent adenoviral vectors with negligible helper-virus contamination. Nat Biotechnol. 2001; 19:582–585.

Urnov FD, Rebar EJ, Holmes MC, Zhang HS, Gregory PD. Genome editing with engineered zinc finger nucleases. Nat Rev Genet. 2010; 11:636-46. Review.

V

Van Oostrum J, Burnett RM. Molecular composition of the adenovirus type 2 virion. J Virol. 1985; 56:439-48.

Vellinga J, van den Wollenberg DJ, van der Heijdt S, Rabelink MJ, Hoeben RC. The coiled-coil domain of the adenovirus type 5 protein IX is dispensable for capsid incorporation and thermostability. J Virol. 2005; 79:3206-10.

Vetrini F, Brunetti-Pierri N, Palmer DJ, Bertin T, Grove NC, Finegold MJ*, et al.* Vasoactive intestinal peptide increases hepatic transduction and reduces innate immune response following administration of helper-dependent Ad. Mol Ther 2010; 18: 1339-45.

W

Wadell G. Sensitization and neutralization of adenovirus by specific sera against capsid subunits. J Immunol 1972; 108: 622-32.

Wang H, Cao H, Wohlfahrt M, Kiem HP, Lieber A. Tightly regulated gene expression in human hematopoietic stem cells after transduction with helper-dependent Ad5/35 vectors. Exp Hematol. 2008; 36:823-31.

Wang Q, Jia XC, Finer MH. A packaging cell line for propagation of recombinant adenovirus vectors containing two lethal gene-region deletions. Gene Ther. 1995; 2:775-83.

Watts KL, Adair J, Kiem HP. Hematopoietic stem cell expansion and gene therapy. Cytotherapy. 2011; 13:1164-71. Review.

Wiethoff CM, Wodrich H, Gerace L, Nemerow GR. Adenovirus protein VI mediates membrane disruption following capsid disassembly. J Virol. 2005; 79:1992-2000.

Wilson CB, Embree LJ, Schowalter D, Albert R, Aruffo A, Hollenbaugh D*, et al.* Transient inhibition of CD28 and CD40 ligand interactions prolongs adenovirus-mediated transgene expression in the lung and facilitates expression after secondary vector administration. Journal of virology 1998; 72: 7542-50.

Weaver EA, Nehete PN, Nehete BP, Buchl SJ, Palmer D, Montefiori DC*, et al.* Protection against Mucosal SHIV Challenge by Peptide and Helper-Dependent Adenovirus Vaccines. Viruses 2009; 1: 920.

Weber JM. Adenain, the adenovirus endoprotease (a review). Acta Microbiol Immunol Hung. 2003; 50:95-101. Review.

Weiss RS, Javier RT. A carboxy-terminal region required by the adenovirus type 9 E4 ORF1 oncoprotein for transformation mediates direct binding to cellular polypeptides. J Virol. 1997; 71:7873-80.

Welsh MJ, Rogers CS, Stoltz DA, Meyerholz DK, Prather RS. Development of a porcine model of cystic fibrosis. Trans Am Clin Climatol Assoc 2009; 120: 149-62.

White G, Monahan P. Gene therapy for hemophilia A. In: Lee C., Berntrop E., Hoots K., editors. Textbook of Hemophilia. Oxford, UK: Blackwell Publishing 2005; 226–28.

Wodrich H, Henaff D, Jammart B, Segura-Morales C, Seelmeir S, Coux O, *et al*. A capsid-encoded PPxY-motif facilitates adenovirus entry. PLoS Pathog. 2010; 6:e1000808.

Wold WS. Adenovirus genes that modulate the sensitivity of virus-infected cells to lysis by TNF. J Cell Biochem. 1993; 53:329-35. Review.

Wolff G, Worgall S, van Rooijen N, Song WR, Harvey BG, Crystal RG. Enhancement of in vivo adenovirus-mediated gene transfer and expression by prior depletion of tissue macrophages in the target organ. Journal of virology 1997; 71: 624-9.

Wonganan P, Clemens CC, Brasky K, Pastore L, Croyle MA. Species differences in the pharmacology and toxicology of PEGylated helper-dependent adenovirus. Mol Pharm 2011; 8: 78-92.

Worgall S, Wolff G, Falck-Pedersen E, Crystal RG. Innate immune mechanisms dominate elimination of adenoviral vectors following in vivo administration. Hum Gene Ther 1997; 8: 37-44.

X

Xia H, Mao Q, Eliason SL, Harper SQ, Martins IH, Orr HT, *et al*. RNAi suppresses polyglutamine-induced neurodegeneration in a model of spinocerebellar ataxia. Nat Med. 2004; 10:816-20.

Xu Z, Qiu Q, Tian J, Smith JS, Conenello GM, Morita T, *et al*. Coagulation factor X shields adenovirus type 5 from attack by natural antibodies and complement. Nat Med. 2013; 19:452-7.

Y

Yang Y, Ertl HC, Wilson JM. MHC class I-restricted cytotoxic T lymphocytes to viral antigens destroy hepatocytes in mice infected with E1-deleted recombinant adenoviruses. Immunity. 1994a; 1:433-42.

Yang Y, Nunes FA, Berencsi K, Furth EE, Gonczol E, Wilson JM. Cellular immunity to viral antigens limits E1-deleted adenoviruses for gene therapy. Proceedings of the National Academy of Sciences of the United States of America 1994b; 91: 4407-11.

Z

Zhang W, Imperiale MJ. Interaction of the adenovirus IVa2 protein with viral packaging sequences. J Virol. 2000; 74:2687-93.

Zhang W, Low JA, Christensen JB, Imperiale MJ. Role for the adenovirus IVa2 protein in packaging of viral DNA. J Virol. 2001; 75:10446-54.

Zhou H, O'Neal W, Morral N, Beaudet AL. Development of a complementing cell line and a system for construction of adenovirus vectors with E1 and E2a deleted. J Virol. 1996; 70:7030-8.

Zhu J, Huang X, Yang Y. Innate immune response to adenoviral vectors is mediated by both Toll-like receptor-dependent and -independent pathways. J Virol 2007; 81:3170-80.

Zinn KR, Szalai AJ, Stargel A, Krasnykh V, Chaudhuri TR. Bioluminescence imaging reveals a significant role for complement in liver transduction following intravenous delivery of adenovirus. Gene Ther 2004; 11:1482-6.

Zong S, Kron MW, Epp C, Engler T, Bujard H, Kochanek S*, et al.* DeltaE1 and high-capacity adenoviral vectors expressing full-length codon-optimized merozoite surface protein 1 for vaccination against Plasmodium falciparum. J Gene Med 2011; 13:670-9.

Zou L, Yuan X, Zhou H, Lu H, Yang K. Helper-dependent adenoviral vector-mediated gene transfer in aged rat brain. Hum Gene Ther 2001; 12:181-91.

Zsebo K, Yaroshinsky A, Rudy JJ, Wagner K, Greenberg B, Jessup M, *et al*. Long-term effects of AAV1/SERCA2a gene transfer in patients with severe heart failure: analysis of recurrent cardiovascular events and mortality. Circ Res. 2014; 114:101-8.